NEUROPHYSIOLOGICAL CORRELATES OF SENSORY-ATTENTIONAL PROCESSING IN MIGRAINE DURING THE INTERICTAL PHASE

Angela Marti Marca

Doctoral Thesis

This thesis is dedicated to:

Aldo
For your love and unwavering support every step of the way

Mama, Tata, and Miki
For your love, support, and encouragement no matter the distance

ACKNOWLEDGEMENTS

This PhD dissertation would not have been possible without the support of many important individuals and organizations. Before delving into its contents, I would like to take a moment to acknowledge some of the people who made the greatest impact on my development as a PhD student, shaping me as both a researcher and a person.

To my lab mates and cherished companions, thank you for your feedback and encouragement. Your comments, criticisms, and suggestions were of great help in putting together this final work. A special thank you, in particular, to Nara Ikumi and Xim Cerdà-Company, whose kindness, counsel, and our many hours in the lab helped me to achieve this milestone.

To my collaborators at the Pompeu Fabra University, Salvador Soto Faraco and Mireia Torralba, I cannot thank you enough for the hours you put into discussing and improving the design, methodology, and analyses of this research thesis. I am very grateful for your help, guidance, and attentiveness.

To the Universitat Autònoma de Barcelona and the Vall d'Hebron Research Institute for providing me with the space and the opportunity to complete this PhD dissertation. A special thank you to the Vall d'Hebron Research Institute for the grant which co-funded my research for three out of the five years.

To my family, thank you for letting me fly even though it meant being so far away. Your belief in my abilities carried me to new heights that I never would have dreamed possible. Thank you, always, for your love and support! This PhD thesis is for us!

To Aldo, I can't put into words how much your support has meant to me over these past five years. Without a doubt, you kept me sane and truly accompanied me in this process. Your love and unfaltering belief in me led me to this end goal and this PhD thesis would not have been possible without you. I love you.

Thank you to my tutor, José Alvarez-Sabín for providing me with the opportunity to complete a PhD under your supervision.

And finally, a huge thank you to my thesis directors, Adrià Vilà-Balló and Patricia Pozo-Rosich. Adrià, thank you for always pushing, guiding, and helping me to accomplish this goal. You

went above and beyond as a thesis director, and I am beyond thankful to you. Patricia, thank you for the space and guidance to work on this PhD thesis. All that I know about migraine I can attribute to you.

Without your support, this journey would not have been feasible. Thank you from the bottom of my heart.

LIST OF ABBREVIATIONS

AEP	Auditory evoked potential
AIC	Akaike information criterion
ANOVA	Analysis of variance
rmANOVA	Repeated measures analysis of variance
ANT	Attention network test
ASRS	Attention deficit hyperactive disorder self-report scale
BDI-II	Beck depression inventory-II
BF_{10}	Bayes factor
BOLD	Blood-oxygen-level-dependent
BSI	Brief symptoms inventory
rCBF	Regional cerebral blood flow
CGRP	Calcitonin gene-related peptide
Chisq	Chi-square test on model log-likelihoods
CM	Chronic migraine
CMS	Common mode sense
CN	Cochlear nuclei
CNS	Central nervous system
CNV	Contingent negative variation
CPT	Continuous performance test
CSD	Cortical spreading depression
DALY	Disability-adjusted life-years
DRL	Driven right leg
DRN	Dorsal raphe nucleus
DST	Digit span test
E	Excitatory synapse
EEG	Electroencephalography
E/I	Excitation/inhibition
EOG	Electro-oculogram
EM	Episodic migraine
EP	Evoked potential
EPSP	Excitatory post-synaptic potential
ER	Evoked response

ERP	Event-related potential
ERSP	Event-related spectral perturbation
ESS	Epworth sleepiness scale
FDR	False discovery rate
FIR	Finite impulse response
FHM	Familial hemiplegic migraine
fMRI	Functional magnetic resonance imaging
GABA	Gamma-aminobutyric acid
GBD	Global burden of disease
GÜF/THF	Hypersensitivity to sound test
H0	Null model
H1	Alternative model
HIT-6	Headache impact test-6
HR	Hazard rate
Hz	Hertz
I	Inhibitory synapse
IAF	Individual alpha frequency
IC	Inferior colliculus
ICHD-3	International classification of headache disorders, 3rd edition
IDAP	Intensity-dependent auditory evoked potential
IIB	Interictal burden
IIR	Infinite impulse response
IPAQ	International physical activity questionnaire
ipRGC	Intrinsically photosensitive retinal ganglion cell
IPS	Intraparietal sulcus
IPSP	Inhibitory post-synaptic potential
IQR	Interquartile range
IPS	Intermittent photic stimulation
ITC	Inter-trial coherence
JND	Just noticeable difference
LARES	Large analysis and review of European housing and health status
LC	Locus coeruleus
LDL	Loudness discomfort level
LGN	Lateral geniculate nucleus

LMM	Linear mixed-effects model
MA	Migraine with aura
MFG	Middle frontal gyrus
MIDAS	Migraine disability assessment test
Mig-S-Cog	Subjective cognitive impairment for migraine attacks
MMN	Mismatch negativity
MO	Main objective
MSQ	Migraine-specific quality of life questionnaire
MwoA	Migraine without aura
NMDA	N-methyl-D-aspartate
OPN	Olivary pretectal nucleus
PAG	Periaqueductal gray
PC	Pulvinar complex
PET	Positron emission tomography
PFC	Prefrontal cortex
PN	Paraventricular nucleus
PPC	Posterior parietal cortex
PR	Pattern-reversal
PR-VEP	Pattern-reversal visual evoked potential
QoL	Quality of life
REDCap	Research electronic data capture
RGC	Retinal ganglion cell
ROI	Region of interest
RON	Re-orienting negativity
RS	Research study
RT	Reaction time
SAT	Sensory aversion threshold
SC	Superior colliculus
SCN	Suprachiasmatic nucleus
SD	Standard deviation
SEM	Standard error of the mean
SGN	Spiral ganglion neuron
SIAM	Single-interval adjustment matrix
SN	Supraoptic nucleus

SO	Secondary objective
SOC	Superior olivary complex
SOA	Stimulus onset asynchrony
SPQ	Sensory perception quotient
SPS	Sensory processing sensitivity
SpV	Spinal trigeminal nucleus
SSEP	Steady-state evoked potential
SSN	Superior salivatory nucleus
SSVEP	Steady-state visual evoked potential
STAI	State-trait anxiety inventory
STFT	Short time Fourier transform
TCC	Trigeminocervical complex
TG	Trigeminal ganglion
TMT-A	Trail making test A
TMT-B	Trail making test B
TNC	Trigeminal nucleus caudalis
UI	Uncertainty interval
V	Volts
VEP	Visual evoked potential
VHIR	Vall d'Hebron Institute of Research
WAIS-R	Wechsler adult intelligence scale revised
YLD	Years [of life] lived with disability
YLL	Years [of life] lost to premature mortality

INDEX OF FIGURES

INDEX OF TABLES

TABLE OF CONTENTS

ABSTRACT

Migraine is a complex, neurosensory disorder, which is frequently characterized by head pain and altered sensory processing. It is very prevalent and highly disabling, affecting on average one out of every seven people and severely impacting quality of life. Migraine is also a cyclic disorder, fluctuating between acute attack (ictal) periods and relative normality (interictal), although impairments have been reported even outside of the acute attack phase. In fact, evaluating sensory-attentional processing during the interictal phase may provide important information about areas that are often disregarded in terms of treatment and clinical importance as well as for anticipating and ideally predicting future attacks. In particular, the influence of stimulus-driven (exogenous) and internally modulated (endogenous) mechanisms on potential alterations of sensory-attentional processing in patients with episodic migraine (EM) interictally as compared to headache-free controls (HC), remains to be elucidated.

One of the tools that is frequently used to study neural activity is the electroencephalogram, which has several important advantages, including high temporal resolution, permitting the researcher to examine different stages of information processing with a fine-grained tool to detect individual differences. Using event-related potentials (ERPs) it is possible to assess the neural response to stimuli or events. Furthermore, time-frequency decomposition of the resulting signal can provide additional information about the underlying neural oscillatory activity, helping to better delineate cognitive processes. Importantly, a combination of ERPs and time-frequency measures can permit the researcher to obtain a variety of neurophysiological correlates of sensory-attentional processing, which can be used to assess alterations in clinical samples, such as in patients with migraine.

For the purposes of this research thesis, electroencephalographic (EEG) recordings were paired with distinct experimental paradigms to study the neurophysiological correlates of sensory-attentional processing in HC and EM during the interictal phase. Four research studies were carried out to explore four secondary objectives (SO). Specifically, we began with the goal of developing a task to study the exogenous and endogenous mechanisms of sensory-attentional processing in the visual domain [SO1]. Subsequently, we wanted to apply this task to EM in the interictal phase and their HC [SO2]. In parallel, we aimed to resolve some of the discrepancies in the literature, by studying the exogenous mechanisms of sensory processing in the visual modality in patients with EM, interictally as compared to HC [SO3]. Finally, we moved to the auditory modality to assess the exogenous and endogenous mechanisms of sensory-attentional processing in patients with EM, during the interictal phase, and their HC [SO4].

First, to accomplish SO1, in Research Study 1 we modified a pre-existing cued visual detection task with bilateral entrainers to elicit neural entrainment, the inherent capacity of neural oscillatory activity to synchronize to rhythmic stimulation. Next, a sample of headache-free

participants completed the task while we recorded the resulting EEG activity and extracted the inter-trial coherence (ITC) and phase alignment, among other measures. After, we ran a series of analyses to check that the paradigm effectively elicited neural entrainment. The results of this study confirmed the presence of neural entrainment, through a significant phase alignment of the neural activity to the periodic external stimuli and persistence of this phase alignment beyond the offset of the driving signal.

Next, to respond to SO2, in Research Study 2 we applied the cued visual detection task with bilateral entrainment along with a series of questionnaires, to patients with EM in the interictal phase and their age- and gender-matched HC. The results indicated that the exogenous response to the repetitive stimulation was similar between groups as seen by a lack of differences between EM and HC in the ITC and phase alignment to the driving signal. Furthermore, and interestingly, we also found similar phase alignment and persistence of the signal after the offset of the external stimuli, in EM and HC.

In parallel, we wanted to assess whether the previously reported sensory-attentional alterations in EM interictally were comprehensive representations of the impairments during this phase. In Research Study 3, which consisted of two experiments, we wanted to assess visual processing in interictal patients with EM and their HC [SO3]. The first experiment assessed young adults with EM and their age- and gender-matched HC, whereas the second experiment evaluated middle-aged patients with EM and their age- and gender-matched HC. In both experiments, participants completed a series of questionnaires as well as an EEG recording during a pattern-reversal task from which we obtained pattern-reversal visual evoked potentials, specifically N1-P1 peak-to-peak amplitude differences. N1-P1 peak-to-peak amplitude differences were obtained for each trial as well as averaged into blocks (100 trials per block) and analyzed using traditional analysis methods as well as a novel approach based on linear mixed-effects models. The results yielded lower scores on the Sensory Perception Quotient in EM as compared to HC. Additionally, N1-P1 peak-to-peak amplitude differences were found to be similar between EM and HC during the first block, related to cortical excitability, and a significant decrement in this measure, used to assess habituation, was observed when comparing the first and last blocks/trials in both groups.

Finally, Research Study 4 was meant to respond to SO4, which wanted to investigate exogenous and endogenous mechanisms of sensory-attentional processing, in the auditory modality. Here, young patients with EM in the interictal phase and their age- and gender-matched HC were compared in terms of questionnaires and their responses to an active, auditory oddball task, during an EEG recording. We obtained behavioural measures, spectral power and phase synchronization of theta, alpha, and beta-gamma, and ERPs for standard stimuli (N1, P2, N2 amplitudes) as well as for

4

target and novel stimuli (MMN, early and late P3a, P3b, and RON amplitudes). The results of our study showed an increased N1 and greater theta phase synchronization to auditory stimuli in EM as compared to HC. We also found a lower early P3a, increased late P3a, and reduced RON to novel stimuli, in EM as compared to HC, related to the post-sensory response, allocation of attentional resources, and attentional orienting, respectively.

The present research thesis studied the neurophysiological correlates of sensory-attentional processing in patients with EM during the interictal phase and their HC. First, we were able to successfully design a task to study the exogenous and endogenous mechanisms of sensory-attentional processing. Next, with regard to the case-control studies (Research Study 2-4), our results would suggest that certain processes and mechanisms are preserved in patients with EM interictally while others are impaired. In particular, in Research Study 2, we found similar neural entrainment, as seen by a lack of significant differences in either phase alignment or ITC between groups, which would suggest that the exogenous and endogenous mechanisms of sensory-attentional processing, related to this process, are preserved in EM interictally. In Research Study 3, on the other hand we found no significant differences on the pattern-reversal task, in either cortical excitability or habituation, in EM or HC, although EM did report subjective visual hypersensitivity, which could be indicative of some level of alterations in the exogenous mechanisms of visual processing. Finally, in Research Study 4, the results yielded auditory hypersensitivity in EM as compared to HC as seen by an increased N1 and greater theta phase synchronization, as well as a reduced post-sensory response and a compensatory increase in the allocation of attentional resources, shown by a reduced early P3a and increased late P3a. Furthermore, patients with EM also had a significantly reduced RON as compared to HC indicating trouble shifting attention away from novel stimuli and back to the main task. Taken together, the results of these studies would suggest that patients with EM interictally may already exhibit certain deficits in sensory-attentional processing, although the results are more limited than previously thought.

RESUMEN

La migraña es un trastorno neurosensorial complejo que se caracteriza frecuentemente por dolor de cabeza y alteración del procesamiento sensorial. Es muy prevalente y altamente discapacitante, afectando de media a una de cada siete personas y repercutiendo gravemente en la calidad de vida. La migraña es también un trastorno cíclico, que fluctúa entre periodos de ataque agudo (ictal) y relativa normalidad (interictal), aunque se han descrito alteraciones incluso fuera de la fase de ataque agudo. De hecho, la evaluación del procesamiento sensorial-atencional durante la fase interictal puede proporcionar información importante sobre áreas que a menudo no se tienen en cuenta en términos de tratamiento e importancia clínica, así como para anticipar e idealmente predecir futuros ataques. En particular, queda por dilucidar la influencia de los mecanismos impulsados por estímulos (exógenos) y modulados internamente (endógenos) en las posibles alteraciones del procesamiento sensorial-atencional en pacientes con migraña episódica (ME) interictales en comparación con controles sin cefalea (CS).

Una de las herramientas que se utiliza con frecuencia para estudiar la actividad neuronal es el electroencefalograma, que presenta varias ventajas importantes, entre ellas una alta resolución temporal, lo que permite al investigador examinar distintas etapas del procesamiento de la información con una herramienta de gran precisión para detectar diferencias individuales. Mediante los potenciales relacionados con eventos (ERPs) es posible evaluar la respuesta neuronal a estímulos o eventos. Además, la descomposición tiempo-frecuencia de la señal resultante puede proporcionar información adicional sobre la actividad oscilatoria neuronal subyacente, ayudando a delinear mejor los procesos cognitivos. Es importante destacar que una combinación de ERPs y medidas de tiempo-frecuencia puede permitir al investigador obtener una variedad de correlatos neurofisiológicos del procesamiento sensorial-atencional, que pueden utilizarse para evaluar alteraciones en muestras clínicas, como en pacientes con migraña.

Para los fines de esta tesis doctoral, los registros de electroencefalografía (EEG) se emparejaron con distintos paradigmas experimentales para estudiar los correlatos neurofisiológicos del procesamiento sensorial-atencional en CS y ME durante la fase interictal. Se llevaron a cabo cuatro estudios de investigación para explorar cuatro objetivos secundarios (OS). En concreto, comenzamos con el objetivo de desarrollar una tarea para estudiar los mecanismos exógenos y endógenos del procesamiento sensorial-atencional en el dominio visual [OS1]. A continuación, quisimos aplicar esta tarea a ME en fase interictal y a sus CS [OS2]. Paralelamente, nos propusimos resolver algunas de las discrepancias en la literatura, estudiando los mecanismos exógenos de procesamiento sensorial en la modalidad visual en pacientes con ME, en fase interictal y sus CS [SO3]. Finalmente, nos trasladamos a la modalidad auditiva para evaluar los mecanismos exógenos

y endógenos del procesamiento sensorial-atencional en pacientes con ME, durante la fase interictal, y sus CS [SO4].

En primer lugar, para lograr el OS1, en el Estudio de Investigación 1 modificamos una tarea de detección visual preexistente con estimulación bilateral para provocar entrainment, la capacidad inherente de la actividad oscilatoria neural para sincronizarse con la estimulación rítmica. A continuación, una muestra de participantes sin cefalea completó la tarea mientras registrábamos la actividad EEG resultante y extraíamos la coherencia (ITC) y la alineación de fase, entre otras medidas. A continuación, realizamos una serie de análisis para comprobar que el paradigma provocaba efectivamente entrainment neural. Los resultados de este estudio confirmaron la presencia de entrainment neural, a través de una alineación de fase significativa de la actividad neural con los estímulos externos periódicos y la persistencia de esta alineación de fase más allá del desplazamiento de la señal impulsora.

A continuación, para responder al SO2, en el Estudio de Investigación 2 aplicamos la tarea de detección visual con estimulación bilateral, junto con una serie de cuestionarios, a pacientes con ME en la fase interictal y a su CS emparejados por edad y sexo. Los resultados indicaron que la respuesta exógena a la estimulación repetitiva fue similar entre los grupos, como se observa por la ausencia de diferencias entre ME y CS en el ITC y la alineación de fase con la señal de conducción. Además, y de forma interesante, también encontramos una alineación de fase y una persistencia de la señal similares tras la desaparición de los estímulos externos, en ME y CS.

Paralelamente, queríamos evaluar si las alteraciones sensoriales-atencionales previamente descritas en pacientes con ME interictales eran representaciones exhaustivas de las alteraciones durante esta fase. En el Estudio de Investigación 3, que consistió en dos experimentos, quisimos evaluar el procesamiento visual en pacientes interictales con ME y sus CS [SO3]. El primer experimento evaluó a adultos jóvenes con ME y a sus CS emparejados por edad y sexo, mientras que el segundo experimento evaluó a pacientes de mediana edad con ME y a sus CS emparejados por edad y sexo. En ambos experimentos, los participantes completaron una serie de cuestionarios, así como un registro EEG durante una tarea de inversión de patrones de la que obtuvimos potenciales evocados visuales de inversión de patrones, específicamente diferencias de amplitud pico a pico N1-P1. Las diferencias de amplitud pico a pico N1-P1 se obtuvieron para cada ensayo, así como promediadas en bloques (100 ensayos por bloque) y analizadas utilizando métodos de análisis tradicionales, así como un enfoque novedoso basado en modelos lineales de efectos mixtos. Los resultados arrojaron puntuaciones más bajas en el Cociente de Percepción Sensorial en ME en comparación con CS. Además, se observó que las diferencias de amplitud pico a pico N1-P1 eran similares entre ME y CS durante el primer bloque, en relación con la excitabilidad cortical, y se

observó una disminución significativa en esta medida, utilizada para evaluar la habituación, al comparar el primer y el último bloque/ensayo en ambos grupos.

Por último, el Estudio de Investigación 4 debía responder al OS4, que quería investigar los mecanismos exógenos y endógenos del procesamiento sensorial-atencional en la modalidad auditiva. Aquí, se compararon pacientes jóvenes con ME en la fase interictal y sus CS de la misma edad y sexo, en términos de cuestionarios y sus respuestas a una tarea auditiva activa, durante un registro de EEG. Se obtuvieron medidas conductuales, potencia espectral y sincronización de fase de theta, alfa y beta-gamma, y ERPs para estímulos estándar (amplitudes N1, P2, N2) así como para estímulos diana y novedosos (amplitudes MMN, P3a temprana y tarde, P3b y RON). Los resultados de nuestro estudio mostraron un aumento de N1 y una mayor sincronización de la fase theta con los estímulos auditivos en ME en comparación con CS. También se observó una menor P3a temprana, una mayor P3a tarde y una menor RON ante estímulos nuevos en ME en comparación con CS, en relación con la respuesta postsensorial, la asignación de recursos atencionales y la orientación atencional, respectivamente.

La presente tesis de investigación estudió los correlatos neurofisiológicos del procesamiento sensorial-atencional en pacientes con ME durante la fase interictal y sus CS. En primer lugar, pudimos diseñar con éxito una tarea para estudiar los mecanismos exógenos y endógenos del procesamiento sensorial-atencional. A continuación, con respecto a los estudios de casos y controles (Estudio de investigación 2-4), nuestros resultados sugerirían que ciertos procesos y mecanismos están preservados en pacientes con ME durante la fase interictal, mientras que otros están deteriorados. En particular, en el Estudio de Investigación 2, encontramos un entrainment neural similar, como se observa por la ausencia de diferencias significativas tanto en el alineamiento de fase como en el ITC entre los grupos, lo que sugeriría que los mecanismos exógenos y endógenos del procesamiento sensorial-atencional, relacionados con este proceso, están preservados en la ME interictal. En el Estudio de Investigación 3, por otra parte, no encontramos diferencias significativas en la tarea de inversión de patrones, ni en la excitabilidad cortical ni en la habituación, ni en ME ni en CS, aunque ME sí informó de hipersensibilidad visual subjetiva, lo que podría ser indicativo de algún nivel de alteraciones en los mecanismos exógenos del procesamiento visual. Por último, en el Estudio de Investigación 4, los resultados arrojaron hipersensibilidad auditiva en ME en comparación con CS, como se observa por un aumento de N1 y una mayor sincronización de la fase theta, así como una respuesta postsensorial reducida y un aumento compensatorio en la asignación de recursos atencionales, mostrado por una P3a temprana reducida y una P3a tarde aumentada. Además, los pacientes con ME también presentaban una RON significativamente reducida en comparación con los CS, lo que indicaba problemas para desviar la atención de los estímulos nuevos y volver a la tarea principal. En conjunto, los resultados de estos estudios sugieren que los pacientes con ME interictales

pueden presentar ya ciertos déficits en el procesamiento sensorial-atencional, aunque los resultados son más limitados de lo que se pensaba.

1. INTRODUCTION

"[Getting a migraine] was like there was a monster that would show up in your house whenever it felt like it and there was nothing you could do about it."- Whoopi Goldberg

1.1. Migraine: Understanding the disease

The word **migraine** is thought to originate from 'hemicrania' of Greek origin with 'hemi' meaning half and 'crania' referring to cranium or skull, effectively describing the symptoms and pain frequently reported on one half of the head.(1) For centuries, this invisible illness has plagued humans with its earliest descriptions, in Mesopotamian poems, dating as far back as 3000 B.C.(1,2) In ancient Egypt, many documents refer to headaches and probable migraine alongside a variety of treatments, including applying pressure to the affected area and the more invasive process of drilling a hole into the skull, or trepanation.(2) In fact, Hippocrates [460 – 370 B.C.], the father of modern medicine, was thought to be the first to document the visual alterations that accompany the disorder, describing it [presumed migraine] as severe pain on one side of the head, co-occurring with visual disturbances.(1,2) Over the years, many references to this disease have been made and countless people, including many famous historical figures, such as Julius Caesar, Charles Darwin, and Sigmund Freud, have been thought to suffer with it, with a deep impact on their daily lives.(3,4) In fact, in 2019, the **global prevalence of migraine was estimated to be around 1.1 billion cases**.(5)

1.1.1. Diagnostic criteria and clinical evaluation

Given its **high prevalence and profound impact**, individuals with migraine require proper treatment. However, to be able to provide optimal care, a diagnosis is necessary. The **International Classification for Headache Disorders** is a hierarchical, diagnostic tool of headache disorders, first published in 1988 and currently in its third edition (ICHD-3).(6) This classification system separates headache disorders into two categories: primary and secondary. **Primary headache disorders** are idiopathic, with no known cause whereas **secondary headache disorders** occur as a result of another condition, such as infection, trauma, or vascular disease.(7) Migraine [code 1 in ICHD-3 (6)] is a primary headache disorder, which consists of periodic, moderate to severe headache attacks with an average duration of 4 to 72 hours in adults and a series of transient, reversible symptoms including **photophobia** (aversion to light) and **phonophobia** (aversion to sound) or nausea and vomiting. Migraine is also frequently subdivided into **migraine without** [MwoA; code 1.1. in ICHD-3 (6)] and **migraine with aura** [MA; code 1.2. migraine with aura in ICHD-3,(6)] (see Figure 1). For clarity, **aura** is a series of heterogeneous, neurological, transient, and reversible symptoms that frequently occur prior to headache, although this is not always the case, comprised of altered visual, sensory,

motor, speech and/or language function.(6) In patients diagnosed with MA, visual aura is the most frequent (90% of patients), followed by sensory disturbances and speech and/or language impairments.(6) Additionally, patients with MA can also have attacks without aura.(6)

Migraine without aura (MwoA)

A. At least five attacks fulfilling criteria B-D

B. Headache attacks lasting 4-72 hours (untreated or unsuccessfully treated)

C. Headache has at least two of the following four characteristics:
   1. unilateral location
   2. pulsating quality
   3. moderate or severe pain intensity
   4. aggravation by or causing avoidance of routine physical activity (e.g., walking or climbing stairs)

D. During headache at least one of the following:
   1. nausea and/or vomiting
   2. photophobia and phonophobia

E. Not better accounted for by another ICHD-3 diagnosis

Migraine with aura (MA)

A. At least two attacks fulfilling criteria B and C

B. One or more of the following fully reversible aura symptoms:
   1. visual
   2. sensory
   3. speech and/or language
   4. motor
   5. brainstem
   6. retinal

C. At least three of the following six characteristics:
   1. at least one aura symptom spreading gradually over ≥5 minutes
   2. two or more aura symptoms occur in succession
   3. each individual aura symptom lasts 5-60 minutes
   4. at least one aura symptom is unilateral
   5. at least one aura symptom is positive
   6. the aura is accompanied, or followed within 60 minutes by headache

D. Not better accounted for by another ICHD-3 diagnosis

Figure 1. Diagnostic criteria for migraine without aura (MwoA) and migraine with aura (MA) according to the International Classification for Headache Disorders, 3rd edition (ICHD-3). These criteria were taken from the ICHD-3 codes 1.1. and 1.2.(6)

Furthermore, aside from classifications based on the presence or absence of aura, migraine can also be categorized according to its frequency (number of headache/migraine days a month), with most diagnoses requiring a minimum number of attack days over a certain period of time. In fact, a more extreme manifestation of migraine, **chronic migraine** (CM) is diagnosed when patients report headaches occurring on 15 or more days per month with at least eight of those days having migraine-like symptoms, for at least three months [code 1.3. in ICHD-3,(6)] (see Figure 2 for more details). Importantly, although the ICHD-3 does not yet have a formal diagnostic category for it, the term episodic migraine (EM) is frequently used to refer to patients with migraine that do not meet the criteria for CM, based on headache/migraine days/month.(8)

Chronic migraine (CM)

A. Headache (migraine-like or tension-type-like) on ≥15 days/month for >3 months, and fulfilling criteria B and C

B. Occurring in a patient who has had at least five attacks fulfilling criteria B-D for 1.1 *Migraine without aura* and/or criteria B and C for 1.2 *Migraine with aura*

C. On ≥8 days/month for >3 months, fulfilling any of the following[2]:
   1. criteria C and D for 1.1 *Migraine without aura*
   2. criteria B and C for 1.2 *Migraine with aura*
   3. believed by the patient to be migraine at onset and relieved by a triptan or ergot derivative

D. Not better accounted for by another ICHD-3 diagnosis.

Figure 2. Diagnostic criteria for chronic migraine (CM) according to the International Classification for Headache Disorders, 3rd edition (ICHD-3). These criteria were taken from the ICHD-3 code 1.3.(6)

To evaluate patients for the presence of a headache disorder, clinicians normally conduct a general neurological examination and collect information relative to family history, age of onset, headache features, lifestyle factors, and comorbid conditions.(7) For migraine, there are no specific diagnostic tests, however a **headache diary** is an excellent tool to confirm a suspected diagnosis and retrieve relevant information as to headache characteristics and acute medication, among other things. Headache diaries can be filled out on paper or digitally (**eDiary**) and consist of a daily log where patients must report the presence or absence of headache, along with its characteristics such as intensity, duration, accompanying symptoms, and acute medication. Other information can also be added, for example regarding menstruation and sleep quality. Importantly, aside from their effectiveness as measurement tools, headache diaries have also been shown to help patients reduce their use of medication and improve their perceived quality of life (QoL).(9) Furthermore, headache diaries are also frequently used in research applications. Patients are usually asked to complete a headache diary for at least thirty days prior to entering a research study to obtain a baseline headache frequency, confirm the suspected diagnosis (particularly when patients are recruited from the general population), and ensure that the patient is headache-free in the time window surrounding the experimental session. Additionally, it is good practice to ask presumed headache-free controls (HC) to complete a baseline headache diary too. This is because HC may sometimes downplay headaches. In fact, in one study over 30% of HCs were excluded from further analyses due to reports of multiple headache days in their headache diaries, with the authors emphasizing the importance of careful screening to avoid introducing bias into the sample.(10)

1.1.2. Characteristics and clinical phases

Aside from the characteristic pain, which is often defined as moderate or severe in intensity and frequently unilateral,(6) migraine is a cyclic neurosensory disorder, frequently accompanied, during and between attacks, by a variety of physiological, sensory, and other symptoms. In fact, the migraine cycle can be divided into phases, with their own characteristic symptoms and impairments (see Figure 3), which include the: **prodrome**, **aura**, **ictal**, **postdrome**, and **interphase**.(11–14)
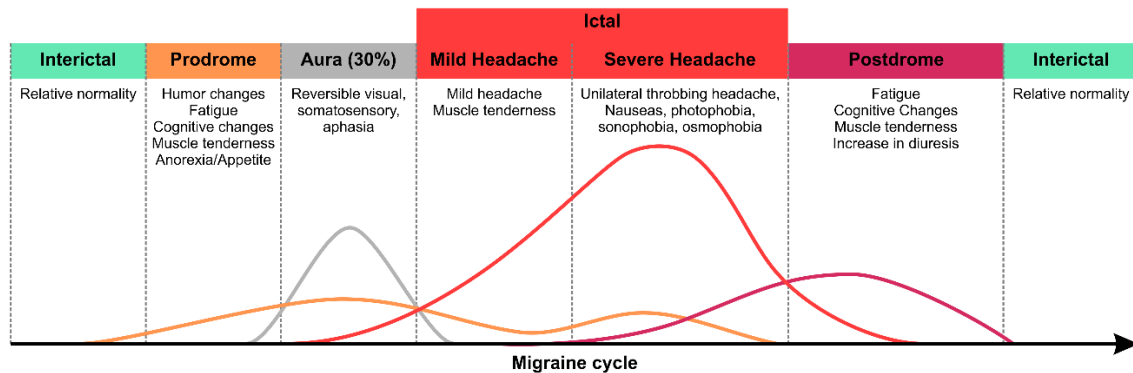
Figure 3. Timeline of the cyclic phases associated with migraine. During the interictal phase, patients experience a relatively normal state, followed by the onset of the prodrome where a variety of changes including fatigue, mood, and cognitive changes occur. In approximately one third of patients, aura, or reversible visual, motor, or cognitive alterations occurs next, followed by headache and its accompanying symptoms, including nausea, and photophobia/phonophobia. Finally, the postdrome phase takes over, during which patients may experience fatigue and cognitive changes among other symptoms, and then a return to normality, again. Adapted from Linde.(12,13)

The **prodrome**, also sometimes referred to as the pre-ictal or premonitory stage, is best defined as the period prior to headache onset,(6) when certain alterations, referred to as prodromes or premonitory symptoms can occur. These frequently include: tiredness or fatigue, yawning, mood or behavioral alterations, appetite changes, thirst, sensory sensitivities, and gastrointestinal complaints.(15–17) Given the nature of premonitory symptoms, a hypothalamic disturbance has been proposed since this brain structure is involved in functions related to appetite control, water retention, circadian rhythms, and endocrine control.(18) Not surprisingly, research studies using functional magnetic resonance imaging (fMRI) would appear to confirm this hypothesis, showing increased hypothalamic activity in patients with migraine during the prodrome.(19,20) These changes have been proposed as a neural correlate of this phase,(19,20) although these results have some important methodological issues including a lack of information about premonitory symptoms at the time of the scan and certain questionable definitions of migraine phases.(21) Another area that would appear to be more active during the prodrome is the spinal trigeminal nucleus (SpV), related to pain and temperature processing,(22,23) which has been found to be coupled to the hypothalamus during this

phase.(24) Activation of the SpV, due to its role in relaying nociceptive information, has been related to the perception of pain and the presence of sensory alterations.(25)

Additionally, about one third of patients with migraine report **aura**.(26) Many researchers do not consider aura as a separate phase because it is not present in all patients and, in those diagnosed with MA, attacks without aura are also common.(6) Furthermore, aura without headache, sometimes termed 'silent migraine' does occur and aura may also overlap into the ictal phase or develop alongside headache.(11) Silent migraines have been reported in older patients, particularly those with a previous MA diagnosis but are not unique to this population.(27–33) In fact, transient visual disturbances have been reported in other diseases such as epilepsy,(34) syncope,(35) cluster headache and other primary headache disorders.(36,37) Aura is therefore not migraine-specific with some researchers even arguing for a different genetic basis for aura as compared to headache.(38–40)

Next, the **ictal** period, most frequently characterized by moderate to severe headache, usually lasting 4-72 hours, and accompanied by photo- and phonophobia or nausea and vomiting, occurs.(6) Interestingly, photo- and phonophobia during a migraine attack can actually exacerbate other symptoms, including head pain, nausea, and vomiting,(41) a phenomenon otherwise termed **photo-** and **phonocephalodynia**. During this time, a number of brain regions have been found to exhibit increased regional cerebral blood flow (rCBF) measured using positron emission tomography (PET), in patients with migraine as compared to headache-free controls. These include the brainstem, auditory and visual association cortices,(42) as well as the dorsolateral pons, anterior cingulate, posterior cingulate, cerebellum, and temporal lobes.(43–45) In particular, the increased blood flow in the dorsolateral pons, located within the brainstem, is thought to play an important role in the migraine attack given its function as a hub for major sensory and motor inputs and outputs as well as pain modulation.(46) On the other hand, activation of the cingulate cortex has previously been linked to the emotional processing of pain.(47–49) Furthermore, increased rCBF in the visual and association cortices may explain the presence of photophobia and phonophobia during the migraine attack.(42)

Once the ictal phase is over, the patient enters the **postdrome**, sometimes called the post-ictal stage, and frequently referred to as the "migraine hangover." During this stage, the patient may report a variety of symptoms, also known as postdromes or postmonitory symptoms, including tiredness or fatigue, difficulty concentrating, stiff neck, muscular weakness, reduced appetite, residual discomfort related to headache, and mood changes.(50–53) Given the wide variety of symptoms, postdromes (and predromes) can be separated into four different categories: neuropsychiatric, sensory, gastrointestinal, and general.(52) Most of these symptoms resolve in a 24-hour period,(51,53) although this phase remains relatively understudied.(54) Using fMRI, one study found increased activation of the visual cortex during the post-ictal phase, which might explain the lingering

sensory sensitivity.(20) Nonetheless, it remains unclear whether the same structures that are more active during the ictal and postdrome phases underlie the reported alterations during this stage.

Finally, once the postdrome dissipates, the patient arrives at the **interphase** or **interictal** stage, often considered the attack-free return to normality. However, many patients continue to report symptoms, such as sensory alterations, here.(55,56) This is consistent with the results from fMRI, which found impaired activity and connectivity between sensory networks suggesting impaired sensory processing, interictally.(57) During this phase, patients also report significant anxiety with regard to future headaches,(58) which may have a significant toll on their QoL and lead to the avoidance of certain stimuli/events, resulting in important lifestyle modifications.(59) Furthermore, the recurrent nature of migraine may lead to a behavioral response termed 'learned helplessness' in some patients, or the belief that no matter what they do bad things will continue to occur, further exacerbating negative feelings.(58) In fact, the impact of migraine during the interictal phase has earned its own term, the Interictal Burden (IIB).(58) Importantly, this phase and its potential alterations continue to be relatively unexplored [for a review, see (60)] although patient complaints in the clinic, would appear to indicate that they continue to experience pervasive symptoms, which affect their QoL. Recently, more interest has been given to this phase, with some clinical trials even including interictal metrics as outcome measures.(60) Without a doubt, better comprehending the alterations that may occur at this stage, may permit us to **improve patient QoL, refocus treatments and outcomes, anticipate or ideally predict future headache attacks, and better understand this complex brain disorder**.

1.1.3. Pathophysiological models

Early theories of migraine pathophysiology were of either vascular or neural origin. For example, work by Peter Wallwork Latham in the 1870s (61,62) proposed that the source of migraine was vasodilation as a consequence of aura, which prompted the **vascular** or **vasogenic theory of migraine**. This notion was revisited in the 1940s by Wolff and colleagues who did research on cranial blood vessels, after observing that the administration of ergot alkaloids such as ergotamine tartrate, which provoke vasoconstriction, had an abortive function on migraine attacks.(63–66) They proposed that the origin of migraine was an initial intracerebral vasoconstriction resulting in aura and a subsequent intra- and extracerebral vasodilation leading to the depolarization of primary nociceptive neurons, causing headache and pain.(64) Other research on the induction of migraine attacks found that nitroglycerin, a known vasodilator, provoked headache,(67) whereas vasoconstrictors including ergotamines and serotonin-norepinephrine reuptake inhibitors eliminated it [(68,69) despite (65,70)]. Additionally, studies on changes in the velocity of blood flow through middle cerebral arteries on the

side of the head affected by headache found reduced velocity suggesting vasoconstriction.(71,72) Nonetheless, the conceptualization of migraine as a uniquely vascular disorder, is unnecessarily reductionist,(65) primarily due this theory's inability to explain a number of headache-related phenomena such as prodromes and postdromes, sensory, attentional, and cognitive alterations, and aura. Additionally, despite the hypothesis proposed by vascular theory, that vasodilation elicits headache, patients with MwoA actually had reduced rCBF during headache,(73) and migraine-like headache was found to occur only once the initial vasodilation had subsided.(65,74,75) However, Asghar and colleagues have recently cautioned against the removal of vascular mechanisms from migraine models, seeing as some level of vascular change does appear to occur during the ictal phase, specifically vasodilation of intra- and extra-cerebral arteries on the side of the headache.(76)

Alternatively, a second set of models to explain migraine pathophysiology were of neural origin. Specifically, around the same time as the original work on vascular theory emerged, Edward Liveing proposed a **neurogenic theory**, claiming that migraine was the result of a nerve-storm.(77) Early proponents of this theory claimed that vascular changes, such as altered blood flow, could result due to abnormal neuronal activity in patients with migraine highlighting a potential relationship between cranial blood vessels and trigeminal nerves [(78,79) for a review, see (80)]. In 1979, Moskowitz proposed the **trigeminovascular** or **inflammatory hypothesis**, after observing that trigeminovascular axons from blood vessels release vasoactive peptides, which produce inflammation.(81,82) As a result of inflammation, the trigeminal ganglion (TG) induces neurogenic protein extravasation of peptides including **calcitonin gene related peptide (CGRP)**. CGRP is one of the most well-known neuropeptides associated with migraine and acts as a potent vasodilator.(83) It is thought that neurogenic inflammation, alongside the impact of CGRP on surrounding tissue, may act as the mechanism underlying pain during the migraine attack.(84) However, neurogenic models have their own share of criticisms, including the fact that not all attacks are CGRP-dependent (85) and that many compounds used in preclinical studies of dural neurogenic inflammation have not been found to work in human models.(86)

Similarly, to neurogenic theory, the **neurological theory** attempted to conceptualize migraine as a disorder of neural origin. In this theory, neuronal activation in migraine is thought to occur as a result of **cortical spreading depression (CSD)** (see Figure 4), an initial wave of excitation followed by an inhibition of cortical neurons and glial cells, causing transient but reversible suppression of neuronal activity.(87) The occurrence of CSD is largely supported by animals models, where the application of potassium ions locally resulted in this series of events (88,89) and is thought to represent the neural correlate of aura.(68,90) Importantly, neurological theory does not entirely discard vascular influence as cerebral blood flow changes have been found to occur during CSD.(91)

However, the presence of CSD is inconsistent in migraine and its effects are very heterogenous in humans.(65) Moreover, aura does not occur in all patients with migraine (26) and aura without headache is not uncommon.(6) Furthermore, the brain itself does not have pain sensory fibers, which makes it difficult for neurological theory to explain where the pain stems from.
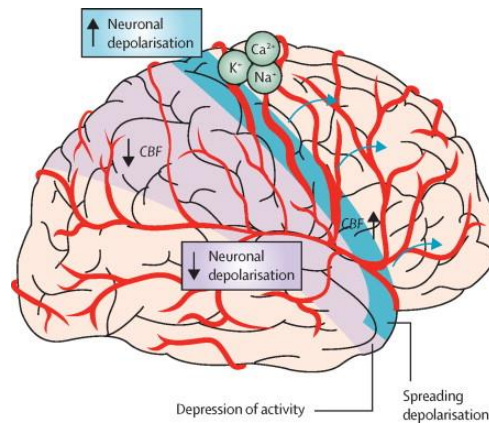
Figure 4. The processes underlying cortical spreading depression (CSD), frequently considered as the electrophysiological generator of aura.(92–94) According to basic research using animal models, CSD occurs as a result of a transient wave of neuronal and glial depolarization, which spreads over the cortex and elicits fluctuations in transmembrane ion concentration, resulting in inhibition of both spontaneous and evoked neuronal activity.(92) Reproduced from Ferrari et al.(95)

Nowadays, the most accepted theory is the **neurovascular theory** (for a schematic representation, see Figure 5), which unites both neural and vascular mechanisms and suggests that migraine originates within the central nervous system (CNS). In particular, the activation of peripheral, trigeminal sensory afferents by the dilation of meningeal blood vessels, results in a nociceptive signal being sent to the thalamus, via the TG and the trigeminocervical complex (TCC).(96–98) The thalamus in turn has connections to brainstem regions such as the periaqueductal gray (PAG) and the locus coeruleus (LC), which may explain the physiological symptoms that tend to accompany migraine.(99) Additionally, co-occurring sensory symptoms may result due to the altered activity in the TCC and thalamus.(25,100) Furthermore, a deficient thalamo-cortical drive, or '**thalamo-cortical dysrhythmia**' was recently proposed to occur in migraine due to a serotonergic disconnection of the thalamus from its controlling inputs, such as the brain stem nuclei, resulting in low-frequency activity.(101) This deficient thalamocortical drive has been related to altered function of sensory cortices and pain processing in patients with migraine.(102) In conclusion, although aspects of migraine pathophysiology remain elusive, it seems clear that **migraine is a disorder of neural (and vascular) origin, and although the brain is difficult to study, there are different techniques, such as electroencephalography (EEG) (see Section 1.2.), which permit us to do so**.
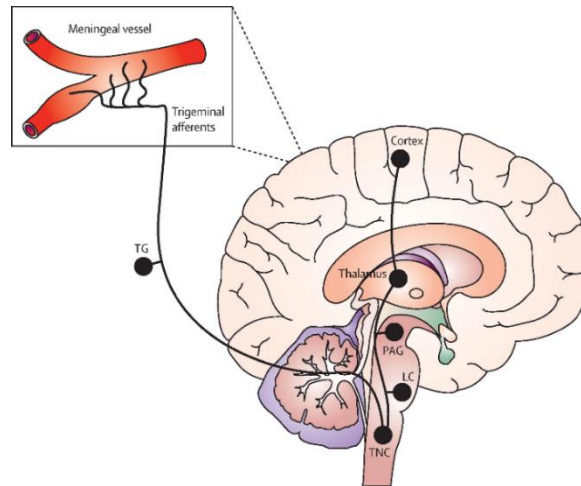
Figure 5. The neurovascular theory of migraine. In this theory, trigeminal sensory afferents encircle cranial blood vessels. When these afferents are activated, the signal moves through the trigeminal ganglion (TG) to the trigeminocervical complex (TCC). Calcitonin gene-related peptide (CGRP) provides the mechanism for this to occur, acting as the main neurotransmitter.(103) The signal then continues to the thalamus and modulation occurs as a result of connections with brainstem regions, including the periaqueductal gray (PAG) and the locus coeruleus (LC).(99) Figure reproduced from Ferrari et al.(95)

1.1.4. Prevalence and economic impact

According to the 2016 Global Burden of Disease (GBD) Study, migraine was ranked as the **sixth most prevalent disorder** according to a list of 328 diseases and injuries.(104) Specifically, 1.05 billion [1.00 – 1.09, 95% uncertainty interval (UI)] individuals were estimated to live with migraine, with approximately 18.9% [18.1 – 19.7] of the global age-standardized prevalence attributed to women and 9.8% [9.4 – 10.2] to men.(104) In Spain this number was found to be around 9.45 million [9.00 – 10.00, 95% UI]. Migraine also ranked as the second highest cause of disability-adjusted life-years (DALYs) according to the 2016 GBD Study, best defined as the years of health/life lost to a disease or disorder and comprised of the sum of years lived with disability (YLDs) and those lost to premature mortality (YLLs).(104) Specifically, migraine contributed to a global 45.1 million [29.0 – 62.8, 95% UI] YLDs with an estimated 792.83 of these YLDs per 100,000 being reported in Spain [189.16 – 1,692.89]. Importantly, the number of YLDs attributed to migraine has increased by approximately 51.2% [49.7 – 52.8] since 1990, highlighting the importance of migraine treatments and research. The amount of YLDs, when age-standardized, was also found to be higher in women than men with a peak in prevalence and YLDs being reported between the ages of 35 and 39. This is not surprising given previous reports of migraine being around three times more prevalent in women than in men [see (105) for a review]. Additionally, migraine is the most frequent cause of disability in individuals, particularly young adults and middle-aged women, under 50 years old (104,106)

Migraine also has an important **economic impact**, which can be attributed to the effect of

headache-related pain and resulting psychosocial and psychiatric problems on work, social relationships, and global disability, among others.(107) For example, patients with migraine tend to report **higher rates of absenteeism**, **less efficiency** at work, and decreased time inverted into their job as well as **consequences on their relationships** with family and friends.(107) In fact, patients with migraine/other headache disorders tend to lose approximately 7 days of work per year with migraine/headache disorders being the second highest contributors to days out of role.(108) Also, in terms of cumulative burden, 11.8% of patients reported that migraine negatively affected their education, 7.4% their career and 5.9% their earnings.(109) Migraine is also highly comorbid with psychiatric illness, with greater comorbidity occurring with increased headache frequency.(110,111) In one study using regression models that accounted for sociodemographic variables, patients with migraine were found to have a significantly higher likelihood of insomnia, depression, and anxiety, than those without migraine.(110) These psychiatric comorbidities not only affect patient QoL, but have also been related to a higher risk of developing CM and overusing medication.(112,113)

Given its high prevalence, significant personal and economic impact, as well as a number of unsolved questions with regard to migraine pathophysiology, it remains clear that more research is required to better understand this disabling brain disorder. One potential avenue of exploration, given the neurosensory nature of migraine relies on the use of EEG as a tool to study migraine, which will be discussed in the following section.

1.1. KEY MESSAGES

1. Migraine can be classified according to the presence or absence of aura (MA and MwoA) as well as the number of headache days/month (EM and CM).
2. Headache diaries are excellent clinical and research tools for recording information relevant to headache, as well as confirming presumed diagnoses and ensuring a headache-free window around the time of the experimental session.
3. Migraine is a cyclic disorder that can be separated into distinct phases: prodrome, aura, ictal, postdrome, and interictal. Studying the latter is particularly relevant to see whether alterations continue outside of the ictal phase, as well as to understand migraine and improve patient QoL.
4. The neurovascular theory of migraine pathophysiology is the most accepted and posits a relationship between neural and vascular elements, of which the neural mechanisms remain to be elucidated.
5. Migraine presents a high economic burden, and results in serious psychosocial and psychiatric difficulties.

1.2. Electroencephalography: The technique

As resumed in the previous section [1.1], migraine is a complex brain disorder of neurovascular origin, with reports of altered neural electrical activity, among other things. To better understand the differences in function during the interictal phase, **this PhD thesis will use EEG as the primary research tool** to elucidate potential impairments in patients with migraine as compared to headache-free controls.

1.2.1. Electroencephalography

The word electroencephalography, stems from the Greek 'electro' referring to electric, 'enkephalo' referring to the head, and 'graphia' referring to drawing or writing, and refers to the study of the temporal dynamics of human cortical activity.(114) Specifically, **electroencephalography is the study of electrical brain activity** and the **electroencephalogram** is the tool used to measure this activity. Nevertheless, to understand both the study and the tool, it is essential to begin by comprehending the origins of the neural signal that is quantified. Cells communicate using **action potentials**, or waves of electrical activity,(115) which result in voltage spikes. These spikes have an effect on the **resting membrane potential**, which has a relatively constant voltage (usually around -40 to -90 mV),(115) and trigger the release of neurotransmitters, which bind to membrane receptors of post-synaptic neurons.(114–116) This binding process causes ion channels to open and close, causing a **post-synaptic potential**, or a change in the electric potential across the resting cell membrane.(115,116) These changes in potential can arrive at the neuron from a large number of inputs and can either be depolarizing [i.e., **excitatory post-synaptic potentials (EPSPs)**] or hyperpolarizing [i.e., **inhibitory post-synaptic potentials (IPSPs)**].(114–116) Depending on the summation of these excitatory and inhibitory inputs, a subsequent action potential can occur (see Figure 6 for a schematic representation).(115) This action potential occurs in an **all-or-nothing** fashion, depending on the membrane potential of the axon hillock, which once a certain voltage or **threshold potential** is reached, fires.(115) These action potentials occur very quickly, usually lasting only about one ms, whereas post-synaptic potentials take place much slower, over a time range in the tens or hundreds of ms. For this reason, **EEG is thought to provide a measure of post-synaptic electrical activity**.(114)
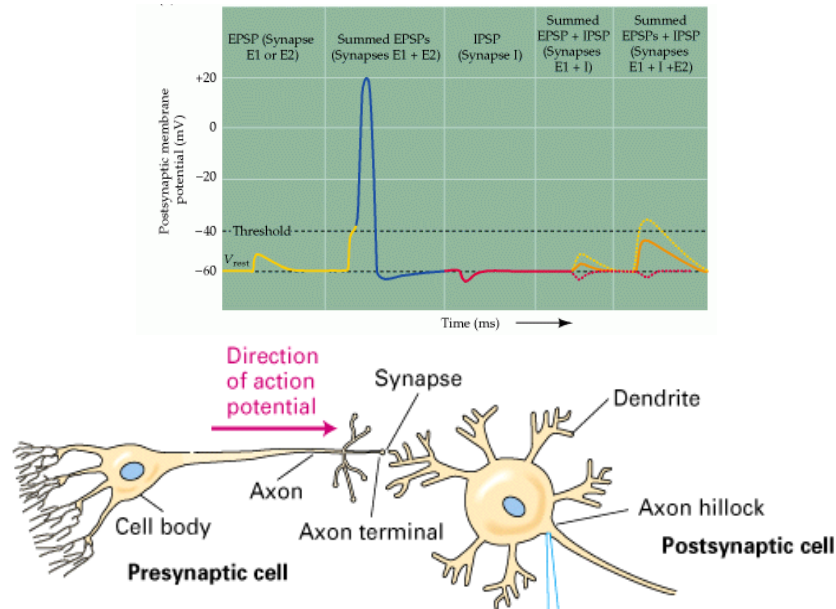
Figure 6. A schematic representation of the summation of post-synaptic potentials (top) and pre- and post-synaptic cell activity (bottom). In the top illustration, a variety of hypothetical synaptic activity scenarios are depicted. Synapses on the post-synaptic cell can be either excitatory (E) or inhibitory (I) in nature. When only one excitatory synapse (E1 or E2) on the post-synaptic cell is stimulated, a subthreshold excitatory post-synaptic potential (EPSP) occurs. When two synapses (E1 and E2) are stimulated, a subthreshold EPSP occurs, leading to the generation of a postsynaptic action potential. In turn, if an inhibitory synapse is stimulated (I1) then an inhibitory post-synaptic potential (IPSP) occurs. Next, if E1 and I1 are stimulated together, then the resulting EPSP occurs, but with a diminished amplitude. Finally, the sum of E1, E2, and I1 leads to an EPSP but of insufficient strength to result in a postsynaptic action potential. Please note, the membrane changes: with EPSPs being excitatory and IPSPs hyperpolarizing. In this graph, EPSPs are represented in yellow, post-synaptic action potentials in blue, IPSPs in red, and the sum of E and I synapses in orange. Top figure reproduced from (115) and bottom figure from (116).

Furthermore, given that the electroencephalogram is placed on the scalp, several other factors contribute to this signal being picked up at a distance. First, ions generate electrical fields and the summation of the electrical fields of a large number of ions can be measured at a distance.(114) Additionally, EPSPs and IPSPs, result in electric **dipoles** (a positive and negative charge pair separated by a distance).(114) When these dipoles occur across many neurons and are similarly oriented, their collective charge can sum to a big enough magnitude to be measured at the scalp.(114) For a review of dipole theory, see work by Niedermeyer.(117) Finally, the amplification of these signals is possible due to specific properties of neural tissue which permit **volume conduction**, allowing electrical fields to propagate through biological tissue to reach the skull.(114) Consequently, the EEG technique permits us to measure the combined post-synaptic activity of large aggregates of cortical neurons (for a visual representation of the biophysical properties of neurons as they relate to the EEG, see Figure 7).(118)
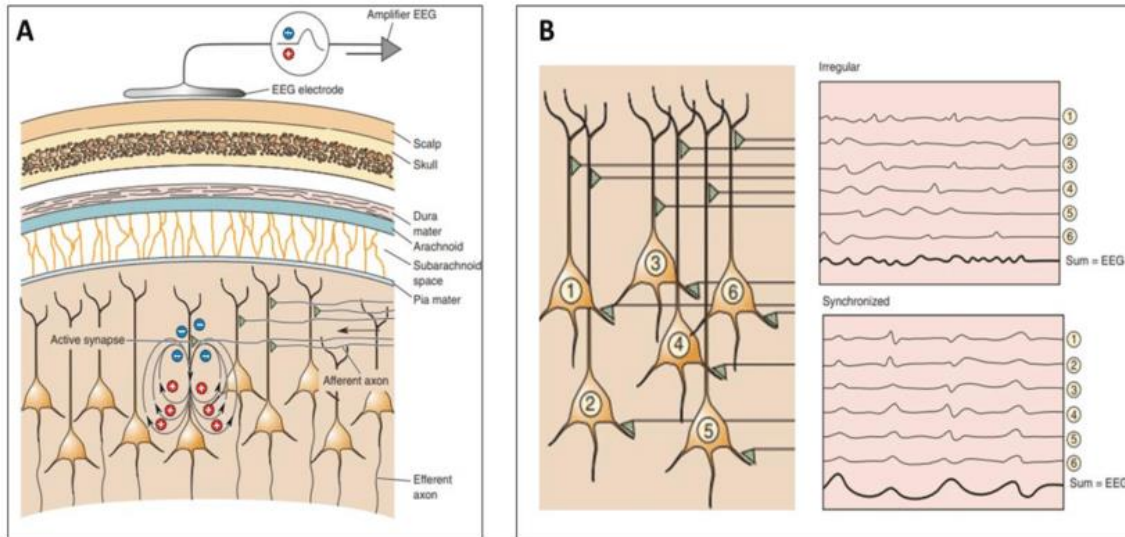
Figure 7. A visual representation of the biophysical properties of neurons as they relate to electroencephalography (EEG). A. Aggregate post-synaptic activity of large numbers of neurons result in electric dipoles, which as a result of the nature of neural tissue with regard to volume conduction, can lead to the signal arriving at the scalp to be picked up by an EEG electrode. B. The EEG signal is affected both by the intensity of the signal as well as the synchronization of neuronal activity. Figure reproduced from Bear et al.(119)

Subsequently, to capture this electrical activity using EEG, four steps are essential: [i] **transduction** or conversion of the neural electrical potentials to an electrical current, [ii] **transmission** from electrode to amplifier, [iii] **amplification** of the resulting activity, and [iv] **conversion** from analog to digital.(114) The EEG activity is recorded using an electrode cap placed on the head and transduction occurs due to the electrode gel, placed on the surface of the electrode, which permits the electrical signal to propagate further.(114) Next, the signal is transmitted to the amplifier, at which point sources of noise (e.g., mechanical, environmental, and physiological) can be introduced into the recording. This is why it is very important to isolate the experimental chamber both acoustically and electromagnetically and to remove unnecessary electrical equipment. Physiological artifacts, on the other hand, can occur due to eye movements, muscular contractions, cardiac activity, and more. To reduce these, participants are normally instructed to remain still, decrease blinking, and maintain their eyes in the center of the screen. Nonetheless, there are post-processing measures in place to deal with these artifacts through visual inspection and the removal of trials with noise. Finally, the signal is amplified, and converted from analog to digital input.

In terms of its efficacy and reliability as a measurement tool, EEG does have certain disadvantages. The principal one is that it does not provide spatial resolution, meaning that we cannot ascertain which cortical areas the signal is coming from. Furthermore, EEG measures provide the end result (a perceived voltage distribution), but it is impossible to know the locations and orientations of

the signal generators, due to the infinite number of possibilities arriving at the same result. This problem is frequently referred to as the '**inverse problem**'. Effects can also be very small, meaning that many trials (repetitions) are necessary to draw any conclusions, which can make experiments very long, leading to fatigue and a lack of motivation. Nonetheless, despite these disadvantages the technique is widely used due to some significant advantages. First, of all due to its high temporal resolution (< 1 ms), EEG measures allow researchers to examine which stages of information processing are affected by different experimental manipulations. Also, given its ability to measure neural activity online, overt responses are not necessarily required. EEG is also not invasive and inexpensive compared to neuroimaging such as fMRI or PET. Consequently, and taking into account both its advantages and disadvantages, EEG techniques should be applied to experiments seeking to identify which neurocognitive processes are affected by a given experimental manipulation rather than those requiring neuroanatomical specificity [for a review see (120)].

1.2.2. Event-related potentials

On its own, EEG provides very little information so to study sensory and attentional processes, specific tasks are designed to elicit neural processes of interest. Consequently, evoked potentials (EPs), also sometimes termed evoked responses (ERs), and most frequently referred to as **event-related potentials (ERPs)** are obtained. Simply put, **ERPs consist of a metric of neural response, quantified according to a deflection or [voltage] change in the neural electrical activity, to an event or stimulus**.(121) They can be stimulus or response-related and provide an important tool, the **event-related potential technique**, to study the neural activity underlying a variety of sensory and attentional processes, among others.(120) In fact, specific ERPs have been related to different stimulus properties and/or neural functions. ERPs are normally studied over a series of trials during the realization of an experimental task and while the ongoing brain activity is recorded using an electroencephalogram (see Figure 8 A).(120,122) Importantly, to effectively study ERPs a series of steps must be carried out. First, anyone that has ever seen a real-time EEG (-100 micro volts, or µV to +100 µV) knows that it is difficult to perceive ERPs within the recording (see Figure 8 B and 9, for an illustration of the raw signal post-amplification). This is in part due to the small nature of ERP deflections, which are in the -10 or µV to +10 µV range, thus requiring additional signal processing to extract the ERP, or 'signal', from the EEG activity, or 'noise'. Therefore, post-EEG recording segments, termed epochs, are extracted and the neural activity is lined up to a temporal moment of interest, through a process referred to as **time-locking**.(120) For example, activity can be lined up to stimulus onset (**stimulus-locked**; for an example see Figure 9) or to the response (**response-locked**), which is considered the 0 ms point within the resulting time-locked waveform.

28

Time-locking is carried out for each segment, resulting in a number of single-trial, individual waveforms (see Figure 8 C, left).(120) Once these single-trial waveforms have been obtained, a signal-averaging procedure is carried out to obtain an **averaged waveform** for each electrode and participant (see Figure 8 C, right).(120) Finally, averaged waveforms from each participant tend to be averaged across subjects to obtain a **grand average ERP waveform**. This is done to minimize individual variability given the high between-subject variability that is common to ERP experiments.(120) The use of grand average waveforms also makes it easier to compare results between experiments while essentially canceling out the background EEG activity, leaving the ERP behind.(120)
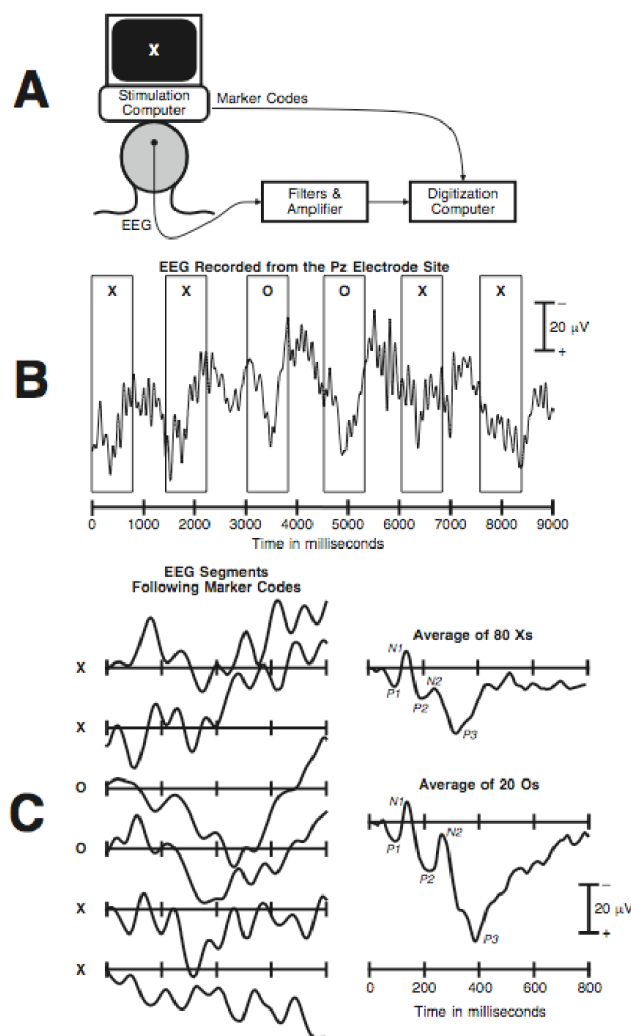
Figure 8. An example of an event-related potential (ERP) experiment. A. The experimental set-up is shown. The participant watches stimuli (frequent Xs and infrequent Os) appear on a computer screen, while their neural responses are recorded using an electroencephalogram. B. The raw signal is observed following filtering and amplification. C. The single-trial data is shown. As can be seen there is a large inter-trial variability, but a P3 (ERP component) can be observed after the presentation of an O stimulus. D. The averaged ERPs can be seen for both the X and O stimuli, separately. Reproduced from Luck.(120)
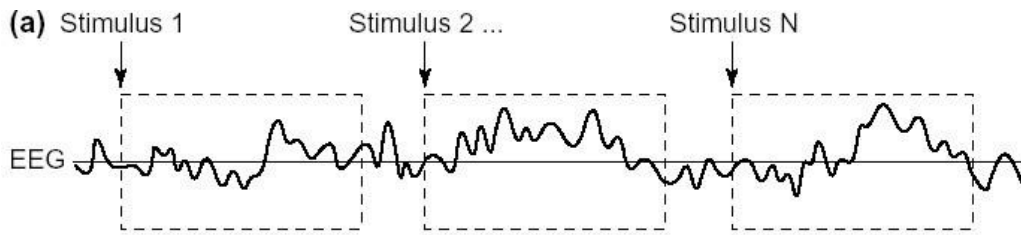
Figure 9. A schematic representation of stimuli (1 to N) being presented during an ongoing EEG recording. As can be seen the activity is too small to be noted and requires further processing. Reproduced from Luck et al.(123)

The averaged waveform is normally made up of a sequence of consecutive peaks and troughs indicating positive and negative voltage deflections. These deflections are commonly referred to as peaks, waves, or components (120) and are normally named according to their voltage (P for positive, N for negative) and ordinal position (1,2,3) although nomenclature can vary.(120) Components are most frequently described according to their amplitude and latency (see Figure 10).(120) In terms of amplitude, peak or mean measures can be used and consist of defining a time window for each component and then finding the maximum voltage in that time window (peak measure) or averaging the voltage over this same time window (mean measure). With regard to latency, or the time to peak appearance in the waveform, the researcher must locate the peak amplitude and associate it with its temporal occurrence. Components also tend to be associated to specific scalp distributions, which are thought to reflect where they were generated although the spatial resolution of the EEG technique is, as previously mentioned, poor.(120)
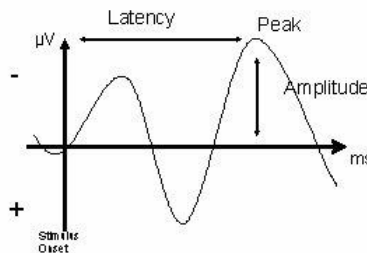
Figure 10. A schematic representation of the characteristics of an ERP component. Figure reproduced from Rinker.(124)

ERP components may differ as a function of sensory modality. Early-latency components, likely generated by primary sensory cortices, are thought to be predominantly modality-specific.(125) In contrast, later-latency ERPs, whose origin is thought to be related to multiple cortical areas, may reflect an aggregate of unimodal and multimodal components.(126–128) Given the interest of this research thesis in vision and audition, the most typical sensory-attentional components associated with each modality will be discussed in Table 1 (visual) and Table 2 (auditory).

30

Table 1. Cascade of typical visual event-related potential (ERP) components related to sensory-attentional processing.

Type of stimuli	Component	Polarity	Peak (ms)	Site	Cognitive related processes
Visual	C1 or N1	-/+	80-100	Occipito-parietal	Reflects V1 processing,(129) sensitive to stimulus characteristics including contrast, spatial frequency, and stimulus location(120,130)
	P1	+	100-130	Lateral-occipital	Sensitive to stimulus characteristics including contrast, luminance, and brightness (120,131,132) Also linked to the direction of spatial attention, arousal, and affective processing(133–136)
	N2	-	100-150 150-200	Parietal Lateral-occipital	Sensitive to stimulus characteristics such as contrast (132) as well as spatial attention (early N1) and discriminative processing/stimulus salience (late N1) (133,134,137–142)
	N170	-	150-200	Lateral occipito-temporal	Sensitive to faces (face specificity) (143,144)
	P2	+	150-275	Anterior-central	Sensitive to simple target features and infrequent targets,(145) early attentional allocation and conscious awareness (146)
	N2b	-	200-350	Posterior	Early sensory detection of unexpected change to task-relevant stimuli (147)
	N2pc	-	200-350	Posterior-contralateral	Sensitive to classification tasks and focusing of spatial attention on target (147)
	CNV	-	260-470	Fronto-central	Related to attention and arousal (148)

In response to a visual stimulus, a cascade of event-related potentials (ERPs) occurs, which include, in order of appearance the C1, P1, N1, P2, N170 (stimulus-related components). Some of these ERPs only appear under certain circumstances (response-related) such as the N2b, N2pc, and the contingent negative variation (CNV). Based on: (147,146,145,144,143,142,141,140,139,129,120,130–138)

Table 2 Cascade of typical, auditory event-related potential (ERP) components related to sensory-attentional processing.

Type of stimuli	Component	Polarity	Peak (ms)	Site	Cognitive related processes
	Brainstem evoked responses	-/+	10	Frontal	Used to assess auditory pathology (149)
	Mid-latency components	-/+	10-50	Central	Used to assess auditory pathology Sensitive to stimulus characteristics of intensity, temporal frequency (150–152)
	P1	+	50-100	Fronto-central	Sensitive to stimulus features and temporal frequency (153,154) Related to attention, inhibition of unattended information, arousal (155,156)
	N1	-	75-150	Fronto-central and central	Sensitive to stimulus features such as pitch and temporal frequency (157) Also reflects attention, change/stimulus detection, feature extraction, and early discrimination (158,159)
Auditory	P2	+	175-200	Central	Sensitive to stimulus characteristics, specific sounds as well as stimulus classification and encoding May also serve for alerting (160)
	Mismatch negativity (MMN) or N2a	-	175-225	Fronto-central	Early sensory detection of unexpected change elicited by infrequent stimuli, sensitive to attention (161) and pitch (162)
	N2b	-	200-350	Central	Early sensory detection of unexpected change to task-relevant stimuli(163)
	Early P3a	+	225-275	Central	Post-sensory detection of unexpected (task-irrelevant) events (164,165)
	Late P3a	+	275-325	Frontal and parietal	Involuntary attentional processing of unexpected (infrequent, task-irrelevant) events (161,164–167)
	P3b	+	300-600	Centro-parietal	Contextual memory comparisons, necessary to the behavioural response, index of voluntary attention (165,168,169)
	Re-orienting negativity (RON)	-	350-600	Fronto-central	Disengagement from stimuli and re-orientation back to the main task (164)

In response to an auditory stimulus, a cascade of event-related potentials (ERPs) occurs, which include, in order of appearance the brainstem evoked responses, middle latency components, P1, N1, and P2. Some of these ERPs only appear under certain circumstances such as the mismatch negativity (MMN), N2b, early P3a, late P3a, P3b, and re-orienting negativity (RON). Based on: (120,149–161,163–170,170)

1.2.3. Time-frequency analysis

Traditional ERP analyses, also termed the 'additive ERP model', often assume that the underlying or ongoing background activity is 'noise', from which the ERP must be extracted, and whose oscillatory properties are not related to the neural processing reflected by the ERP. However, this belief has been challenged due to evidence indicating that event-related changes occur in the oscillatory metrics of the underlying EEG activity at specific frequencies, which shape event processing.(171,172) Therefore, the EEG recording also contains rhythmic information, reflecting neuronal oscillatory activity, which is thought to determine baseline neural excitability.(173–175) This rhythmic activity is comprised of multiple frequencies [measured in Hertz (Hz)] and a number of typical frequency bands have been found to occur in the adult brain, including delta, theta, alpha, beta, and gamma, linked to different cognitive processes (see Table 3 and Figure 11).

Table 3. Typical frequency bands in the adult brain along with the cognitive processes, which they reflect.

Frequency Band	Spectral Boundary (Hz)	Cognitive related processes
Delta	1-4	Reflects motivational processes and emotional processing, role in deep sleep, behavioral inhibition, and memory formation (176–179)
Theta	4-7	Related to memory and emotional processing, role in information encoding, spatial navigation, salience detection (176,180–182)
Alpha	7-14	Linked to idling, role in inhibition of irrelevant task information,(183) perceptual awareness,(184–189) and attentional control (190)
Beta	14-30	Associated with voluntary and mental movements, emotional processing,(191) language processing,(192) perception (187,193,194)
Gamma	30-100	Reflects object representation and feature binding as well as integration of information and cognitive processes (195)

Based on: (176–187,187,187,189–194,196)
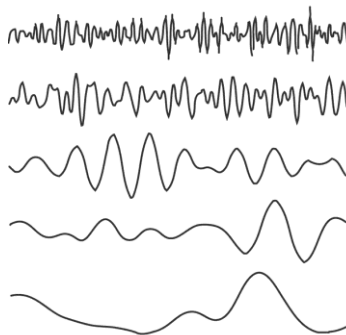
Figure 11. The typical frequency bands in human cortex from delta, theta, alpha, beta, gamma (in order from bottom to top). Reproduced from Kent.(197)

33

Importantly, oscillatory activity can be defined according to three properties: frequency, power, and phase (see Figure 12). **Frequency** (Hz) refers to the number of cycles or oscillations per second (cycles/s). **Power** (μV^2) can be defined as the amount of energy in the oscillatory activity at a given frequency or frequency range.(172) It is also thought to reflect changes in neuronal synchrony.(198,199) Finally, **phase** can be considered as the point on the sine wave with respect to time and can range from −180° to 180° (degrees) or −π to π (radians).(172) EEG activity or ERPs are typically decomposed into **time-resolved spectral power** and phase-consistency, or **inter-trial phase coherence** (ITC). The ITC is obtained by normalizing the amplitude and averaging these numbers across trials and frequencies and is considered to be a measure of neural synchronization, ranging between 0 (zero phase alignment) and 1 (perfect phase alignment).(189)
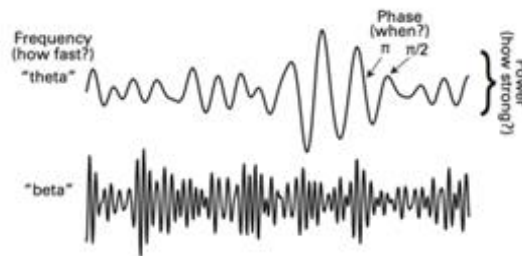
Figure 12. A visual representation of the three typical properties of oscillatory activity. Adapted from Cohen.(200)

The EEG signal can also be observed in a variety of ways. When looking at data in the **frequency domain** (see Figure 13 A), the resulting plot will indicate the power or phase at each frequency.(120) In contrast, the **time domain** (see Figure 13 B), permits the observation of the power or phase at each point in time.(120) The ability to move between one form of visualizing the data and the other is achieved using the Fourier analysis. Furthermore, **time-frequency analyses**, combining information from both the time and frequency domain (see Figure 13 D) allow us to visualize the power or phase at each frequency and time point, permitting the study of what has frequently been referred to as 'event-related brain dynamics'.(171) Finally, when analyzing single-trial EEG data, the EEG activity is multiplied by a transformation function, such as a Morlet wavelet, centered on a segment of the EEG data, an operation referred to as **convolution**.(172) When this transformation function is moved over the EEG activity over time, a complex number can be obtained for each time point, trial, and also over trials allowing the extraction of both power and phase information. Subsequent operations can be carried out on both metrics, such as obtaining the mean power for a frequency at any point in time by squaring and averaging the magnitude [for more details see (172)]. Different approaches to time-frequency decomposition through the application of transformation

functions with different properties exist since there is a balance between temporal and frequency resolution (larger time windows result in greater frequency resolution but poorer temporal resolution).
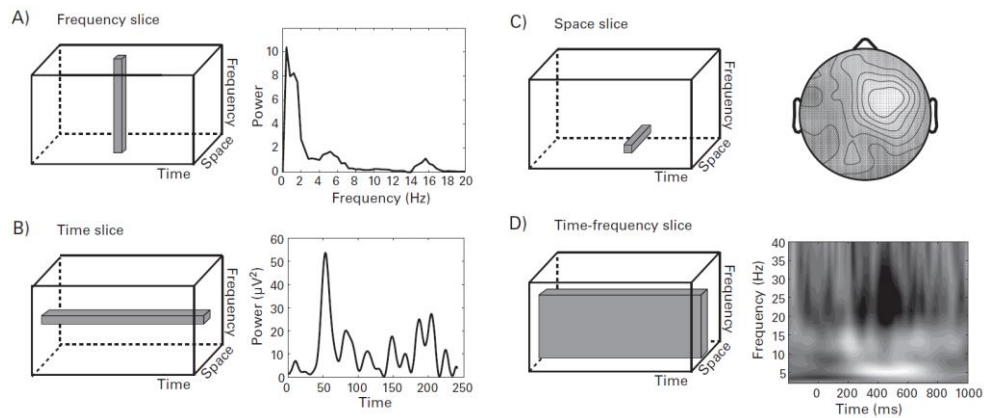
Figure 13. A schematic representation of the different ways to visualize EEG data in the 3-D conceptualization of time, space, and frequency. A. In the frequency domain. B. In the time domain. C. In the space domain. D. In the time-frequency domain. Reproduced from Cohen.(200)

Importantly, the use of time-frequency analyses provides an important complement to EEG research. First of all, results can be interpreted taking into account oscillatory properties, which offer important insights into the functional significance of neural oscillations.(201) Additionally, time-frequency analyses provide more information, if we consider the 3D time-frequency-space conceptualization (Figure 13) than ERPs, and therefore may reflect a more accurate measure of cognitive processes.(200) Finally, in many clinical disciplines, including migraine, the use of time-frequency measures is still rather minor despite the potential of these analyses to identify pathophysiological differences.(172)

1.2.4. Exogenous and endogenous components and oscillations

ERPs and oscillatory activity can also be categorized based on a spectrum of exogenous, mesogeneous, and endogenous components/activity.(202,203) In terms of ERPs, components that occur earlier in the waveform (≤100 ms), tend to be more **exogenous**, meaning that their properties (amplitude, latency, and distribution) appear to be modulated by physical characteristics of sensory stimuli, such as luminance (131) and contrast.(132) These components are frequently referred to as 'sensory components'. Early components also tend to occur at specific cortical sites, with visual potentials occurring at occipital areas and auditory ones at either central or frontal areas. Exogenous components are also largely involuntary, should be present in all individuals, and are often considered to be a sign of healthy brain function.(149,151) **Endogenous** components, on the other hand, also

sometimes called 'cognitive components' usually occur later in the waveform (>100 ms) and their properties tend to be modulated by attention, task or goal-oriented factors, or relevance thus depending on the subject's interaction with the event or stimulus.(202,204,205) Given that these components are frequently task-dependent, they may be absent from the waveform. Endogenous components tend to be present more diffusely, across many cortical sites. Nonetheless, it is often difficult to classify components as belonging to one category, largely due to the continuous nature of the waveform which results in many components overlapping with each other or resulting from the sum of underlying components.(120,206) Components that do not fit neatly into either category, are frequently termed **mesogenous**, and are sensitive to both stimulus characteristics and the interaction with the stimulus/event.(203)

In terms of neural oscillations, a similar classification system can be established. **Exogenous oscillations** occur in response to [are driven by] rhythmic external stimulation and are usually related to sensory systems. Two examples include steady-state visual evoked potentials (SSVEPs) and auditory steady state responses.(207,208) **Endogenous oscillations,** on the other hand, result due to internal processes and once again depend on the task, goal, and interaction between the subject and the event.(209) Normally, we think of the typical frequency bands of the adult brain (see Figure 11) as being endogenous.(209) Endogenous oscillations can also be present in the absence of stimulus input.(210) Nonetheless, one would expect a combination of exogenous and endogenous oscillations in response to repetitive stimuli.(210)

<div style="border:2px solid">

1.2. KEY MESSAGES

1. EEG measures are good at identifying which neurocognitive processes may be affected by specific experimental manipulations.
2. ERPs provide insight into the temporal course of neural information processing.
3. Time-frequency measures allow us to consider the underlying neural oscillatory activity. They also appear to provide a more accurate measure of cognitive processes and in migraine, their use is still very minor, despite their potential in identifying pathological differences.
4. ERPs can be defined according to the exogenous-endogenous spectrum. Exogenous components tend to be sensitive to physical properties of the stimulus or event, whereas endogenous components tend to reflect the interaction between the subject and stimulus/event.
5. Oscillatory activity can be categorized in the same way with exogenous oscillatory activity occurring in response to rhythmic stimulation (SSVEPs for example) and endogenous activity resulting due to internal processes (related to the typical frequency bands like alpha and beta).

</div>

1.3. Sensation and perception

"We must remember that we do not observe nature as it actually exists, but nature exposed to our methods of perception. [...] Reality is an illusion, albeit a persistent one." – Albert Einstein

1.3.1. Definition

As Albert Einstein once said, reality is an illusion. Despite our senses being exposed to the outside world, we build our worldview based on what our neural systems choose to perceive. Simply put, our "perceptions are built from sensations, [but] not all sensations result in perception".(211) To effectively interact with the world, the human body is equipped with specialized sensory receptors including those related to the typical senses, such as vision, hearing, smell, taste, and touch but also balance, movement, pain, and temperature. Importantly, **sensation** occurs when **sensory receptors detect a stimulus** and the process of transforming energy related to the stimulus into neural signals is called **transduction.**(212) Sensation can be considered an automatic, stimulus-driven process, by which our senses receive information from external stimuli.(212) Sensation normally travels from specialized receptors, through the peripheral nervous system (PNS) to the CNS. **Perception**, on the other hand, relates to **how our brains organize, interpret, and put into context sensory information** and relies on a series of internal processes.(213)

The study of sensation and perception most likely dates all the way back to 600 B.C. and the musings of Greek philosophers such as Heraclitos and Protagros. Nonetheless, Fechner, the father of psychophysics was one of the first to attempt to quantify these concepts. The branch of science known as **psychophysics** is frequently used in research on sensation and perception due to its interest in understanding the relationship between stimulus and percept/behaviour.(214) Some of the most well-known measures include the **absolute** or **detection threshold**, or the minimum stimulation that is required to be detected 50% of the time, as well as the **difference** or **discrimination threshold**, related to the **just noticeable difference (JND)**, indicating the minimum amount of change necessary to detect that two stimuli are not identical.(212) Discomfort levels, such as the loudness discomfort level (LDL), also frequently referred to as **sensory aversion thresholds** (SATs), provide a third metric to measure sensory processing, particularly in clinical populations that are thought to exhibit an exaggerated response to sensory stimuli.(56,215,216) Other commonly used tools in the study of sensation and perception, and particularly in clinical research due to their accessibility, ease of application, and short administration time, are self-report questionnaires and validated neuropsychological tests. Unlike psychophysical thresholds, which usually assess a single

characteristic of a specific sensory modality, self-report questionnaires and neuropsychological tests can allow the researchers to capture information related to many stimuli and their relative properties.

When studying these concepts, it is important to be aware of a couple important points. First, individual differences can occur at a mechanistic level (e.g., damage to receptors or pathways) or at a neurocognitive level (e.g., due to impaired perceptual or attentional mechanisms). Second, aside from the potential for individual differences at the receptors, pathways or neural levels, a variety of factors besides stimulus characteristics, such as internal states, expectations, and motivation, can also influence perception.(217–219) Therefore, when studying sensation and perception it is of interest to determine whether differences stem from alterations at the level of processes/mechanisms or as a result of the factors that modulate them.

1.3.2. Pathways, models, and neurophysiological correlates

This **PhD thesis chose to focus on vision and audition**, given that these are the sensory modalities that are primarily affected in patients with migraine (see 1.5. for more information).

1.3.2.1. Vision

The visual sensory experience begins at the level of the eye. **Light** enters the eye through the pupil with the cornea and lens focusing and projecting it onto the **retina** where transduction takes place.(220) The retina is comprised of sensitive **photoreceptors**, called **rods** and **cones**.(221) Cones are located in the center of the retina (fovea) and help us to see colour and fine detail whereas rods detect grey scale and are primarily used in peripheral vision.(222,223) The retina also contains three layers of cell bodies and two layers of synapses.(223) The top layer is made up of rods and cones whereas the medial retinal layer consists of bipolar, horizontal, and amacrine cells. The bipolar cells activate **retinal ganglion cells (RGCs)**, whose axons form the **optic nerve**. The optic nerve axons from each eye meet at the **optic chiasm** below the hypothalamus, at which point some of the axons cross over to the other side of the brain (contralateral) while others continue on the same side (ipsilateral). These axons now make up the **optic tracts**, of which many project on to the **lateral geniculate nucleus** (LGN). As a side note, it is important to mention that there are different types of RGCs, which are engaged in different retinal circuits specific to a variety of tasks.(224–226) Some of these RGCs project to the lateral geniculate nucleus (LGN) and the thalamus, whereas others project to the superior colliculus (SC), involved in rapid eye movements, and other areas such as the olivary pretectal nucleus (OPN), the supraoptic nucleus (SN), the suprachiasmatic nucleus (SCN), the pulvinar complex (PC), the dorsal raphe nucleus (DRN), and the paraventricular nucleus (PN) [for a review see (226)]. In terms of those that reach the LGN, inputs from the left visual field arrive at the

right LGN, whereas right visual field inputs arrive at the left LGN [for a review see (227)]. Additionally, visual topography is maintained given that neighboring RGCs send inputs to neighboring LGN cells.(228–230) Next, second-order relay neurons also referred to as **thalamocortical neurons**, project the information on to the **primary visual cortex**, which is divided into five areas (V1 to V5), with each one playing a specific role in visual processing. The cells within these areas are feature-specific and project to associative cortical regions and frontal cortex (for a schematic representation of the visual pathway from the eye to the brain, see Figure 14). Importantly, deficits in any of the components of the visual pathway can result in severe visual impairment [for a review see (227)]. Abnormalities along the visual pathways are frequently detected using visual evoked potentials (VEPs), which have been shown to have better functional integrity than neuroimaging techniques.(231)
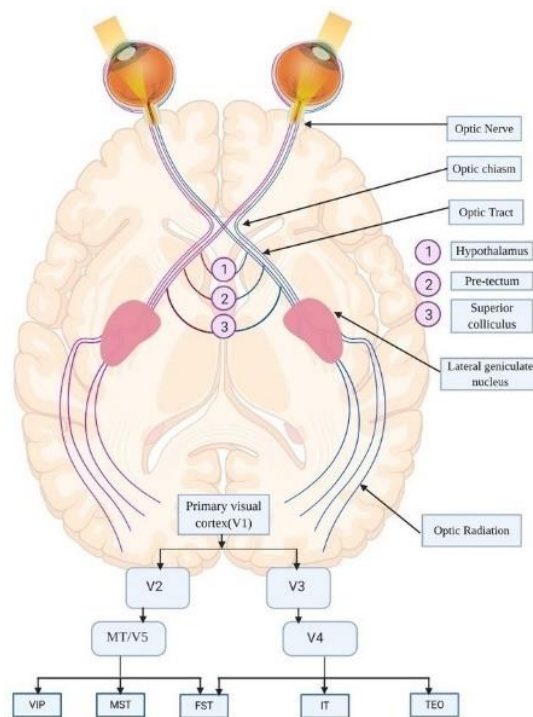
Figure 14. A representation of the visual pathway from the eye to the visual cortex. Light enters the eye and goes through transduction at the retina. This signal then travels through the retinal ganglion cells (RGCs) of the optic nerve, through the optic tract, and to the thalamus where it is sent to the visual cortex and other primary and association areas for further processing. Figure reproduced from Ahirwal.(232)

Aside from detecting impairments in visual pathways, EEG measures also provide insight into the stages of sensory-perceptual processing. Initial activity can be detected in early-latency ERP components that tend to be exogenous in nature. In the visual modality, in order of appearance, N1 has been found to reflect changes in contrast and spatial frequency (120,130) and is suggested to be

the first stimulus-related response in both striate and extrastriate areas.(233–235) Next, P1 has been shown to be modulated by stimulus properties including contrast, luminance, and brightness (120,131,132) whereas visual N2, has been found to be sensitive to contrast, among other properties.(132)

In terms of underlying, neural oscillatory activity, alpha activity has been shown to play a central role in sensation and perception. In fact, out of all the frequency bands, the strongest response to periodic visual stimulation has been found to occur in the alpha band.(236,237) Furthermore, the ability to detect a target is modulated by alpha power, with stronger pre-stimulus alpha power reflecting a lower likelihood of stimulus detection.(184–189) This pattern of activity would indicate that when alpha power is high, the brain's capacity to detect low-intensity stimuli is low, meaning that stimuli near the detection threshold may be missed, with low alpha power yielding opposite results.(189,238) Furthermore, alpha phase immediately prior to stimulus onset has been found to exert an even stronger influence on performance.(189) This may be related to the fact that neural oscillatory activity fluctuates between states of high and low excitability (173–175), which depending on the phase of the oscillation at the time of stimulus onset, may benefit performance (see Figure 15 for a visual representation).(189) For example, in one study by Busch and colleagues, visual stimuli that were presented at near threshold were more likely to be detected if the stimulus aligned with the phasic peak in excitability, highlighting the role of alpha oscillatory activity in sensory-perceptual processes.(189)
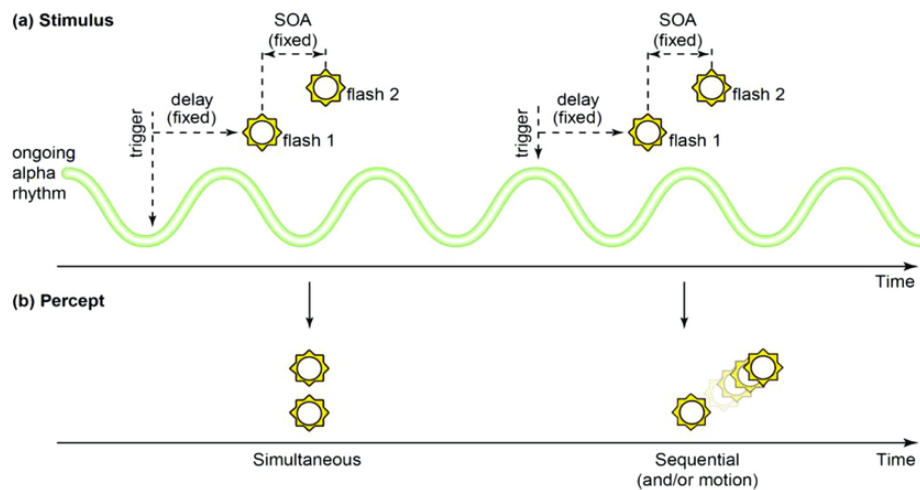
Figure 15. An example of the effect of alpha phase on stimulus detection. In this case, two flashes presented temporally close together can be perceived as occurring simultaneously if they align with the phase trough (low excitability) or as sequential flashes if they occur in line with the phase peak (high excitability). Reproduced from Sanchez.(239)

40

1.3.2.2. Audition

Audition, on the other hand, occurs because of **sound waves**, which travel through the air due to a series of vibrations.(212) These sound waves arrive at the outer ear and are channelled inside along the auditory canal until they make contact with the **tympanic membrane**. The vibrations of the tympanic migraine set three small bones called the **ossicles** in motion, which channel the vibrations into the inner ear or **cochlea**. This part of the ear is filled with fluid and contains sensitive hair cells, called **stereocilia**, which pick up on the sound vibrations and perform transduction.(212,240) Different stereocilia are sensitive to different ranges of sound and encode information related to intensity, frequency, and timing [for a review see (241)]. Stereocilia project the auditory information to **spiral ganglion neurons (SGN)**, which relay the information to the **cochlear nuclei (CN)** along the vestibucochlear nerve.(212) It is important to note, that the auditory ascending pathways are more complex than those of other sensory systems and more in-depth description is outside the scope of this research thesis [for a review see (242)]. In short, the primary auditory pathways, use **second-order relay neurons** to pass the signal to the **superior olivary complex (SOC)** after which processing continues to the **inferior colliculus (IC)**, which projects information to the **medial geniculate nucleus (MGN)** of the thalamus and finally to the auditory cortex (for a visual representation of the pathway from the ear to the brain, see Figure 16).(212,240) Similarly, to vision, impairments along this pathway can result in severe auditory impairments,(243) which can be identified using auditory evoked potentials (AEPs).(244)

In the auditory domain, brainstem evoked responses have been used to evaluate hearing loss in infants (149,245), whereas mid-latency components are modulated by stimulus intensity and temporal frequency.(246) The following components of P1, N1, and P2 have also been found to be sensitive to a variety of stimulus characteristics including temporal frequency (153,154,158,159) and pitch, among others.(157) Furthermore, similarly to vision, the power and phase of ongoing oscillatory activity can also have an impact on auditory sensation and perception. For example, theta phase has been related to auditory detection (247,248) in a similar manner as alpha in the visual modality.
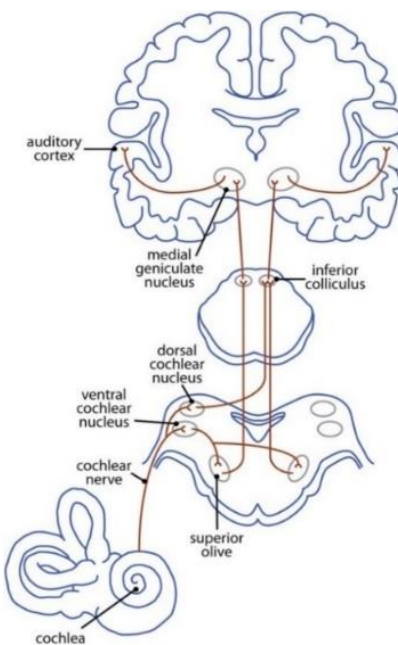
Figure 16. Schematic representation of the auditory pathway from the ear to the auditory cortex. Sound enters the ear and reaches the cochlea, where it is transduced and transmitted to the cochlear nerve, superior olivary complex (SOC), inferior colliculus (IC), medial geniculate nucleus (MGN), and finally the auditory cortex and other primary and association areas for further processing. Reproduced from Butler and Lomber.(249)

1.3.3. Sensory sensitivity

One of the concepts that will be studied in this research thesis is that of sensory sensitivity, which can be operationally defined as an abnormal response to sensory stimuli, potentially leading to changes in behavior.(250) Importantly, in light of this definition, Schultz and Stevenson (251) recently discussed the importance of clearly distinguishing between two different constructs that are often confounded: **sensory sensitivity** and **sensory reactivity** or **responsivity**. Sensory sensitivity is defined as **the capacity to detect and perceive a sensory stimulus**.(251) In other words, individuals that are high in sensory sensitivity may find it easier to detect weaker stimuli and may perceive sensory inputs as stronger (e.g., louder) than those that report lower sensory sensitivity. This construct can be measured using psychophysical thresholds as well as self-report questionnaires and neuropsychological tests, such as the Sensory Perception Quotient (SPQ),(252) which separates between sensory sensitivity and reactivity. Sensory reactivity, on the other hand, **refers to the visible, behavioral responses to sensory inputs**, and is frequently measured using self-report and third party questionnaires.(251) Nonetheless, despite their apparent connection, it is important to emphasize that while altered sensory sensitivity may lead to changes in reactivity, heightened sensory reactivity may also occur in the absence of sensory sensitivity, meaning that the perception of the stimulus may be

42

unchanged but the behavioral response is abnormal.(251) Importantly, **in this research thesis, the focus will be placed on assessing sensory sensitivity**.

One way to conceptualize sensory sensitivity is according to a spectrum. For example, individuals that are on the extreme ends may exhibit **hyposensitivity** (lower than normal sensory sensitivity) or **hypersensitivity** (higher than normal sensory sensitivity). In fact, individuals that score very high or very low on this spectrum, may exhibit sensory processing difficulties, with an impact on QoL (253). Hypo- and/or hypersensitivity are commonly reported in neurological and psychiatric conditions, including but not limited to anxiety,(254,255) attention-deficit/hyperactivity disorder,(256) depression,(255,257) autism,(258–262) and migraine.(55,263) Importantly, extreme hypersensitivity can lead to a subjective experience of aversion and even pain [i.e., **photophobia, phonophobia, osmophobia** (aversion to smell), and **allodynia** (aversion to light touch)].(25) Some researchers have conceptualized heightened sensory processing (or hypersensitivity) as a genetic trait, according to the sensory processing sensitivity (SPS) theory.(255) In fact, this trait has been proposed to serve an evolutionary function, allowing the organism to detect and respond to more subtle changes, although at a cost of time and energy.(253,264–266) Aron et al., proposed that SPS may arise from a sensitive CNS, and is comprised of: [i] behavioral inhibition in order to attend to novel or conflicting stimuli, [ii] increased awareness of stimulus characteristics and subtleties, [iii] deeper information processing, using past experience and memory traces, and [iv] heightened emotional response.(253) Importantly, the presence of one of these points without the rest could be indicative of altered information processing with no evolutionary advantage, or pathology.(253)

Nonetheless, the neural mechanisms and pathways underlying sensory sensitivity are complex and it remains unclear how these are shared among different conditions. Currently, several candidate pathways have been identified to explain visual hypersensitivity or photophobia. Importantly, a specific subgroup of RGCs with a specialized photoreceptive capacity have been found to play an important role in all three potential pathways.(267,268) These RGCs contain melanopsin, a protein responsible for photoreception,(269) and are referred to as melanopsin-containing intrinsically photosensitive retinal ganglion cells (ipRGCs).(268) ipRGCs have been found to mediate the pupillary light reflex (constriction to light),(270–272) as well as align with the circadian changes of light, termed circadian photo-entrainment, among other things.(267)

The first candidate pathway relies on the activation of these ipRGCs by light, which pass the transduced signal along to the OPN and the superior salivatory nucleus (SSN). The SSN then acts on ocular blood vessels resulting in vasodilation,(273) which triggers the trigeminothalamic pathway related to pain processing. The ensuing nociceptive signal is then sent to the trigeminal nucleus caudalis (TNC), posterior thalamus, and higher cortical areas. In the second candidate pathway, photic

stimulation modulates the activity of trigeminovascular thalamic neurons, which relay information between the retina and distinct cortical areas.(274) Specifically, [i] light undergoes transduction at the retina through ipRGCs, which send the resulting signal, via the optic nerve, to posterior thalamic neurons. [ii] Some of these thalamic neurons also receive nociceptive (pain) inputs, which arrive from the dura mater via the trigeminothalamic tract. [iii] Convergence of both signals occurs here, and the axons of these light- and dura-sensitive neurons then project to various other cortical areas, in particular S1 and S2, related to nociception and the visual cortex, associated with visual processing. Finally, the third pathway relies on the fact that ipRGCs, although predominantly located in the retina,(275) have also been found in the iris.(276) In this circuit, light is transduced at the level of the iris and the signal is directly projected to trigeminal nerve afferents.(276–278), related to nociceptive processing. For a schematic representation of all three pathways, see Figure 17.

In terms of auditory hypersensitivity or phonophobia, a similar neuroanatomical substrate, to the second candidate pathway of photophobia, has been proposed. Specifically, at the level of the thalamus, convergence of both auditory inputs from sound receptors (sound-sensitive) and nociceptive inputs from the dura mater (dura-sensitive) occurs in thalamic neurons, located in the posterior and lateral nuclei. The axons of these neurons then project to distinct cortical areas including the primary auditory and association cortices as well as S1 and S2.(25,279)
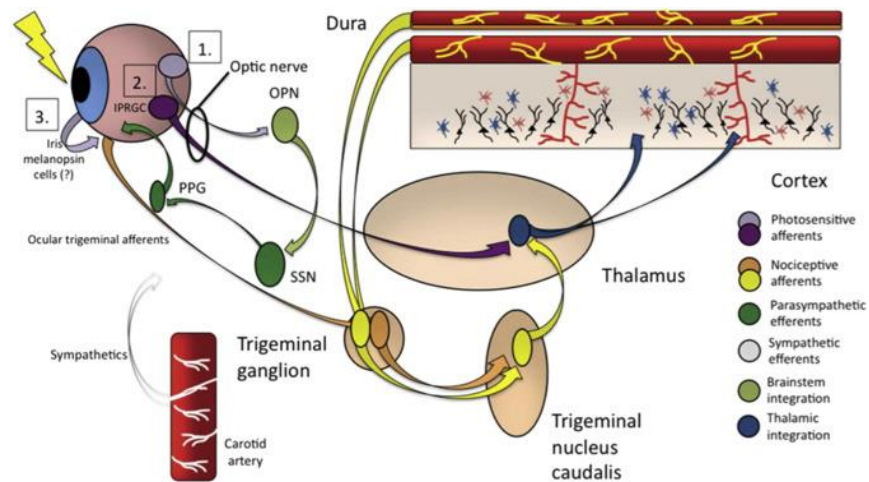
Figure 17. Candidate pathways related to visual hypersensitivity/photophobia. Pathway [i] connects the intrinsically sensitive retinal ganglion cells (ipRGCs) to the olivary pretectal nucleus (OPN), and then to the superior salivatory nucleus (SSN). The SSN alongside the pterygopalatine ganglion induces ocular vasodilation, which leads to the activation of pain-related ocular trigeminal afferents. These afferents project to the trigeminal nucleus caudalis (TNC), thalamus, and cortex. Pathway [ii] links ipRGCs directly to the thalamic neurons, which also receive nociceptive inputs from the trigeminal ganglion (TG) and the TNC. Neurons in the thalamus are therefore sensitive to both pain and light, and this information is then projected to the sensory and association cortices. Finally, pathway [iii] relies on ipRGCs in the iris, which activate the TG and TNC directly, without passing through the optic nerve. Figure reproduced from Digre and Brennan (275) and based on the results of a number of studies.(273,276,280,281)

1.3.4. Cortical excitability

Although the mechanisms leading to visual and auditory hypersensitivities and altered sensory perceptions remain elusive, there is some evidence to indicate that altered cortical excitability may play a role. **Cortical excitability** can be operationally defined as **the strength and/or likelihood of a neural response to external stimulation** and is a reflection of **neuronal reactivity**, or the probability of an action potential being elicited in response to a stimulus, and **specificity**, or the specialized response properties of different neurons to specific stimulus properties.(282,283) The link between hypersensitivity and cortical excitability requires further research, however some evidence suggesting a mechanistic relationship has been proposed. For example, at a purely theoretical level, SPS theory claims that those with this genetic trait display a 'hypersensitive brain', related to increased responses in the default mode and salience networks linked to the processing of sensory stimuli.(284) In line with this theory, animal studies using 5-HTT knockout, showed that faster sensory processing was related to a decreased inhibition of excitatory principal neurons, which have been found to modulate both cortical excitability and sensory gating, or a reduced response to irrelevant or repetitive stimuli.(285,286) Furthermore, transcranial magnetic stimulation, applied to the occipital cortex to reduce cortical excitability, was also found to decrease photophobia.(287) One of the ways to study cortical excitability is through the use of EEG. In particular, the amplitude of early-latency ERP components and their peak-to-peak amplitude differences, especially prior to or during the initial presentation of sensory stimuli have been found to be good neurophysiological correlates of cortical excitability.(288) Importantly, if an alteration in cortical excitability underlies impaired sensory sensitivity, then treatments can be devised to normalize this activity and improve the QoL of those affected by it.

To better understand cortical excitability, it is important to comment on the two underlying systems, which modulate it; the **excitatory** and **inhibitory systems** function in unison and are fundamentally inseparable.(289) Through their combined effects on neurotransmitter regulation and receptor action, these systems determine the neural state of cortical excitability, and by extension impact cortical function and processing.(289) In fact, cortical excitability can be enhanced either through increased excitatory mechanisms or decreased inhibitory ones. The excitatory system is primarily related to glutamatergic principal cells, which largely release glutamate, an excitatory neurotransmitter, and act upon N-methyl-D-aspartate (NMDA) and non-NMDA receptors.(290) In contrast, the inhibitory system is highly associated with interneurons, related to gamma-aminobutyric acid (GABA), an inhibitory neurotransmitter, and GABAa and GABAb receptors.(291–293)

Excitatory and inhibitory systems exert a reciprocal influence on each other in several ways (for a schematic representation of different neural network configurations, see Figure 18). First,

although interneurons act on principal cells by inhibiting them, principal cells also have an opposite, excitatory effect on interneurons. This simultaneous inhibitory action exerted by interneurons and excitatory effect from local principal cells is often termed **feedback** or **recurrent inhibition**. Furthermore, excitatory inputs arrive as a result of both local and long-range connections, with the latter being referred to as **feedforward inhibition**. These feedforward inhibitory circuits, act on both principal excitatory cells and inhibitory interneurons.(294) Furthermore, interneurons also exert an inhibitory influence on each other. Ultimately, these different local and long-range circuits, work together and according to the **classical theory of balanced networks** the **ratio between excitation and inhibition (E/I ratio)** at both the individual neuron and network level, should remain relatively balanced to ensure stable brain function.(289) In particular, at the neuronal level this ratio should be maintained between excitatory and inhibitory synaptic inputs, whereas at the network level the balance should be maintained among the different excitatory and inhibitory circuits.(295,296) Nonetheless, this ratio is dynamic and depending on its current status can impact neural response specificity and/or reactivity. For example, a disbalance in favor of excitation can be beneficial at times, such as when processing sensory stimuli,(297,298) however prolonged disbalance, towards either excitation or inhibition, activates homeostatic, compensatory mechanisms to return the system to a balanced state.(299–302) Importantly, **prolonged disbalance of the E/I ratio has been linked to altered sensory perception** (303–305) as well as, in chronic cases, the **generation of neurological and psychiatric conditions**, such as autism, schizophrenia, and migraine.(306–309)
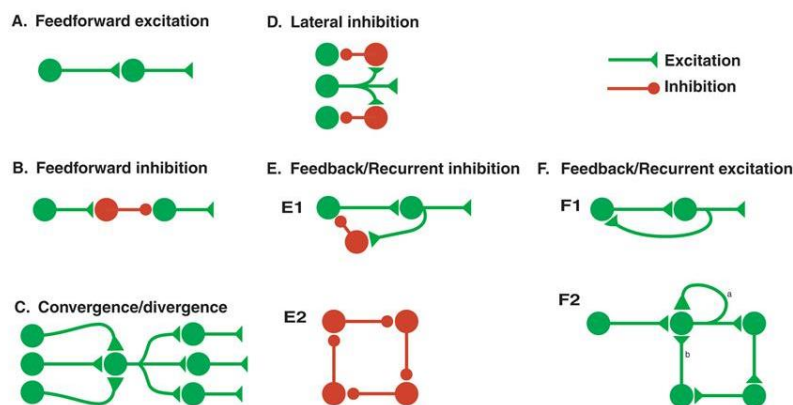
Figure 18. A schematic representation of different types of neural circuits. A. Feedforward excitation where one neuron excites the next. B. A presynaptic neuron excites an inhibitory interneuron, which then inhibits the following neuron. This impedes further excitation. C. A single neuron receives inputs from many neurons (convergence) and is also connected to several other neurons (divergence). D. A pre-synaptic excitatory neuron excites inhibitory interneurons, which then inhibit neighboring excitatory cells. E1. A pre-synaptic excitatory neuron excites another excitatory neuron, which then excites an inhibitory interneuron. This inhibitory interneuron, in turn inhibits the pre-synaptic cell. E2. Each neuron in this closed circuit inhibits the next. F1. A pre-synaptic neuron excites a post-synaptic neuron, which then excites the pre-synaptic neuron. F2. A pre-synaptic neuron excites a post-synaptic neuron, which then can excite itself or other excitatory neurons, which ultimately come back to it too. Figure reproduced from Byrne.(310)

When a prolonged disbalance between excitatory and inhibitory inputs is detected, compensatory mechanisms are activated to return the brain to a stable state. Within the brain, there are two types of mechanisms leading to plastic change, **Hebbian** or **positive feedback processes** and **anti-Hebbian** or **negative feedback mechanisms**. Although, Hebbian mechanisms, which strength the connection between neurons that fire together (311), are crucial to learning, memory, and normal development (312) they always move toward a maximum or minimum and if left uncontrolled can result in serious neural consequences. Anti-Hebbian mechanisms, on the other hand use negative feedback mechanisms to keep neural excitability within a certain range, by acting upon neuronal reactivity,(313,314) synaptic strength or efficacy,(314) synaptic number, feedback and forward-feedback mechanisms, and/or meta plasticity.(302,314) In terms of neuronal reactivity, anti-Hebbian homeostatic mechanisms can decrease or increase the threshold necessary for an action potential to occur, through changes to voltage-gated sodium or potassium channels.(315,316) At the synaptic level a variety of homeostatic changes can occur at both excitatory and inhibitory synapses [for a review see (302)]. One of the most well-known mechanisms of synaptic homeostasis, termed **synaptic scaling**, functions at the network level on principal neurons, by adjusting the strength of excitatory synapses up or down in an effort to regulate firing.(314) All in all, an interplay between Hebbian and anti-Hebbian mechanisms maintains the E/I balance and by extension normal cortical function.

1.3.5. Habituation and sensitization

Sensory sensitivities and abnormal perception may also be exacerbated by impaired adaptive mechanisms. The environments through which living organisms navigate daily are filled with innumerable sensory stimuli, which if handled improperly, can rapidly lead to an overwhelming, chaotic lived experience, and, in worst cases scenarios, to pathology. Basic research has found that even in the simplest of organisms ranging from single-celled amoeba and sea cucumbers to rats and humans (317–322) [for a review see (323)] there exists a response decrement to repetitive or constantly applied sensory stimuli, termed **habituation**, which is different from sensory adaptation or fatigue. The opposite process, or a response increment, called **sensitization**, to repetitive or constant, high intensity or painful stimuli has also been found to occur.(323) The work of Kandel (322) was particularly influential in showing that these innate abilities are the most basic forms of learning (324) or behavioral plasticity (323) and are fundamental to environmental adaptation (325) and evolutionary survival.(326) Importantly, both habituation and sensitization are non-associative learning mechanisms, occurring without the necessity of stimulus pairing or feedback and are relatively stimulus-specific.(327) Habituation in particular, has been suggested to act as a protective

mechanism against overstimulation, while also providing an additional measure of cortical excitability.(328) To better operationally define habituation, Thompson and Spencer (329) elaborated a list of nine properties that has since been expanded upon by Groves and Thompson (330) and recently revisited by Rankin et al. (327). These include:

(i) If the presentation of a repetitive or constant stimulus leads to a response decrement, this should manifest as a reduced magnitude, duration, or frequency. This reduction can take the form of a negative linear or exponential function and in some cases even an initial increment.(330)

(ii) If the stimulus is withheld once habituation has occurred, then a **spontaneous** full or partial **recovery** of the response should occur.

(iii) If habituation and spontaneous recovery are cyclically repeated, habituation will occur more rapidly each time, a process termed **potentiation of habituation**.

(iv) At higher stimulation frequencies, both habituation and subsequent spontaneous recovery are quicker and/or more apparent.

(v) At weaker stimulus intensities, habituation occurs quicker and/or is more pronounced. Habituation may not occur at all at stronger stimulus intensities.

(vi) Habituation does not necessarily stop once no response is achieved. Its effects may continue to accumulate leading to slower spontaneous recovery.

(vii) Habituation appears to show some stimulus specificity within the same modality; and generalization to other stimuli can be tested by examining changes between the response to the novel and habituated stimuli.

(viii) If another stimulus, or **dishabituating stimulus**, is presented after a response decrement has occurred than usually the subsequent response will be incremented. **Dishabituation** should be assessed with reference to the original stimulus not to the novel one.

(ix) If this dishabituating stimulus is repeated, then the effects on the original response will habituate too (**habituation of dishabituation**).

(x)   In some cases, habituation can last for longer periods of time (hours, days, or even weeks), in which case it should be termed **long-term habituation**.

Over the years, several theories of habituation have been proposed [for a review see (329–331)]. In a recent review by Thompson,(331) three theories, were highlighted as being especially relevant and will be discussed briefly here. The first theory, is the **dual-process theory of habituation** (330) by Groves and Thompson. In this theory, two separate forms of non-associative learning, specifically habituation and sensitization, interact to determine the final behavioural outcome. Habituation typically results in a response decrement whereas sensitization evokes the opposite. This theory might explain why, in experimental research, an initial response increment is frequently observed followed by the anticipated decrement. Furthermore, stimulus characteristics such as frequency and intensity have an important modulatory effect on the net outcome in this theory.(330,332) In particular, stimulus intensity has been inversely correlated to habituation, whereas stimulus frequency reflects an inverse-U shaped function relationship to habituation.(332)

The second theory, or **opponent-process theory** was based on the work of Solomon and Corbit, and established that there are two sets of processes, which occur in response to an event.(333) First, there is a primary process A or the initial, observable response to the stimulus, which is followed by an opponent process B, which attempts to re-establish equilibrium by suppressing or counteracting process A.(333) Importantly, for habituation to take place, primary process A must gradually weaken whereas primary process B should strengthen, occur earlier, and decay slower. Process B, in particular can be modulated by stimulus intensity, duration, and frequency of exposure.(334,335) Finally, opponent processes tend to occur more quickly in response to future exposures of the initial stimulus, a phenomenon termed the savings principle.(334,335)

Last, is a set of cognitive theories of habituation commonly explained together, which began with the work of Sokolov (336) who proposed the **stimulus-model comparator theory** (see Figure 19), based on the results of one of the earliest studies on habituation using EEG. According to this theory, exposure to a stimulus leads to the formation of a neuronal model [of the stimulus] within the cerebral cortex. Repeated exposure to the same stimulus activates the matching neural model, and consequently results in a decrement and eventual response extinction. A new stimulus, however, leads to a response increment given that the system detects a mismatch requiring the creation of a new neuronal model. Ultimately, Sokolov's stimulus model comparator theory (336) proposed the presence of two parallel systems; one amplifying the response and the other inhibiting it, based on the presence or absence of a matching pre-existent model. Following the revolutionary work of Sokolov, Konorski (337) proposed a theory, which was later expanded upon by Wagner (338), to

form the **Konorski-Wagner theory**. In this theory, habituation is the result of so-called **gnostic** units or memory traces that are created upon contact with a stimulus. Repetitive experience with the same stimulus may lead to response suppression and similar stimuli can activate the same gnostic unit, a phenomenon termed **associative influence**. The Konorski-Wagner theory also accounted for environmental noise, a criticism of the stimulus-comparator model, by accounting for failures in stimulus recognition despite previous experience and the presence of a matching gnostic unit. Additionally, this theory proposed that habituation can provoke long-lasting, not immediately reversible changes, which may distinguish between short-term and long-term habituation.(326,338)
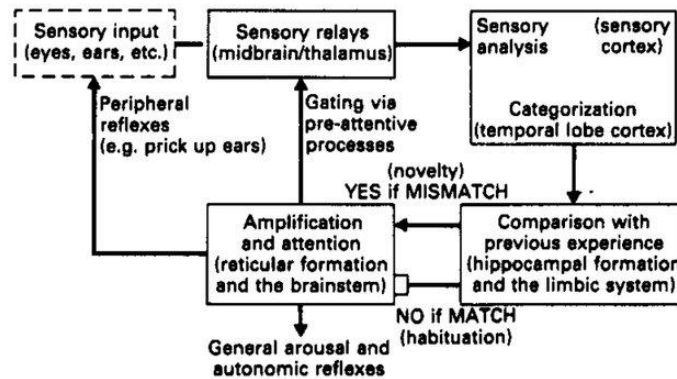
Figure 19. A schematic representation of Sokolov's stimulus-model comparator theory. Reproduced from Kirvelis and Vanagas.(339)

Importantly, all of the above-mentioned theories concur that habituation is not a peripheral process but most likely occurs at the level of interneurons in the CNS.(330) Primary sensory afferent neurons do not habituate, rather habituation occurs somewhere between the sensory and motor level, affecting the likelihood of our system effectuating a response. This is important as it signals the importance of measuring habituation using tools, which focus on the CNS rather than sensory receptors. In fact, **EEG has often been used as a means to study habituation and a decrement of ERPs has been found to be a good neurophysiological correlate of habituation**.(340,341) Computer-based tasks such as the pattern-reversal and oddball with EEG provide an additional way for the researcher to control stimulus characteristics important to habituation such as frequency and intensity.

1.3.6. Research paradigms associated with sensation and perception

1.3.6.1. Pattern-reversal

Within the literature on visual processing, the pattern-reversal (PR) is one of the most well-known and validated paradigms and is the preferred technique for clinical purposes.(342) Paired with EEG, it involves the presentation of a checkerboard pattern of an equal number of black and white squares, which reverse (from black to white and white back to black) at a predefined temporal frequency quantified according to the number of Hz (see Figure 20). The parameters of the checkerboard are carefully established both with respect to luminance, field size, contrast, and spatial frequency, which is typically defined according to the visual angle. Additionally, stimulation is presented consecutively usually 600 trials, divided post-recording into blocks of 100 trials (6 blocks).

In terms of the resulting waveform, at higher temporal frequencies (> 6 Hz) (343) SSVEPs can occur, as the components overlap to form a sinusoidal signal. On the other hand, at lower temporal frequencies, the resulting waveform is best termed a transient VEP, where the discrete positive and negative deflections can be easily identified (see Figure 20). An advantage of pattern-reversal visual evoked potentials (PR-VEPs), especially for clinical applications, is that there is very little variation both within and across participants.(342) The resulting PR-VEPs normally consist of the N1 (also called N70, N75 or N80), P1 (or P100), and N2 (also called N135 or N145) peaks (see Figure 20). N1, is usually considered as the most negative peak between 60-90 ms post-stimulus, P1 as the most positive peak after N1 and between 80-120 ms post-stimulus, and N2 as the most negative peak after P1 and between 90-200 ms.(341) These peaks, or neurophysiological correlates of sensation and perception, are sensitive to stimulus characteristics and tend to be predominantly exogenous, in nature. N75, is modulated by contrast (132) and spatial frequency (344) whereas P1 is sensitive to luminance (131) and contrast (132) among other characteristics. It is also common to calculate the peak-to-peak amplitude difference (N1-P1) to minimize the amplitude distortion of later components such as P1 by earlier components, such as N1.(120) One of the most frequent uses of this task, is to assess cortical excitability and habituation to repetitive stimuli. In fact, these concepts are frequently studied in clinical populations that report visual hypersensitivity or photophobia such as migraine (101,341) and epilepsy,(345,346) as potential pathophysiological mechanisms underlying sensory alterations. Cortical excitability is normally assessed by examining first block N1-P1 peak-to-peak amplitude difference,(288) whereas habituation is quantified according to the difference in first block N1-P1 peak-to-peak amplitude difference and last block N1-P1 peak-to-peak amplitude difference,(341,347) with a reduction confirming habituation. To avoid ocular artifacts, subjects are

instructed to maintain their eyes on a fixation cross in the middle of the screen. In this PhD thesis, a PR task will be used to study the exogenous mechanisms of visual processing.
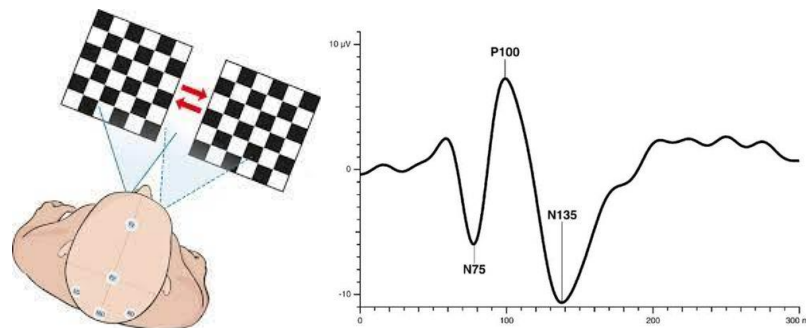
Figure 20. Pattern-reversal stimulus (left) and typical waveform response (right). The event-related potentials that are most commonly elicited in response to this type of stimulation are the N75, P1, and N135. The image on the left is reproduced from Sand et al.(348) and the one on the right from Lee et al.(349)

1.3.6.2. Oddball

Another experimental paradigm that is frequently used to explore sensory-attentional processing (see 1.4.5.2. for information relative to attention) is the auditory oddball alongside an EEG recording. Oddballs can consist of single stimulus, two-stimulus, or three-stimulus paradigms. If a single stimulus is used, a target is presented infrequently without the presence of any other stimuli. In the two-stimulus oddball, a chain of standard stimuli (repetitive and frequent) is presented with the presence of an occasional, infrequent target, which differs from the standards. If a three-stimulus oddball is used, the participant is presented with the same chain of events as the two-stimulus oddball but with an occasional novel, also sometimes called deviant or distractor, stimulus. The oddball paradigm can be either active, requiring a response from the participant, or passive, not requiring an overt response. In the active version of the oddball paradigm, participants must respond to targets while ignoring standard and novel stimuli (see Figure 21).
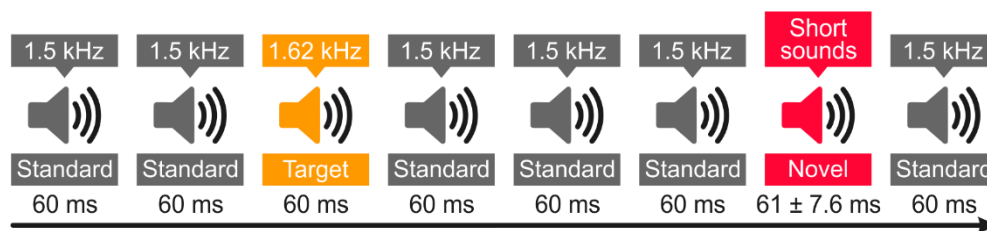
Figure 21. Schematic representation of an active auditory oddball paradigm. In this example, infrequent target sounds (1620 Hz, 60 ms duration) occur with a probability of P = 0.2 and are embedded in a stream of standard tones (1500 Hz, 60 ms duration), occurring with a P = 0.6 probability. Novel sounds (short excerpts of environmental sounds) are also included with a probability of P = 0.2 (average duration: 60.95 ± 7.61 ms).

The oddball task permits the researcher to study, among other things, the electrophysiological response to standard, repetitive stimuli alongside sensory and attentional processes. In terms of standard stimuli, the auditory N1 and P2 ERP components have been linked to evaluative processing of repetitive stimuli and are primarily exogenous in nature. N1 is identified as the most negative peak between 75-150 ms post-stimulus and has been shown to be sensitive to stimulus salience.(146,350) P2, on the other hand, is the most positive peak after N1, appearing between 150-250 ms post-stimulus, and reflecting higher level perceptual processing.(146) Next, the mismatch negativity (MMN) is a preattentive ERP component, which occurs in response to stimuli that differ from the standards in either tone, duration, volume, or timbre (146,351) and is calculated from the difference wave of distractors minus standards. It is considered to be stimulus-driven and occurs automatically without the necessity of an overt behavioral response, or even conscious awareness.(146,352) Importantly, although ERPs provide useful information relative to the time-course of sensory processing, time-frequency measures can supply additional information about underlying processes. For example, in response to standard, but also target or novel stimuli, there is an increase in theta activity, coinciding with N1 maximum amplitude. Furthermore, phase-synchronization measures, alongside power, might contribute to ERP activity,(353) and may provide additional information particularly with regard to the processing of repetitive stimuli.

Summary

Please consult Table 4 for a summary of processes and mechanisms related to sensation and perception that will be examined in this PhD thesis. Information about the cued visual detection task with bilateral entrainment can be found in Section 1.4.3 and 1.4.4.1.

Table 4. A summary of the processes and mechanisms related to sensation and perception, of interest in this PhD thesis.

Sensory modality	Cognitive process	Neural mechanism	Research paradigm	Neurophysiological correlate(s)
Visual	Perception	Cortical excitability	Pattern-Reversal	P1-N1 amplitude (first block)
		Habituation		P1-N1 amplitude (last block vs. first block)
		Neural entrainment	Cued detection with bilateral entrainment	Phase alignment Inter-trial coherence
Auditory	Perception	Habituation	Oddball	N1, P2, N2 amplitudes Theta, alpha, beta-gamma power and phase-synchronization (last block vs. first block)

P1-N1 refers to the P1-N1 peak-to-peak amplitude difference.

1.3. KEY MESSAGES

1. Psychophysical thresholds and self-report questionnaires and/or validated neuropsychological tests are some of the most frequently used tools to study sensation and perception.
2. Sensory ERPs, such as the visual N1 and P1, are modulated by characteristics related to the physical stimulus, such as contrast or luminance.
3. The alpha-band (8-12 Hz) has also frequently been related to sensation and perception, with changes in power and phase being related, for example to the likelihood of perceiving a stimulus.
4. Sensory sensitivity is best defined as the capacity to detect and perceive a sensory stimulus and can be characterized according to a spectrum ranging from hypo- to hyper-sensitivity.
5. Cortical excitability can be defined as the strength and/or likelihood of a neural response to external stimulation and reflects neuronal reactivity as well as specificity.
6. Habituation refers to a response decrement to repetitive or constantly applied sensory stimulation.
7. The pattern-reversal and auditory oddball task can be used to study sensation and perception.

1.4. Attention

1.4.1. Definition

Although we are intimately acquainted with the concept of attention, it is difficult to define all of its facets, given that attention is often used as an umbrella term to refer to a variety of phenomena.(354) Nonetheless, a general definition of attention would most aptly consider two things: [i] that the brain and the resources available to information processing form a limited capacity system, and [ii] the subject has some level of control [whether conscious or not] over what information enters the system.(355) Therefore, **attention is the mechanism that permits us to allocate our resources to process select stimuli and/or events, thus bringing them into conscious awareness**. Some of the aspects of attention that have been explored over the years include the link between attention and perception, the voluntary and/or involuntary nature of attention, as well as the clarity which attention can provide to information processing.(356) However, it is important to consider that attention is a broad term that encompasses a variety of different situations, and can therefore be categorized according to different types or functions of attention. Some of these subtypes (not a comprehensive list) include the selection of which information to process and which to suppress or ignore [selective attention], the ability to notice novel and/or unexpected stimuli and events [attentional capture], and the capacity to shift our resources towards them [attentional orienting] and back to the previous locus of attention [attentional re-orienting].(354) Some of the most prominent models of attention will be discussed below, with **particular emphasis being placed on selective attention, attentional capture and orienting/re-orienting**, the subtypes of attention that will be explored in this PhD thesis.

One of the first models of selective attention, was a theory by Broadbent, heavily inspired by information theory, called **filter theory**(357) (see Figure 22 for a simplified version). In this model, Broadbent proposed the existence of two stages of attentional processing. In the first preattentive stage, all of the information arriving at the senses is temporarily stored for further processing. Here, information processing occurs in parallel and input information is stored as a function of stimulus characteristics and modality, among other things. The second stage is defined as a limited capacity processing system whereby only a fraction of the previously processed information is directed for further handling based on physical characteristics of the inputs. This reduction of initial information creates an **attentional bottleneck,** where only one of the initially collected inputs is sent for further cognitive processing. Inputs that are not selected are held in short-term stores at the pre-attentive stage and are thought to rapidly decay. Finally, depending on the selected input, the motor system and its consequent response is activated at the end of this second stage.
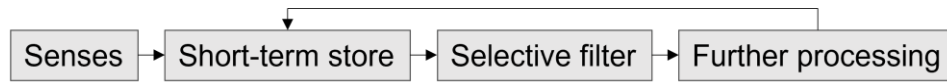
Figure 22. Broadbent's model of selective attention (filter theory).(357) Figure adapted from Jackson and Cottrell.(358)

Understandably, Broadbent's theory has been updated throughout the years with one of the most well-known modifications being the **filter-attenuation theory** by Treisman (359) (see Figure 23 for a comparison of both models). One of the criticisms of Broadbent's theory was that it struggled to explain the processing of unattended stimuli, such as the **cocktail party phenomenon** (360,361) where you can hear your name in a noisy environment (such as a cocktail party) even if your attention is directed elsewhere. Treisman's theory sought to account for this, by revisiting the action of the filter. In filter-attenuation theory information enters the system through parallel channels and is examined for stimulus characteristics. However, here the filter strengthens some inputs and attenuates others but does not eliminate them, meaning that weakened signals can still get through to further processing. At later stages, inputs are compared to dictionary units, or pre-existing concepts within the system, and a response can be executed. Importantly, some of these so-called dictionary units have lower thresholds, particularly for biologically or emotionally relevant stimuli. This would help to explain why in real-world instances, attention can be triggered by unattended stimuli. Furthermore, these thresholds can vary based on instructions or context.(362–364)
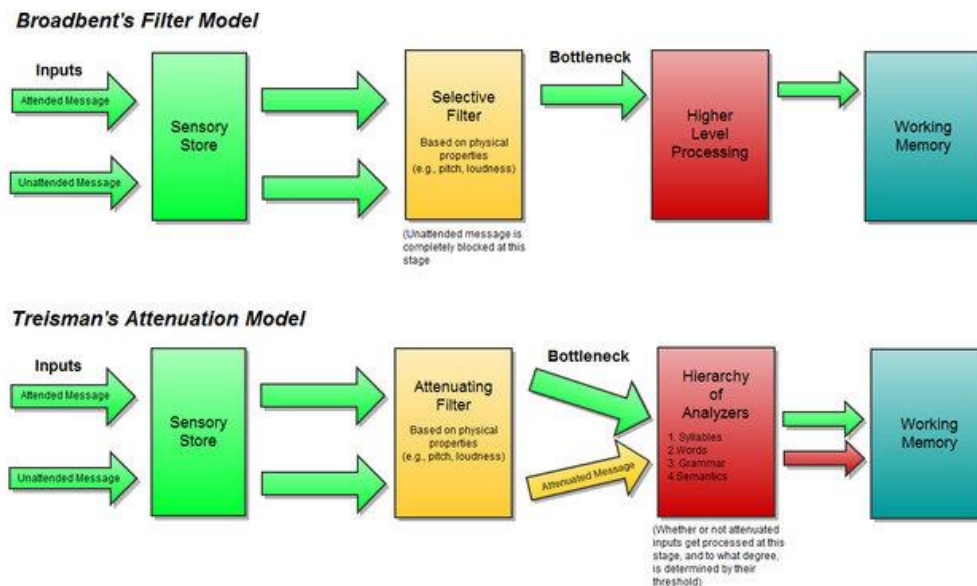
Figure 23. Schematic representations of Broadbent's filter model (top) and Treisman's attenuation model (bottom). Note the differences in the properties of the filter in both models. In Broadbent's model, only the selected input gets forwarded on for further processing, whereas in Treisman's model, both selected and attenuated inputs continue past the filter stage. Based on Broadbent (357) and Treisman,(359) figure reproduced/adapted from Atmaja.(365)

56

Treisman's filter attenuation theory was met with some criticism due to its redundancy, therefore, Deutsch and Deutsch proposed an alternative **selection model**.(366) In their model, the initial filter sensitive to physical characteristics is non-existent and input is relayed directly to the dictionary units. In this model, all inputs are assessed for meaning and then a selection is made. Responses are determined according to the weight of the dictionary unit rather than the strength of the signal itself and the most heavily weighted stimulus (i.e., the most relevant) becomes the focus of attention. If another signal is weighted more heavily than an attentional shift occurs.

These three early models all considered **attention as a selective filter mechanism**, enabling individuals to process vast quantities of information by prioritizing some things and ignoring or suppressing others.(367) Given limitations on the amount of energy available to the brain (368) and the high cost of neural firing,(369) this function of attention allows the individual to ensure that they are not wasting precious resources on irrelevant or distracting information. Importantly, within the research on selective attention, a few key matters have been identified.(370) The first stems from the attentional bottleneck itself and focuses on clarifying where this selection process takes place. Two predominant approaches have been conceptualized and consist of early-selection and late-selection models. **Early-selection models** such as Broadbent's filter theory and Treisman's filter attenuation theory claim that information is selected according to physical or sensory attributes prior to reaching the semantic stage whereas **late-selection models**, such as the selection model posit that all inputs reach the semantic stage and selection occurs here [for a review see (371)]. The debate between these two types of models is still ongoing, although in recent years more evidence would appear to support the early-selection view.(372) Recently, the two types of selection models have been unified according to a **hybrid model** modulated by perceptual load, related to manipulations of display set size and task requirements.(373,374) Specifically, smaller displays and easier tasks (e.g., detection task vs. identification of a specific position of target stimulus) require less resources and therefore exert a lower perceptual load. In this view, the type of selection whether or early or late depends entirely on the perceptual load whereby high perceptual loads lead to early selection and low perceptual loads to late selection mechanisms.

The two other subtypes of attention discussed in this thesis, attentional capture and attentional orienting/re-orienting consist of the process of an external stimulus or event **seizing our attentional resources**, which usually occurs in response to a novel, but also a significant, rare, surprising and/or unfamiliar stimulus (375–377) after which the brain may choose to **maintain attentional resources where they are or flexibly orient** to the novel stimulus or event.(378,379) This ability to redirect attention and modify behaviour according to the presence of novel or unexpected stimuli is important for safely and effectively navigating our busy environments.(380) In fact, the shift in attention

required to elicit an orienting response has been likened to the switches used for task or rule switching (381,382), which may also suggest that these processes and cognitive flexibility share interconnected mechanisms.

One of the most important aspects of attentional capture, orienting/re-orienting but also selective attention, has to do with the direction of processing, which can be either **bottom-up** or **top-down** (370) (see Figure 24 for a schematic representation). Attention can be externally induced [exogenous], such as through changes in luminance or motion, which occurs through **automatic, involuntary, and stimulus-driven mechanisms, frequently termed bottom-up**.(383–387) For example, in the spatial domain, an external cue can provoke a shift in attention to a cued location (388) whereas in the temporal domain, attentional capture can occur in response to rhythmic or predictable stimuli.(389–391) Usually, this mechanism occurs very quickly, peaking at approximately 100 ms, and tends to have a more transient nature,(392) [for a review see (367,385,393)]. Bottom-up attention also appears to be phylogenetically older and plays a role in detecting and responding to salient or novel events that appear unexpectedly or outside of our attentional focus.(394)
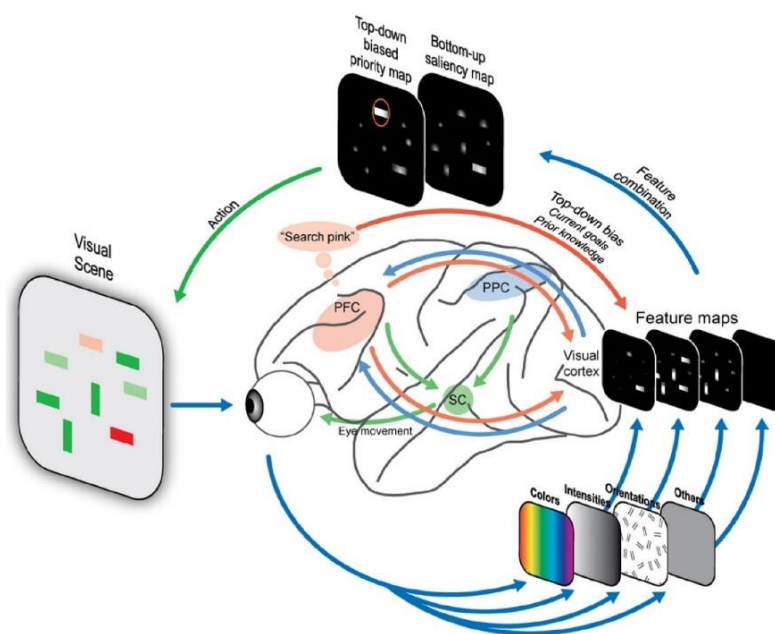
Figure 24. A visual representation of bottom-up and top-down attention. The external arrows represent the flow of information related to bottom-up saliency, which integrates with top-down priority maps to yield action. The schematic representation of the brain in the center of the image depicts the cortical pathways related to visual attention. Arrow colors represent bottom-up (blue), top-down (red), and eye movement (green) signal processing. Visual information enters the system through the eye and is processed according to different features such as color. Feature maps assemble these components and integrate them into a saliency map, with the goal of orienting attention to the most salient stimulus. Saliency is processed simultaneously in the prefrontal cortex (PFC) and the posterior parietal cortex (PPC). Importantly, bottom-up processing can be modulated by top-down mechanisms, such as goals and prior knowledge. The combination of bottom-up and top-down processing is represented using a priority map. In particular the PFC is thought to affect how the input is represented throughout the cortical pathway. The area with the most activation in the map is the target of attention. Eye movements, generated by the superior colliculus (SC) are ultimately carried out. Figure reproduced from Katsuki and Constantinidis.(395)

Top-down, or **endogenous** attentional mechanisms, on the other hand are more closely related to goals, expectancies, and incentives.(387) Endogenous, voluntary, or goal-directed attention, occurs as the result of a choice to deploy attentional resources to a particular location or object.(385,392) In the temporal domain, it can occur in response to informative, symbolic cues, similarly to the spatial domain.(396) Attentional capture and subsequent re-orienting are also modulated by top-down, internal cognitive control processes.(381,382,397) Top-down attention is also much slower and more prone to interruption,(387) however it can be sustained for longer periods of time.

Importantly, bottom-up [exogenous] and top-down [endogenous] attention are tightly related. In fact, some authors claim that exogenous attention can be modulated and even suppressed by endogenous attention,(383,392,398) [despite (399,400)]. One of the theories related to the mechanisms underlying this interaction is the **biased competition model of attention** by Desimone and Duncan, whereby objects compete for access to cognitive resources and top-down signals bias this competition by enhancing the representation of objects that are considered to be relevant to the task, goal, or behavior.(401) In terms of functional and anatomical neural networks related to bottom-up and top-down attentional mechanisms (380,402) two pathways have been proposed: a **ventral** fronto-parietal network related to bottom-up attentional mechanisms and a **dorsal** fronto-parietal network linked to top-down processes.(380,402) The dorsal fronto-parietal network is made up of the: dorsal parietal cortex, specifically the intraparietal sulcus (IPS) and the SPL, frontal eye fields, and the dorsal frontal cortex.(387) This network has been shown to activate as a function of goals or expectations and to guide motor responses, for example with regard to the appearance of a stimulus at an attended location.(387) In contrast, the ventral fronto-parietal network includes the: right ventral frontal cortex, including parts of the middle frontal gyrus (MFG), inferior frontal gyrus, anterior insula, and frontal operculum, as well as the right temporo-parietal junction.(387) This network responds to task-relevant or behaviorally-relevant stimuli, for example to unattended locations (387) and does not seem to be modulated by participant expectancies.(403) Importantly, unexpected or irrelevant stimuli appear to activate a different network made up of the bilateral dorsal basal ganglia, anterior cingulate, left dorsolateral prefrontal cortex, and the left anterior insula.(387,404) Both networks would appear to congregate at the lateral prefrontal cortex and compete for attention.(387) A theory by Corbetta and Shulman, related to attentional orienting has suggested that in the presence of novel information, the ventral network acts as a 'circuit-breaker' halting processing of the dorsal network by redirecting attention to the novel stimulus or event [for a review see (380) and a visual representation see Figure 25].(402)
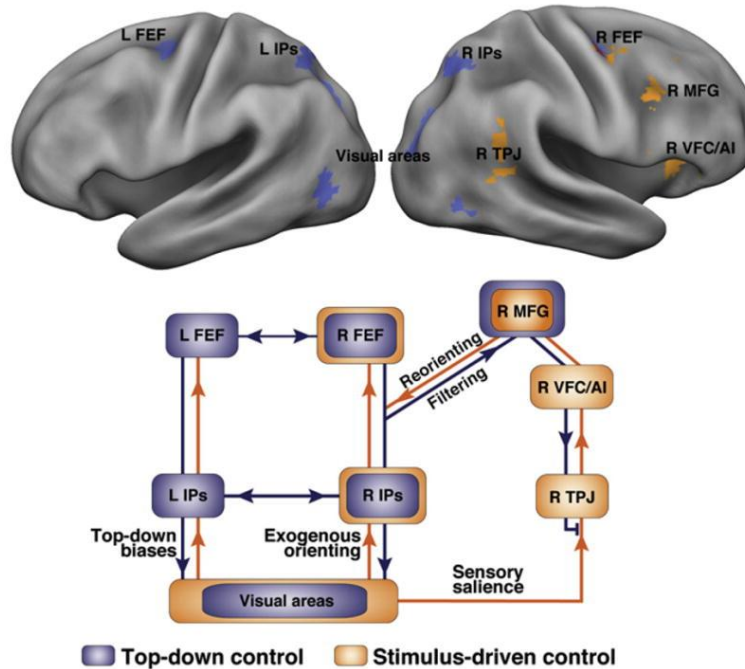
Figure 25. A visual representation of the interaction between ventral and dorsal networks, with particular emphasis on the re-orienting response. The figure on the top represents the activation of different brain regions to informative, central cues [blue] and those that respond to behaviorally relevant, unexpected stimuli through a re-orienting response. On the bottom, a model of the interaction between the two systems is represented. The dorsal network biases processing through activity from the frontal eye fields (FEF) and the intraparietal sulcus (IPS), via the middle frontal gyrus (MFG) (filtering signal) to the ventral network, thus inhibiting responses to stimuli that are behaviorally important. However, in response to a salient stimulus and subsequent stimulus-driven re-orienting, the ventral network acts on the dorsal network through a re-orienting signal sent through the MFG. Reproduced from Corbetta et al.(380)

In recent years, the bottom-up and top-down dichotomy has been met with some criticism (405) particularly with regard to a failure to adequately represent attentional capture in response to emotional stimuli or those associated with incentives, which can still capture attention, even if not necessarily related to the goal.(406,407) It seems clear that both endogenous and exogenous attention shape sensory information processing in distinct but relevant ways.(408,409) Given the nature of our environments, multiple stimuli are constantly competing between each other for neural representation and these competitive interactions can be affected or biased by both bottom-up and top-down mechanisms.(401,410,411) Nonetheless, few research studies have found a way to successfully isolate these processes.(412,413)

Finally, selective attention, attentional orienting, and attentional capture can occur in an **overt** or **covert** manner, with overt being related to eye or head movements and covert occurring in the absence of these.(414) In fact, covert attention tends to precede ocular saccades.(415) For example, selective attention can be overtly activated by looking at something directly, or covertly induced due to cueing. Michael Posner's work on spatial cueing has been particularly influential in understanding

covert shifts of attention by indicating that selective attention can be manipulated by cueing the participant, to the likely location of a target in space.(388)

1.4.2. Neurophysiological correlates of attention

The use of ERPs permits researchers to explore the stages of attention, as well as its relationship to selection and perception.(206) In terms of the visual modality, early studies used flash stimulation to examine ERPs and were the first to report modulations of component amplitudes with attention.(416–418) The earliest visual component, N1 [80-100 ms] (also called C1) tends to be exogenous and does not appear to be affected by attentional modulation [(419–424) despite (425,426)]. P1 [100-130 ms] and N2 [100-200 ms] (the following ERPs to appear in the waveform) also tend to be exogenous, although some evidence exists that on cued attentional tasks, they may show attentional modulation (see Figure 26). Attentional effects in these early components tend to occur when participants are cued to covertly attend to locations in space. In particular, P1 would appear to be related to suppressing unattended stimuli and facilitating stimulus processing at attended locations whereas N2 has been linked to discrimination and amplification of attended stimuli with a possible role in attentional orienting towards relevant stimuli.(142,206,427,428) Additionally, both P1 and N2 amplitudes have been shown to be reliably enhanced in response to attended stimuli, as well as to precued stimuli.(133,137,141,142,206,417) In this light, some researchers have proposed that **selective attention may act as a gain control mechanism on sensory information**, effectively amplifying attended stimuli.(420) The increased amplitudes of P1 and N2 have also been correlated to behavioural effects, with enhanced amplitudes being correlated with improved detection and faster reaction times (RTs).(137,141,142) Nevertheless, despite some evidence for attentional modulation, these components are usually considered to be predominantly exogenous.
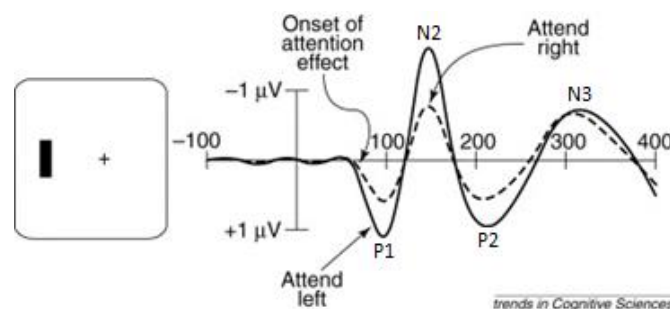
Figure 26. A schematic representation of a typical attentional paradigm used to elicit attentional effects in visual event-related potentials (ERPs). Participants are told to fixate on a cross in the center of the screen and covertly attend to either the right or left visual field. Next a stimulus is presented to the right or to the left over a series of trials. On the right, the expected result is shown for a left visual field stimulus, where a larger P1 and N2 can be observed in response to attended (participant told to 'attend left') as compared to unattended (participant instructed to 'attend right') condition. Figure adapted from Luck et al.(123)

61

In the auditory modality, on the other hand, early-latency components tend to be more exogenous. For example, brainstem auditory evoked potentials (peak < 10 ms post-stimulus) and mid-latency components (peak 10-50 ms post-stimulus) do not appear to reflect attentional processes [(160,429–431) despite (432–435)]. The following component N1 (peak 75-150 ms post-stimulus) also tends to be exogenous, but has been found to show an enhanced amplitude in response to stimuli presented at the attended ear vs. the unattended one (see Figure 27) [(155,416,436) despite (437,438)]. Next, P2 (peak 150-250 ms post-stimulus) has also been related to early attention and orienting (127,146) alongside the MMN (peak 175-225 ms post-stimulus) (439) although, once again these three components [N1, P2, and the MMN] tend to be exogenous and contamination from later-latency, endogenous components may explain these attentional effects.(437,438,440) P3, on the other hand, tends to be more endogenous, reflecting attentional effects on its amplitude.(441,442) It is usually decomposed into early P3a (peak 225-275 ms post-stimulus) and late P3a (peak 275-325 ms post-stimulus), which occur earlier in response to novelty, and P3b (peak 300-600 ms post-stimulus), which occurs later in response to target stimuli.(443) Finally, the re-orienting negativity (RON) (peak 400-600 ms post-stimulus) has frequently been used as a neurophysiological correlate of attentional disengagement from a target and subsequent re-orientation to the task.(170,444)
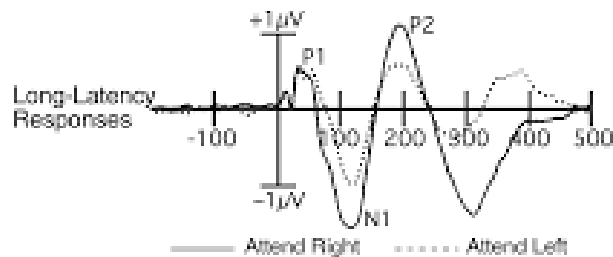
Figure 27. Auditory event-related potentials in response to stimuli presented to the right ear, when the subject was attending to the right versus to the left ear. This data would appear to indicate an early effect of attention on N1, P2, and later components. Adapted from Woldorff et al.(435,445)

Aside from research on ERPs, time-frequency analyses have permitted researchers to go further in studying the brain's endogenous frequencies and their relation to attention [for a review see (446)]. In fact, more recent attentional theories such as the **blinking spotlight theory** (447) have proposed that attentional sampling and ultimately selection may occur due to a rhythmic underlying mechanism. Basic science research has evidenced that attention has a modulatory impact on baseline neuronal excitability (448,449) and impacts internal neuronal rhythmicities, including those of well-known frequency bands (see Table 3). In fact, perhaps the most well-known neurophysiological correlate of attention is the **alpha** rhythm, which has been suggested to act as an attentional gating mechanism, suppressing task-irrelevant information while facilitating task-relevant events.(450,451)

Importantly, the relationship between alpha and attention has been found across sensory modalities, including evidence from both the visual (452,453) and auditory (454,455) domains. When alpha power is reduced attention to task-relevant stimuli is enhanced.(188,189). Specifically, alpha power shows an identifiable hemispheric pattern in that it tends to be suppressed in the contralateral and enhanced in the ipsilateral hemisphere with reference to an attended visual field (see Figure 28),(186,456) despite some discrepancies,(457–462) mainly attributed to the presence of strong distractors on the unattended side.(463)
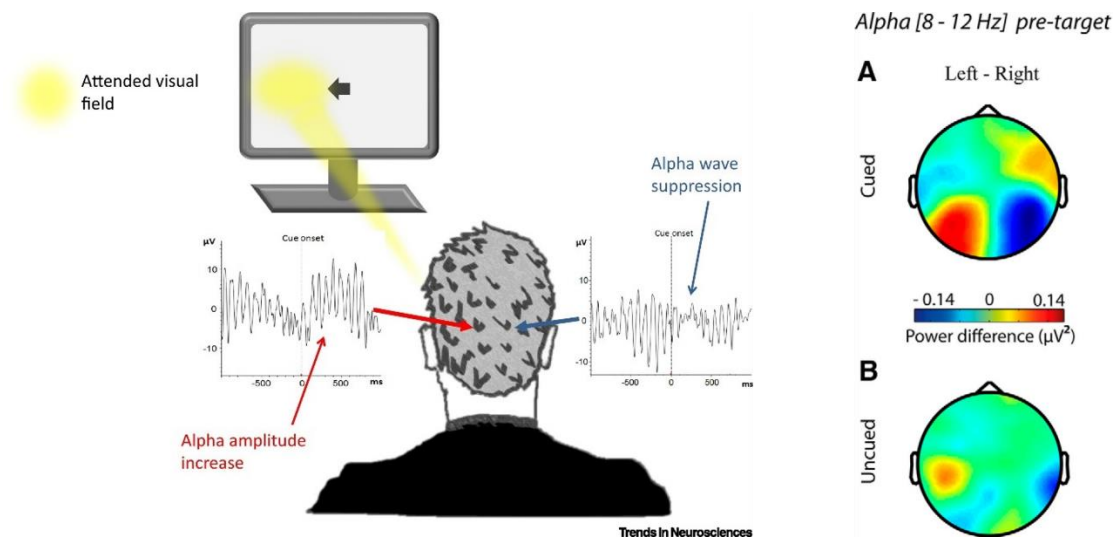
Figure 28. Alpha oscillatory activity as a mechanism of selective attention. On the left, a classic paradigm is shown where the participant is cued to attend to a location in space. On the right, the identifiable hemispheric pattern is shown (cued – top, and uncued – bottom), with suppression on one side and enhancement on the other. The figure on the left was reproduced from Peylo et al.(464) whereas the one on the right is from van Diepen et al.(465)

An effect of attention on alpha phase has also been reported, with larger **phase locking**, or the capacity of a neuron to synchronize with a stimulus or event, being reported in response to increased attention.(466) Furthermore, due to its important role in attention, alpha has been the central player of several oscillation-based theories of attention. First, the **inhibition-timing hypothesis** (183) suggests that alpha power is the mechanism underlying the functional inhibition and facilitation of cognitive processing. When alpha power is decreased, cognitive processing is inhibited, whereas when the opposite is true, cognitive processing is facilitated. Another theory putting alpha rhythms at the forefront is the **gating-by-inhibition hypothesis** put forward by Jensen and Mazaheri.(451) Similar to the inhibition-timing hypothesis, alpha rhythms are proposed to play an inhibitory role in the processing of sensory information through pulsed activity and accompanying gamma power increases. Gamma band oscillations have also been related to attention and bottom-up sensory processing.(467,468) In a recent study by Clayton et al. (469) the interaction between theta (4-8 Hz)

and gamma (< 30 Hz) frequency bands has been unified in a gamma-theta phase-power coupling model of attention proposing an attentional sampling role for theta-gamma.(470–472) In this case, inhibition or suppression of task-irrelevant processes is modified by theta power whereas the facilitation or excitation of task-relevant stimuli is controlled by gamma power.(469,473) On their own, theta oscillations have been proposed to provide the necessary flexibility to perform attentional shifts, as discussed in a recent rhythmic theory of attention, and may provide long-range control (473,474) [for a review see (475)]. However, the role of theta remains to be explored (476) particularly because it continues to be unclear whether theta oscillations are an active response or a passive by-product of attentional modulations. In summary, alpha oscillatory activity would appear to provide the most robust evidence of an oscillatory neurophysiological correlate of attention.

1.4.3. Neural entrainment and photic driving

Neurons possess an intrinsic capacity to oscillate both spontaneously and also in response to stimuli.(477) This ability can occur at a microscopic, or individual neuron level, with changes to membrane permeability or nerve impulses (478) and also at the macroscopic level (across groups of neurons), resulting in the generation of synchronized activity at different frequencies.(479) These rhythmic fluctuations (see Table 3) have been shown to underlie baseline neural excitability, at a variety of temporal and spatial scales, with an effect on sensation, perception, and action.(173–175) Oscillatory activity has also been proposed to act as a gating mechanism in terms of communication between different brain areas.(471,480,481) Interestingly, the brain has a natural tendency to synchronize these underlying oscillations to rhythmic external stimuli, often referred to as **neural entrainment** and operationally defined by Obleser and Kayser as "**the temporal alignment of an observed neural process with the regularities in an exogenously occurring stimulus**".(482) This inherent mechanism may provide a variety of benefits, particularly attentional ones (452,483,484) related to stimulus expectation.(485)

Given that oscillations are characterized by a peak and a trough of excitability, neural entrainment permits the alignment of peak neural activity with the onsets of periodic external stimulation. This results in enhanced sensory representation, amplifying stimuli that are aligned with the high excitability phase of neural oscillations and attenuating those that are in line with the low excitability phase [for a review see (486)]. Furthermore, neural entrainment may have an impact on action by optimizing behavior, through quicker reaction times (485) and increased hit rates.(487–489) It is believed that neural entrainment most likely occurs as a result of a phase-reset of the internal oscillator to match the external one (see Figure 29).(483,490) In fact, neural entrainment does not need to be accompanied by an increase in power, as is the case for evoked responses, but rather

involves an alignment of phase, or **phase-locking**, between internal and external oscillators.(210,491) Therefore, phase concentration metrics provide an important tool to study neural entrainment.(492)
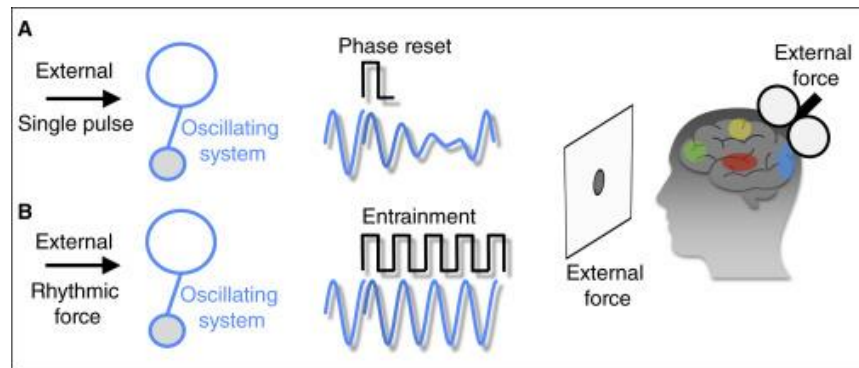
Figure 29. A visual representation of phase reset as compared to neural entrainment. A. A single external input causes phase reset, or a modulation of the phase of the internal oscillators to a specific value at the temporal moment of the arrival of the external signal into the system. If, no other external signals are delivered, the internal oscillators return to their natural, or eigenfrequencies. B. Neural entrainment in response to rhythmic external inputs. This results in modulation of the wavelength and amplitude through a series of probable, rhythmic phase resets. The wavelength is altered to line up with the rhythmic input, which resets the internal oscillatory phase. Reproduced from Lakatos et al.(493)

In recent years, the definition of neural entrainment has been further elaborated on, to effectively distinguish this process from steady-state evoked potentials [SSEPs] (494,495) or other forms of neural activity, whose temporal superposition may look like an alignment between internal and external activities.(210) One of these processes, which closely resembles neural entrainment is **photic driving**, a robust neurophysiological correlate of sensory sensitivity,(496) and arousal,(497) which has frequently been used on studies of clinical populations, including epilepsy,(498) autism,(496) Alzheimer's,(499,500) migraine,(501–503), attention-deficit hyperactive disorder,(504) and schizophrenia.(505) Photic driving, or a **rhythmic exogenous synchronization of internal oscillatory activity to the frequency of periodic, external stimulation**, is frequently elicited using intermittent photic stimulation (IPS), involving the presentation of a series of light flashes, using a strobe light, for 4-10 s and with frequencies increasing from 1-30 Hz.(506) At alpha frequencies photic driving would appear to have the largest effect.(507,508) Furthermore, when photic driving is carried out at the alpha frequency it has been shown to generate a relaxing effect, which has been confirmed by measuring heart rate, galvanic skin resistance, and breathing rate (509) and has actually been applied therapeutically.(483,510–512) Importantly, alterations in photic driving, particularly an increased effect could explain photic hypersensitivity in patients with sensory alterations such as autism (496) and migraine.(501–503,513)

Nonetheless, despite certain similarities, photic driving is considered separately from neural entrainment and recent studies have highlighted **a number of criteria that should be used to**

differentiate true neural entrainment or '**neural entrainment in the narrow sense**' from a more general temporal alignment between external stimuli and internal activity, or '**neural entrainment in the broad sense**'.(210,482) These criteria will be detailed upon continuation and should be referred back to throughout the thesis when referring to neural entrainment.

> [i] Neural oscillations should occur spontaneously (in the absence of external stimulation) or persist after stimulus offset.

> [ii] Neural oscillators possess 'eigenfrequencies', or natural frequencies around, which they tend to oscillate [Arnold tongue concept] and when exposed to rhythmic stimuli they should adjust their frequencies within certain bounds. Nevertheless, post-stimulus offset they should return to their natural frequencies, exhibiting a resilience to perturbation.

> [iii] Post-stimulus offset, neural oscillators should maintain their frequency around the entrained frequency for a little while longer, before returning to their eigenfrequency, thus displaying a persistence of the entrained signal.

Neural entrainment would also appear to be modality-independent, with research in the visual,(488,514–516) auditory,(485,487,517,518) olfactory,(519) and somatosensory (520–522) domains yielding similar results and focusing on different neural frequency bands, including delta,(485,487,515,523,524) theta,(518) alpha,(237,452,488,514,516,517) beta,(522) and gamma.(522) Nonetheless, in recent years the neural entrainment of alpha frequency oscillations [7-14 Hz] has received special interest because of alpha's role in selective attention [see 1.4.2.].(484,525) It would appear that alpha oscillations participate in the mechanisms involved in: representing task-relevant information at specific temporal moments,(526) determining the amount of neural representation of an external stimulus,(527) and preparing the system to respond by either enhancing or suppressing inputs [for a review, see (528)]. The inhibition-timing hypothesis (183) would support the conceptualization of entrained alpha as a mechanism to filter and gate sensory inputs while enhancing neural coding based on temporal features.(482,483) In fact, some studies have theorized that maybe two systems, related to alpha power and alpha phase synchronization, interact with each other for the selection or suppression of stimuli representation/response.(411)

Furthermore, it is important to clarify that most brain responses contain both evoked responses and endogenous oscillatory activity and it can be difficult to dissociate them.(210) Given that neural entrainment tends to persist for some time after the external periodicity has been removed,

an opportunity to isolate and study the endogenous, underlying oscillatory activity without the influence of evoked responses exists. This ability is relevant because it provides a unique ability to dissociate bottom-up and top-down mechanisms, at a mechanistic level, and in the case of clinical populations, could indicate which of the two systems, if any, are impaired. Particularly in patients with sensory alterations, neural entrainment can provide a window to independently assess the influence of exogenous and endogenous mechanisms on sensory-attentional processing.

Lastly, some neural entrainment tasks can be used to study both temporal and spatial attention.(484) In this case, temporal aspects of the stimulus can improve visual discrimination through more efficient processing of targets presented in-time with entrainers (529,530) whereas, spatial elements, linked to a visuospatial attentional mechanism, can act as a pulsed inhibition.(461)

1.4.4. Research paradigms associated with attention

1.4.4.1. Cued visual detection with bilateral entrainment

Given the natural ability of external rhythms to entrain internal oscillatory activity [see 1.4.3.], tasks used to elicit neural entrainment frequently entail the presentation of periodic stimulation alongside an EEG recording. Lakatos and colleagues established a series of building blocks, which can be useful when designing experimental tasks meant to generate neural entrainment.(493) First, neural entrainment is not frequency specific, although it does tend to be stronger around the individual alpha frequency (IAF),(507,508) which means that it can occur in response to all of the typical frequency ranges.(493) Therefore, the frequency of stimulation can be selected according to other criteria, such as processes of interest. Neural entrainment is also tolerant to changes in input timing,(493) meaning that stimuli such as speech or music can be used in experimental tasks, and can occur in response to a variety of rhythmic inputs, including environmental, self-produced, autonomic, and top-down.(493) Importantly, tasks can be set up based on specific research questions, for example by introducing target-absent trials, which can be used to study underlying neural oscillatory activity without the influence of evoked responses.(484) Neural entrainment can also be coupled with different computer-based tasks, to study potential behavioral benefits or hypothesized impairments in clinical populations.(484,485,487,488) Furthermore, bottom-up, exogenous mechanisms can be studied alongside top-down, endogenous ones, with the ability to separately isolate their influence.

1.4.5.2. Oddball

One experimental paradigm that is frequently used to study sensory-attentional processing is the oddball [for information about the sensory-perceptual functions of this task, see 1.3.6.2]. In terms of attentional mechanisms, this task is useful to study behavioral readjustments as a function of environmental demands by studying the neurophysiological response to novel and target stimuli. Novel stimuli lead to a cascade of ERPs including, in order of appearance, the MMN, early and late P3a, and finally the RON, whereas target stimuli elicit the MMN, P3b, and the RON (see Table 7). The MMN can be an index of attentional capture (see Table 7). Additionally, the most well-known component elicited by the oddball paradigm is the P3, which occurs when a new stimulus is detected that does not match the existing schema of the previously presented stimuli (531) and can be subdivided into P3a (early and late) and P3b subcomponents. The P3a normally underlies attentional allocation of resources as well as orienting to environmental change, such as to infrequent novel stimuli,(532) with larger amplitudes being related to increased attention.(532) The P3b in contrast occurs in response to infrequent targets, when subjects are instructed to actively respond.(532,533) The amplitude is dependent on the attentional resources provided to the stimulus.(532) The use of a three-stimulus task permits the researcher to study both the P3a and P3b. Finally, the RON is considered to play a role in disengaging from stimuli and re-orientation back to the task and is obtained using the difference wave of standard and novel trials. Time-frequency measures can also provide additional information about the time-course of attentional processing. For example, in response to target or novel stimuli, an increase in theta activity can be seen, which coincides with the maximum amplitude of P3a. Furthermore, greater low-beta activity has been noted in response to novel stimuli.(379,534)

Summary

Please consult Table 5 for a summary of processes and mechanisms related to attention that will be assessed in this PhD thesis.

Table 5. A summary of the processes and mechanisms related to attention of interest in this PhD thesis.

Sensory modality	Cognitive process	Neural mechanism	Research paradigm	Neurophysiological correlate(s)
Visual	Selective attention	Neural entrainment	Cued detection with bilateral entrainment	Phase alignment Inter-trial coherence
Auditory	Allocation of attentional resources		Oddball	N1, P2, P3a amplitude
	Attentional orienting/re-orienting			P3a, Re-orienting negativity (RON) amplitude
	Attentional Capture			Mismatch negativity (MMN) negativity

1.4. KEY MESSAGES

1. Attention acts like a selective mechanism, filtering information for further processing, while also shifting resources to new sources of information or back to the task at hand.
2. Attention occurs through a delicate interplay between bottom-up and top-down mechanisms, which interact to shape sensory-information processing.
3. ERPs, such as the auditory P3 and RON, as well as neural oscillatory activity, in particular alpha, are some of the neurophysiological correlates, which can be used to study attention.
4. Neural entrainment is the natural tendency of neurons to synchronize their internal oscillations to rhythmic, external stimuli.
5. Attentional re-orienting refers to the ability to direct and redirect attention based on novel or unexpected stimuli.

1.5. Sensory-attentional processing in migraine

To explore whether sensory-attentional processing is altered in migraine, a number of different concepts will be examined including sensory sensitivity, cortical excitability, habituation, neural entrainment, photic driving, and the orienting/re-orienting response. The studies listed in the following sections will discuss findings related to EM. Additionally, given the importance of the interictal period [discussed in 1.1.2.] the research presented in the following sections will be focused on this phase, unless explicitly stated otherwise.

1.5.1. Sensory sensitivity in migraine

Photophobia and phonophobia are among the diagnostic criteria of a migraine attack.(6) However, sensory alterations have also been reported in the interictal phase, significantly contributing to the IIB, and provoking discomfort and sensitivity in response to stimuli from different sensory modalities.(55,535) Currently, the mechanisms underlying this sensory hypersensitivity remain unclear, although there are some theoretical propositions, which will be discussed below. Sensory hypersensitivity has traditionally been measured using self-report questionnaires (536,537) and sensory thresholds.(55,215,263,538) One questionnaire used to evaluate sensory sensitivity, while dissociating it from sensory reactivity, is the **Sensory Perception Quotient (SPQ)**, which has been used in both healthy and clinical populations and evaluates both visual and auditory parameters.(252) In the following sections [1.5.1.1. and 1.5.1.2.], research related to the visual and auditory domains will be discussed. It is important to mention that olfactory hypersensitivity or an aversion to smell (osmophobia) and somatosensory hypersensitivity or an aversion to light touch (cutaneous allodynia) are also prevalent in migraine, both ictally and interictally.(539–542) However, in this PhD thesis, we have chosen to focus on vision and audition, which constitute the most prevalent sensory complaints interictally, leaving olfactory and somatosensory hypersensitivity outside of the scope of this thesis [for a review of these two modalities see: (543–545)].

1.5.1.1. Visual sensitivity in migraine

During the interictal phase, many patients continue to report visual hypersensitivity,(55,56) which significantly contributes to the IIB (58) and has also been associated with an increased prevalence of psychiatric comorbidities, including anxiety and depression.(546) In one study, patients with migraine reported a significantly increased number of visual stressors in their environment outside of the headache attack, as a consequence of **enhanced visual sensitivity**, including

sensitivities to glare, flicker, alternate light and shade, contrasting patterns, fluorescent lights, and color.(536,547) To provide additional support to the results of self-report questionnaires and population-based studies, psychophysical **discomfort thresholds would also appear to indicate an increased sensitivity to light**; with patients reporting stimuli as more bothersome at lower light intensities than HC.(55,535) Patients also report more discomfort to grating patterns than HC.(548) This apparent hypersensitivity to visual stimuli, could be related to altered function of one of the candidate pathways of visual hypersensitivity (see section 1.3.3.). First of all, ipRGCs, which are implicated in all three pathways are particularly sensitive to blue light with a particular impact on inflammation of the trigeminal ganglia,(549) and blue light in patients with migraine has been found to exert the greatest amount of photophobia.(550) Furthermore, research studies administering painful stimuli to the face and chin, shown to activate the trigeminal nerves (see Figure 30), found that patients with migraine during the interictal period reported a decreased tolerance to light, post-nociceptive stimulation, as compared to HC.(551–553) Photic stimulation also decreased trigeminal nociceptive thresholds in patients with migraine interictally as compared to HC.(553) These results, taken together would appear to indicate an exacerbated interaction between visual and trigeminal pathways in migraine.(41)
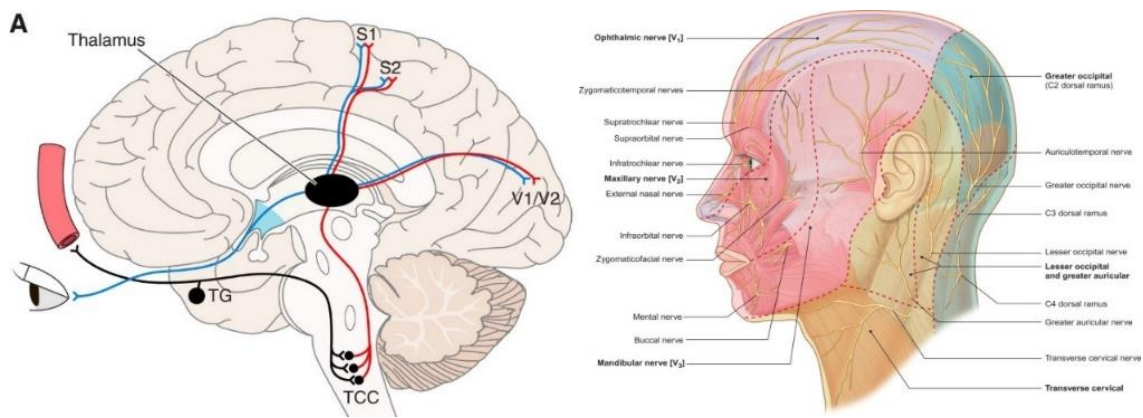
Figure 30. A schematic representation of one of the candidate pathways thought to underlie photophobia, which has been highly related to migraine (on the left) and an anatomical representation of the trigeminal nerves (on the right). Specifically, light entering the eye undergoes transduction and travels from the retina, via the optic nerve, to posterior thalamic neurons. These thalamic neurons also receive nociceptive information from the dura mater, via the trigeminothalamic tract. Therefore, convergence of both photic and nociceptive signals occurs here. This information is transmitted further to areas of the cortex, in particular S1 and S2, related to nociception and the visual cortex, resulting in photocephalodynia and visual hypersensitivity. Reproduced from Goadsby (97) and Fillmore and Seifert.(554)

Neuroimaging studies, using fMRI and PET, have yielded additional insights into sensory sensitivity in interictal migraine. First, heightened blood-oxygen-level-dependent (BOLD) responses in visually driven functional areas have been reported in response to visual stimuli in patients with

migraine, although some studies found the increase in the visual occipital cortex while others found it in associative cortical areas, or both [for a review see Table 1 of (545)]. Other areas that have been shown to have greater activation in patients with migraine interictally are the LGN and the middle temporal cortex, related to motion processing,(555,556) which may suggest that in patients with migraine, hypersensitivity may not necessarily be limited to the visual cortex. In fact, the LGN receives its inputs from the optic tract fibers and the occipital pole, thought to contain the primary visual cortex and association areas, as well as underlie visual processing.(557) This increased pattern of activation, specifically in MA, has been proposed to underlie visual aura, with the hypothesis that greater activation of these areas may lead to CSD.(558,559)

1.5.1.1. Auditory sensitivity in migraine

Aside from visual hypersensitivity, patients also report auditory hypersensitivity and discomfort during the interictal phase.(538) In one study, results from the Large Analysis and Review of European housing and health Status (LARES) survey were used to assess the impact of common everyday noise sources on subjective annoyance and stress and the relationship to different illnesses, including migraine. They found that participants that reported severe or chronic annoyance in response to environmental noise were also at an increased risk of migraine.(560) Furthermore, and similarly to the visual domain, **patients with migraine also report decreased auditory discomfort thresholds** [(55,56,215,561) despite (263)] in response to auditory stimuli, indicating that at lower sound intensities, patients report the stimuli as more bothersome compared to HC. Importantly, this does not appear to be as a result of differences in hearing, given that auditory detection thresholds were not reported as being significantly different between patients and HC.(55,215) This does not however definitively clarify whether differences in sensitivity occur as a result of altered sensation (e.g., damage to receptors or pathways) or perception. In one study that we recently published, the role of protective behaviors (e.g., avoidance) were evaluated to see their impact on auditory discomfort thresholds in patients with migraine interictally and HC.(215) Three different psychophysical methods were used with different levels of predictability including the method of limits [adapted from (561)], the method of constant stimuli, and the adaptive method. The method of limits involves gradually incrementing the intensity of the delivered sound until the participant reports discomfort and is considered highly predictable,(562,563) which may be conducive to the use of protective behaviors to avoid higher intensity sounds. In migraine research, this method is the most commonly used to measure sound aversion thresholds.(55,56,263,561) The method of constant stimuli, on the other hand, consists of pseudorandom delivery of auditory stimuli at different and unpredictable intensities. Interestingly, the only study to utilize this method in patients with migraine,

did not find differences in auditory hypersensitivity between patients and HC.(564) Finally the adaptive method determines the resulting stimulus intensity on each trial based on the stimulus intensity and subsequent response of previous trials and is considered to be moderately predictable. The results of our study yielded lower discomfort thresholds using all three methods in patients compared to HC (see Figure 31), which would suggest that although avoidance behavior may have a modulatory effect on discomfort thresholds and should be considered in future studies, it does not appear to explain auditory hypersensitivity in patients with migraine.(215)

Given the significant literature on the topics of both visual and auditory hypersensitivity, it is important to delve deeper into the mechanisms, which might explain their occurrence. Some studies have suggested alterations in underlying cortical excitability or a habituation deficit as a potential mechanism to explain sensory hypersensitivity in interictal patients (565,565,566) however more research on this topic remains to be done. Furthermore, it remains unclear whether hypersensitivity occurs due to exogenous or endogenous, sensory or attentional impairments, for example through altered 'filtering' of incoming stimuli or difficulty disengaging.
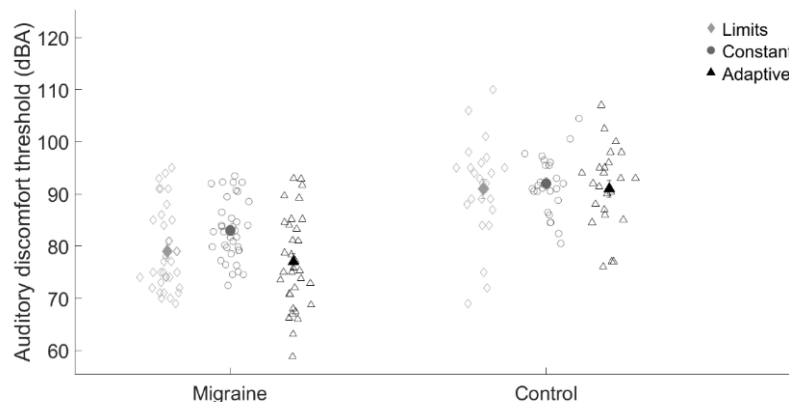
Figure 31. Discomfort thresholds are presented for each experimental method and for migraine patients and headache-free controls. Each symbol represents an individual data point (participant) with diamonds being used for the method of limits, circles for the method of constant stimuli, and triangles for the adaptive method. The filled symbols represent the mean and standard error of the mean for each condition. Reproduced from Ikumi et al.(215)

1.5.2. Cortical excitability in migraine

Nowadays there is a strong push for migraine to be viewed as **a disorder of altered brain excitability** (see Figure 32).(567) This notion would actually date back to the discovery of the CSD,(568) although support for this theory comes from psychophysics, genetic studies, single-pulse, paired-pulse and repetitive pulse transcranial magnetic stimulation, transcranial direct current stimulation, and ERPs [for a review see: (101,569,570)]. Patients with migraine frequently report a

greater number of sensory illusions, perceptual alterations, and increased discomfort to both visual and auditory stimuli interictally, which some researchers have suggested may be a consequence of a hyperexcitable [visual or auditory] cortex.(566,571–575)

Genetic evidence from familial hemiplegic migraine (FHM) would also provide support for theories of migraine as a disorder of altered brain excitability, although it is important to note that susceptibility loci relative to common migraine remain to be identified, likely due to its polygenic and multifactorial nature [see (576) for a review]. In particular, mutations of certain genes in different types of FHM have been related to increased brain excitability. In FHM type 1, P/Q calcium channel gene mutations have been related to increased excitatory neurotransmitter release (577) whereas in FHM type 2, alterations in sodium and potassium ATPase genes have been related to increased neuronal excitability.(578) Finally, in type 3, mutations in sodium channel genes, have been shown to underlie more frequent action potentials.(579) All of these would appear to support a general propensity for hyperexcitability, at least in FHM, although the relation to specific phases is unclear.

Additionally, in terms of transcranial magnetic stimulation some studies have reported **higher phosphene prevalence and lower phosphene thresholds interictally**, neurophysiological correlates of hyperexcitability, in the primary visual cortex of patients with migraine [(580–584) despite (585,586)]. This proposed hyperexcitability has been primarily linked to the occipital cortex.(587) Nonetheless, MT phosphene measures have been subject to criticism with regard to their subjectivity and large amounts of heterogeneity,(588) which some researchers have related to patient heterogeneity and inadequate control of migraine phase, among other things.

ERPs, on the other hand, may provide a more stable measure, particularly if elicited using the PR task, which is well-validated and highly recommended for use in clinical studies (see 1.3.6.1.).(342) In electrophysiology, the amplitude of cortical EPs is thought to be closely related to changes in cortical excitability and in research studies on interictal migraine, **abnormal (both hyper- and hypo-excitability) cortical excitability has been reported in patients** as compared to HC, defined according to PR-VEP amplitude measures (increased or decreased respectively) [for a review see (101)]. Specifically, some studies reported attenuation of the typical PR-VEP components [N1, P1, N2] amplitudes (589–591) whereas others reported enhancement [(592–595) despite (596–600)]. Also, many studies using PR-VEPs to study cortical excitability in patients with migraine have used a peak-to-peak amplitude difference measure, such as N1-P1 and P1-N2 to avoid the distortion of later component amplitudes [e.g., P1] by earlier components [i.e., N1].(120) In this case, some studies once again reported a decreased peak-to-peak amplitude (601) whereas others reported an increase [(602–605) despite (606–609); for a review see (101)]. In both cases, these alterations have been proposed to underlie sensory hypersensitivities.(594)

Upon reviewing the body of literature related to PR tasks in migraine, 26 out of 60 studies reported alterations in early components of visual processing whereas 34 out of 60 did not (see Appendix 1 for a full summary of results). The results of all these studies would appear to yield two theories related to altered cortical excitability in migraine, which continue to be hotly debated. The first is a general theory of **cortical hyperexcitability**,(580,610,611) which could be due to either **increased excitation** (612) or **decreased inhibition** (581) [see (576), for review]. The second is a theory of **cortical hypoexcitability** thought to be due to **low preactivation levels of sensory cortices** (101,581) resulting from either decreased serotonin uptake or thalamocortical dysrhythmia.(101) Finally, other researchers have proposed a general cortical dysexcitability due to the presence of deficient regulatory mechanisms (613–615) with some preferring to use the term 'hyperresponsive' to describe the alterations in cortical excitability found in patients with migraine.
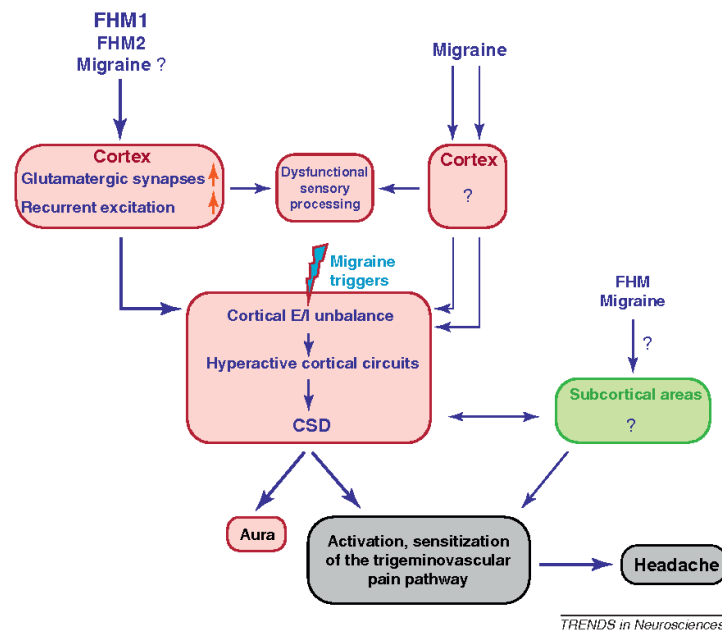
Figure 32. Schematic representation of migraine as a disorder of altered brain excitability. Specifically, migraine involves a dysregulation of the excitation/inhibition (E/I) balance. In familial hemiplegic migraine and potentially also migraine, repetitive glutamatergic neurotransmission may lead to impaired cortical circuits, which result in an E/I unbalance. This may lead to altered sensory processing as well as neuronal hyperactivity, which may underlie CSD and activation of the pain pathways leading to headache. It is also possible that subcortical areas are also impaired, although research is still unclear. Reproduced from Vecchia and Pietrobon.(576)

1.5.3. Habituation and sensitization in migraine

Another reason why patients with migraine may experience altered sensory-attentional processing is due to impaired, internal adaptive mechanisms. Jean Schoenen and colleagues were the first to report a deficit of habituation in patients with migraine during the interictal period as compared to HC, using PR-VEPs.(341) Previous studies often used averaging across stimuli in an attempt to

study sensory alterations, which could hide underlying processes such as habituation and/or potentiation.(341) To control for this, Schoenen et al. separated the continuous PR-VEP recording into temporal blocks [n trials per block] and compared the peak-to-peak amplitudes of N1-P1 and P1-N2 over blocks.(341) Normal habituation would suppose a decrement of these measures over time, however, in patients with migraine this expected decrease was not found and, in some cases, an increment of these components at later blocks was observed, indicating **potentiation**. In patients with migraine, a number of studies have confirmed this deficit of habituation interictally (101,341,606,607,616–621) [for a review see (622)] although this is not always the case (604,608,609,623–626) [see Appendix 2 for a literature review]. Some researchers have even termed this **habituation deficit as the hallmark of interictal migraine** (622) although this has been under some scrutiny.(625–628) Importantly, this lack of habituation appears to be modulated by migraine phase, appearing interictally in patients with EM, but normalizing ictally [(347,617) see Figure 33 and Figure 34].
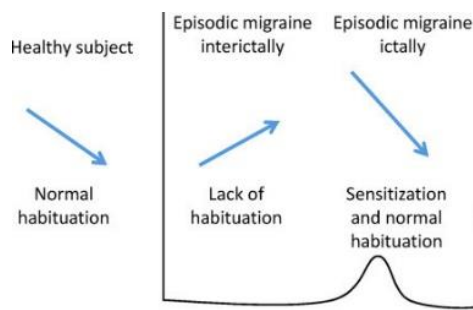
Figure 33. Habituation in patients with migraine as compared to healthy controls, accounting for phasic changes. Reproduced from Coppola et al.(9)
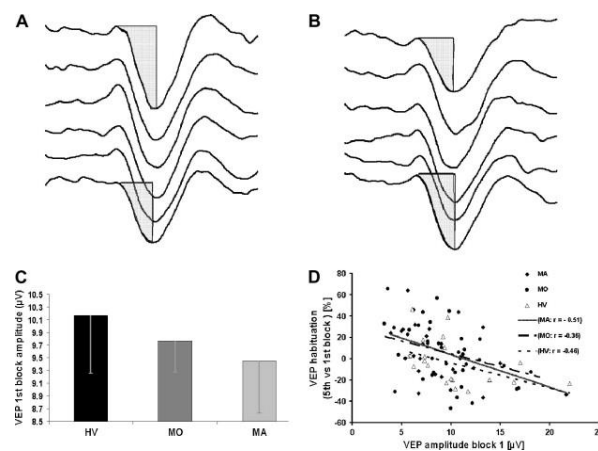
Figure 34. A. Pattern-reversal visual evoked potentials (PR-VEPs) are shown for both a headache-free control, HC (A) and a patient with migraine, M (B). Note that each line represents a block from Block 1 (top) to Block 6 (bottom). A decrease over blocks can be observed for the HC but not for M where the first block amplitude is reduced (C). Finally, in D we can observe a negative correlation between VEP habituation and first block amplitude, suggested to indicate that habituation depends on cortical pre-activation levels. Reproduced from Coppola et al.(622)

In Appendix 2, we assembled the results of 40 studies that assessed habituation in adults with EM and found that 30 reported a deficit of habituation in patients with migraine whereas 10 found normal habituation. However, considering the publication bias surrounding negative studies, which may erroneously inflate positive results, these numbers may not be entirely representative.(629) In an attempt to understand why some studies did not find differences in habituation, a number of aspects were studied. First, clear habituation in HC was only detected when using small check sizes,(604) which would suggest that smaller check sizes may be optimal to observe group differences in habituation, given that bigger check sizes might not elicit the anticipated response decrement. Also, standard analysis methods are lacking given that habituation has been studied using a variety of block ratios, linear regression slopes, least squares slopes and repeated measures ANOVAs among others.(630) This may make it difficult to generalize results and might explain certain discrepancies. Also, as a side note, many of these analysis methods ignore the middle blocks (i.e., only taking into account the first and last block measure), which may contain relevant information. Finally, not all of the previous studies on habituation adequately controlled for preventive treatments and the phase of headache around the time of the recording, which could bias results, particularly if habituation has been shown to vary in a phasic manner alongside cyclic migraine phase. Therefore, it is important to take these things into account prior to running a PR task on patients with migraine.

In the auditory modality, evidence for **an interictal deficit of habituation of AEPs** has also been reported.(631–633) Specifically, paradigms that study the intensity-dependence of auditory potentials (IDAP) have frequently been used and consist of presenting sounds [normally 1000 Hz tones of 50 ms duration] of increasing intensities [40, 50, 60, 70, 80 dB] to participants in randomized order. In patients with migraine, with the exception of one study,(609) the majority have found increased IDAPs when compared to headache-free controls over time, indicating a lack of habituation, and in some cases even potentiation.(606,617,631,632,634) Furthermore, in one study habituation was found to be inversely correlated to IDAP amplitudes, although this is not migraine-specific.(635) Once again, decreased cortical pre-activation levels were suggested to underlie altered habituation.(631)

1.5.4. Attention in migraine

Some of the most frequently reported complaints from patients with migraine outside the ictal phase consist of attention-related deficits and trouble concentrating.(636) Moreover, self-report questionnaires have also suggested a potential relationship between attention difficulties and sensory hypersensitivities,(537) thus guiding future lines of research. The question remains: is migraine a

disorder of sensory processing or does the problem exist at the level of the attentional filter and the mechanisms that gate the entrance of information into the system for further processing?

One of the ways to attempt to objectively quantify the subjective patient experience is through the use of neuropsychological tests, which have yielded somewhat conflicting results [for a review see (636)]. Some of the tests that have been used to study attention in patients with migraine are the Trail Making Test A and B (TMT-A and TMT-B),(637,638) the Digit Span test (DST),(639) Wechsler Adult Intelligent Scale Revised (WAIS-R) Digit Symbol subtest,(640) choice reaction time test,(641), Continuous Performance test (CPT),(642) Stroop test and Stroop Color Word test,(643,644) and the Attention Network Test (ANT).(645) The TMT-A requires participants to draw a line in numeric order between twenty-four numbered circles and is related to visual attention and processing speed whereas the TMT-B alternates between letters and numbers and requires the participant to switch between numeric and alphabetic order, being proposed to measure divided attention, set-shifting, and executive function.(646,647) The results from both TMT-A and TMT-B yielded poorer performance for patients with migraine,(648,649) although some studies did not find these reported group differences.(650–652) The DST Forward test, on the other hand, requires participants to repeat a series of digits back to the experimenter and is often considered a measure of simple attention.(653) In this test, some studies found a deficit in performance in patients with migraine (654) while others did not.(655) Next, the WAIS-R Digit Symbol subtest, linked to working memory, visuospatial processing, and attention consists of participants associating a number with a symbol, with one study reporting slower performance in patients with MA.(656) Choice reaction time tests, on the other hand, require participants to suppress responses to non-target stimuli while attempting to respond as quickly as possible to target stimuli.(657) Here, performance was found to be similar between patients and HC.(648) Finally, with regard to the CPT, associated with both selective and sustained attention, participants were required to respond to a target as quickly as possible when it appears on the screen while ignoring distractors, with no differences being reported.(658) The Stroop test consists of color words (e.g., red), which are presented to the participant in either the same color (red) or different color (e.g., blue) ink. The participant must name the color of the ink out loud. Given that reading is a highly automatic process, it can be quite difficult to name the ink color when the words do not match, an effect referred to as the Stroop effect.(643,644) This ability to suppress interfering information might be altered in migraine seeing as some studies reported differences between patients and HC (650,659) [despite (648,654)]. Finally, the ANT was used to study three separate attentional networks: orienting, alerting, and attentional executive function.(660) Significant differences were found in RTs related to executive function but not to alerting and orienting (654,661) as well as in RTs.(654) These results, coupled with previous

neuropsychological tests including the TMT-A, TMT-B, and DST may support a **potential deficit in attentional executive function**, (654,662) which has been related to conflict monitoring and resolution, attentional shifts, and cognitive flexibility, potentially indicating that **patients with migraine interictally have a hard time suppressing irrelevant information** and/or dealing with tasks that are more cognitively demanding. In fact, one meta-analysis on interictal deficits in patients with migraine found that patients may start to show attentional impairments interictally when tasks require more cognitive resources and have a greater processing demand.(663) Nonetheless, despite their frequent use in clinical studies (664) and the benefits they may provide such as shorter examination time and ease of administration, neuropsychological tests have some important caveats including an important lack of sensitivity and construct validity.(665–668) Therefore, experimental paradigms, particularly if coupled with electrophysiological measures, may provide a better alternative.

In terms of behavioural tasks, specifically the Posner cueing paradigm, some studies found no differences between groups with regard to behavior [RTs (669,670)] whereas others, using a spatial orienting task based on the Posner paradigm found faster RTs and heightened orienting to sudden onset peripheral events in patients with migraine.(671) This final study was particularly interesting given that the authors carried out three separate experiments, two of which were control experiments to ascertain whether other factors might explain the heightened reflexive orienting found in the first. The second experiment allowed them to discard a more general increased attentional response whereas the third provided additional support that the aforementioned differences were not a result of attending to peripheral stimuli.(671) This last study has frequently been cited as preliminary evidence that patients with migraine have a **decreased ability to attenuate behaviorally irrelevant stimuli interictally**, which may be related to the reported lack of habituation and visual hypersensitivities.

One task that has a high degree of efficacy in studying subcomponent processes related to attention and behavioral readjustments to environmental demands is the classic auditory oddball task [see 1.4.5.2 Oddball for an explanation of the task]. In patients with migraine interictally, in the auditory modality, the majority of studies did not find differences in the latencies (672–674) or amplitudes (673,674) of N1, P2 in response to standard and novel tones. However, in one study using a modified auditory oddball task, the N1 was separated into two subcomponents, one of, which [component III] appears when the interstimulus interval (ISI) is more than 4 s and is frequently termed the orienting component [appearing 100 – 120 ms post-stimulus and usually observed at F3, Fz, F4, and Cz electrodes].(127) This component was found to be increased to the first stimulus (always a standard) in patients with migraine as compared to HC, potentially indicating intensified orienting of

attention to unattended auditory stimuli.(675–677) In terms of the MMN amplitude, several studies reported a lack of group differences between patients with migraine and HC.(678,679) On the other hand, some studies found a reduced P3a (680) and/or a reduced P3b (673,681) in migraine, in response to target or deviant stimuli, although this is not always the case.(672,674,679) Results from active oddball paradigms would also appear to be in the direction of reduced P3b amplitudes in patients with migraine.(682) Finally, the RON was evaluated using a modified oddball paradigm (683) and was found to show an increased amplitude. These findings would suggest an impaired response to unexpected or unattended auditory stimuli. Furthermore, given that some studies reported alterations in response to standard stimuli (such as in the N1), this would suggest that patients display increased orienting towards environmental stimuli [see Figure 35].(671,683) This is consistent with theories suggesting that differences in sensory-attentional processing in patients with migraine can be attributed to signal-to-noise issues, in that patients struggle to focus on target stimuli in the presence of distractor noise.(570,588,684) Importantly, despite the advantages offered by time-frequency measures, including providing additional insights about general, underlying processes and offering a more direct link to study potential alterations in thalamocortical activity, **power or phase-synchronization metrics have not been examined in auditory processing in migraine**.
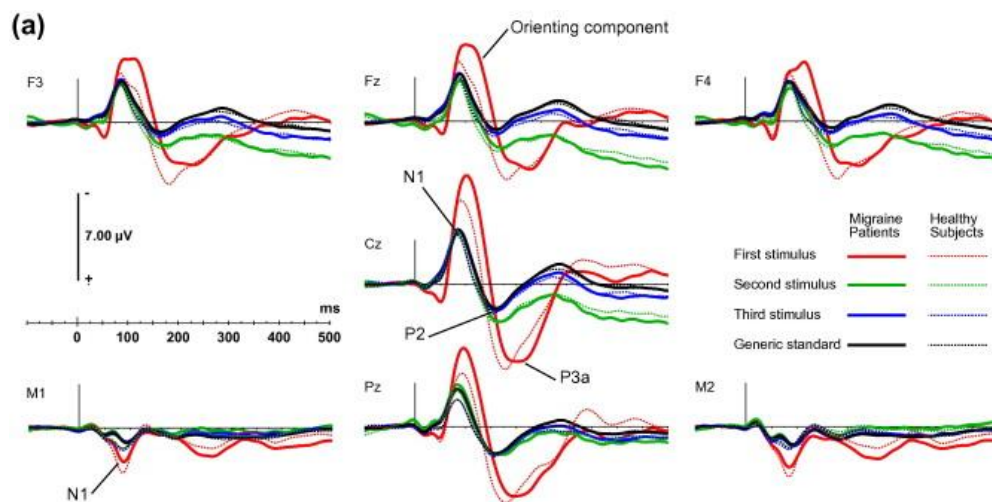
Figure 35. The event-related potential (ERP) waveforms represent the grand average of the response to the first three stimuli (all standard; red, green, and blue, respectively). The black line represents the general response to standards. The results of both migraine patients (lines) and headache-free controls are shown. Notice the exacerbated N1 in response to the first stimulus in patients with migraine. Reproduced from Demarquay et al.(675)

Visual oddball paradigms have seldom been used in migraine, however, some have found delayed latencies of N1 and N2 components in response to novel stimuli,(685) while others have reported increased N2 and P3 amplitudes in response to deviant stimuli.(686) Once again, this would provide support for the notion that migraine patients showcase difficulties in processing irrelevant

81

stimuli.(671) In general, the evidence would tentatively support **abnormal processing and trouble suppressing irrelevant and/or infrequent stimuli** (654,671) with **increased attentional orienting** to sudden-onset stimuli.(671)

Although only a small number of neuroimaging studies have assessed networks related to attention, Mickleborough et al. assessed patients during the performance of a visual spatial-orienting task as compared to controls.(670) They found decreased activation of the right temporal-parietal junction, part of the ventral fronto-parietal network, which has been suggested to respond to task-relevant stimuli, occurring at unattended locations (387) as well as disengaging and re-orienting attention. This may provide additional support to the proposed theories that patients have trouble processing, selecting, and responding to stimuli in unattended space.

1.5.5. The role of endogenous and exogenous processes in migraine

One of the, as of yet, unresolved questions with regard to sensory-attentional alterations in patients with migraine interictally, is whether impairments occur as a result of exogenous, stimulus-driven mechanisms or endogenous, top-down ones.(683) Results from the literature would appear to support impaired exogenous processing, as seen in the results from PR and oddball paradigms as well as studies using flash stimulation. In particular, components such as the visual N1, P1, and P1-N1 as well as the auditory N1, P2 tend to be exogenous in nature and in some studies were found to be altered in terms of amplitudes and/or latencies.(594,604,675–677) Additional support for impaired exogenous processing can also be pulled from SSEP studies. In particular, patients with migraine have been found to show increased photic driving or the "H response".(687) However, many ERP components that tend to be exogenous also show some level of modulation by top-down factors. Furthermore, the nature of the EEG waveform makes it difficult to dissociate evoked activity from the underlying endogenous processes. Therefore, it remains difficult to ascertain whether impairments occur due to alterations in bottom-up exogenous or top-down endogenous mechanisms, or both.

In recent years, there has been growing interest in top-down processes in migraine. Some tentative evidence for endogenous dysfunction comes from the results of studies examining later latency components, which tend to be endogenous such as the contingent negative variation (CNV) and the P300, which have been found to display abnormal amplitudes and latencies.(672,674) In one study, endogenous top-down mechanisms were explored using a visual attention task,(671) following the finding that visual alterations in migraine are often related to the extrastriate visual cortex (688–690), linked to top-down modulations of sensory excitability.(691,692) This study found a late phase effect of lateral-occipital P1 at the parafovea and an increased amplitude of N1 for unattended stimuli at the fovea in patients with migraine. HC also showed an early phase effect of P1, therefore a lack

of this finding in migraine was suggested to represent decreased suppression of unattended stimuli interictally. The N1 results on the other hand, might be linked to altered discrimination of visual stimuli, which may actually lead to enhanced performance. In this study, the authors suggested that top-down processes may be altered in interictal migraine although they may not necessarily have a negative impact on performance. Migraine has also been frequently referred to as a **disorder of impaired inhibitory control** (581,693,694), which would align with one of the main functions of top-down processing, to filter out irrelevant stimuli through the use of inhibitory mechanisms. Increased synchronization of the endogenous alpha-band to repetitive stimuli has also been reported,(695,696) which may be related to altered thalamocortical gating.(238,697) This event-related synchronization has also been shown to persist for longer in patients with migraine, alongside a lower de-locking index to deviant stimuli,(698) which would, again, support the notion that patients struggle to shift attention away from irrelevant stimuli, a top-down function. Increased alpha has frequently been reported in migraine,(699,700) which is important given alpha's role in filtering sensory information.(701) These findings would suggest that endogenous alpha may be abnormal in migraine, suggesting that this frequency band may be the ideal candidate if looking to study bottom-up and top-down mechanisms.

Importantly, due to the type of paradigms used in migraine literature, it remains unclear whether sensory-attentional alterations occur as a result of impaired exogenous or endogenous mechanisms. In particular, since the majority of studies did not separate endogenous activity from the influence of evoked responses, conclusions remain tentative, leading to the interest of this research thesis. To the best of our knowledge, no studies in migraine have managed to definitively isolate top-down endogenous processes from exogenous influence.

1.5. KEY MESSAGES

1. Sensory alterations, including visual and auditory hypersensitivity have frequently been reported in the interictal phase of EM.
2. These sensory alterations have been proposed to be linked to differences in cortical excitability and a lack of habituation in patients with migraine interictally. In fact, migraine has been proposed to be a disorder of altered brain excitability although it remains unclear whether this occurs as a result of hypo- or hyperexcitability.
3. Patients also frequently report attentional difficulties.
4. Finally, it remains unclear whether the alterations in patients with EM interictally occur as a result of altered bottom-up, exogenous or top-down, endogenous mechanisms.

2. HYPOTHESES

As can be seen in the vast literature on sensory-attentional processing in EM interictally, many aspects remain to be elucidated. The use of neurophysiological correlates permits us to better study the temporal stages of sensory-attentional processing while also investigating more general underlying processes through the use of fine-grained measures such as ERPs and time-frequency measures, which better capture individual differences. In this PhD thesis, we wanted to better understand the nature of sensory-attentional processing in EM interictally using neurophysiological correlates (see Table 6 for a comprehensive breakdown of the research studies, techniques, sensory-attentional processes, and hypotheses of this PhD thesis).

To begin and given that previous research studies did not effectively isolate the exogenous and endogenous mechanisms of sensory-attentional processing in migraine, we wanted to design a paradigm, that would allow us to better study these processes [*Research Study 1: The influence of temporal unpredictability on the electrophysiological mechanisms of neural entrainment*]. We focused on neural entrainment and modified a pre-existing task,(484) reducing temporal predictability, checking that the resulting neural entrainment met the requirements for neural entrainment in the narrow sense (482,491) to ensure that the task was suitable for comparing headache-free controls and patients with EM. Additionally, we checked that this task would permit us to assess exogenous processing while also obtaining an uncontaminated measure of endogenous neural activity, free of evoked [exogenous] influence on target-absent trials.(465,702) **We hypothesized that in Research Study 1 if the conditions for neural entrainment in the narrow sense are met, then alignment between the internal oscillators and external rhythms should persist providing an uncontaminated measure of endogenous neural activity on target-absent trials, despite reduced temporal predictability.**

Next, given the advantages provided by neural entrainment to assess both exogenous and endogenous mechanisms of sensory-attentional processing, we decided to administer this task to patients with EM, interictally [*Research Study 2: Neural entrainment of alpha-band oscillations in patients with migraine*]. Exogenous mechanisms have been proposed to be altered in migraine (101,341,687) with some evidence for potential alterations in the endogenous system.(101,673,696,698) Nonetheless, these results are speculative given the continuous nature of the waveform and the fact that many electrophysiological activities overlap with each other or result from the sum of underlying components.(120) Therefore, neural entrainment provides the necessary tool to study exogenous and endogenous mechanisms of sensory-attentional processing in patients with migraine. Furthermore, we specifically entrained alpha band oscillations, given that alterations in this frequency range have previously been reported in EM, interictally.(695,696) **We hypothesized**

that in Research Study 2 patients with migraine would entrain less, indicated by less alignment of alpha oscillatory activity with the entraining signal as compared to headache-free controls, thus indicating altered endogenous processing while also showing an incremented response to the entrainers, indicative of altered exogenous processing.

The results of Research Studies 1 and 2 should permit us to design a neural entrainment task to study exogenous and endogenous mechanisms of sensory-attentional processing and then apply it to patients with interictal episodic migraine.

The following research studies [3 and 4] were planned to assess whether the sensory-attentional alterations reported in the literature, were an accurate representation of the impairments reported by patients with EM, interictally. First, a PR task was used to study the neurophysiological correlates of exogenous, visual processing in patients with EM in the interictal phase. To accomplish this, we carried out two experiments with two distinct samples of patients with EM and a similar PR task, used to evaluate the same processes in both [*Research Study 3: Exploring sensory sensitivity, cortical excitability, and habituation using the pattern-reversal task across the episodic migraine spectrum: A case-control study*]. In particular, we wanted to check whether patients with EM in the interictal phase reported altered sensory sensitivity using a perceptual measure (the SPQ) and then examine, using PR-VEPs, cortical excitability and habituation measures, related to exogenous processing of visual stimuli. In this modality, sensory hypersensitivity, abnormal cortical excitability, and a deficit of habituation have frequently been reported [(55,101,341,703) despite (623,625)]. **Therefore, for Research Study 3, we hypothesized, that patients with EM in the interictal phase should report impaired exogenous sensory processing; specifically visual hypersensitivity, altered cortical excitability, and a lack of habituation**.

Finally, and given negative results in the visual modality, we turned to the auditory modality, and studied, with an active auditory oddball task, whether the neurophysiological correlates of exogenous and endogenous, sensory-attentional processing are altered in patients with migraine, interictally as compared to HC [*Research Study 4: Neurophysiological correlates of abnormal auditory processing in episodic migraine during the interictal period*]. The concepts of sensory sensitivity, cortical excitability, habituation, attentional orienting, and processing of repetitive stimuli were analyzed. However, this time we added the use of power and phase synchronization measures, which have not been used to study auditory processing in oddball tasks in the migraine literature, previously. Past ERP studies on interictal, EM compared to HC reported hypersensitivity, increased cortical excitability, and a lack of habituation.(101,215,263,635,704) **Consequently, we**

hypothesized that in Research Study 4 patients with migraine should present auditory hypersensitivity, increased cortical excitability, and a lack of habituation in both ERPs and time-frequency related measures.

The results of both Research Studies 3 and 4 should provide some clarity as to the nature of the neurophysiological correlates of sensory-attentional processing in interictal episodic migraine.

Table 6. Research paradigms and sensory-attentional processes that will be studied in this research thesis.

Research paradigm	Analyses	Sensory-attentional processes and mechanisms studied	Hypotheses
Cued visual detection task with bilateral entrainment	Time-frequency Phase alignment	Visual processing visual detection selective attention (spatial and temporal) neural synchronization (photic driving, neural entrainment)	[i] Alignment between the internal oscillators and external rhythms should persist providing an uncontaminated measure of endogenous neural activity on target-absent trials [ii] Altered exogenous and endogenous sensory-attentional processing; specifically, incremented response to the entrainers, and less entrainment shown by a decreased alignment of alpha with the driving signal, in patients with EM interictally as compared to headache-free controls
Pattern-Reversal + SPQ	ERPs SPQ scores	Visual processing visual sensitivity cortical excitability habituation	[iii] Impaired exogenous sensory processing; specifically visual hypersensitivity, altered cortical excitability, and a lack of habituation in patients with EM interictally as compared to headache-free controls
Oddball	ERPs Time-frequency	Auditory processing target detection saliency processing novelty processing attentional orienting	[iv] Impaired exogenous and endogenous sensory-attentional processing; specifically auditory hypersensitivity, increased cortical excitability, and a lack of habituation in both ERPs and time-frequency related measures in patients with EM as compared to headache-free controls

3. OBJECTIVES

Main objective (MO):

MO1. To study the neurophysiological correlates of sensory-attentional processing in episodic migraine during the interictal period

Secondary objectives (SO):

SO1. To develop a task to study the exogenous and endogenous mechanisms of sensory-attentional processing

SO2. To study the exogenous and endogenous mechanisms of sensory-attentional processing in patients with episodic migraine in the interictal phase, using a neural entrainment task and time-frequency analyses

SO3. To assess the exogenous mechanisms of visual sensory processing in patients with episodic migraine in the interictal phase, using the pattern-reversal task and event-related potentials

SO4. To investigate the exogenous and endogenous mechanisms of auditory sensory-attentional processing in patients with episodic migraine in the interictal phase, using an active oddball task and event-related potentials as well as time-frequency analyses

4. METHODS

The focus of this thesis was to study sensory-attentional processing in patients with EM interictally as compared to headache-free controls. To accomplish the main and secondary objectives, four different studies were carried out. All studies administered a battery of questionnaires and EEG recordings alongside computer-based tasks. The research studies were approved by the Clinical Research Ethics Committee at the Vall d'Hebron University Hospital and all participants provided their informed written consent, prior to participating. Furthermore, data was collected using coded databases in accordance with the Personal Data Protection Law.

In the studies that recruited patients with migraine, headache diaries were assigned to both patients and controls to determine a baseline headache frequency and provide information relative to migraine phase during the experimental session. For the purposes of this PhD thesis, the student created a digital, headache diary (eDiary) based on ICHD-3 criteria (6) and a set of seven criteria proposed by Hundert et al.(705) The eDiary was hosted using research electronic data capture (REDCap) tools, at the Vall d'Hebron Institute of Research (VHIR) and a daily, automatic reminder system was set up, consisting of an e-mail sent to the participant every evening at the same time, to improve adherence. Participants were instructed to fill out the eDiary every day at the same time, to respond keeping in mind the last 24 hours, and to be as honest and accurate as possible. The eDiary collected information about the presence of headache and its characteristics including intensity, duration, accompanying symptoms, and acute medication as well as additional information about menstruation, sleep-wake cycle, and medication use. Some key points to note [following Hundert et al. (705)] are that the headache diary:

[1] was created with the help of neurologists and a headache nurse specialist who provided their clinical and headache specialist expertise,

[2] has undergone testing over a period of four years [2018-now], to ensure that it is a reliable method of data collection, with updates being made according to patient and neurologist/specialist nurse feedback,

[3] measures clinically relevant headache variables, according to ICHD-3 criteria,(6) and feedback from the Headache Unit's neurologists and headache nurse specialist,

[4] is considered a usable and well-functioning measurement tool,

[5] includes customizable answer options,

[6] uses branching logic and a variety of linking options for multiple variables,

[7] permits data to be exported outside of the software (RedCAP) for analysis purposes.

Furthermore, our eDiary collects information even on days where no headache has occurred, which many eDiaries and headache diary apps do not do.(705) Also, all of the control participants in our research studies, had to fill out a headache diary for at least 30 days prior, during, and 24 hours after the experimental session, similarly to those who were classified as patients. We added this extra screening because control participants may sometimes downplay headaches, which after careful screening may discard them as headache-free participants. In fact, in one study over 30% of control participants needed to be excluded due to multiple headache days post-baseline screening, with the authors emphasizing the importance of careful screening to avoid introducing bias into the sample, which may reduce the odds of finding between-group differences.(10)

Some of the results of this research thesis have already been published in scientific journals (see Appendix 3 and 4). The remaining studies have been presented at scientific conferences as oral communications and posters and are currently being prepared for submission for publication.

4.1. Developing a task to study the exogenous and endogenous mechanisms of sensory-attentional processing

Secondary objective 1 of this research thesis was to design a paradigm that would allow us to study the exogenous and endogenous mechanisms of sensory-attentional processing [*Research Study 1: The influence of temporal unpredictability on the electrophysiological mechanisms of neural entrainment*] (Appendix 3). The methodological aspects will be discussed upon continuation.

Participants

36 young adults (all females, 21.69±2.06 years old, range: 18-28 years) were recruited to participate in this study. All participants were right-handed and had normal or corrected-to-normal vision and hearing. General exclusion criteria included: known morphological brain abnormalities, severe neurological or psychiatric illness, chronic pain conditions, the use of pharmaceutical or non-pharmaceutical drugs that may alter the EEG waveform, and pregnancy. The data obtained for use in this study was part of a prospective case-control research study on migraine [Research Study 2] and was taken from the control group. Aside from the EEG recording, participants also completed the Adult Attention Deficit Hyperactive Disorder Self-Report Scale (ASRS) (706) and the Beck Depression Inventory-II (BDI-II).(707) This research study was approved by the Ethics Board at the Vall d'Hebron Hospital (PR(AG) 376/ 2017) and all participants provided written, informed consent prior to participating. Upon completion, each participant received 25 euros as compensation.

Procedure and paradigm

The experimental session consisted of: [i] completing a series of psychiatric and experimental session questionnaires, [ii] a 5-min resting state recording, which permitted participants to adapt to the dim lighting, and [iii] a neural entrainment task with EEG. Information related to the psychiatric questionnaires can be found in the section above [Participants], whereas the experimental session questionnaire simply collected information relative to menstruation, sleep quality, pain, and medication at the time of the recording. The EEG recording was performed inside a chamber with acoustic and electromagnetic attenuation and participants sat 0.75 m away from the screen.

The neural entrainment paradigm was based on the one by Kizuk and Mathewson,(484) which consisted of a cued, visual detection task with bilateral entrainment (see Figure 36 A). Attention on target-present and target-absent trials was evaluated accordingly. MATLAB R2017a (The Mathworks Inc., 2017) and Psychophysics Toolbox Version 3.0.13 (708,709) software and custom-made scripts were used to program and present the stimuli on a Sony Multiscan G520 Color Monitor CRT screen (1024 x 768 resolution, 120 Hz refresh rate, 21 cd/m^2 background luminance).

Throughout the entire neural entrainment task, a black, central fixation cross (height, width: 0.5°) was present on the screen and participants were instructed to maintain their eyes on the cross, to reduce ocular artifacts and to ensure they were orienting attention covertly. At the beginning of each trial, a black directional arrow cue (isosceles triangle, height: 1°, width: 0.5°) appeared over the fixation cross (5.26° to the north) for 200 ms. After the offset of the cue, a 675 ms fixation period occurred. Next, a stream of synchronous, bilateral entrainers in the shape of annuli (30.47% gray, 7.3 cd/m^2 luminance, 2.25° external annulus diameter, 1.25° internal annulus diameter) appeared on the screen 1.13° above and 4.1° to either the right or the left of the fixation cross. The number of entrainers was variable [8-12], remaining equiprobable within each block and balanced across conditions. This was done to reduce inherent task predictability. The rate of presentation was set at 12 Hz and the duration of each entrainer was 8.33 ms (equal duration on both sides of the screen) followed by a blank interval of 75 ms (thus ensuring 83.33 ms periods, or a 12 Hz rhythm). After the offset of the last entrainer, a target was presented on the screen on 70% of trials (28 per cued side and 14 per stimulus-onset asynchrony or SOA). The target had a similar appearance to the entrainers, consisting of two bilateral annuli with the same positions and dimensions, however one of the annuli contained a Gabor patch with a spatial frequency of 1.68 cycles/pixel (90° orientation, 2.98 pixels sigma, 0 cycles phase). The contrast of the Gabor patch was set according to an individual detection threshold [see Individual detection threshold below for more information]. The remaining 30% of trials consisted of target-absent trials, where neither the target annuli nor the Gabor patch were shown (12 per cued side and 6 per SOA). As soon as the target appeared on the screen on target-present trials, participants were instructed to respond, indicating the target location with either the z (left side) or m (right side) keys with their left and right index fingers, respectively. If no target appeared (target-absent trials), participants were told to refrain from responding. Participants had 800 ms to respond and were told to do so as quickly as possible while maintaining accuracy. Furthermore, they were told to remain conservative and avoid guessing in the case of uncertainty. Lastly, the inter-trial interval randomly varied between 500 ms and 700 ms. Importantly, target-present trials could either be validly cued, meaning that the target appeared at the location previously indicated by the cue (valid trials, ~71%) or invalidly cued, indicating that the target appeared at the location opposite the one indicated by the cue (invalid trials, ~29%). Furthermore, targets could appear at one of four SOAs, two anti-phase with the previous entrainers (41.66 ms and 125.00 ms) and two in-phase with the entrainers (83.33 ms and 166.66 ms). Therefore, four main conditions were obtained: spatially valid anti-phase, spatially valid in-phase, spatially invalid anti-phase, and spatially invalid in-phase.

The entire task lasted ~ 40 minutes and was subdivided into nine blocks of 80 trials. Participants were allowed to rest between blocks and received a training task prior to starting the

experiment, which consisted of 12 easy to detect trials (90% Gabor contrast, three per condition, random presentation) with the same structure as the main task. Upon completing the training, the individual detection threshold was calculated and then participants went on to do the main task. The entire session lasted approximately 3 hours including preparation and clean-up.
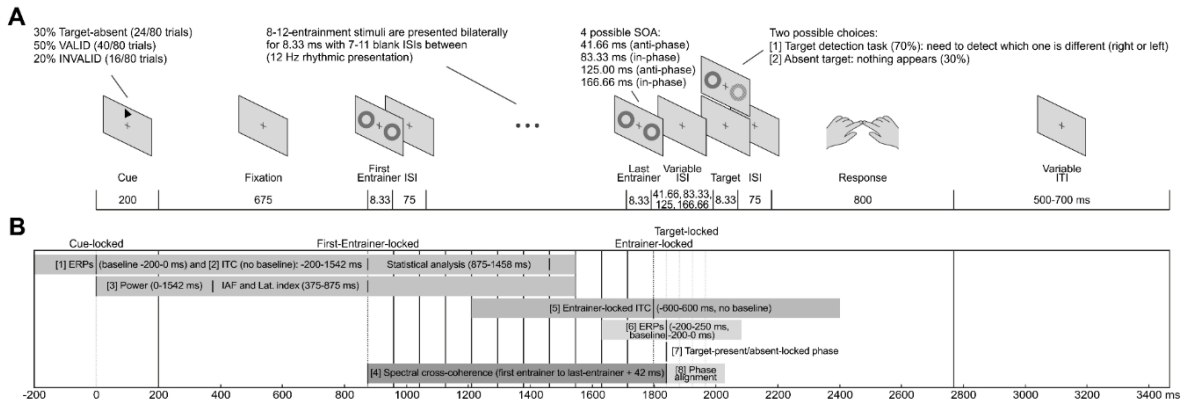
Figure 36. Schematic illustration of a single trial (A) and the time windows used for the neural entrainment task (B). A. Representation of a single trial of the cued, visual detection paradigm with bilateral entrainment. Participants had to fixate on the central fixation cross at all times. Each trial began with the presentation of a directional cue arrow indicating either right or left. After a delay, a series of bilateral, synchronous entrainers (annulus shape) were presented. The sequence of entrainers was variable in length [8-12] and interspersed with fixed inter-stimulus intervals. The inter-stimulus interval between the offset of the last entrainer and target consisted of four different options. Two targets appeared in-phase and two anti-phase with the rhythmic entrainers. Targets appeared on 70% of trials and could occur at spatially valid (gray) or invalid (black) locations and looked similar to the entrainers but with one of the annuli containing a Gabor patch, whose contrast was determined according to a 60% detection threshold obtained prior to the experiment using a single-interval adjustment matrix. On 30% of trials, no target, annuli, or Gabor patch appeared (target-absent trials). Participants were told to respond using the appropriate response keys or withhold their response if no target was present. B. Schematic illustration of the time windows used for each of the analyses. For clarity, entrainer stream length was fixed at 12 entrainers and target-locked analyses were fixed to the first anti-phase target onset. The first analyses used cue-locked data and the following time windows. [i] ERP/SSVEP analyses, time window: -200 ms to 1542 ms (baseline: -200 ms to 0 ms). [ii] Inter-trial coherence (ITC) analyses, same as [i] but no baseline and over the time window of interest from 875 ms to 1458 ms to assess the activity over entrainers 1 to 8. [iii] Power analyses to explore individual alpha frequency (IAF) and lateralized alpha activity over a time window from 0 ms to 1542 ms (no baseline). Spectral power for the IAF and time-frequency lateralization index was obtained between 375 ms and 875 ms. Also, [iv] for the spectral cross-coherence analyses a time window was selected from the onset of the first entrainer to the offset of the last entrainer plus one half cycle (+42 ms), corresponding to the onset of the first anti-phase target. The time window was of variable length depending on the number of entrainers. The next analysis was carried out using entrainer-locked data, with the last entrainer to which activity was locked varying between 8 and 12 depending on the trial. [v] ITC analyses over the time window between -600 ms and 600 ms (no baseline). The final set of analyses used target-locked (target-present or target-absent data), along with their time windows. [vi] ERP analyses, as a function of relative phase (anti-phase/in-phase) on target-present and target-absent trials, time window: -200 ms to 250 ms (baseline: -200 ms to 90 ms). [vii] 12 Hz phase at target onset. Here data were separately time-locked to target onset times (target-present) or when targets were expected to occur (target-absent) and divided as a function of relative phase (anti-phase or in-phase). Finally, [viii] to examine phase alignment post-entrainer offset. This analysis only used target-absent correct trials and looked at a time window from 41.5 ms to 250 ms with respect to the last entrainer, or the equivalent of three cycles of possible target onset times (one cycle was equal to one anti-phase and consecutive in-phase).

Individual detection threshold

To obtain the contrast for the Gabor patch of the target, a single-interval adjustment matrix (SIAM) (710) was used to find each participant's 60% detection threshold. Using a modified version

of the neural entrainment task, with a fixed number of entrainers [10] and only spatially valid, in-phase targets, participants were instructed to respond to targets and refrain from responding if no target was present. In the event of a correct response (hit), the contrast of the Gabor patch on the target stimulus was reduced on the next trial, as a function of the step size. If their response was incorrect (miss or false alarm) the contrast was increased according to the step size on the next trial. A pre-determined adjustment matrix was used to determine the contrast value on the next trial according to the increase/decrease determined by the step size and number of reversals. In this experiment, the step size was set at 0.01 and multiplied by four for the first and second reversal (step size of 0.04), by two for the third reversal (step size of 0.03), and finally by one (step size of 0.01) for the remainder of the reversals. Once twelve reversals were reached, the individual detection procedure was over. To obtain the final mean threshold, the last four reversals were averaged together. Importantly, a separate threshold was obtained for each side (right and left).

EEG recording

Continuous, digitized EEG recordings (500 Hz sampling rate, no online filters) were obtained through a BrainAmp Standard (001 10/2008) amplifier, connected to an actiCHamp Control Box (Brain Products). Electrodes were placed at standard positions and data from 64 active electrodes (10-10 system) was obtained. The ground electrode was positioned at AFz, and an online reference electrode was placed on the nose. Four external electrodes consisting of the left and right mastoids as well as the vertical and horizontal electrooculograms were also used. Impedances were set at 10 kΩ for the duration of the experiment.

Analyses

This research study consisted of a within-subjects design. Each participant completed one experimental session.

Hazard rate

The Hazard rate (HR) was calculated for each target time and served as an objective comparison index of task predictability between this research study and that of Kizuk and Mathewson.(484) To obtain the HR, the probability that a target will occur at time *t* was divided by the probability that the target has not yet occurred:(711)

$$h\left(t\right) = \frac{f\left(t\right)}{\left[1 - F(t)\right]}$$

In this formula, f(*t*) represents the probability distribution of target times whereas F(*t*) refers to the cumulative probability distribution. Due to the variable number of entrainers as well as the four different target SOAs, our study contained 12 different time windows, ranging from 625 ms to 1083 ms, from the offset of the first entrainer to the target onset.

Behavioral analyses

To explore the effect of spatial validity and relative phase, both hit rates and RTs were obtained for spatially valid and invalid conditions as well as for each of the four target SOAs (see Figure 37). If the RT on any trial was less than or equal to 100 ms or greater than three standard deviations (SDs) above the participant's mean RT for the condition (valid/invalid SOA pairing), the trial was excluded (1.17±1.00% of total trials, range: 0-3.04%) and not considered for subsequent analyses. SOAs were collapsed into anti-phase and in-phase conditions. Next, a repeated measures analysis of variance (rmANOVA) was conducted on both hit rates and RTs using a 2 (spatial validity: valid, invalid) x 2 (relative phase: anti-phase, in-phase) design. Both spatial validity and relative phase were within-subject factors. If necessary, post hoc *t*-tests were conducted. Also, the Greenhouse-Geisser epsilon correction was used to correct any violations of sphericity and better estimate epsilon,(712) of adjusted *p* values (p_{adj}). To obtain the effect size of both *t*-tests and rmANOVAs, Cohen's *d* and *f* statistics were calculated.(713) Furthermore, the Bayes factor (BF_{10}) was obtained for the rmANOVAs using JASP software [null model (714–716)] to determine whether the data provided evidence for the alternative model (H1) as compared to the null model (H0). Both spatial validity and relative phase as well as their interaction were included in the model. Finally, to determine whether participants held a response bias (more to less conservative), the response criterion, or the mean of the *z*-score of the hit rate and the *z*-score of the false alarm rate (717) was calculated.

EEG pre-processing

To perform the EEG data analyses, EEGLAB 13.5.4b,(718) ERPLAB 7.0.0,(719) and FieldTrip version 20,161,103 (720) toolboxes, running on MATLAB R2017a (The Mathworks Inc., 2017), were used alongside custom MATLAB R2017a scripts. The mean activity of the left and right mastoid was used to re-reference the EEG activity, offline. Next, a 50 Hz notch filter (type: Parks-McClellan, padding factor 2, smoothing factor 50, sliding window length 4, sliding window step 1, order 180) was applied offline to each recording. No further pre-processing was done for phase analyses. For ERPs, however, an offline band-pass filter (Hamming windowed sinc finite impulse response (FIR), zero-phase) was applied from 0.1 (high-pass: 0.1 Hz frequency, 16501 order, -6 dB

cutoff) to 40 Hz (low-pass: 40 Hz frequency, 167 order, -6 dB cutoff). For ITC, phase, and power analyses no filters were used.

EEG analyses

A detailed description and visual representation of EEG analyses and their corresponding time windows can be found in Figure 36 B. Importantly, five different time windows centered on different trial events were used to analyze the EEG activity. [i] Cue-locked analyses centered on the cue (-200 ms to 1542 ms) and consisting of ERPs, power, time-resolved ITC, and the power spectrum to obtain the IAF. [ii] A cross-coherence analysis used to examine the EEG activity from first entrainer onset to last entrainer offset plus one half-cycle (42 ms). [iii] Entrainer-locked analyses centered on the last entrainer (-600 ms to 600 ms), which included the ITC. [iv] Target-locked analyses centered on the target (-200 ms to 250 ms), which examined ERPs and phase alignment to the times where targets appeared (target-present trials) or were expected to appear (target-absent trials). [v] Persistence of entrainment post-entrainer offset over three cycles of possible target onset times (41.5 ms to 250 ms, centered on the last entrainer). More details about the respective analyses can be found in the following sections. Furthermore, to best assess endogenous activity and ensure that participants were attending to the task, only correct trials (hits or correct rejections) were examined. To ensure an unbiased estimation of the ITC, a minimum of 50 clean, artifact-free trials were required for each condition.(721) ITC, phase alignment, and power analyses were also re-epoched with an additional 2000 ms at each end to avoid edge artifacts. To ensure that trials were void of ocular and muscular artifacts, a visual inspection was carried out on concatenated data, specifically cue-locked, entrainer-locked, and target-locked data. Finally, to replicate the results of Kizuk and Mathewson (484) all of the analyses, with the exception of the lateralized alpha activity, were done using the Pz electrode and additionally repeated at the Oz electrode, where the maximum activity was observed in our research study.

IAF estimation

Cue-locked epochs were used to obtain the IAF, a metric of endogenous activity pre-stimulus [pre-entrainer]. A Hanning window Short Time Fourier Transform (STFT) was used to extract the power spectrum (4-30 Hz, 0.1 Hz step size, zero-padded to 10 s). A time window between 375 and 875 ms post-cue was selected to omit activity, which may be related to the processing of the cue. Furthermore, the length of the time window was selected to have enough cycles to estimate the frequency of interest. In this research study, the power spectrum was averaged across the electrodes of interest, which consisted of PO3, POz, PO4, PO7, PO8, O1, Oz, and O2. A $1/f^{\alpha}$ curve was fitted to

the power spectrum to estimate the background noise.(722,723) Finally, the IAF peak was calculated over a 5-15 Hz window.

Event-related potentials

ERPs were extracted for both cue-locked and target-locked analyses. For cue-locked analyses, ERPs and SSVEPs were obtained over a time window from -200 ms to 1542 ms (baseline -200 ms to 0 ms) and collapsed as a function of target-present/target-absent condition given that the time window did not reach this far. Target-locked ERPs (time window: -200 ms to 250 ms, baseline -200 ms to 0 ms) however, were obtained both as a function of relative phase and target-present/target-absent condition.

Inter-trial coherence

The following analyses were carried out to assess both exogenous and endogenous mechanisms of neural entrainment and to ensure that the entrained activity persisted from the onset of the first entrainer to the offset of the last entrainer and into the target period on both target-present and target-absent trials. To assess this, both cue-locked and last entrainer-locked activity was examined. Frequency-domain multiplication, where the Fourier-derived spectrum was multiplied by a complex Morlet wavelet spectrum with a variable number of cycles (4-10 in logarithmic steps, wavelet time -2 to 2 s), was used to convolute single-trial EEG epochs and obtain the inverse Fourier transform. Separate time series of complex wavelet coefficients, containing both a real and imaginary component, were obtained for each frequency (linear increase of 1 to 40 Hz, 1 Hz steps) and used to extract the ITC (724) for each trial, time point, frequency, and participant. ITC values range from 0 (randomly distributed) to 1 (perfectly aligned) and serve as a metric of phase consistency across trials.(725) For cue-locked epochs (-2200 ms to 3542 ms, time window of interest: -200 ms to 1542 ms), trials were collapsed across target-present and target-absent conditions. Only correct trials were analyzed. For entrainer-locked epochs (-2600 ms to 2600 ms, window of interest: -600 ms to 600 ms), on the other hand, ITC was collapsed across relative phase but separately obtained for both target-present and target-absent conditions. ITC analyses did not use a baseline.

Next, a Montecarlo permutation test (726) was employed to determine whether EEG activity remained significantly concentrated throughout the entrainer stream, specifically with regard to cue-locked data from the onset of the first entrainer to the offset of the eighth entrainer (time window of interest: 875 ms to 1458 ms). For each participant and both Pz and Oz electrodes we obtained a null ITC distribution. Then, for each trial, a randomly chosen phase from the time window of interest was designated and a surrogate ITC was calculated for all of the randomly chosen phases to maintain the trial number constant. These steps were repeated 10,000 times to create a distribution of surrogate

ITCs for each participant, which were then averaged across participants. The proportion of surrogate ITCs which exceeded the ITC was used to calculate an unbiased *p* value.(727) An FDR procedure was used to correct for multiple comparisons on the time series of *p* values (728) and these adjusted *p* values were compared against an alpha of .05 to determine significance.

Spectral cross-coherence

To determine whether the EEG activity and the external entrainers were aligned and therefore provide additional evidence for the presence of neural entrainment, a spectral cross-coherence analysis was executed.(729) Specifically, cross-coherence can provide an index of alignment between two signals, in this case the EEG activity and entrainers, and a peak in the cross-coherence would be anticipated at the entrained 12 Hz frequency. Epochs were separated according to the number of entrainers on each trial [8-12], and a time window from the onset of the first entrainer to the offset of the last entrainer plus one half-cycle (42 ms) was calculated for each one. Only correct trials were included in this analysis. For each epoch length, a series of steps was performed, which included: [i] creating an artificial 12 Hz spiking signal, [ii] obtaining the entire spectrum for both the real and artificial signals, separately using a Hanning window STFT (2.048 padding, frequency range: 1-40 Hz), [iii] calculating the spectral cross-coherence value for each channel, frequency, and participant. The final step was carried out using the ft_connectivityanalysis function in FieldTrip.

Once the spectral cross-coherence values were obtained, a weighted arithmetic mean, of the five different entrainer lengths was calculated for each frequency and participant. The weighting was done according to the number of trials for each of the five entrainer lengths. Next, the peak at 12 Hz was evaluated for statistical significance using the method by Biltoft and Pardyjak.(730) 1024 samples and an average trial number of 351±83 with a mean length of 418 points (ranging from 335 points for eight entrainers to 502 points for twelve entrainers) were used for the FFT estimation. Considering the sampling rate of 500 Hz, the degrees of freedom were set at 143 and the significance cutoff at *p* < .05, implied a peak height of 0.0416 at 12 Hz.

12 Hz phase at target onset on target-present and target-absent trials

Phase opposition during the target period was assessed using target-locked EEG data from correct trials. Importantly, EEG activity was time-locked to target onset (target-present) or expected target onset (target-absent) trials, as a function of in-phase and anti-phase condition. Target-absent trials permitted us to study the endogenous mechanisms of neural entrainment in the absence of evoked (exogenous) activity related to targets. Epochs were selected from -2000 ms to 2000 ms and centered according to target onset or expected target onset. Similarly, to previous analyses, a minimum of 50 artifact-free trials was required for each condition and participant. Single-trial phase

was obtained at 12 Hz for each condition (target-present, target-absent) and participant, separately. Next, these phases were pooled over all trials and participants and a circular V-test (731) was carried out to determine whether the anticipated 180° separation between anti-phase and in-phase trials was present. Also, on target-present and target-absent trials, the mean angular difference for anti-phase and in-phase trials was calculated for each participant as an additional analysis for descriptive purposes only. All circular statistics were carried out using the Circular Statistics Toolbox 1.2.1.(732)

Phase alignment in the absence of external signal

Given the requirements for neural entrainment in the narrow sense, we wanted to see whether neural entrainment persisted for some time after the offset of the rhythmic entrainers, which would provide additional evidence for neural entrainment in the narrow sense. Similarly, to the cue-locked ITC data, a Montecarlo procedure was used to test for statistical significance (see Inter-trial coherence for more details). In this analysis, however, only correct target-absent trials were used, and the time window of interest ranged from 41.5 ms to 250 ms, or three cycles of possible target onset times (one cycle meaning one anti-phase and consecutive in-phase temporal moment).

Control analyses

Five control analyses were carried out using a Hanning windowed STFT of 166 ms length (two cycles of the frequency of interest) to improve temporal resolution and avoid temporal smearing of evoked activity (see Figure 36 for more details). Please note that phases were free of contamination, apart from anti-phase 1. [i] First, last entrainer-locked ITC data for both target-present and target-absent trials was obtained (using the same time window as the analyses carried out using complex Morlet wavelets, -2600 ms prior and 2600 after the first entrainer) and the phase concentration analyses detailed above were executed. [ii] Next, 12 Hz phase was analyzed, centering the activity at target onset or expected target onset and adding 2000 ms at each side. Phase opposition was assessed between anti-phase and in-phase trials and the same statistical analyses were performed as with the complex Morlet wavelets. [iii] Third, circular correlations between the phase at the offset of the last entrainer (10 ms post-onset) and the four expected target SOAs were carried out, for target-absent trials only. This was done to provide additional support to the presence of neural entrainment. A value was obtained for each trial and participant, and the resulting *p* values were combined using the Fisher method (733) across participants, yielding a vector of *p* values over time. Finally, the fourth and fifth analyses examined the effect of 12 Hz phase on performance. For both analyses, EEG data was time-locked 166 ms pre-target and divided according to SOA (anti-phase 1, in-phase 1, anti-phase 2, in-phase 2) and response type (correct, incorrect). 12 Hz phase was obtained for each target onset, response type, trial, and participant as well as RTs for each trial. The fourth analysis, [iv] consisted

of a circular correlation between RT and 12 Hz phase, for each participant and target SOA. The Fisher method (Fisher, 1925) was used to combine *p* values across participants and obtain a single *p* value for each target onset. Finally, the fifth analysis [v] was a phase opposition analysis between correct and incorrect trials. For this analysis, SOAs were collapsed as a function of anti-phase or in-phase. The difference between the mean angle of correct and incorrect trials for each target onset was obtained for each participant and used to calculate a circular V-test.(731) Once again, a 180° separation was anticipated.

Reality check: Lateralized alpha activity

To assess whether participants were orienting attention correctly, alpha activity was analyzed between the cue and entrainer interval to assess preparatory lateralization. Epochs were obtained for cue-left and cue-right conditions (-2200 ms to 2542 ms, window of interest: 0 ms to 1542 ms, no baseline), on correct, valid trials only to ensure proper orienting of attention. A time window of 375 ms to 875 ms post-cue was used to calculate the mean spectral power, which was extracted using a Hanning windowed FFT (zero padding to 1 s). Power was separately obtained for two regions of interest (ROIs) of parieto-occipital electrodes,(186,461) a left ROI (P3, PO3, PO7, P7, P5, P1, PO9, and O1) and a right ROI (P4, PO4, PO8, P8, P6, P2, PO10, and O2). For both cue-left and cue-right conditions (attended-left, attended-right), the average alpha power for the electrodes ipsilateral and contralateral to the cue was calculated. Next the average alpha power of the attended-left (ipsi left minus contra left) was subtracted to the attended-right (ipsi right minus contra right) average alpha power and divided by the sum of the two to obtain an index of alpha lateralization.(186) This index was assessed for statistical significance using a one-sided (right) paired *t*-test against zero. The spectral power analysis was also repeated using a complex Morlet wavelet for illustrative purposes (-2200 ms to 3542 ms time window) and the index of alpha lateralization was computed for the entire time window.

4.2. Assessing the exogenous and endogenous mechanisms of sensory-attentional processing in interictal EM and HC, using a neural entrainment task

Secondary objective 2 of this research thesis was to assess the exogenous and endogenous mechanisms of sensory-attentional processing in patients with episodic migraine in the interictal phase, using a neural entrainment task and time-frequency analyses [*Research Study 2: Entrainment of neural band oscillations in patients with migraine*]. The methodological aspects will be discussed upon continuation.

Participants

61 right-handed, female university students with normal or corrected-to-normal vision and hearing participated in this research study. The participants in Research study 2 participated in two experimental sessions, where they also completed Research Study 3 Experiment 1 [Session 1] and Research Study 4 [Session 2; not all of the participants completed this session]. A neurologist diagnosed 34 participants with EM with or without aura, according to the ICHD-3 (6) diagnostic criteria and the remaining 27 were diagnosed as headache-free controls (HC). The participant groups were age- and gender-matched. All of the participants completed an eDiary for an average of 35±9 days prior, during, and at least 24 hours after the experimental session, which was used to confirm their diagnosis and also to ensure that patients were in the interictal phase at the time of the recording. Participants did not receive confirmation of their diagnosis until the end of the research study and were therefore unsure or unaware of their belonging to either participant group. This helped to ensure that both the researcher and the participant could remain double-blind. Exclusion criteria included severe neurological or psychiatric illness, chronic pain conditions, known morphological brain abnormalities, pregnancy, or the use of pharmaceutical or non-pharmaceutical drugs with an effect on responses or the EEG waveform. In particular, patients could not have been previously diagnosed with CM or any other headache disorder or be using any prophylactic medication, HC could also not have received any previous headache diagnosis or have a first-degree relative with migraine. Importantly, this research study was interested in studying neural entrainment in EM during the interictal period therefore patients that recorded the presence of a moderate or severe headache 24 hours prior, the day of, and 24 hours post-EEG session in their eDiary were excluded from the final sample (72 hour headache-free window). This study was approved by the Research Ethics Board at the Vall d'Hebron Hospital (PR(AG) 376/2017) and all participants provided written informed consent prior to participating. At the end of the study, participants received 25 euros as compensation.

Procedure and paradigm

Participants were contacted through a research participant database provided by the Center for Brain and Cognition at the Pompeu Fabra University and those that replied to the advertisements were sent two questionnaires to complete: [i] a sociodemographic and anthropometric questionnaire, and [ii] a migraine screening questionnaire based on ICHD-3 (6) criteria. These questionnaires permitted the researchers to have an initial filter for inclusion/exclusion. Participants that were designated as fit to continue based on their answers, were subsequently diagnosed by a neurologist and provided with an eDiary to complete. Participants were told to contact the laboratory if they had a headache or were menstruating prior to the experimental session and were rescheduled accordingly.

On the day of the experiment, participants were asked to [i] complete a series of psychiatric, clinical, and experimental session questionnaires, which alongside the eDiary were hosted using REDCap tools at the VHIR. The psychiatric questionnaires included the: BDI-II,(707) State-Trait Anxiety Inventory (STAI),(734,735) and the ASRS.(706) Clinical questionnaires, on the other hand, consisted of the: Headache Impact Test-6 (HIT-6),(736) Migraine Disability Assessment Test (MIDAS),(737) and Migraine-Specific Quality of Life Questionnaire (MSQ).(738) The researchers also collected information relative to sensory sensitivity, using the SPQ (252) and the state of the participant at the time of the research session (experimental session questionnaire), which included information relative to headache, tiredness, and pain. Upon completing the questionnaires, participants underwent a [ii] 5-minute resting state recording, which permitted them to adjust to the dim lighting, and [iii] a neural entrainment task with a simultaneous EEG recording.

The neural entrainment task was the same as the one detailed in Section 4.1. (739) and adapted from Kizuk and Mathewson (484) consisting of a cued visual detection paradigm with bilateral entrainment (Figure 36 A). Experimental set-up, length, and training was also the same as detailed in Section 4.1.

The entire session lasted approximately three hours including preparation and clean-up.

Individual detection threshold

The procedure used to calculate the individual detection threshold was the same as the one described in Section 4.1. For more information please consult 4.1. Individual detection threshold.

EEG recording

The details of the EEG recording were the same as the ones described in Section 4.1. For more information, please see Section 4.1. EEG recording.

Analyses

The following software and toolboxes were used for the statistical analyses: R, (R Core Team, 2021, version 4.1.1), RStudio Software (RStudio Team, 2021, version 1.4.1717), MATLAB R2017a, (The Mathworks Inc., 2017), the Circular Statistics Toolbox 1.21,(732), and custom-made scripts. Meanwhile, for electrophysiological pre-processing and analyses: EEGLAB 13.5.4b,(718) ERPLAB 7.0.0,(719) and the Fieldtrip toolbox for EEG/MEG analysis (720) were used. Please note that the analyses detailed upon continuation are very similar to those used in RS1, with the exception of group comparisons. However, for the ease of the reader, we have decided to maintain all of the information below.

Psychiatric, clinical, and experimental session questionnaires

Categorical variables and scores were reported using percentages, continuous normally distributed variables using means and SDs, and continuous not normally distributed variables using medians and interquartile ranges (IQR). Group effects were assessed using Fisher's exact test or two-sided unpaired t-tests of equal variance if the population variances did not significantly differ. However, if the population variances were not equal, then a two-sided, nonparametric Mann-Whitney U test was applied. Values including W, t, and p were reported.

Behavioral analyses

To assess the effect of spatial validity, relative phase, and participant group, hit rates and RTs were obtained for spatially valid and invalid conditions and the four target SOAs. RTs that were less than or equal to 100 ms and greater than three SDs from the participant's mean RT for the condition were removed. Also, participants with more than 90% accuracy on spatially invalid conditions (519) or a false alarm rate greater than 30% were excluded.(484,739) SOAs were collapsed as a function of in-phase and anti-phase. Next, rmANOVAs with a 2 (spatial validity; valid, invalid) x 2 (relative phase: anti-phase, in-phase) x 2 (participant group: EM, HC) design were calculated for both hit rates and RTs. Spatial validity and temporal validity made up the within-subjects factors whereas participant group was a between-subject factor. Post hoc t-tests were carried out, when necessary. Finally, to correct for potential violations of sphericity a Greenhouse-Geisser epsilon correction was applied, and adjusted p values were reported.

EEG pre-processing

The EEG pre-processing procedure was the same as the one described in Section 4.1. For more information, please consult 4.1. EEG pre-processing.

EEG analyses were divided into five different time windows locked to distinct events. For a pipeline of analyses and their respective time windows see Figure 36 B. [i] Cue-locked analyses (-200 ms to 1542 ms, with respect to the cue) included ERPs, power, time-resolved ITC, and the power spectrum for the IAF. [ii] Cross-coherence analyses (from the first entrainer onset to the last entrainer offset plus one-half cycle (42 ms)). [iii] Last entrainer-locked analyses (-600 ms to 600 ms, from the last entrainer) only included the ITC. [iv] Target-locked analyses (-200 ms to 250 ms, with respect to target onset) were comprised of ERPs and phase alignment analyses on target-present and target-absent trials. [v] Persistence of entrainment after entrainer presentation offset (41.5 ms to 250 ms, with respect to the last entrainer). Only correct trials were included and a minimum of 50 artifact-free trials for each condition was required,(721) to ensure a non-biased estimation of the ITC. To avoid edge artifacts, epochs were reepoched with 2000 ms at both ends for ITC, phase alignment, and power analyses respectively. Furthermore, to ensure artifact-free trials, a manual rejection process and subsequent visual inspection were used to remove ocular and muscular noise. In the previous study (RS1), we observed that the measured effects were the same at Pz and Oz electrodes. Therefore, for the current research study (RS2) we decided to use the Pz electrode, with the exception of the analysis on lateralized alpha activity, which utilized ROIs, given that it is more frequently used in the literature.(484,514,740)

Reality check: IAF estimation

Cue-locked epochs were used to calculate the power spectrum for the IAF for both EM and HC. The first step was to extract the power spectrum using a Hanning windowed STFT (4-30 Hz in 0.1 Hz steps, zero-padded to 10 s) over a time window from 375 ms to 875 ms and average it over the electrodes of interest (PO3, POz, PO4, PO7, PO8, O1, Oz, and O2). Next, a $1/f^{\alpha}$ curve was fitted to the power spectrum to estimate background noise.(722,723,739) The IAF was defined as the largest peak (local maximum) for a frequency range of 5 to 15 Hz.

Event-related potentials

ERPs were obtained for both cue-locked and target-locked data. Only correct, artifact-free trials were used. For cue-locked data, ERPs and SSVEPs (-200 ms to 1542 ms, baseline: -200 ms to 0 ms) were obtained collapsing across target-present and target-absent conditions, given that the time window of interest did not reach the target period. For target-locked data, on the other hand (-200 ms to 250 ms, baseline: -200 ms to 0 ms), ERPs were separately obtained both as a function of target-present and target-absent and also relative phase (anti-phase, in-phase).

Inter-trial coherence

To assess whether neural entrainment persisted over the length of the entrainment, ITC analyses were carried out. For these analyses, activity was locked to the onset of the cue (cue-locked) and also to the onset of the last entrainer (entrainer-locked). Only correct, artifact-free trials were included. A frequency domain multiplication, which consisted of multiplying the Fourier derived spectrum by a complex Morlet wavelet spectrum (variable number of cycles, 4-10 in logarithmic steps), was used to convolute the single-trial EEG data and take the inverse Fourier transform. Next, a separate time series of complex wavelet coefficients was obtained for each frequency from 1 to 40 Hz, in 1 Hz steps. These complex coefficients, contained both real and imaginary components and were used to calculate the ITC (724) for each trial, time point, frequency, and participant.(739) Similarly to previous analyses, cue-locked data was collapsed across target-present and target-absent conditions (-2200 ms to 3542 ms, window of interest: -200 ms to 1542 ms). Entrainer-locked data on the other hand was separated as a function of target-present or target-absent but collapsed across the relative phase (-2600 ms to 2600 ms, window of interest: -600 ms to 600 ms). Two-sided unpaired *t*-tests of equal variance were used to assess group differences between HC and EM. For cue-locked epochs, the frequency range of interest was set at 10 to 14 Hz and three separate time windows were examined, which included: [i] throughout the presentation of the cue (0 to 200 ms), [ii] from cue offset to first entrainer onset (200 ms to 875 ms) and [iii] from first entrainer onset to eighth entrainer offset (875 ms to 1542 ms). Entrainer-locked data used the same frequency range and examined two different time windows: [i] over the last entrainers (-600 ms to 0 ms) and [ii] during the target or expected target period (0 ms to 167 ms).

Montecarlo permutation tests (726) were carried out to see whether the phase remained concentrated around 12 Hz for the cue-locked data and over the duration of the first eight entrainers (875 ms to 1458 ms). First, a null distribution of ITC values was obtained for each participant and the Pz electrode. A phase from a random time within the window of interest was selected for each trial and a surrogate ITC was calculated for these phases to maintain the same number of trials. This step was repeated 10,000 times to obtain a distribution of surrogate ITCs, and these were averaged across participants. Next, the group-averaged surrogate ITCs were compared to the ITC to see how many times the former exceeded the latter, and the resulting proportion was used to obtain an unbiased *p* value.(727) To correct for multiple comparisons, a false discovery rate correction (FDR) was carried out on the time series of *p* values.(728) The corrected *p* values were compared to an alpha of .05 to determine significance.

Spectral cross-coherence

To assess the alignment of EEG activity to the external entrainers, a spectral cross-coherence analysis (729) was carried out for both HC and EM. Given the entrainment frequency, we expected a peak in the cross-coherence at 12 Hz. Epochs were subdivided based on the number of entrainers [8-12] and time windows were created taking into account first entrainer offset to last entrainer offset plus one half cycle (42 ms). Only correct trials were considered for this analysis. For each epoch length, a set of steps was carried out: [i] creating an artificial 12 Hz spiking signal, [ii] obtaining the spectrum for both the artificial and real signals using a Hanning windowed STFT (2.048 padding, 1 to 40 Hz frequency range), and [iii] calculating a spectral cross-coherence value for each channel, frequency, and participant.

Next, a weighted arithmetic mean was obtained for all five epoch lengths and for each frequency and participant. To determine whether the peak was statistically significant a procedure by Biltoft and Pardyjak (730) was applied. 1024 samples were used for the FFT estimation. HC had an average of 317±79 trials and EM had an average of 364±106 trials. The mean trial length was 418 points for both groups with a range between 335 points for eight entrainers and 502 points for twelve. If significance was set at $p < .05$, then HC had 129 degrees of freedom and a peak height of 0.046, whereas EM had 149 degrees of freedom and a peak height of 0.040.

12 Hz phase at target-present and target-absent trials

To determine whether there was phase opposition during the target period, EEG data was time-locked to the onset of targets (target-present trials) or expected target onsets (target-absent trials), separating as a function of relative phase. Only correct, artifact-free trials were used. Epochs were selected with a time window from -2000 ms to 2000 ms and the single trial phase at 12 Hz was extracted for each participant and condition. Phases were pooled over trials and participants and a circular V-test (731) was carried out to assess whether the anticipated 180° was present in the data between anti-phase and in-phase conditions. The circular mean phase and radial difference (anti-phase minus in-phase) were also obtained for target-present and target-absent trials. For both HC and EM, some descriptive circular statistics were calculated including the: mean circular direction, median circular direction, mean length, circular variance, circular standard deviation, circular skewness, and circular kurtosis. Also, to check for group differences, a Watson-Williams test was carried out on the difference in mean phase, which is a two-sample *t*-test equivalent for circular statistics.

Lastly, several concentration metrics were obtained for in-phase target-absent trials, which included kappa concentration, mean vector length, and mean angular direction. Montecarlo

randomization tests were carried out 10,000 times to compare these concentration metrics between participant groups and assess the presence of potential group differences.

Reality check: Alpha power lateralization

Preparatory alpha activity over the time window between the offset of the cue and the onset of the first entrainer was assessed to ensure that participants were orienting their attention correctly. Only correct, artifact-free, and spatially-valid trials were used. Epochs were obtained for both cue-left and cue-right conditions (-2200 ms to 3542 ms, window of interest: 0 ms to 1542 ms no baseline). The time window in question was between 375 ms (post-cue) and 875 ms and the mean spectral power was extracted using a Hanning windowed FFT (zero padding to 1 s). Two ROIs of parieto-occipital electrodes (186) were used to calculate the spectral power, a left ROI (P3, PO3, PO7, P7, P5, P1, PO9, and O1) and a right one (P4, PO4, PO8, P8, P6, P2, PO10, and O2). Power for the electrodes ipsilateral and contralateral to the cue on both left and right cue (attended-left/attended-right) trials, between 7 and 14 Hz, was obtained. The attended-left (ipsi left-contra left) power was subtracted from the attended-right (ipsi right-contra right) power and divided by the sum of the two, to calculate an index of alpha lateralization for each participant group.(186) This index was assessed for statistical significance using a one-sided (right), paired *t*-test against zero for both HC and EM, separately. The indices of both participant groups were also compared using a two-sided unpaired *t*-test of equal variance to assess for group differences.

Correlations

To check for potential correlations between demographic/clinical variables and experimental measures, we ran circular-linear and circular-circular correlations on: age, migraine frequency (EM only), kappa concentration, mean vector length, mean angular direction, cue-locked ITC (all three time windows), last entrainer-locked ITC (both time windows), as well as questionnaire scores including STAI-state, STAI-trait, ASRS, BDI-II, SPQ Total, SPQ Vision, and all of the SPQ Vision subtypes. Clinical questionnaires including MIDAS, HIT-6, and MSQ were also correlated for EM only. To correct for multiple comparisons an FDR procedure was carried out. Correlation (*r*) values and adjusted *p* values were reported.

4.3. Studying the exogenous mechanisms of visual sensory processing in interictal EM and HC, using a pattern-reversal task

Secondary objective 3 of this research thesis was to assess the exogenous mechanisms of visual processing in patients with interictal EM and HC, using a pattern-reversal task and event-related potentials [*Research Study 3: Exploring sensory sensitivity, cortical excitability, and habituation using the pattern-reversal task across the episodic migraine spectrum: A case-control study*]. The following research study was divided into two experiments. Experiment 1 included young adults with EM recruited from a research participant database provided by the Center for Brain and Cognition and their age- and gender-matched HC. Experiment 2, on the other hand, consisted of middle-aged adults with EM sampled from an out-patient clinic, jointly with their age- and gender-matched HC. The methodological aspects will be discussed upon continuation.

4.3.1. Experiment 1

Participants

63 female university students, that were right-handed, and reported normal or corrected-to-normal vision and hearing took part in this research study. A neurologist assigned a diagnosis of EM with or without aura according to criteria established by the ICHD-3 (6) to 35 participants and a diagnosis of headache-free control (HC) to the remaining 28 participants. Please note that the participants in this experiment were the same as the ones from Research Study 2 (plus two additional participants [one HC and one EM] that did not complete the entrainment task) and Research Study 4. Participant groups were age and gender-matched and great care was taken to obtain homogenous and clinically similar participants, to reduce bias and potentially confounding variables. Prior to completing the experimental session, all participants completed a baseline eDiary for an average of 34±8 days before their experimental session. This eDiary was continued on the day of the experimental session and for at least 24 hours after, to ensure that patients were in the interictal phase at the time of the recording. Participants were also not informed of their diagnosis until the end of the research study. Also, participants were screened for exclusion criteria, which included: morphological brain abnormalities, neurological disorders, severe psychiatric illness, chronic pain conditions, pregnancy, and/or the use of any kind of pharmaceutical or non-pharmaceutical drug with an effect on the EEG waveform. Furthermore, specific exclusion criteria for patients included no previous diagnoses of CM or any other headache disorder or current use of prophylactic medication. Controls were also excluded if they had received a previous headache diagnosis or had any first-degree relatives with diagnosed migraine. Given that migraine phase can have an impact on measures

including sensory sensitivity and habituation, patients outside of the interictal phase were also excluded [see 5.3.]. In our study, the interictal phase was defined as the absence of a moderate or severe headache 24 prior, the day of, and 24 hours post-experimental session, thus capturing a 72-hour headache-free time window (confirmed with eDiary). This study was approved by the Ethics Committee at the Vall d'Hebron Hospital (Experiment 1: PR(AG) 376/2017) and all participants provided written, informed consent prior to participating. Upon completion, all participants received 25 euros as compensation.

Procedure and paradigm

Participants received notice of the research study through a research participant database at the Pompeu Fabra University and prior to being admitted into the research study, were asked to fill out two questionnaires: [i] a sociodemographic and anthropometric questionnaire and [ii] a migraine screening questionnaire based on ICHD-3 (6) diagnostic criteria. Those that fulfilled the initial inclusion and exclusion criteria were subsequently diagnosed by a neurologist and all participants received an eDiary. Importantly, if the patients reported a headache or were menstruating prior to the experimental session, their session was postponed accordingly.

On the day of the experimental session, participants first responded to a series of psychiatric, clinical, and experimental session questionnaires. The psychiatric questionnaires consisted of the BDI-II,(707) STAI,(734,735) and ASRS.(706) Clinical questionnaires including the MIDAS,(737) HIT-6,(736) and MSQ (738) were also administered. Sensory sensitivity was assessed with the SPQ,(252) with lower scores indicating increased sensory sensitivity. Finally, a custom-made experimental session questionnaire asked participants about headache presence, acute and other medication use, and level of fatigue at the time of the experiment. All of the questionnaires as well as the eDiary were hosted by REDCap at the VHIR.

Next, participants underwent an EEG recording, which was performed inside a chamber with acoustic and electromagnetic attenuation. First, a resting state recording (5-minute duration) was carried out, which helped participants adapt to the dim lighting. Next, they completed a PR task and were instructed to maintain their eyes on the fixation point at all times. The PR stimulation was comprised of a black and white checkerboard pattern with a 93% contrast, which reversed its pattern at a temporal frequency of 1.55 Hz (see Figure 48 A). Reversal frequency was based on Coppola et al. and the check size was set at 0.1725 cm (6 min of arc or 6') given that the participants sat at a distance of 0.75 m from the screen (0.23 cm or 8' at 1 m is the recommended size).(741) Stimulation was delivered binocularly on a visual field of 30.7 cm x 22.5 cm. A red fixation point was present on the center of the screen throughout the duration of the task to reduce ocular artifacts. All stimuli were

programmed and presented using MATLAB R2017a (The Mathworks Inc., 2017) and Psychophysics Toolbox Version 3.0.13 (708,709) custom-made scripts on a Sony Multiscan G520 Trinitron Color Monitor (CRT screen, 120 Hz refresh rate, 1024 x 768 resolution, and 21 cd/m^2 resolution), running on Windows XP. The Black Box Toolkit (accuracy of < .005 s; Black Box Toolkit Ltd, Sheffield, UK) was used to confirm accurate stimulus timing. The task consisted of 600 trials with a duration of 3.23 min, which were segmented into six blocks of 100 trials post-recording. The duration of the session was approximately three hours.

EEG recordings

Digitized, continuous EEG recordings with no online filters (500 Hz sampling rate) were obtained through a BrainAmp Standard (001 10/2008) amplifier connected to an actiCHamp Control Box (BrainVision Analyzer, Version 2.2.2., Brain Products GmbH, Gilching, Germany). Electrodes were placed at standard positions using the 10-10 system and 64 active electrodes were used including a ground electrode at AFz and an online reference electrode positioned on the nose. Four external electrodes were placed including the left and right mastoids and vertical and horizontal electrooculograms. The impedance cut-off was set at 15 kΩ and maintained throughout the experiment.

EEG pre-processing

EEG data analyses were carried out using EEGLAB 13.5.4b, (718) ERPLAB 7.0.0,(719) and MATLAB R2017a (The Mathworks Inc., 2017) software and custom-made scripts.(742)

Pre-processing of EEG data included applying an offline, 50 Hz notch filter (type: stop-band Parks-McClellan Notch, order 180) to each recording. Next, the recordings were inspected and any electrodes experiencing technical problems during the recording were interpolated. A Hamming windowed sinc FIR band-pass filter (zero-phase), ranging from 0.1 Hz (high-pass: 0.1 Hz frequency, 16501 order, -6dB cutoff) to 60 Hz (low-pass: 60 Hz frequency, 111 order, -6dB cutoff) was also applied to each recording. Also, the mean activity of both the left and right mastoid was used to re-reference the activity offline. Epochs were time-locked to the reversals and segmented from 0 ms to 300 ms as well as normalized by the mean activity of each one. Finally, epochs were inspected for ocular artifacts including blinks and horizontal eye movements, as well as muscular noise, and a manual rejection process was performed to remove epochs with noise.

Analyses

R (R Core Team 2021, version 4.1.1) and RStudio (RStudio Team 2021, version 1.4.1717) software were used for statistical analyses. The following packages were used: base, car, dgof, dplyr,

emmeans, ggpubr, ggResidpanel, graphics, lattice, lme4, nlme, multiplyr, nortest, pgirmess, psych, rstatix, and stats.

Psychiatric, clinical, and SPQ questionnaires

Categorical values and scores obtained from the psychiatric, clinical, and SPQ questionnaires were reported using percentages, whereas continuous data was represented with means and SDs if normally distributed and medians and IQRs otherwise. To evaluate potential group effects, Fisher's exact test, two-sided unpaired *t*-tests of equal variance or two-sided, nonparametric Mann-Whitney U tests were used.

Electrophysiological data

PR-VEP. N1 and P1 amplitudes and latencies as well as the peak-to-peak (N1-P1) amplitude difference, at the Oz electrode, were separately obtained for each trial [1-600] and participant. Oz was used as the electrode of interest based on past literature in migraine using the PR task.(101,341,616) Only clean, artifact-free trials were included in subsequent analyses. Each block [1-6] was comprised of a maximum of 100 trials and in this experiment, the mean number of clean trials was 89.46±9.093 [range: 30-100] per participant per block. Furthermore, out of a maximum of 600 trials, participants had a grand mean of 536.78±36.962 [range: 435-595] clean trials. Through the use of visual inspection and peak latencies (reversal-locked), N1 was identified as the most negative peak between 65-95 ms (peak: 80 ms; window: ±15 ms) and P1 as the most positive peak between 86-126 ms (peak: 106 ms; window: ±20 ms). To extract the amplitudes of N1 and P1, used to calculate the N1-P1 peak-to-peak amplitude, an automatic detection system based on the one used by Coppola et al.(743) accompanied by visual inspection to confirm the results, was used.

Classic block analyses. First, we ran classic block analyses (744) on the N1-P1 peak-to-peak amplitudes. Specifically, a type III two-way mixed analysis of variance (ANOVA) with Block (1 and 6) as the between-subject factor and Group (EM and HC) as the within-subject factor was executed. Post hoc tests were performed accordingly using Bonferroni adjusted *p* values (padj).

Block linear mixed-effects model. Similarly, to the classic block analyses, the aim of the current analysis was to explore the concepts of cortical excitability and habituation, using N1-P1 data. However, in contrast to the previous analysis, linear mixed-effects models (LMM) were fitted to the data using the nlme package in R (745) with Block (1 and 6) and Group (EM and HC) as the fixed effects variables and Participant as the random effects variable. Furthermore, an autocorrelation structure of order 1, with Participant nested within Trial, was applied to the model. A number of

120

model comparisons were carried out using the Akaike Information Criterion (AIC) and a chi-square test on the model log-likelihoods (Chisq),(746) to ensure that the final model best explained the data. Once a final model was obtained, a type III ANOVA was executed with Kenward-Roger "F" tests and Satterthwaite degrees of freedom. The within-subject factor was Block and the between-subject factor was Group. The resulting F and p values were reported at a confidence level of 0.95. To ensure the normality and homoscedasticity of the measures, a visual inspection of residual plots was carried out. If a significant interaction between Block x Group was detected, then post hoc tests and pairwise comparisons were carried out using estimated marginal means. Z ratios and p values were reported accordingly and the FDR correction was applied to adjust for multiple comparisons.

Importantly, the peak-to-peak first block amplitude was compared between participant groups to assess potential differences related to cortical excitability with a significantly lower amplitude suggesting hypo- and a significantly greater amplitude hyper-excitability in one group as compared to the other.(288) The change in peak-to-peak amplitude between the first and last block was also evaluated within and between groups to assess habituation. For this analysis, only data from the first and last block were used seeing as the majority of studies assessing habituation in the literature, only used data from the first and last blocks [see Table 5 in (625)]. If a decrement was observed, then normal habituation was confirmed.(341,347) Meanwhile, a lack of significant differences between the peak-to-peak amplitude first and last block measures indicated a lack of habituation and even potentiation (increment). In order to properly evaluate these differences, a Block x Group interaction was necessary.

Trial linear mixed-effects model. Given that the previous block model was based on past literature comparing first and last block measures and only took into account averaged block data from blocks 1 and 6, we decided to run one more LMM analysis but this time taking trial-by-trial fluctuation into account. This trial LMM fitted using the nlme package in R (745) therefore permitted us to account for both individual (Participant) and temporal (Trial) variability. In this model, Group and Trial (numeric) were the fixed effects variables whereas Participant was the random effects variable and once again, an autocorrelation structure of order 1, with Trial nested within Participant, was applied. Models were compared using the AIC and Chisq to obtain the best alternative and a type III ANOVA table with Kenward-Roger "F" tests and Satterthwaite degrees of freedom was obtained. For this ANOVA, Trial was considered as the within-subject factor and Group as the between-subject factor. F and p values were reported and the confidence level was set at 0.95. To ensure the homoscedasticity and normality of the measures, residual plots were inspected.

To explore cortical excitability using the trial LMM, the main effect of Group was examined since the temporal variability introduced through the use of Trial made post hoc comparisons difficult to interpret. Similarly, habituation was assessed through a main effect of Block and confirmed through visual inspection.

Correlations

Spearman correlations were executed between age, migraine frequency (EM only), sensory sensitivity, cortical excitability, and habituation. Sensory sensitivity was assessed according to the scores from the SPQ-Vision subscale, cortical excitability according to the first block N1-P1 amplitude, and habituation as the difference between the last block and first block N1-P1 measures and r and p values were reported. Finally, FDR correction was applied to adjust for multiple comparisons.

4.3.2. Experiment 2

Participants

66 middle-aged participants between the ages of 18 and 65 years old, with normal or corrected-to-normal vision were included in this experiment. In particular, 36 were diagnosed with EM by a neurologist according to ICHD-3 criteria (6) and 30 were assigned HC status and age- and gender-matched to the EM group. The inclusion criteria were similar to Experiment 1, with the exception being that patients were recruited from a specialized Headache Clinic resulting in increased disease severity. In fact, Welch's t-tests confirmed that patients with EM in Experiment 2 were significantly older (Welch's t-test: $t(19.786) = -8.867$, $p = 2.51\text{x}10^{-8}$) and had a greater headache frequency (headache days/month: $t(35) = -3.043$, $p = .004$) than patients with EM in Experiment 1. This second experiment was carried out to due to the fact that we did not find the frequently described habituation deficit in patients using either classic block analyses or LMMs in Experiment 1 and wanted to assess these variables in older patients with greater disease severity. Exclusion criteria were the same as Experiment 1. This experiment was approved by the Ethics Committee at the Vall d'Hebron Hospital (EudraCT 2019-002224-32) and all participants provided their written informed consent prior to participating. At the end of the experiment, HC received 35 euros as compensation and EM were administered preventive treatment.

Procedure and paradigm

The procedure was the same as in Experiment 1 and included: [i] completion of psychiatric, clinical, and experimental session questionnaires; [ii] a 5-min resting state recording and, [iii] a 3.23

min PR task recording. Stimuli were programmed and presented using MATLAB R2017a (The Mathworks Inc., 2017) and Psychophysics Toolbox Version 3.0.13 (708,709) custom-made scripts on a BenQ XL2411P CRT screen monitor (120 Hz refresh rate, 1024 x 768 resolution, 21 cd/m^2 background luminance). Once again, the BlackBox Toolkit (Black Box Toolkit, Ltd., Sheffield, UK) was used to confirm stimulus timing.

In this experiment, the stimulation parameters were practically the same except for an incremented reversal rate of 3.1 Hz. Furthermore, the recordings were segmented into 12 blocks of 100 trials, post-recording. The reversal rate was increased in Experiment 2 given that several authors have proposed that incrementing this rate may help to detect the lack of habituation in patients with migraine.(624,625,747). Furthermore, a large number of studies reporting a habituation deficit applied a 3.1 Hz reversal rate.(101,341,607,616)

EEG recording

Continuous, digitized EEG recordings (1000 Hz sampling rate, 50 Hz online notch filter) were obtained using a BrainAmp32 Standard amplifier connected to a BrainVision recorder polybox BP-BM-30 actiCAP32 (Brain Products GmbH). Electrodes were placed in standard positions and 32 active electrodes were used including a ground electrode inserted at AFz and an online reference electrode on the nose. External electrodes included right and left mastoids as well as vertical and horizontal electrooculograms. Impedances were set at 15 kΩ. and maintained throughout the experiment.

EEG pre-processing

EEGLAB 13.5.4b,(718) ERPLAB 7.0.0,(719) and MATLAB R2017a (The Mathworks Inc., 2017) software and custom-made scripts were used for EEG data analyses. The order of procedure was the same as in Experiment 1, except that the notch filter had already been applied online and epochs were segmented from 0 ms to 150 ms. The FIR filters used for Experiment 2 yielded the following metrics: [i] high-pass: 0.1 Hz frequency, 33001 order, -6dB cutoff, and [ii] low-pass: 60 Hz frequency, 221 order, and -6dB cutoff.

Analyses

Psychiatric, clinical, and SPQ questionnaires

The same analysis procedure was used as in Experiment 1 (see above).

Electrophysiological data

       PR-VEP. The same procedure was used as in Experiment 1 (see above). N1, P1 amplitudes and latencies as well as N1-P1 at Oz, were separately obtained for each trial (1-1200) and participant. Each block had a maximum of 100 trials and in this experiment, the mean number of clean trials was 93.72 ± 6.912 (range: 56-100) per participant. Furthermore, participants had a grand mean of 1124.58 ± 57.203 clean trials (range 971-1197) out of a maximum of 1200. Components were identified according to visual inspection and peak latencies. In this experiment, N1 was the most negative peak between 73-101 ms (peak: 88 ms; window: ± 15 ms) and P1 was the most positive peak between 96-136 ms (peak: 116 ms; window: ± 20 ms).

       Classic block analyses. The experimental procedure was the same as in Experiment 1 (see above) only that the Block factor consisted of Blocks 1 and 12.

       Block linear mixed-effects model. The experimental procedure was the same as in Experiment 1 (see above), except the fixed effects variable Block of the LMM consisted of blocks 1 and 12, and the within-subject factor of the ANOVA also included blocks 1 and 12.

       Trial linear mixed-effects model. The experimental procedure was the same as in Experiment 1 (see above) but with the fixed effects variable Trial including trials 1 to 1200, same with the within-subject factor of the ANOVA.

Correlations

       The experimental procedure was the same as in Experiment 1.

4.4. Investigating the exogenous and endogenous mechanisms of auditory sensitivity processing in interictal EM and HC, using an oddball task

Secondary objective 4 of this research thesis was to study the exogenous and endogenous mechanisms of auditory sensory-attentional processing in patients with episodic migraine during the interictal phase, using an active oddball task and ERPs as well as time-frequency analyses [*Research Study 4: Neurophysiological correlates of abnormal auditory processing in episodic migraine during the interictal period*] (Appendix 4). The methodological aspects will be discussed upon continuation.

Participants

45 young, right-handed females, with normal or corrected-to-normal vision and hearing, were selected to take part in this research study. The same participants that took part in Research Study 2 and Research Study 3 (Experiment 1), were invited to participate in a second session, approximately one week later, although not all of the original participants took part. Participants that were included in the study were diagnosed by a neurologist, according to the ICHD-3 criteria, with 23 participants being diagnosed with EM, with or without aura, and 22 as HC. Groups were age- and gender-matched. Patients and controls were carefully matched to ensure a homogenous and clinically similar sample of participants, in an effort to reduce bias and the impact of confounding variables. Furthermore, the patients in this study had never been formally diagnosed therefore were unsure or unaware of their migraine status. Participants were not informed of their diagnosis until the experiment was over so that both the researcher and the participant could remain double-blind. All participants were asked to complete an eDiary (same as for the other research studies) for around 30 days prior to the experimental session (which they continued on the day of the session and at least 24 hours post). General exclusion criteria included severe psychiatric or neurological illness, known morphological brain abnormalities, chronic pain conditions, pregnancy, as well as the use of pharmaceutical or non-pharmaceutical drugs, which may alter the EEG waveform. Patients could not be using prophylactic medication or have been diagnosed with CM or any other headache disorder and controls could not have any first-degree relatives with migraine or been previously diagnosed with a headache disorder. Patients had to be in the interictal phase to be included in further analyses, defined as the absence of moderate or severe headache 24 hours prior, the day of, and 24 hours post-experimental session (confirmed by eDiary, 72-hour headache-free window). The Ethics Committee at the Vall d'Hebron hospital approved this study (PR(AG) 376/2017) and all participants provided informed, written consent prior to participating. At the end of the experimental session, participants received 15 euros as compensation.

Procedure and paradigm

Participants that contacted the laboratory in response to recruitment advertisements had to fill out two questionnaires: [i] a sociodemographic and anthropometric questionnaire, and [ii] a migraine screening questionnaire based on ICHD-3 criteria.(6) Next, a neurologist checked the diagnoses of those that were flagged as fit to continue and all of the participants were provided with an eDiary. If participants reported a headache or menstruation in the 24 hours prior to the experimental session, then their session was postponed accordingly. On the day of the EEG recording participants had to complete a series of psychiatric, clinical, and experimental session questionnaires. The psychiatric questionnaires consisted of the: BDI-II,(707) ASRS,(706) STAI,(734,735) and the Brief Symptoms Inventory (BSI).(748) Clinical questionnaires included the: HIT-6,(736) MIDAS,(749) MSQ,(738) Subjective Cognitive Impairment Scale for Migraine Attacks (Mig-S-Cog),(750) Epworth Sleepiness Scale (ESS),(751) International Physical Activity Questionnaire (IPAQ),(752) and Hypersensitivity to Sound Test (GÜF/THS).(753) The questionnaires and eDiary were hosted using REDCap at the VHIR.

Next, participants underwent an EEG recording while performing a variant of the active auditory oddball paradigm.(379,534) A stream of auditory tones was presented binaurally and included standard 1500 Hz tones (probability of p = 0.6), infrequent 1620 Hz target tones (probability of p = 0.2), and novel sounds (probability of p = 0.2) (see Figure 21). Both the standard and infrequent target tones had a 60 ms duration and a rise and fall time of 5 ms. Novel sounds consisted of short excerpts of environmental sounds such as a car honking or dog barking and had an average duration of 60.95±7.61 ms. Auditory stimulation was presented using Presentation Software 18.1 (NeuroBehavioral Systems, San Francisco, CA, USA) through Sony MDR-ZX310APB headphones at a sound pressure level (SPL) of 75 dB. The order of presentation was pseudo-random along with a SOA of 1200 ms (±100 ms). A black fixation cross (height, width: 13 pixels) was present in the center of the screen, on a black background, throughout the entire experiment and participants were instructed to maintain their eyes on the cross, at all times. They were also told to respond to the target tones as quickly and accurately as possible, while ignoring both the standard and novel sounds. The total duration of the auditory oddball paradigm was 25 minutes, and 500 trials (five blocks of 100 trials) were presented. The entire experimental session lasted approximately 2.5 hours, including preparation and clean-up.

EEG recording

Continuous, digitized EEG recordings (500 Hz sampling rate, no online filters) were obtained using an Enobio (Neuroelectrics Enobio, Barcelona) 20-electrode EEG cap. Electrodes were placed

at standard positions and consisted of Fp1/Fp2, F3/F4, F7/F8, Fz, Cz, Pz, C3/C4, T7/T8, P3/P4, P7/P8, O1/O2. A common mode sense (CMS) and driven right leg (DRL) electrode at the right mastoid were also applied. An electrode placed at the infraorbital ridge (right eye) was used to monitor eye movements. EEG activity was re-referenced offline to the mean activity of all the electrodes. The impedance cut-off was set at 15Ω and maintained throughout the experiment.

EEG pre-processing

First, a 50 Hz, offline notch filter (type: stop-band Parks-McClellan Notch, order 180) was applied to each recording. The next pre-processing steps were different depending on whether or not the EEG data came from ERPs and power or ITC. This was done to avoid nonlinear phase distortions of the ITC.(200) Specifically for ERPs and power, a Butterworth infinite impulse response (IIR) band-pass filter was applied from 0.1 Hz (high-pass: 0.1 Hz frequency, 2 order, -6 dB cutoff) to 100 Hz (low-pass: 100 Hz frequency, 4 order, -6 dB cutoff). On the other hand, for ITC, a Hamming windowed sinc FIR band-pass filter (zero-phase) was applied from 0.1 Hz (high-pass: 0.1 Hz frequency, 16500 order, -6dB cutoff) to 100 Hz (low-pass: 100 Hz frequency, 66 order, -6dB cutoff). Epochs were segmented for ERPs (100 ms to 1000 ms) and power/phase synchronization (-2000 ms to 2000 ms post-stimulus onset) for standard, target, and novel sounds, separately. A baseline correction from -100 ms to 0 ms (post-stimulus onset) was also applied.(379,534) Importantly, only correct trials were considered when obtaining the epochs and consisted of correct detection of the infrequent target sounds and no response to either standard or novel tones. For this kind of nested case-control study design, a sample size of 10-25 participants and at least 20 artifact-free trials per condition was determined to be sufficient.(754,755) Participants that did not meet the requirement of at least 20 artifact-free trials were excluded from further analyses (0 participants in our research study). An automatic detection process with subsequent visual inspection was used to remove trials with ±100 µV in the EEG or electro-oculogram (EOG).

Frequency-domain multiplication, which consists of the multiplication of the Fourier-derived spectrum of the ERP data by the wavelet spectrum was used for single trial convolution, and the inverse Fourier transform of the result was taken.(200) A complex Morlet with six cycles was used. Furthermore, for each frequency from 1 Hz to 40 Hz (linear increase), we extracted a separate time series of complex wavelet coefficients, which contained both real and imaginary components and were used to obtain the power and phase synchronization (ITC).(200) The baseline was used to get the power and both power and phase synchronization were extracted for each trial and averaged within-participants prior to achieving the grand average.

Analyses

Behavioral analyses

Several behavioral metrics were obtained including RTs, the percentage of no-response (miss) trials (number of misses/number of hits), and the false alarm rates in response to standard and novel tones (number of standard/novel trials with a response/total number of standard/novel trials). Trials with RTs ±3 SDs from the participant's mean were excluded. Group differences were assessed using two-sample *t*-tests. Finally, an ANOVA for standard stimuli values was executed with Time (Blocks 1-5) as the within-subject factor and Group (EM or HC) as the between-subject factor.

Electrophysiological analyses

Separate analyses were carried out for standard trials and target/novel ones. With regard to standard trials, the amplitude of each component was obtained for each block and participant. The ERP mean amplitude was set-centered on the peak activity of each component, with N1 being the most negative peak between 75 ms and 125 ms; P2 the most positive peak between 175 ms and 225 ms, and N2 the most negative peak between 250 ms and 350 ms. Meanwhile, for power and phase-synchronization, frequency ranges were identified according to maximum activity as well as past literature (379,534) and consisted of theta (3-8 Hz, 0-400 ms), alpha (8-12 Hz, 0-200 ms) and beta-gamma (12-40 Hz, 0-200 ms).

For target/novel trials, we calculated the difference waveform ERPs between novel/target and standard trials. Different components were obtained depending on whether the trial contained a novel or target stimulus (see Table 7 for a description of the cascade of sensory and attentional processes from MMN to RON involved in processing novel and target stimuli). In particular, for novel stimuli the: MMN (175-225 ms), early P3a (225-275ms), late P3a (275-325 ms), and RON (350-450 ms) were obtained. For target stimuli, on the other hand the components were: MMN (175-225 ms), P3b (450-550 ms), and RON (400-600 ms). The mean amplitude for each component was set-centered on the peak activity.

Next, a rmANOVA was carried out on data from standard trials, with Electrode Location (Fz, Cz, Pz) and Block (1-5) as within-subject factors and Group (EM or HC) as between-subject factors. Similarly, for novel/target trials, a rmANOVA was executed with Electrode location (Fz, Cz, Pz) as the within-subject factor and Group (EM or HC) as the between-subject factor. Post hoc *t*-tests were carried out, if necessary and *p* values were corrected for nonsphericity using the Greenhouse-Geisser correction, when needed.

Table 7. Cascade of novel and target stimuli effects on the sensory-attentional system.

Type of Stimuli	Component	Polarity	Peak (ms)	Site	Cognitive related processes
Novel	MMN	-	175-225	Fronto-central	Early sensory detection of unexpected changes. Related to automatic attentional capture.
	Early P3a	+	225-275	Central	Post-sensory detection of unexpected events
	Late P3a	+	275-325	Frontal and parietal	Attentional processing of unexpected events
	RON	-	350-450	Fronto-central	Disengagement from stimuli and re-orientation back to the main task. Related to attentional resources, processing ease, and/or efficiency
Target	MMN	-	175-225	Fronto-central	Early sensory detection of unexpected changes. Related to automatic attentional capture.
	P3b	+	300-600	Centro-parietal	Related to memory comparisons based on context, required for behavioral response
	RON	-	400-600	Fronto-central	Disengagement from stimuli and re-orientation back to the main task. Related to attentional resources, processing ease, and/or efficiency

In response to novel stimuli, the following ERPs appear (in order of appearance): mismatch negativity (MMN), early P3a, late P3a, and re-orienting negativity (RON).(161,164,165) In response to target stimuli, the following ERPs appear (in order of appearance): MMN, P3b, and RON.(161,164,165,170,679). Reproduced from Vilà-Balló et al.(756)

5. RESULTS

5.1. Developing a task to study the exogenous and endogenous mechanisms of sensory-attentional processing

Analyses

Participants

        Six participants were discarded for a variety of reasons including a: mean false alarm rate > 30% (one participant), mean hit rate > 90% on invalidly-cued trials (484) (two participants), technical problems (two participants), and less than 50 clean trials on any condition post-artifact rejection (see EEG analysis section). Once the exclusions were carried out, 30 participants remained in the final sample (21.70±2.18 years old, range: 18-28 years). Scores on the psychiatric questionnaires remained within the normal range for both ADHD (ASRS: 1.73±1.62) and depression (BDI-II: 4.83±4.57).

Hazard rate

        To assess the predictability of our task as compared to the original paradigm,(484) HRs were calculated (see Figure 37 E). In our research study, the HR was fairly constant between the first and last conditions (small slope) in comparison to the HR reported for Kizuk and Mathewson,(484) which differed a lot more between the first and last conditions (larger slope). This would indicate that in Kizuk and Mathewson's task target predictability differed a lot between conditions, consistent with a common bias in temporal attention paradigms, whereas in our task this bias would appear to be reduced, with similar target predictability in each condition.

Behavioral analyses

        To assess the effect of spatial validity and relative phase on behavioral performance, separate rmANOVAs were carried out on hit rates and RTs. Hit rates were categorized according to spatial validity (valid, invalid) and relative phase (anti-phase, in-phase) (see Figure 37 A, B). The four possible target SOAs (anti-phase 1, in-phase 1, anti-phase 2, in-phase 2) were collapsed as a function of relative phase (anti-phase or in-phase) for the subsequent behavioral analyses. Spatial validity and relative phase were considered as the within-subject factors for the subsequent rmANOVA analysis. First, a significant main effect of spatial validity was detected, $F(1,29) = 22.166$, $p = -5.7 \times 10^{-5}$, $f = .874$, $BF_{10} = 2.1 \times 10^{11}$, indicating that hit rates in response to valid trials were increased (62.0±19.5%) as compared to invalid trials (40.6±26.6%). In contrast, the main effect of relative phase was not significant $F(1,29) = 1.448$, $p = .239$, $f = .225$, $BF_{10} = .261$, which would imply that hit rates between anti-phase (56.5±17.7%) and in-phase (55.3±19.8%) were similar. The interaction between spatial validity and relative phase was also not significant, $F(1,29) = .016$, $p = .901$, $f = .032$, $BF_{10} = .284$,

meaning that these two variables did not modulate each other. Importantly, the Bayes Factor estimates provided strong evidence in favor of H1 with regard to spatial validity and moderate evidence in favor of H0 for relative phase and the interaction between the two.

Next, RTs were assessed using the same rmANOVA design (see Figure 37 C, D). Two participants did not have any correct responses on invalid trials and were not included in this analysis, although this did not serve as an exclusion criterion for other analyses. In terms of spatial validity, a significant main effect was reported $F(1,27) = 43.432$, $p = 4.5 \times 10^{-7}$, $f = 1.269$, $BF_{10} = 1.3 \times 10^9$, meaning that participants were significantly faster to respond to validly cued trials (454.5±14.0 ms) than invalidly cued ones (493.1±14.5 ms). However, with regard to relative phase, the main effect was not significant, $F(1,27) = .968$, $p = .334$, $f = .190$, $BF_{10} = .217$, which would indicate that RTs in response to anti-phase (458.0±14.3 ms) targets was not significantly different from the RTs in response to in-phase (462.7±13.7 ms) targets. The interaction between the two variables of spatial validity and relative phase was also not significant $F(1,27) = .257$, $p = .616$, $f = .095$, $BF_{10} = 0.287$, indicating once again that these variables exerted independent effects on behavioral performance. The Bayes Factors estimates indicated strong evidence in favor of H1 for spatial validity and moderate evidence in favor of H0 for both temporal validity and the interaction between the two variables.

Finally, to examine the presence of a potential response bias in either direction, we calculated a response criterion. In this research study, the response criterion was -4.5103×10^{-17}, which is practically equal to 0, indicating that participants did not hold a response bias.

Individual alpha frequency

To assess the IAF, we plotted and assessed the results of a violin plot. As seen in Figure 37 F, most of the data in the shaded area (median: 10.80 Hz; IQR: 9.25-12.35 Hz) was concentrated around 11 Hz, within the alpha band frequency range.
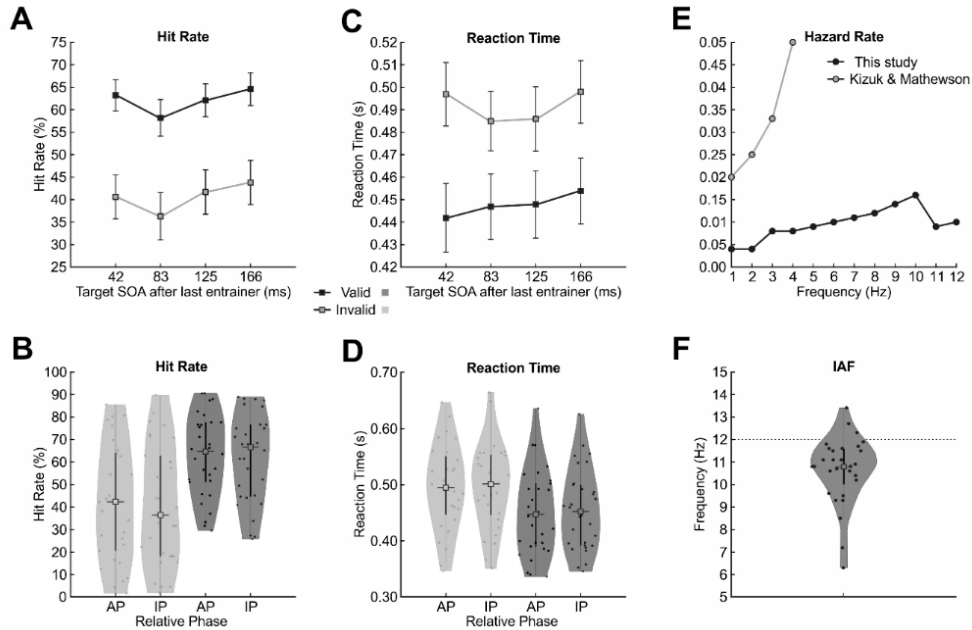
Figure 37. Visual representations of the behavioral analyses on hit rates and reaction times (RTs) as well as the Hazard rate (HR) and IAF. A. Mean hit rates with their standard errors of the mean (SEM), represented using line graphs, as a function of relative phase (x axis) and spatial validity (separate lines). **B.** Hit rates represented using violin plots and separated as a function of spatial validity and relative phase (anti-phase, in-phase). Dots depict individual data, central squares the median, and vertical lines the interquartile range (IQR). **C.** Mean RTs with their SEM represented using line graphs, as a function of relative phase (x axis) and spatial validity (separate lines). **D.** Reaction times represented using violin plots and separated as a function of spatial validity and relative phase (anti-phase, in-phase). Dots depict individual data, central squares the median, and vertical lines the IQR. Dark grey lines and bars refer to spatially valid whereas light grey represent spatially invalid data. **E.** The HR for our task (12 time points) and Kizuk and Mathewson's task (515) (four times). **F.** IAF (5-15 Hz), depicted using a violin plot, at the selected ROI. An alpha peak was detected in all participants except one.

Cue-locked EEG data analysis

Data was time-locked to different temporal points and a visual inspection of cue-locked ERPs and ITC (see Figure 38) was carried out at both Pz and Oz electrodes. The cue-locked time window permitted us to examine neural entrainment over the course of the first eight entrainers, common to all trials. Here, target-present and target-absent trials were collapsed together given that the time window of interest (-200 ms to 1542 ms; baseline: -200 ms to 0 ms) did not extend into the target period. A visual inspection of the ERPs yielded an alignment between the peaks in the neural activity and the entrainer onset times. Next, in terms of ITC, an increase was observed around the entrained 12 Hz frequency, which persisted throughout the entire entrainer period, providing tentative support for neural entrainment. This effect was visible at both electrodes, although it did appear to be greater at the Oz electrode, both in terms of ERP alignment and ITC activity. In the next section, we will discuss the statistical analyses carried out on cue-locked data.

135
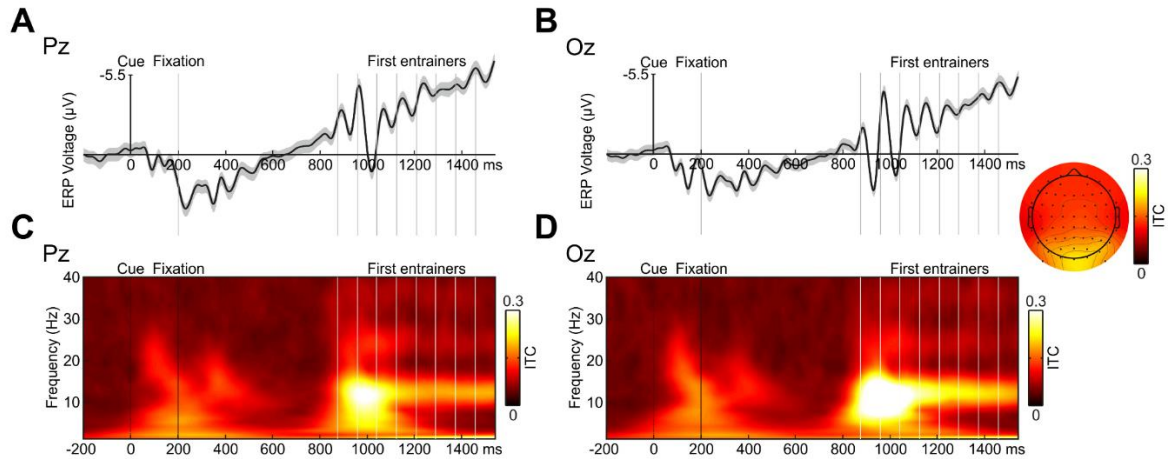
Figure 38. Cue-locked data event-related potentials (ERPs) and inter-trial coherence (ITC) for both the Pz and Oz electrodes. A. Cue-locked grand average ERP, with the shaded area corresponding to the standard error of the mean (SEM), at Pz electrode. B. Cue-locked grand average ERP, with the shaded area corresponding to the SEM, at Oz electrode. C. Cue-locked ITC at the Pz electrode. D. Cue-locked ITC at the Oz electrode. The time window of interest for this analysis was -200 ms to 1542 ms (baseline -200 ms to 0 ms). The vertical lines represent, in order of appearance, the cue, fixation cross, and first eight entrainers. Only correct trials were analyzed and data was represented across spatial validity and relative phase, as well as target-present and target-absent trials. An increase in the ITC at 12 Hz is observed throughout the series of entrainers. A topographical map of the ITC between 10-14 Hz is shown (representing the time window from the first to the eighth entrainer).

Cross-coherence between entrainers and EEG response

  To assess the alignment between the internal oscillatory activity and the external entrainers, during the presentation of the first eight entrainers, a cross-coherence analysis was carried out. The value of the spectral cross-coherence between the real and artificial signal was extracted for all frequencies and averaged across both trials and participants. Next, the output was investigated to check for the presence of a peak at the entrained 12 Hz frequency. The results indicated an average peak height of 0.24 for the Pz electrode and 0.28 for the Oz electrode at 12 Hz. When these peaks were evaluated for significance, both yielded a significant *p* value (Pz: 5×10^{-9}; Oz: 5×10^{-10}), which would indicate the presence of the anticipated 12 Hz frequency peak in the cross-coherence between the neural oscillatory activity and the entrainers.

Entrainer-locked analysis

  To further confirm the presence of neural entrainment, activity was time-locked to the last entrainer (entrainer-locked) and the time window ranging from the last entrainers to the target period was examined. Here, trials were separated as a function of target-present and target-absent conditions (Figure 39). Complex Morlet wavelets were used to estimate the ITC and for visualization purposes. An inspection of Figure 39 would indicate an increase of the ITC around the entrained 12 Hz frequency throughout the last entrainers and into the target period, for both Pz and Oz electrodes.

136

Importantly, this increment in the ITC persisted in both electrodes on both target-present and target-absent trials, indicating that, even in the absence of target stimuli, endogenous activity remained entrained for some time post-entrainer offset.
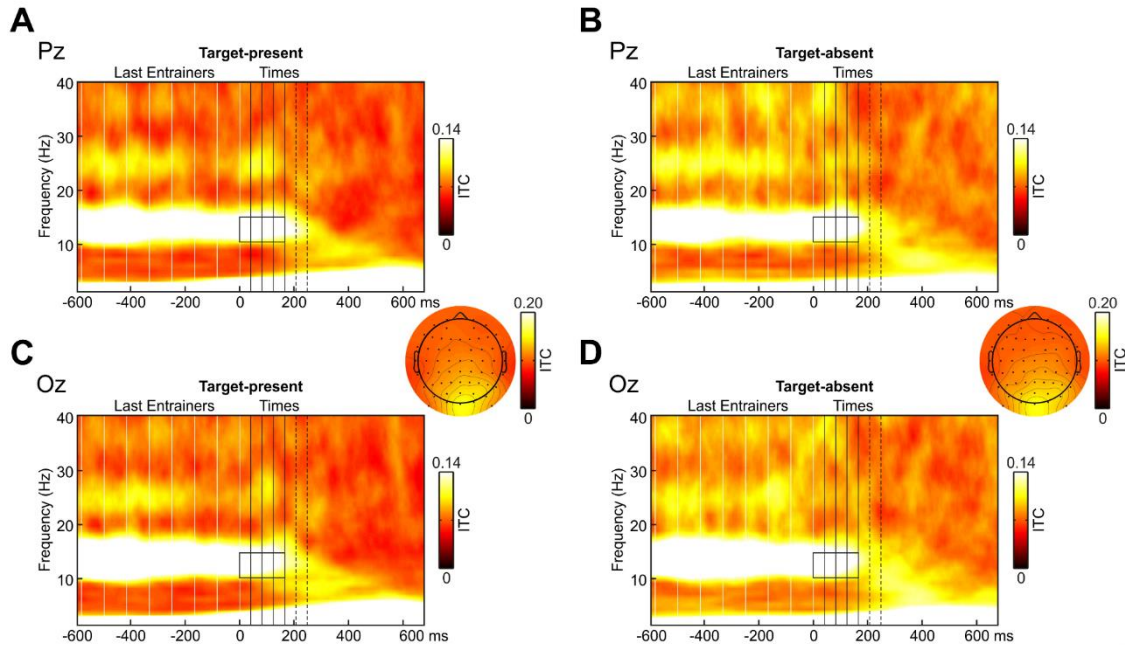
Figure 39. Entrainer-locked data inter-trial coherence (ITC) for target-present and target-absent trials, at both Pz and Oz electrodes. For visual purposes, the data represented was obtained using complex Morlet wavelets. A. ITC on target-present trials (Pz electrode). B. ITC for target-absent trials (Pz electrode). C. ITC for target-present trials at the Oz electrode. D. ITC for target-absent trials (Oz electrode). The time window for this analysis was -600 ms to 675 ms (no baseline). The last entrainers are represented using white vertical lines whereas black solid lines illustrate the four possible anti-phase and in-phase times (41.5, 88.3, 125, 166.6 ms post-last entrainer). Black pointed lines represent one additional cycle (anti-phase: 208.25 ms and in-phase: 250 ms) for the phase alignment analyses. Only correct trials were included, and epochs were collapsed across relative phase and spatial validity. Once again, an increase in the ITC around 12 Hz was observed throughout the last entrainers and in the target period. Separate topographies are shown for target-present (left) and target-absent (right) trials of the ITC at 10 to 14 Hz from the onset of the last entrainer to the last possible target onset time.

12 Hz phase at target onset on target-present and target-absent trials

Phase alignment to anti-phase and in-phase target onsets was statistically analyzed using target-locked data, where EEG activity was time-locked to target onset on target-present trials and expected target onset on target-absent trials. These analyses were carried out at both Pz and Oz electrodes and only correct, artifact-free trials were included. The mean phase at anti-phase and in-phase onsets was calculated for both target-present and target-absent trials and all participants, with the latter being of particular importance to study endogenous oscillations without the influence of evoked activity from ERPs in response to the target.(465,702) For each participant, the single-trial phase for each condition (target-present anti-phase, target-present in-phase, target-absent anti-phase, target-absent in-phase) was extracted and used to calculate the angular difference (anti-phase – in-

137

phase). To provide support for the persistence of neural entrainment into the target period, we anticipated a 180° phase separation between anti-phase and in-phase temporal moments at the entrained 12 Hz frequency for both target-present and target-absent conditions (see Figure 40). The circular V-test was significant at the Pz electrode for both target-present, $p = 1.12 \times 10^{-5}$ and target-absent, $p = 3.58 \times 10^{-4}$ trials, and similar results were obtained for Oz (target-present $p = 6.26 \times 10^{-6}$, target-absent: $p = 5.22 \times 10^{-5}$). These results would indicate that the angular differences between anti-phase and in-phase trials at the 12 Hz entrained frequency and both target-present and target-absent conditions were not randomly distributed. Specifically, the difference between anti-phase and in-phase (angular difference) temporal moments was around the expected 180° indicating opposite alignment of single-trial phase, contingent on relative phase (descriptive statistics in Table 8).
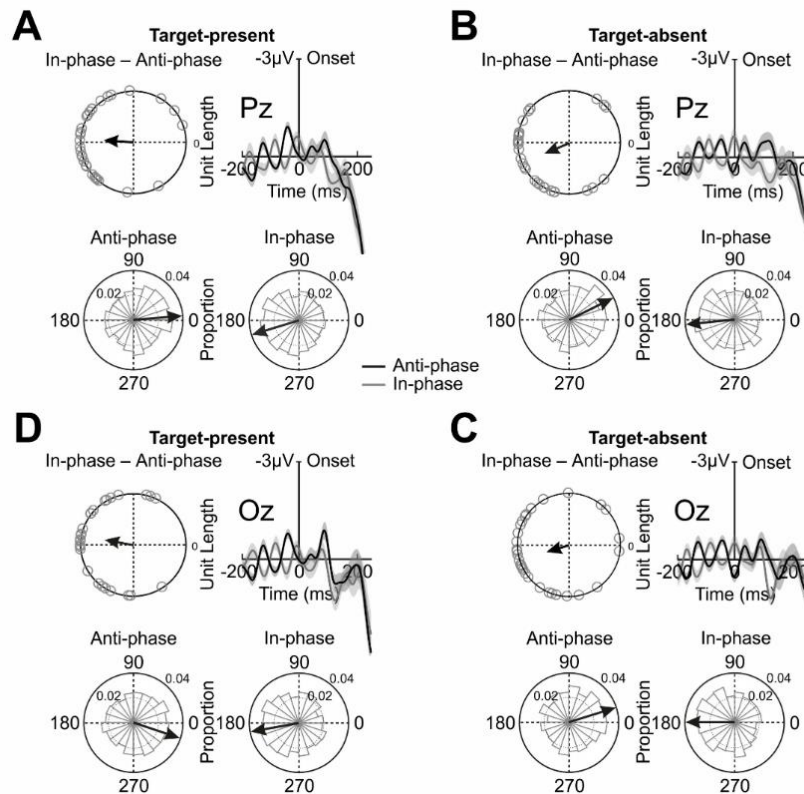
Figure 40. Schematic illustrations of the activity on target-locked trials, separating as a function of target-present and target-absent data. Once again, for visual purposes, the phases were obtained using complex Morlet wavelets. A. Target-present trials at Pz electrode. B. Target-absent trials at Pz electrode. C. Target-present trials at Oz electrode. D. Target-absent trials at Oz electrode. Each section contains four graphs. The top right illustrates the broadband ERPs with the shaded areas representing the SEM, time-locked to target onset (target-present) or expected target onset (target-absent trials) over a time window from -200 ms to 250 ms (baseline: -200 ms to 0 ms). On the top right, the circular graphs show for each participant (dots), the mean angular difference of the phase between in-phase and anti-phase trials. The length of the arrow indicates how representative the grand average of the mean difference is. A 180° difference can be observed at 12 Hz between in-phase (grey) and anti-phase (black) trials. The bottom (right and left) indicates circular histograms. The bars indicate the proportion of trials (pooled across participants with no phase re-alignment for the twenty bins) for anti-phase (left) and in-phase (right). An opposite phase preference for in-phase and anti-phase can be observed on both target-present and target-absent trials.

138

Table 8. Circular separation (in-phase – anti-phase) analyses as a function of target-present and target-absent trials and Pz and Oz electrodes.

Electrode	Condition	Circular degrees (°)	Separation (in-phase – anti-phase)
Pz	Target-present anti-phase	4.69°	158.41°
	Target-present in-phase	163.1°	
	Target-absent anti-phase	26.5°	147.8°
	Target-absent in-phase	174.3°	
Oz	Target-present anti-phase	18.52°	151.28°
	Target-present in-phase	169.80°	
	Target-absent anti-phase	17.27°	162.13°
	Target-absent in-phase	179.40°	

Data was extracted using complex Morlet wavelets.

Phase alignment in the absence of external signal

To provide further support for the presence of neural entrainment in the narrow sense, an additional analysis was carried out to check whether neural entrainment persisted post-entrainer offset for some time before the neural oscillators relaxed back to their eigenfrequencies. To evaluate the phase concentration around the entrained 12 Hz frequency, a similar Montecarlo procedure was carried out (see Cue-locked analyses) on entrainer-locked data from 41.5 ms to 250 ms post-last entrainer. This time window was selected to evaluate three cycles after the offset of the last entrainer, with a single cycle referring to one anti-phase and successive in-phase temporal moment. The resulting p values were corrected using the FDR procedure and when compared to the pre-established significance value ($p < .05$). All of the p values were statistically significant at all of the time points and for both electrodes. Therefore, the internal oscillators remained aligned to the external rhythm and this alignment persisted for at least three cycles post-entrainer offset, which would support the presence of neural entrainment in the narrow sense.

Control analyses

To ensure that the previous results were not altered due to temporal smearing of evoked activity, a series of control analyses using STFTs were carried out. [i] In terms of phase concentration over the last eight entrainers, last-entrainer locked ITC data was examined and significant phase

concentration over all time points and at both electrodes was found ($p < .05$; FDR was applied to p values to adjust for multiple comparisons). [ii] Phase opposition results were replicated and once again the anticipated 180° phase separation was confirmed, as seen through the significant circular V-test results. This would indicate that the phase was not randomly distributed and was confirmed for both target-present (Pz: $p = 1.15 \times 10^{-3}$; Oz: $p = 2.99 \times 10^{-4}$) and target-absent trials (Pz: $p = 2.60 \times 10^{-4}$; Oz: $p = 3.65 \times 10^{-5}$) (see Table 9). [iii] Circular correlations on target-absent trials were explored comparing the 12 Hz phase post-last entrainer offset (10 ms post-onset) and the 12 Hz phase at all four expected target SOAs (anti-phase 1, in-phase 1, anti-phase 2, in-phase 2). The results of these circular correlations were all significant, at all time points and both electrodes (Table 10).

Finally, to check whether 12 Hz phase had an influence on behavior, [iv] a circular correlation between phase and RTs was carried out. In this case the phase was extracted at 166 ms pre-target to avoid contamination from the target and RTs considered all four possible target onsets. Results yielded a significant correlation at in-phase 1 between 12 Hz phase and RTs, but not at any of the other onsets (see Table 11). Finally [v] a phase opposition analysis comparing response type (correct, incorrect) and target onset time as a function of relative phase (anti-phase, in-phase) was carried out. The results of this analysis were not significant between correct and incorrect trials (see Table 12).

Table 9. Circular separation (in-phase – anti-phase) analysis as a function of target-present and target-absent trials and the Pz and Oz electrodes.

Electrode	Condition	Circular degrees (°)	Separation (in-phase – anti-phase)
Pz	Target-present anti-phase	18.34°	171.60°
	Target-present in-phase	160.00°	
	Target-absent anti-phase	21.91°	163.93°
	Target-absent in-phase	177.22°	
Oz	Target-present anti-phase	37.42°	165.52°
	Target-present in-phase	153.75°	
	Target-absent anti-phase	6.57°	168.16°
	Target-absent in-phase	169.02°	

Data was extracted using short time Fourier transforms.

Table 10. Circular correlations between 12 Hz phase (10 ms after last entrainer offset) and on the temporal moments where targets should occur on target-absent trials, as a function of the four possible target onset times.

Electrode	Last vs. Anti-phase 1	Last vs. In-phase 1	Last vs. Anti-phase 2	Last vs. In-phase 2
Pz	$p < 1.000 \times 10^{-100}$	$p = 7.545 \times 10^{-73}$	$p = 4.481 \times 10^{-26}$	$p = 6.470 \times 10^{-10}$
Oz	$p < 1.000 \times 10^{-100}$	$p = 6.727 \times 10^{-61}$	$p = 6.989 \times 10^{-14}$	$p = 2.816 \times 10^{-08}$

Table 11. Circular correlations between 12 Hz phase at 166 ms pre-target onset and the reaction-times for target-present trials, as a function of the four possible target onset times.

Electrode	Anti-phase 1	In-phase 1	Anti-phase 2	In-phase 2
Pz	$p = .595$	$p = .049$	$p = .656$	$p = .608$
Oz	$p = .948$	$p = .008$	$p = .855$	$p = .699$

Table 12. Phase (166 ms pre-target) opposition between correct and incorrect trials, post-last entrainer offset, as a function of target onset time type (anti-phase, in-phase).

Electrode	Anti-phase	In-phase
Pz	$p = .979$	$p = .976$
Oz	$p = .955$	$p = .999$

EEG alpha power lateralization

Alpha activity in the pre-stimulus window (between the offset of the cue and the onset of the first entrainer) was examined to see whether the cue prompted the expected inter-hemispheric imbalance of alpha power typical to spatial attention orienting. Only correct trials were used, and alpha lateralization was examined over 7-14 Hz. Cue-locked data (0 ms to 1542 ms) was used to obtain power and the lateralization index (ipsi – contra) was assessed between 375 ms to 875 ms over the left ROI. The inter-subject average lateralization index was compared using a right-tailed paired *t*-test against zero (see Figure 41 for a violin plot of the individual distribution). The results of this *t*-test were significant, $t(29) = 1.882$, $p = .035$, $d = .344$, which would provide support for correct orienting of spatial attention post-cue (see Figure 41).
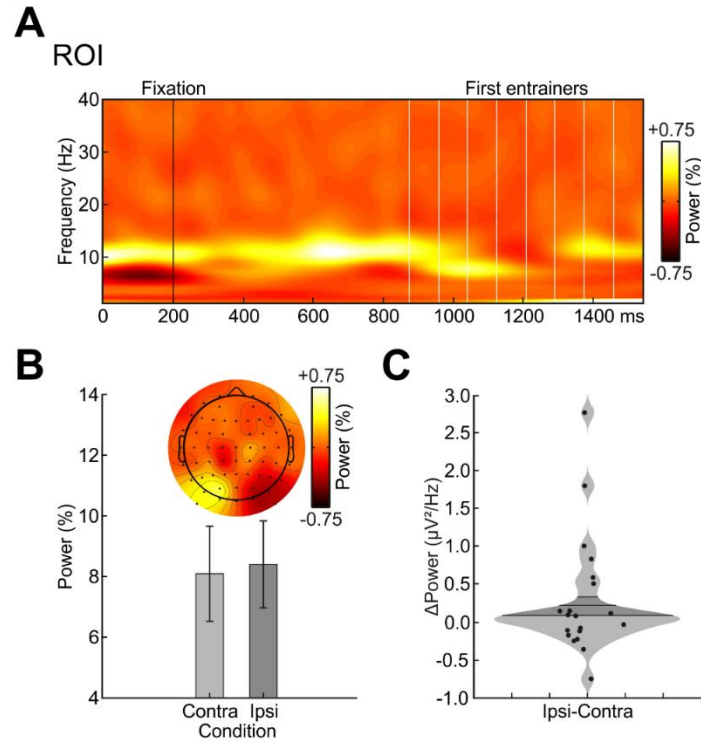
Figure 41. Alpha power lateralization analyses. A. Alpha (7-14 Hz) power lateralization over the time window from 0 ms to 1542 ms (no baseline, post-cue). Only correct trials were included. The lateralization index was obtained subtracting attended left average alpha power (ipsi left – contra left) from the attended-right average alpha power (ipsi right – contra right) and dividing by the sum of the two. The topographic plot showed the average alpha power (7-14 Hz) for each electrode ipsilateral and contralateral to the cue on both left and right cue (attended-left/attended-right) trials, computed over the time window between 375 ms to 875 ms (relative to the cue and 500 ms before the first entrainer). We used real activity for the left electrodes and simulated activity for the right electrodes. Similarly for the left cue, we used the real activity for the right electrodes and the simulated for the left electrodes. B. The bar graph shows the average alpha power at 7 – 14 Hz over the time window from 375 ms to 875 ms relative to the cue onset, for the electrodes contralateral (light grey) and ipsilateral (dark grey) to the cue on both left and right cue sides (attended-left/attended-right). C. The lateralization index plotted using a violin plot (dots represent individual participant data).

5.2. Assessing the exogenous and endogenous mechanisms of sensory-attentional processing in interictal EM and HC, using a neural entrainment task

Analyses

Participant demographics and migraine characteristics

Once the experimental session was finalized, exclusion criteria were revised, and several participants were excluded from the final sample. Fourteen EM were excluded in total. The reasons consisted of technical problems (three EM), a mean false alarm rate > 30% (two EM), a hit rate > 90% on invalid trials (one EM), matching (one EM), < 50 clean trials post-artifact rejection (one EM), and for being outside of the interictal phase during the experimental session (six EM; confirmed with eDiary). Meanwhile, seven HC were discarded for the following reasons: technical problems (one HC), a mean false alarm rate > 30% (one HC), < 50 clean trials post-artifact rejection (one HC) and for matching purposes (three HC). Post-exclusions, 40 participants, specifically 20 EM and 20 HC, made up the final sample. Both groups were age- and gender-matched. In terms of questionnaire results, no significant differences between groups were observed regarding psychiatric variables or sensory sensitivity (see Table 13). Despite their low-frequency diagnosis, the clinical questionnaires indicated that EM had some headache-related impact and moderate disability (see Table 13).

Table 13. Descriptive statistics and the results of two-sided, unpaired *t*-tests of equal variance, or two-sided, nonparametric Mann-Whitney U tests on demographic, clinical, and psychiatric variables between healthy controls and patients with episodic migraine.

Variables	EM	HC	*p*
N	20	20	-
Gender (% of females)	100	100	-
Age, years Mean ± SD Range	22.76 [2.610] 20-33	22.06 [2.265] 19-28	.152
Education level	7.00 [0.000]	7.00 [0.250]	.729
STAI-State (score)	11.50 [10.750]	10.50 [5.500]	.818
STAI-Trait (score)	23.45±11.06	19.8±5.36	.192
BDI-II (score)	4.00 [4.250]	2.00 [4.250]	.253
ASRS (score)	1.50 [2.000]	1.00 [2.250]	.309
Frequency(days/month)	2.65±2.66	NA	-
MIDAS (score)	11.00 [21.500]	NA	-
HIT-6 (score)	54.95±6.920	NA	-
MSQ (score)	33.92 [11.315]	NA	-
Accompanying symptoms of headache (%) of participants			
Aura	55.00	NA	-
Nausea/vomiting	65.00	NA	-
Photophobia	75.00	NA	-
Phonophobia	80.00	NA	-
SPQ Total (score)	113.11±18.460	117.05±18.120	.505
SPQ Vision (score)	28.79±4.590	30.40±4.790	.291
SPQ Motion (score)	8.00 [2.500]	7.00 [2.500]	.955
SPQ Brightness (score)	5.42±1.770	6.15±1.310	.151
SPQ Color (score)	5.00 [2.500]	6.00 [2.000]	.070
SPQ Acuity (score)	11.00 [1.000]	10.50 [2.500]	.909

Continuous normally distributed variables were reported using means and standard deviations (mean±SD) whereas not normally distributed variables were reported with medians and interquartile ranges (median [IQR]). Null hypotheses were assessed using two-sided, unpaired *t*-tests of equal variance and two-sided, non-parametric Mann-Whitney U tests, respectively. Bold values indicate significant differences between groups.

Behavioral analyses

To examine the effects of spatial validity, relative phase, and participant group on behavioral performance, rmANOVAs were executed using a 2 (spatial validity: valid, invalid) x 2 (relative phase: anti-phase, in-phase) x 2 (participant group: EM, HC) design on both hit rates and RTs (see Figure 42). For analysis purposes, the four target SOAs were collapsed as a function of anti-phase or in-phase. First, in terms of hit rates (Figure 42 A and C), a main effect of spatial validity was observed, $F(1,38) = 32.140$, $p = 1.62 \times 10^{-6}$ indicating increased hit rates in response to spatially valid targets (61.9±17.7%) as compared to spatially invalid ones (44.4±25.7%). The main effect of relative phase, on the other hand, was not significant, $F(1,38) = 0.315$, $p = .578$, which would imply that the hit rates on anti-phase trials (53.4±23.4%) did not significantly differ from those on in-phase trials (53.0±24.0%). Furthermore, the interaction between spatial validity and relative phase was also not significant, $F(1,38) = 0.642$, $p = .428$, which would appear to indicate that these variables were not mutually dependent. In terms of group differences, the main effect of Group was not significant, $F(1,38) = 0.288$, $p = .595$, meaning that both HC (54.8±25.6%) and EM (51.5±21.6%) had similar hit rates. The remaining interactions were also not significant: spatial validity x relative phase x participant group: $F(1,38) = 0.186$, $p = .669$; spatial validity x participant group: $F(1,38) = 0.702$, $p = .407$; and relative phase x participant group: $F(1,38) = 3.527$, $p = .068$, which would indicate that none of these variables modulated each other.

The same analysis was repeated on RTs (Figure 42 B and D). Two participants were excluded from this analysis due to a lack of correct responses to invalid conditions (only correct trials were included). Similarly, to (739) this was not a criterion for exclusion from other analyses. Once again, the rmANOVA yielded a main effect of spatial validity, $F(1,36) = 34.546$, $p = 1.01 \times 10^{-6}$, indicating decreased RTs to spatially valid trials (0.462±0.064 ms) as compared to spatially invalid ones (0.497±0.066 ms). No significant main effect of relative phase was observed, $F(1,36) = 0.916$, $p = .345$, with similar RTs in response to anti-phase (0.477±0.07 ms) and in-phase targets (0.481±0.065 ms). The interaction between spatial validity and relative phase was also not significant, $F(1,36) = 1.721$, $p = .198$, once again indicating that these variables did not appear to modulate each other. Concerning group effects, the lack of a main effect of Group also confirmed that RTs were similar between HC (0.474±0.08 ms) and EM (0.484±0.05 ms). Finally, none of the remaining interactions involving the factor Group were significant: spatial validity x relative phase x participant group: $F(1,36) = 0.065$, $p = .800$; spatial validity x participant group: $F(1,36) = 1.568$, $p = .219$; relative phase x participant group: $F(1,36) = 0.047$, $p = .830$, suggesting that these variables were not interdependent.
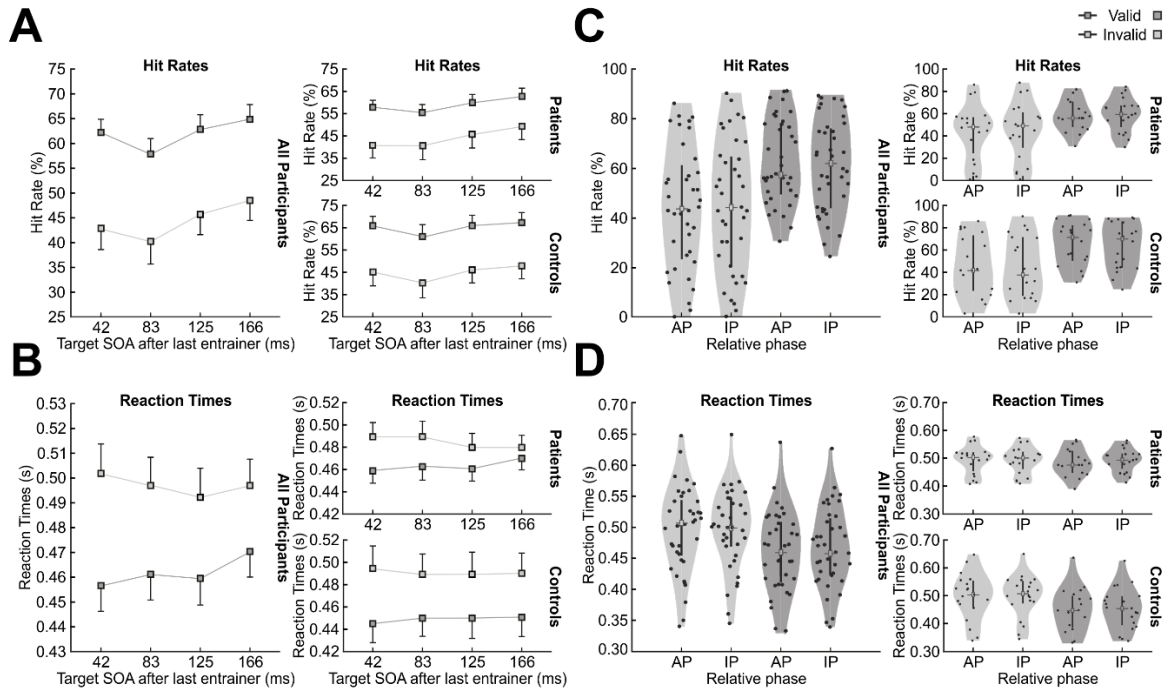
Figure 42. Behavioral analyses of hit rates and reaction times (RTs) for all participants, patients, and controls. A. Line graphs of the mean hit rates with their standard errors of the mean (SEM) with relative phase represented on the x-axis and spatial validity plotted using separate lines. B. Line graphs of the mean RTs with their SEM. Relative phase is represented on the x-axis and spatial validity plotted using separate lines. C. Violin plots of the hit rates with relative phase on the x-axis and spatial validity plotted separately. In this plot, the four target SOAs (anti-phase 1, in-phase 1, anti-phase 2, in-phase 2) are collapsed into two categories, anti-phase and in-phase. Individual data is plotted using dots and the median and interquartile range (IQR) correspond to the central squares and vertical lines, respectively. D. Violin plots of the RTs with relative phase on the x-axis and spatial validity plotted separately. In this plot, the four target SOAs are collapsed into two categories, anti-phase and in-phase. Individual data is plotted using dots and the median and IQR correspond to the central squares and vertical lines, respectively. In all four graphs, dark grey lines and bar colors indicate spatially valid conditions, whereas light great represent spatially invalid ones. Additionally, in each set of graphs, the data of all participants is plotted on the left, patient data is plotted on the top right and control data is plotted on the bottom right.

Reality check: IAF

Next, the IAF was evaluated post-cue and prior to entrainer onset to see at which frequency we could observe a peak. Both participant groups were found to have peaks in the alpha frequency range, as seen by looking at the shaded area of the violin plots representing the kernel density estimation (Figure 43). HC had a median value of 10.95 Hz (IQR: 10.15 Hz – 11.55 Hz) and EM had a median value of 11.20 Hz (IQR: 10.65 Hz – 11.58 Hz).
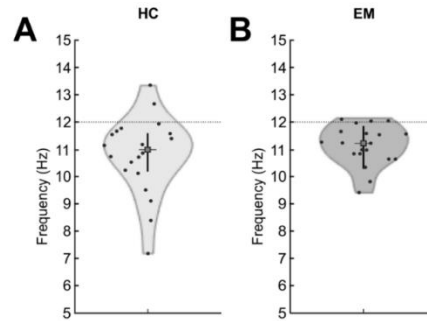
Figure 43. Violin plots of the individual alpha frequency (IAF) for both headache-free controls (HC) and patients with episodic migraine (EM). A. Violin plot of the IAF between 5 and 15 Hz at the pre-established ROI for HC. All HC had a peak in alpha. B. Violin plot representing the IAF between 5 and 15 Hz at the pre-established ROI for EM. An alpha peak was detected in all of the EM, with one exception.

Cue-locked analysis

To examine neural entrainment over the first eight entrainers (common to all trials), EEG activity was time-locked to the onset of the cue (-200 ms to 1542 ms, baseline: -200 ms to 0 ms), and ERPs and ITC were extracted (see Figure 44). Given that this time window did not extend into the target period, target-present and target-absent trials were collapsed together along with spatial validity and relative phase conditions. A preliminary look at the ERPs indicated alignment of the ERP peaks with the entrainer onset times. Furthermore, an increase and persistence of the ITC over the entrainer period was observed (Figure 44). These observations were seen in both EM and HC.

Next, to evaluate whether the phase remained concentrated around 12 Hz throughout the first eight entrainers (875 ms to 1458 ms), Montecarlo permutation tests on the phase were executed. Significant *p* values (alpha cut-off for significance: $p < .05$; FDR-corrected) were detected at all time points and for both participant groups. The results of this analysis would provide additional support for the presence of neural entrainment in both HC and EM.

Finally, ITC values were evaluated over 10-14 Hz between HC and EM. Three different time windows were inspected including: [i] the cue window (0 ms to 200 ms), [ii] from cue offset to first entrainer onset (200 ms to 875 ms), and [iii] between first entrainer onset and eighth entrainer offset (875 ms to 1542 ms). No significant differences in ITC between groups were detected at any of the three time windows: [i] $t(38) = -1.738$, $p = .090$; [ii] $t(38) = -0.061$, $p = .951$ and [iii] $t(38) = -0.361$, $p = .720$, which would appear to indicate that both groups had similar neural synchronization.

Cross-coherence

Next, to evaluate whether the internal oscillatory activity was significantly aligned with the entrainment signal, a cross-coherence analysis was carried out on both participant groups, separately. The cross-coherence values were calculated and assessed for a significant peak at 12 Hz. HC

displayed the expected peak in the cross-coherence at 12 Hz with an average height of 0.245 and an associated p value of 1.860×10^{-8}. EM also displayed a peak at 12 Hz with an average height of 0.285 and a p value of 2.006×10^{-11}. Given the significant p values in both groups, additional evidence was provided for the presence of neural entrainment in both HC and EM.
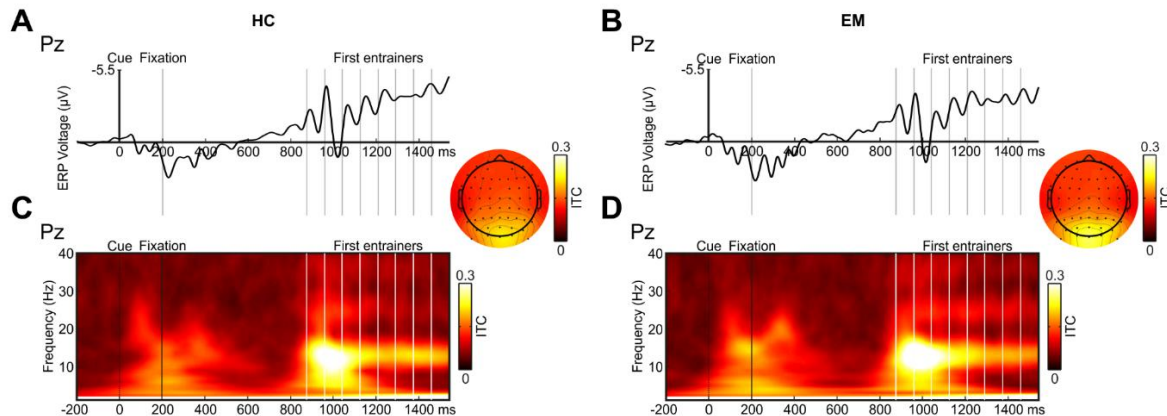
Figure 44. Cue-locked data event-related potentials (ERPs) and inter-trial coherence (ITC) for both patients with episodic migraine (EM) and headache-free controls (HC) at the Pz electrode. A. Plot of the grand-average ERP and its SEM at the Pz electrode for HC. B. Plot of the grand-average ERP and its SEM at the Pz electrode for EM, interictally. C. Cue-locked ITC at the Pz electrode for HC. D. Cue-locked ITC at the Pz electrode for EM. The time window of interest for these graphs went from -200 ms to 1542 ms (baseline: -200 ms to 0 ms). Vertical lines were used to represent the cue, fixation cross, and the first eight entrainers. Only correct, artifact-free trials were used and data epochs were collapsed across both spatial validity, relative phase, and also target-present/target-absent conditions. As can be seen, an increase in the ITC over the first eight entrainers, around 12 Hz was observed. A topographical plot for both HC (left) and EM (right), of the ITC at 10-14 Hz over the entrainer period is shown.

Entrainer-locked analysis

Given that the previous analyses only examined neural entrainment over the first eight entrainers, we wanted to verify that neural entrainment extended through the last entrainers and into the target period (see Figure 45). To accomplish this, EEG activity was time-locked to the last entrainer offset (-600 ms to 600 ms) and separated according to target-present and target-absent conditions for both participant groups. In this case, we collapsed all of the target SOAs (anti-phase 1, in-phase 1, anti-phase 2, in-phase 2) together. Here, the ITC was estimated using complex Morlet wavelets. Once again, as seen in Figure 45, an increase of the ITC around the entrained 12 Hz frequency was apparent in both participant groups, across the last eight entrainers as well as during the target period, on both target-present and target-absent trials. This would indicate that the entrained activity persisted into the target period, even in the absence of a target.

Next, for statistical analyses we began by assessing phase alignment in both groups over the time window from 41.5 ms to 250 ms, with respect to the last entrainer using a similar Montecarlo procedure as the cue-locked analyses. The length of this time window was expressly selected to

148

contain three cycles of anti-phase and in-phase temporal moments. When the resulting FDR-corrected p values were compared to the pre-established significance value ($p < .05$), all of them were deemed to be statistically significant across the length of the time window and for both participant groups. This analysis would indicate the presence of persistent alignment at the 12 Hz frequency, as seen for at least three cycles post-entrainer offset, between the internal oscillators and the external rhythm. Subsequently, group comparisons on the ITC values from 10-14 Hz were assessed at two different time windows: [i] over the last entrainers (-600 ms to 0 ms) and [ii] during the target period (0 ms to 167 ms), for target-present and target-absent trials separately. For the first time window [i] no significant differences between groups were found on either target-present, $t(38) = -0.051$, $p = .960$, or target-absent $t(38) = -0.440$, $p = .663$, trials. At the second time window [ii], ITC values were also similar between groups, with no significant differences on either target-present, $t(38) = 0.099$, $p = .922$, or target-absent, $t(38) = 0.197$, $p = .845$ trials. These results would appear to indicate that neural synchronization over these time windows was similar in both EM and HC.
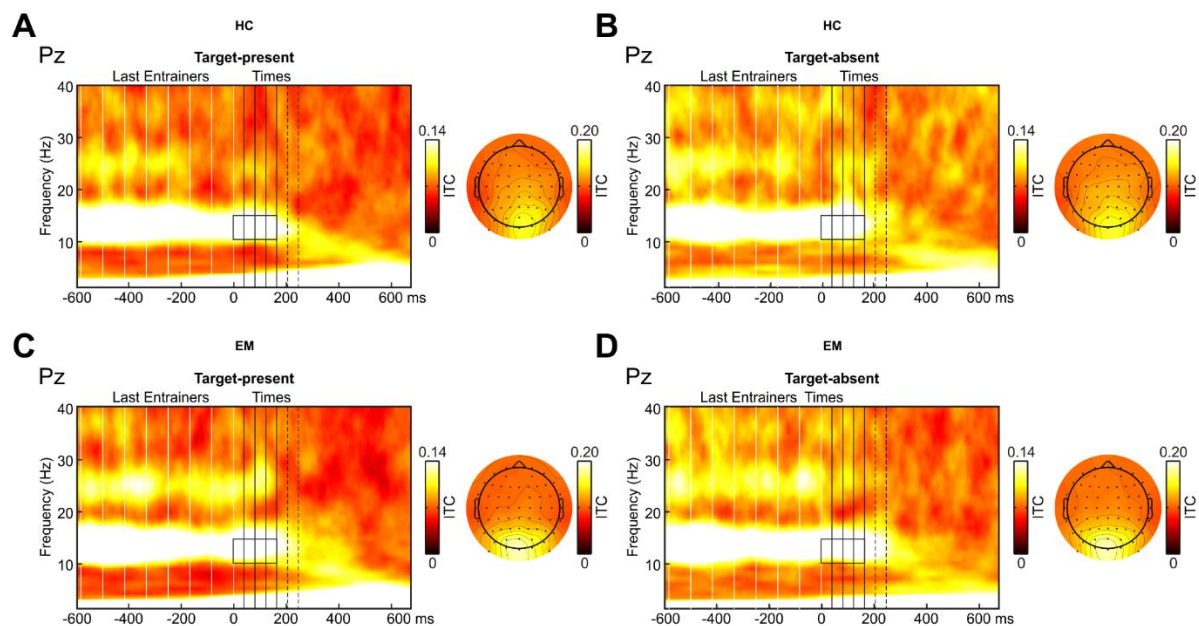
Figure 45. Entrainer-locked inter-trial coherence (ITC) data from complex Morlet wavelets for both patients and controls at the Pz electrode. A. Target-present data at the Pz electrode for HC. B. Target-absent data at the Pz electrode for HC. C. Target-present data at the Pz electrode for EM. D. Target-absent data at the Pz electrode for EM. The time window of interest here went from -600 ms to 675 ms (no baseline). Vertical lines depict the last eight entrainers (white), the four target SOAs (black, solid) and one additional cycle on anti-phase and in-phase times (black, discontinuous). Only correct artifact-free trials were included and epochs were collapsed across both spatial validity and relative phase. A clear increase in the ITC around 12 Hz can be observed through the last entrainers and the target period. Separate topographical maps are also shown for both target-present and target-absent trials of the ITC from 10-14 Hz. The time window for the topographies is from the last entrainer onset to the last possible target time point.

12 Hz phase at target-present and target-absent trials

To assess phase opposition, EEG activity was time-locked to the target onset (target-present) or expected target onset (target-absent). Trials were further separated as a function of anti-phase or in-phase targets. Only correct trials were included in these analyses and a minimum of 50 artifact-free trials per condition was required. Single trial phase values were obtained for each participant and condition at 12 Hz. ERPs as well as single trial phase values were plotted (Figure 46). In terms of the ERPs, phase opposition between anti-phase and in-phase was observed at target or expected target onset (0 ms, see Figure 46) for both target-present and target-absent conditions and HC and EM. The circular histograms of the single trial phases pooled over trials, also showed nonuniform and opposite distributions of anti-phase and in-phase temporal moments, for both target-present and target-absent conditions and both participant groups (Figure 46). Finally, the mean angular difference between anti-phase and in-phase trials, as seen in the circular graphs (Figure 46), appeared to show a concentration around 180° for both participant groups and target-present and target-absent conditions, which seemed similar in both groups.

Next, statistical analyses were carried out to provide support to the visual observations. First, circular V tests,(731) with the single trial phase pooled over all trials and participants, were carried out at Pz. An a-priori hypothesis of 180° phase separation between anti-phase and in-phase temporal moments was expected to confirm neural entrainment. The circular V test was significant for both target-present (HC: $p = .008$, EM: $p = 1.745 \times 10^{-5}$) and target-absent conditions (HC: $p = .044$, EM: $p = 9.800 \times 10^{-4}$), which would indicate that the radial differences were nonuniform and had a specific mean direction (in this case the expected 180°) (see Table 14 and 15 for descriptive circular statistics). Next, a Watson-Williams test was carried out to test for group differences and no significant differences were found at either target-present, $p = .466$, or target-absent, $p = .527$ conditions. Therefore, both participants groups had similar mean radial differences. Also, concentration metrics including kappa, mean vector length (longer vector lengths indicate greater concentration around a certain point), and mean angular direction (direction of the data) were tested to assess potential group differences using the Montecarlo procedure. No statistical differences were observed for any of the three concentration metrics, between groups: $p = .551$, $p = .567$, and $p = .533$, respectively. This would suggest that EM and HC did not differ in terms of the strength and direction of concentration.
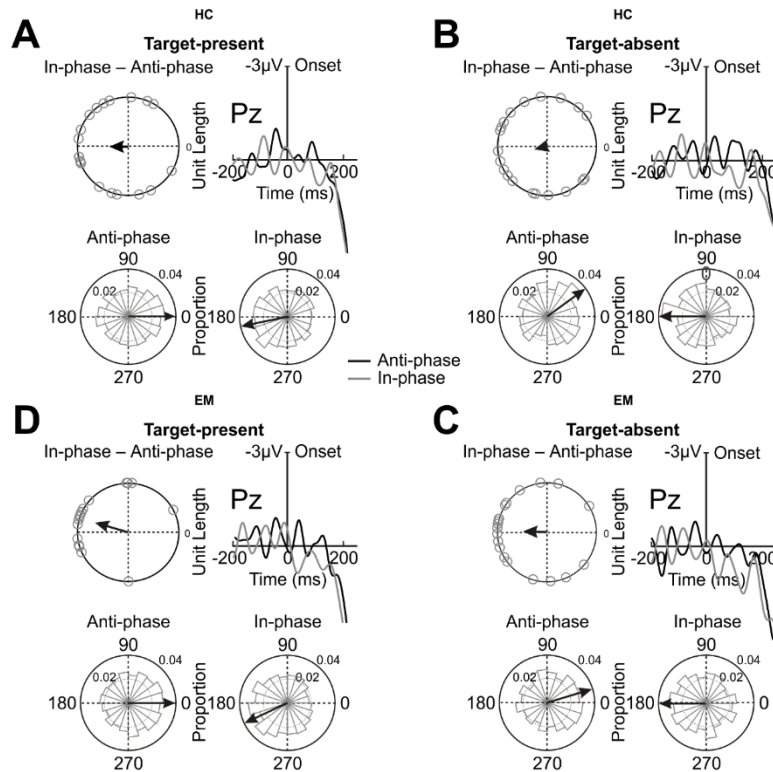
Figure 46. Schematic illustrations of the activity on target-locked trials, separated as a function of target-present and target-absent data for both patients and controls. A. Plots of the activity difference on target-locked trials for both target-present and target-absent data. Only correct, artifact-free trials were included, and phases were extracted using complex Morlet wavelets. A. Target-present trials at the Pz electrode for HC. B. Target-absent trials at the Pz electrode for HC. C. Target-present trials at the Pz electrode for EM. D. Target-absent trials at the Pz electrode for EM. Each section has four graphs, which correspond to the following. On the top right, the broadband ERP is represented, time-locked to either target onset (target-present trials) or expected target onset (target-absent trials) over a time window of interest from -200 ms to 250 ms, baseline: -200 ms to 0 ms. On the top left, the mean angular difference between in-phase and anti-phase trials is represented using circular graphs, with dots representing individual participant data. The length of the arrow represents the grand average of the mean differences, and the phase difference is approximately 180° for all of the conditions and both participant groups. On the bottom left and right, circular histograms show the proportion of trials, pooled across participants with no phase re-alignment for the twenty phase bins, for both anti-phase (left) and in-phase (right). A preference for the opposite phase can be seen for both target-present and target-absent conditions.

Table 14. Descriptive circular statistics for both patients with episodic migraine and headache-free controls. Variables are separated as a function of participant group and target-present or target-absent condition.

Participant group and condition	Mean direction	Median direction	Mean vector length	Circular variance	Circular standard deviation	Circular skewness	Circular kurtosis
HC target-present	179.87	167.73	0.37	0.62	1.11	0.01	0.03
EM target-present	163.21	163.48	0.68	0.32	0.80	0.15	0.38
HC target-absent	165.65	167.78	0.28	0.72	1.20	0.03	0.03
EM target-absent	178.83	173.12	0.49	0.51	1.01	0.09	0.23

Table 15. Analysis of circular separation (in-phase – anti-phase) for target-present and target-absent trials, extracted with short time Fourier transforms, as a function of participant group (patients with episodic migraine and headache-free controls).

Electrode	Condition	HC	Separation	EM	Separation
			Mean Angular Phase		
	Target-present anti-phase	-17.23°	179.87°	-2.10°	163.21°
	Target-present in-phase	-162.09°		-165.63°	
Pz					
	Target-absent anti-phase	31.74°	-165.65°	14.38°	178.83°
	Target-absent in-phase	-167.12°		-174.67°	

EEG alpha power lateralization

The following analyses were carried out to determine whether both participant groups exhibited the expected inter-hemispheric imbalance of alpha power, which is typical of orienting on spatial attention tasks. The topoplots yielded the expected pattern of activity in both HC and EM, showing an increase in alpha power over the time window post-cue and pre-entrainer (Figure 47). An analysis of the alpha lateralization index in both groups using a one-sided (right) paired t-test against zero, yielded a significant index in EM, $t(19) = 1.962$, $p = .032$ and a trend in HC, $t(19) = 1.678$, $p = .055$, which would provide evidence that both groups oriented attention correctly. When the lateralization index was compared between groups, no significant difference was found $t(19) = 0.211$, $p = .835$, indicating that EM and HC did not differ in terms of preparatory alpha.
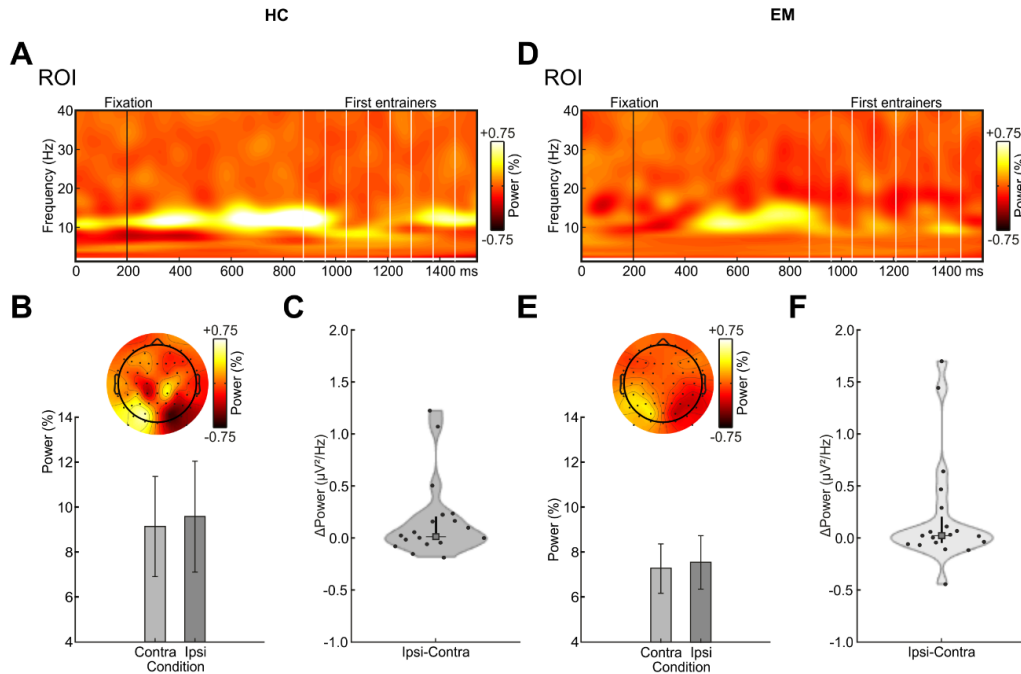
Figure 47. Alpha power lateralization analyses for both patients and controls. A. Plot of the alpha (7-14 Hz) power lateralization for HC over a time window of interest from 0 ms to 1542 ms (no baseline, post-cue). Only correct, artifact-free trials were used for this analysis. Average attended-left alpha power (ipsi left – contra left) was subtracted from the average attended-right alpha power (ipsi right – contra right) and divided by the sum of the two. **B.** The average power between 7-14 Hz was represented using a bar graph over a time window of interest from 375 ms to 875 ms (post-cue). Contralateral electrodes (light grey) and ipsilateral (dark grey) to the cue, for left and right sides (attended-left – attended- right) are shown for HC. **C.** A violin plot representing the alpha lateralization index for HC (dots represent individual participant data). **D.** Plot of the alpha (7-14 Hz) power lateralization for EM over a time window of interest from 0 ms to 1542 ms (no baseline, post-cue). Only correct, artifact-free trials were used for this analysis. Average attended-left alpha power (ipsi left – contra left) was subtracted from the average attended-right alpha power (ipsi right – contra right) and divided by the sum of the two. **E.** The average power between 7-14 Hz was represented using a bar graph over a time window of interest from 375 ms to 875 ms (post-cue). Contralateral electrodes (light grey) and ipsilateral (dark grey) to the cue, for left and right sides (attended-left – attended- right) are shown for EM. **F.** A violin plot representing the alpha lateralization index for EM (dots represent individual participant data). Topographies were shown to represent the average alpha (7-14 Hz) power for each electrode ipsilateral and contralateral to the cue on left and right cue sides (attended-left/attended-right), over the same time window (375 ms to 875 ms). Importantly, real activity was used for the left electrodes and simulated activity was used for the right electrodes.

Correlations

The circular-linear and circular-correlations did not yield any significant correlations for either HC or EM for any of the variables ($p > .100$). This would appear to indicate that clinical and experimental variables were not related.

5.3. Studying the exogenous mechanisms of visual sensory processing in interictal EM and HC, using a pattern-reversal task

5.3.1. Experiment 1

Analyses

Participant demographics and migraine characteristics

After completing the EEG recording, one EM and one HC were excluded due to technical problems. Furthermore, the eDiaries were monitored post-recording, which led to 5 EM being excluded for being outside of the interictal phase during the experimental session. Therefore, the final sample included 18 EM and 27 age- and gender-matched HC. Six patients reported aura as an accompanying symptom of headache, however no significant differences between patients with and without aura were found with respect to: sensory sensitivity (SPQ Vision scale; $t(15) = -1.037$, $p = .316$), cortical excitability (first block N1-P1 amplitude difference; $t(16) = 0.150$, $p = .883$), and/or habituation (last block N1-P1 amplitude difference – first block N1-P1 amplitude difference; $t(16) = -0.757$, $p = .460$). Consequently, patients were collapsed for further analyses. In terms of the psychiatric questionnaire results, no significant differences between EM and HC were reported (see Table 16). Finally, although patients reported low-frequency EM, some impact of headache and mild to moderate disability was found, according to the clinical questionnaires (see Table 16).

Sensory perception questionnaire

Sensory sensitivity was assessed using the SPQ with particular attention provided to the Total SPQ score, Total Vision score, and all the subsections related to Vision including Vision-Brightness, Vision-Color, Vision-Motion, and Vision-Acuity. For this analysis only, the EM sample size was 17 because one patient did not complete the SPQ questionnaire. The resulting scores were compared between participant groups and EM reported significantly lower Total Vision, Vision-Brightness, and Vision-Color scores as compared to HC. The remaining scores did not significantly differ between groups (see Table 16).

155

Table 16. Experiment 1. Descriptive statistics and results of two-sided, unpaired *t*-tests of equal variance or two-sided, nonparametric Mann-Whitney U tests on demographic, clinical, and psychiatric variables between healthy controls and patients with episodic migraine.

	Experiment 1		
Variable	**HC**	**EM**	***p***
N	27	18	-
Gender (% of females)	100.00	100.00	-
Age (years old)	21.81±2.031	22.81±1.885	.105
STAI-State (score)	12.22±6.204	11.06±5.896	.532
STAI-Trait (score)	20.44±6.727	21.11±7.962	.764
BDI-II (score)	2.00 [5.000]	3.00 [3.000]	.898
ASRS (score)	1.00 [3.000]	1.00 [2.000]	.785
Migraine frequency (headache days/month)	NA	5.09±3.235	-
MIDAS (score)	NA	7.00 [8.750]	-
HIT-6 (score)	NA	54.06±5.985	-
MSQ (score)	NA	30.36 [11.603]	-
Accompanying symptoms of headache (% of participants)			
Aura	NA	31.58	-
Subjective presence of photophobia	NA	52.63	-
Subjective presence of phonophobia	NA	52.63	-
Nausea/vomiting	NA	31.58	-
SPQ Total (score)	116.11±18.29	108.88±17.01	.197
SPQ Vision (score)	31.37±5.077	27.36±4.358	**.010***
SPQ Motion (score)	7.67±1.797	7.24±1.985	.461
SPQ Brightness (score)	5.96±1.743	4.59±1.770	**.015***
SPQ Color (score)	6.00 [1.500]	5.00 [3.000]	**.026***
SPQ Acuity (score)	21.04±2.915	10.00 [2.000]	.091

Continuous normally distributed variables were reported using means and standard deviations (mean±SD) whereas not normally distributed variables were reported with medians and interquartile ranges (median [IQR]). Null hypotheses were assessed using two-sided, unpaired *t*-tests of equal variance and two-sided, non-parametric Mann-Whitney U tests, respectively. Bold values with (*): significant differences between groups.

Electrophysiological analyses

   Classic block analysis. The ANOVA yielded a main effect of Block ($F(1,43) = 8.895$, $p =$ .005) but no main effect of Group ($F(1,43) = 2.279$, $p = .138$) or significant Block x Group interaction ($F(1,43) = 0.497$, $p = .485$). The significant main effect of Block would appear to indicate that both groups habituated normally (confirmed through visual inspection of Figure 48 B and C). Furthermore, no main effect of Group as well as the lack of a significant Block x Group interaction would provide preliminary evidence for similar cortical excitability and habituation in both participant groups.
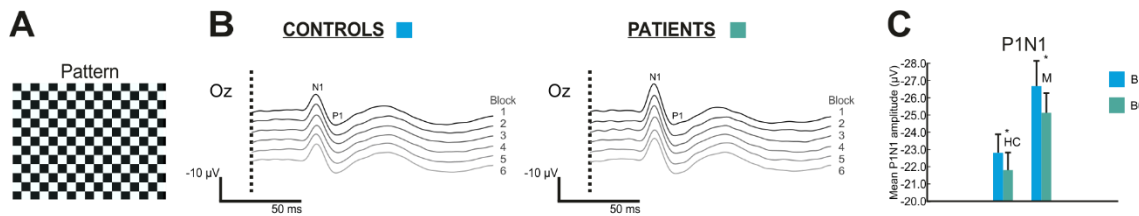
Figure 48. Checkerboard pattern and Experiment 1 visual evoked potentials (VEPs) and habituation. A. Checkerboard pattern used for the Pattern-Reversal task. B. Visual-evoked potentials (VEPs) at the Oz electrode, observed for each block (1 to 6) during the Pattern-Reversal task, for both groups (EM on the right, HC on the left). C. Bar graph depicting habituation of the N1-P1 between Block 1 and 6 (green corresponds to EM and blue to HC). Notice the decrement in amplitude from the 1st to the 6th block.

   Block linear mixed-effects model. To assess both cortical excitability and habituation while accounting for individual variability, a LMM was fitted to the P1-N1 data for Blocks 1 and 6. First, trials were inspected for the presence of extreme outliers or any data point that was ± three times the IQR. Eleven trials were removed from subsequent analyses. Following a series of comparisons using the AIC and Chisq, the model which best fit our data was found to be:

$$N1 - P1 \sim Block * Group, random = \sim 1 \mid Participant,$$
$$correlation = corAR1(form = \sim Trial \mid Participant)$$

The results of the ANOVA yielded a significant main effect of Block ($F(1,7963) = 11.499$, $p = .0007$). However, no main effect of Group ($F(1, 43) = 2.710$, $p = .100$), or Block x Group interaction ($F(1, 7963) = 2.287$, $p = .130$) were found. These results were consistent with those of the classic analyses. The main effect of Block continued to confirm normal habituation in both groups (see Figure 49 A for a visual representation). No main effect of Group or significant Block x Group interaction also indicated that EM and HC had similar results. This would appear to indicate that the participant groups did not differ with respect to cortical excitability and habituation.

Trial linear mixed-effects model. Next, we chose to extend the modelling of our data to account for both individual and temporal variability, by considering individual trials instead of just the first and last block. Once again, extreme outliers were removed prior to the analysis. After running model comparisons, the trial model that was deemed the best fit was the following:

$$N1 - P1 \sim Trial * Group, random = \sim 1|Participant,$$
$$correlation = corAR1(form = \sim Trial \,|\, Participant)$$

The results of the ANOVA indicated a significant main effect of Trial ($F(1,24056) = 228.601$, $p = 2\text{x}10^{-16}$), which was consistent with the Block model results. Furthermore, no main effect of Group ($F(1,43) = 1.954$, $p = .162$), and no significant interaction (Trial x Group: $F(1,24056) = 1.772$, $p = .183$) were reported. These findings would suggest that EM and HC habituate normally and have similar cortical excitability (see Figure 49 B for a visual representation).

Figure 49. Visual representations of the data used in both the block and trial linear mixed-effects models (LMMs) for Experiment 1. A. Visual representation of the data used in the block LMM, for both groups (EM in green, HC in blue). B. Visual representation of the data used in the trial LMM, for both groups (same colors). Please note, that trials were grouped into bins of ten trials to facilitate visual inspection by reducing trial-to-trial variability.

Correlations

A series of Spearman correlations were carried out to examine whether age or migraine frequency (only EM) were associated with any of the experimental measures including sensory sensitivity scores (SPQ Vision), cortical excitability (first block N1-P1 peak-to-peak amplitude difference), or habituation (Block 6 N1-P1 peak-to-peak amplitude difference – Block 1 N1-P1 peak-to-peak amplitude difference). In the case of HC, none of the experimental measures were correlated with age or with each other (see Table 17 for a full breakdown of *r* and FDR-corrected *p* values). In EM, on the other hand, a positive correlation between age and SPQ-Vision was found, meaning that EM reported less sensory sensitivity (higher SPQ score) with increasing age. Furthermore, a negative

correlation between first block amplitude and habituation was reported. This would suggest that greater first block amplitudes were correlated with larger differences between Block 6 and Block 1 (i.e., more habituation) and smaller first block amplitudes were associated with reduced differences between Block 6 and Block 1 (i.e., less habituation). None of the other variables were significantly associated with each other (see Table 17 for a full breakdown of *r* and FDR-corrected *p* values).

Table 17. Experiment 1. Spearman correlation tests assessing the association between age, headache frequency (migraine patients only), sensory sensitivity (SPQ Vision score), cortical excitability (first block N1-P1 peak-to-peak amplitude difference), and habituation (Block 6 N1-P1 peak-to-peak amplitude difference – Block 1 N1-P1 peak-to-peak amplitude difference).

			Experiment 1			
Group	**Variable**	**Age**	**Headache Days**	**SPQ Vision**	**First Block Amplitude**	**Habituation**
EM	**Age**	-	0.52 (*.060*)	0.70 (*.005**)	0.20 (*.501*)	-0.23 (*.501*)
	Headache Days	0.52 (*.060*)	-	0.30 (*.408*)	0.38 (*.232*)	-0.19 (*.501*)
	SPQ	0.70 (*.005**)	0.30 (*.408*)	-	0.13 (*.632*)	0.19 (*.501*)
	First Block Amplitude	0.20 (*.501*)	0.38 (*.232*)	0.13 (*.632*)	-	-0.72 (*.003**)
	Habituation	-0.23 (*.501*)	-0.19 (*.501*)	0.19 (*.501*)	-0.72 (*.003**)	-
HC	**Age**	-	NA	0.14 (*.654*)	-0.20 (*.524*)	0.10 (*.718*)
	SPQ Vision	0.14 (*.654*)	NA	-	0.21 (*.524*)	0.06 (*.773*)
	First Block Amplitude	-0.20 (*.524*)	NA	0.21 (*.524*)	-	-0.39 (*.116*)
	Habituation	0.10 (*.718*)	NA	0.14 (*.654*)	-0.39 (*.116*)	-

Spearman correlations were executed, and the False Discovery Rate (FDR) was applied to adjust for multiple comparisons. The resulting *r* and adj. *p* values $r(p_{adj})$ are reported with significant values in bold with a (*).

5.3.2. Experiment 2

Participant demographics and migraine characteristics

Following the experimental session, three participants were excluded due to technical problems (two EM, one HC) and two due to an insufficient number of clean trials post-artifact rejection (two EM). Also, 17 patients were excluded due to the presence of moderate or severe headache in the 72-hour time window surrounding the EEG session. Therefore, a total of 19 EM and 29 age- and gender-matched HC were included in the final sample. Five patients reported aura as an accompanying symptom. That being said patients with migraine with and without aura did not significantly differ on any of the experimental measures related to sensory sensitivity ($t(14) = 1.412$, $p = .180$), cortical excitability ($t(14) = 0.232$, $p = .820$), and/or habituation ($t(14) = -1.965$, $p = .070$). Therefore, the two subgroups were collapsed to augment statistical power. Regarding the results of the psychiatric questionnaires, and as would be anticipated in a sample of patients with higher migraine frequency, EM had significantly higher scores on measures of anxiety (STAI) and depression (BDI-II) than HC, but not on the ASRS (see Table 18). Clinical questionnaires also indicated that patients reported severe headache-related disability and impact (Table 18).

Table 18. Experiment 2. Descriptive statistics and results of Fisher's exact test, two-sided, unpaired *t*-tests of equal variance, or two-sided, nonparametric Mann-Whitney U tests on demographic, clinical, and psychiatric variables between healthy controls and patients with episodic migraine.

	Experiment 2		
Variable	**HC**	**EM**	***p***
N	29	19	-
Gender (% of females)	82.8%	84.2%	1.00
Age (years old)	39.24±8.842	40.89±8.679	.527
STAI-State (score)	5.00 [7.500]	11.00 [6.000]	**.002***
STAI-Trait (score)	12.00 [7.000]	19.00 [7.500]	**.001***
BDI-II (score)	2.00 [6.000]	6.00 [4.500]	**.003***
ASRS (score)	1.00 [2.000]	1.00 [2.000]	.801
Migraine frequency (headache days/month)	NA	12.68±4.028	**-**
MIDAS (score)	NA	52.32±27.885	**-**
HIT-6 (score)	NA	62.11±5.666	**-**
MSQ (score)	NA	52.96±14.131	**-**
Accompanying symptoms of headache (% of participants)			
Aura	NA	26.32	**-**
SPQ Total (score)	110.31±23.23	106.47±23.33	.579
SPQ Vision (score)	30.45±4.961	26.16±4.045	**.003***
SPQ Motion (score)	7.00 [1.000]	7.00 [2.500]	.359
SPQ Brightness (score)	5.00 [2.000]	4.00 [3.000]	**.011***
SPQ Color (score)	5.00 [2.000]	5.00 [1.000]	.194
SPQ Acuity (score)	12.00 [3.000]	10.00 [2.500]	**.012***

Continuous normally distributed variables were reported using means and standard deviations (mean±SD) whereas not normally distributed variables were reported with medians and interquartile ranges (median [IQR]). Null hypotheses were assessed using Fisher's exact test, two-sided, unpaired *t*-tests of equal variance or two-sided, non-parametric Mann-Whitney U tests, respectively. Bold values and (*): significant differences between groups.

Sensory perception questionnaire

To assess potential group differences in sensory sensitivity, SPQ scores were compared between groups. In this experiment, EM had significantly lower scores on Vision, Vision-Brightness, and Vision-Acuity than HC, which would suggest that patients exhibited hypersensitivity to visual stimuli and in particular to characteristics of brightness and acuity. No significant differences were found with respect to the Total SPQ score, Vision-Motion or Vision-Color (see Table 18).

Electrophysiological analyses

Classic block analyses. The results of the type III two-way mixed ANOVA on N1-P1 data were assessed. A main effect of Block ($F(1,46) = 24.082$, $p = 1.2 \times 10^{-5}$) was found, although the main effect of Group ($F(1,46) = 0.872$, $p = .355$) and the interaction between the two variables ($F(1,46) = 2.384$, $p = .129$) were found to be not significant. This would suggest the presence of normal habituation in both groups (confirmed by a visual inspection of Figure 50). Furthermore, EM and HC would appear to show similar levels of cortical excitability, as seen through a similar first block N1-P1 amplitude.
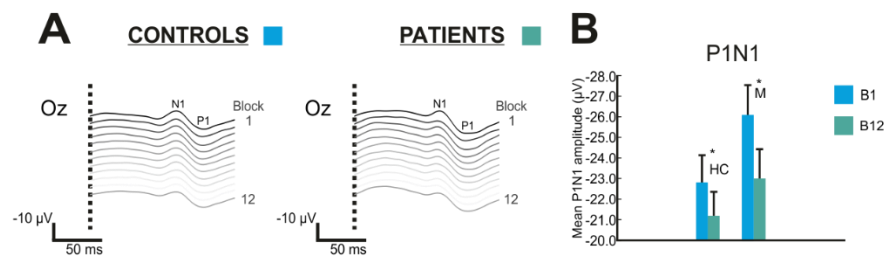
Figure 50. Experiment 2 visual evoked potentials (VEPs) and habituation. A. VEPs at the Oz electrode, observed for each block [1-12] during the Pattern-Reversal task, for both groups (EM on the right, HC on the left). B. Habituation of the N1-P1 between Block 1 and 12 (green corresponds to EM and blue to HC).

Block linear mixed-effects model. First, the data was inspected for the presence of significant outlier trials, or any trial that was ±three times the IQR, yielding 35 extreme outliers that were removed from further analysis. Only Blocks 1 and 12 were included in this analysis.(625) Model comparisons were carried out and the fit was determined according to the following model:

$$N1 - P1 \sim Block * Group, random = \sim 1 \,|\, Participant,$$
$$correlation = corAR1(form = \sim Trial \,|\, Participant)$$

The ANOVA on the resulting model yielded a significant main effect of Block ($F(1, 8888) = 30.130$, $p = 4.039 \times 10^{-8}$), no main effect of Group ($F(1,46) = 1.514$, $p = .219$), and a significant Block x Group

interaction ($F(1,8888) = 12.215$, $p = 4.741\text{x}10^{-4}$). To further explore the results, the interaction was decomposed. When comparing the N1-P1 amplitude between Blocks 1 and 12, both HC ($t = 5.489$, $p < .0001$) and EM ($t = 8.990$, $p < .0001$) showed a significant decrease. This would provide support, once again, for normal habituation in both participant groups (see Figure 51 A). Additionally, at both Blocks 1 and 12, the N1-P1 amplitude in EM and HC was found to be similar, $t = -1.230$, $p = .337$ (Block 1) and $t = -0.659$, $p = .616$ (Block 12), respectively. This would indicate that both participant groups had similar cortical excitability.

Trial linear mixed-effects model. The same trials were rejected as for the Block model and the final model, following model comparisons yielded the following:

$$N1 - P1 \sim Trial * Group, random = \sim 1|Participant,$$
$$correlation = corAR1(form = \sim Trial \,|\, Participant)$$

Once again, the results of the two-way mixed ANOVA were assessed and a main effect of Trial was found ($F(1,53803) = 264.649$, $p = < 2\text{x}10^{-16}$). Furthermore, there was a significant main effect of Group, ($F(1,46) = 5.529$, $p = .019$) as well as a significant interaction between Trial x Group ($F(1,53803) = 627.299$, $p = < 2\text{x}10^{-16}$). The main effect of Trial indicated the presence of differences between some trials. However, given the high number of trials, this is not unexpected and most likely indicates normal habituation as supported by a visual inspection of the first and last trial amplitudes in Figure 51 B. The main effect of Group and significant interaction, however, would perhaps lend some support to increased hyperexcitability in EM as compared to HC as well as differences in the habituation slope. Importantly, in this experiment differences in the habituation slope would not provide evidence as to a deficit of habituation as previously reported in some studies, but rather suggest that the habituation slope is different between groups. In this case, it would appear that EM actually habituated more. These results differ from those found in the Block LMM.
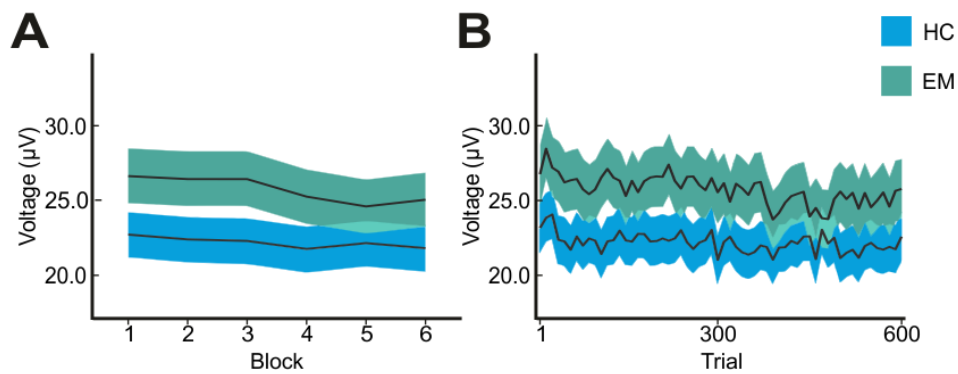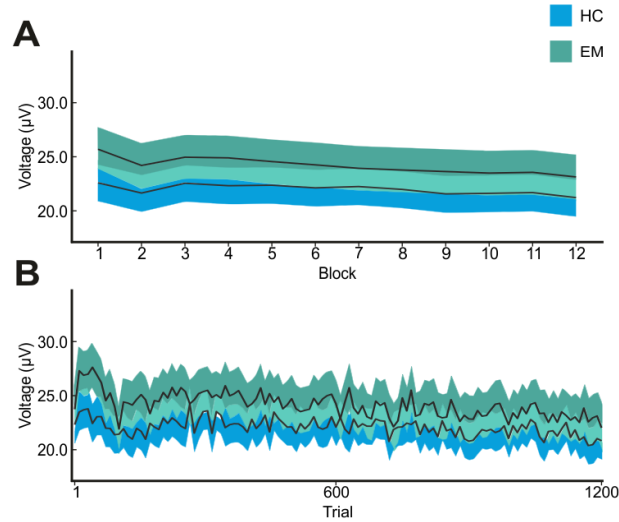
Figure 51. Visual representations of the data used in both the block and linear mixed-effects models (LMMs) for Experiment 2. A. Visual representation of the data used in the block LMM, for both groups (blue refers to HC and green to EM). B. Visual representation of the data used in the trial LMM, for both groups (same colors). Please note, that trials were grouped into bins of ten trials to facilitate visual inspection by reducing trial-to-trial variability.

Correlations

Spearman correlations were carried out to check for potential associations between age and migraine frequency (EM group only) and the experimental measures related to sensory sensitivity (SPQ Vision), cortical excitability (first block N1-P1 amplitude difference), and habituation (last block N1-P1 amplitude difference – first block N1-P1 amplitude difference). In EM, neither age nor migraine frequency were significantly correlated to any of the experimental measures. Furthermore, in contrast to Experiment 1, no correlations between the experimental measures were found either (see Table 19 for *r* values and FDR-corrected *p* values). HC also did not yield any correlations between age and any of the experimental measures, however first block amplitude and habituation were negatively correlated (see Table 19 for *r* values and FDR-corrected *p* values). This would appear to indicate that greater first block amplitude was related to greater difference between last block and first block N1-P1 amplitude difference, or more habituation.

Table 19. Experiment 2. Spearman correlation tests assessing the association between age, headache frequency (migraine patients only), sensory sensitivity (SPQ Vision score), cortical excitability (first block N1-P1 peak-to-peak amplitude difference), and habituation (Block 12 N1-P1 peak-to-peak amplitude difference – Block 1 N1-P1 peak-to-peak amplitude difference).

Group	Variable	Age	Headache Days	SPQ Vision	First Block Amplitude	Habituation
Experiment 2						
EM	**Age**	-	0.05 (*.994*)	0.02 (*.994*)	0.00 (*.994*)	0.22 (*.684*)
EM	**Headache Days**	0.05 (*.994*)	-	-0.07 (*.994*)	-0.27 (*.684*)	0.05 (*.994*)
EM	**SPQ**	0.02 (*.994*)	-0.07 (*.994*)	-	0.20 (*.684*)	0.25 (*.684*)
EM	**First Block Amplitude**	0.00 (*.994*)	-0.27 (*.684*)	0.20 (*.684*)	-	-0.25 (.684)
EM	**Habituation**	0.22 (*.684*)	0.05 (*.994*)	0.25 (*.684*)	-0.25 (.684)	-
HC	**Age**	-	NA	-0.16 (*.541*)	-0.34 (*.135*)	0.13 (*.541*)
HC	**SPQ Vision**	-0.16 (*.541*)	NA	-	0.12 (*.541*)	-0.28 (*.237*)
HC	**First Block Amplitude**	-0.34 (*.135*)	NA	0.12 (*.541*)	-	-0.55 (***.005*****)
HC	**Habituation**	0.13 (*.541*)	NA	-0.28 (*.237*)	-0.55 (***.005*****)	-

Spearman correlations were executed, and the False Discovery Rate (FDR) was applied to adjust for multiple comparisons. The resulting *r* and adjusted *p* values $r(p_{adj})$ are reported with significant in bold with a (*).

5.4. Investigating the exogenous and endogenous mechanisms of auditory sensitivity processing in interictal EM and HC, using an oddball task

Analyses

Participants

Following artifact rejection, three participants were excluded for having an insufficient number of trials post-artifact rejection (two EM, one HC) leaving a final sample of 21 patients with EM with or without aura (22.99±1.99 years old; 4.38±2.91 headache days/month) and 21 age- and gender-matched HC (21.95±2.20 years old; $t(40) = -1.598$, $p = .118$).

Questionnaire results

For a breakdown of descriptive and inferential statistics related to clinical and psychiatric questionnaires see Table 20 and Table 21, respectively. No significant differences between groups were found using independent sample t-tests with respect to the psychiatric questionnaires.

Table 20. Descriptive statistics related to the clinical questionnaires.

	Migraine	
Clinical questionnaires	M	SD
HIT-6	51.00	7.10
MIDAS	6.38	6.82
Mig-S-Cog	4.52	3.86
MSQ (points)	25.96	8.72

The following clinical questionnaires were assessed: the Headache Impact Test (HIT-6), Migraine Disability Assessment (MIDAS), Migraine Subjective Cognitive Symptoms Questionnaire (Mig-S-Cog), and the Migraine-Specific Quality of Life Questionnaire (MSQ, points). Mean (M) and standard deviation (SD).

Table 21. Descriptive statistics and results of the independent sample *t*-tests on the psychiatric questionnaires.

	HC		EM			
Questionnaires	M	SD	M	SD	*t*	*p*
ASRS	1.57	1.83	2.29	1.76	-1.287	.206
BDI	4.52	4.09	4.90	3.96	-.306	.761
BSI (depression)	.47	.50	.51	.52	-.261	.795
BSI (hostility)	.39	.46	.46	.51	-.444	.660
BSI (somatization)	.39	.38	.43	.34	-.302	.764
BSI (obsession-comp.)	.65	.54	.76	.57	-.648	.520
BSI (interpersonal sens.)	.75	.75	.82	.73	-.312	.757
BSI (anxiety)	.54	.61	.75	.43	-1.314	.196
BSI (phobic anxiety)	.26	.41	.22	.33	.332	.741
BSI (paranoid ideation)	.54	.56	.38	.49	.998	.324
BSI (psychotism)	.49	.60	.38	.49	.615	.542
ESS	9.19	3.71	9.38	3.01	-.183	.856
IPAQ (intense)	1247.71	1455.16	1497.14	1814.63	-.495	.623
IPAQ (moderate)	794.29	936.64	1613.73	2571.25	-1.372	.182
IPAQ (walking pace)	1686.14	1668.89	2578.71	3951.55	-.954	.346
IPAQ (total)	3726.14	2995.33	5689.59	7180.71	-1.156	.258
STAI (state)	12.71	7.88	12.14	5.73	.269	.790
STAI (trait)	21.00	6.70	23.48	7.49	-1.129	.266
THF	5.29	5.26	5.10	2.81	.146	.884

The questionnaires analyzed above include the Adult ADHD Self-Report Scale (ASRS), the Beck Depression Inventory (BDI-II), the Brief Symptoms Inventory (BSI), the Epworth Sleepiness Scale (ESS), the International Physical Activity Questionnaire (IPAQ), the State-Trait Anxiety Inventory (STAI), and the Test of Hypersensitivity to Sound (GÜF/THF). No differences were found. Significance was set at $p < .05$.

Behavioral results

Behavioral performance on both novel and standard trials was evaluated between groups to assess potential differences. First, in response to novel stimuli, similar RTs were reported between HC (512.53±73.29 ms) and EM (486.13±41.19 ms; $t(40) = 1.602$, $p = .117$). Furthermore, no differences between groups were found with regard to the percentage of misses (HC: 4.86±3.79%, EM: 5.61±5.63%; $t(40) = -0.506$, $p = .616$) or the false alarm rate (HC: 3.29±1.65%, EM: 3.91±2.24%; $t(40) = -1.023$, $p = .312$). This would appear to indicate similar behavioral performance between HC and EM in response to novel stimuli. Second, with regard to standard trials, the ANOVA on false alarm rates yielded no main effect of Block ($F(4,160) = 2.466$, $p = .106$), Group ($F(1,40) = 0.001$, $p = .978$) or Block x Group interaction ($F(4,160) = 0.102$, $p = .854$). This would appear to indicate that false alarm rates were not modulated by either Block or Group.

Electrophysiological results

Repetitive stimuli ERPs. The anticipated N1, P2, and N2 ERP components were identified and observed across blocks. For a visual observation of the results and statistics related to the rmANOVAs, see Figure 52 and Table 22. The main effect of Electrode Location was significant for all components and signaled a central distribution for N1 and P2 components and a frontocentral distribution for N2. In contrast, there was no main effect of Block or significant Block x Electrode interaction for either N1 or N2 components, which would imply that the amplitude of these components did not significantly change over time, suggesting a lack of habituation. However, both a main effect of Block and a significant Block x Group interaction were reported for the P2 component, which would indicate a decrement in the amplitude, or normal habituation.

In terms of group differences, there was a trend for a main effect of Group regarding the N1 component, with EM patients exhibiting increased amplitudes of N1 as compared to HC. No main effect of Group or significant Block x Group interaction were reported for the remaining components. Furthermore, given the lack of significant three-way interaction (Block x Electrode x Group) and two-way interaction (Block x Group), it seemed that both participant groups displayed comparable habituation patterns with a lack of habituation of N1 and N2 and habituation of P2.
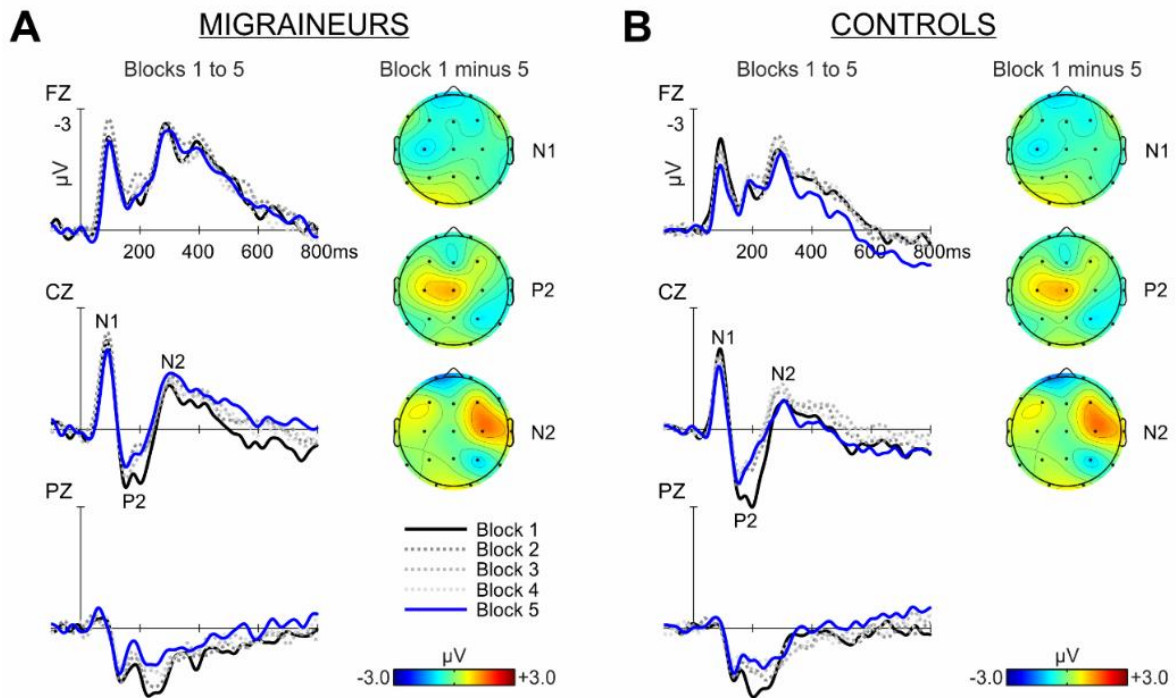
Figure 52. Grand mean event-related potential (ERP) waveforms for standard trials. Data is displayed over Blocks: 1 (solid black line), 2 (pointed dark grey line), 3 (pointed medium grey line), 4 (pointed light grey line), and 5 (solid blue line) for midline electrodes (Fz, Cz, and Pz) over the time window of interest from -100 ms to 800 ms, -3 to +3 µV, for both EM (A) and HC (B). The scalp distribution (-3 to +3 µV), for the 1st minus 5th Block of standard trials includes the N1, P2, and N2 components.

Table 22. Results of the repeated measures analysis of variance (rmANOVA) on the event-related potential (ERP) components related to standard trials.

	B		B x G		E		E x G		B x E		B x E x G		G	
ERP	*F*	*p*	*F*	*p*	*F*	*p*	*F*	*p*	*F*	*p*	*F*	*p*	*F*	*p*
N1	0.830	.498	1.412	.237	34.504	**<.001**	1.582	.214	1.652	.130	0.691	.664	3.772	.059
P2	3.968	**.006**	0.919	.447	68.364	**<.001**	.303	.713	2.562	**.022**	0.554	.757	0.019	.891
N2	0.534	.676	1.656	.175	35.351	**<.001**	1.933	.153	0.957	.447	1.114	.354	2.582	.116

N1 (175-225 ms), P2 (350-450 ms), and N2 (250-350 ms) ERP components were assessed. The rmANOVA included Block (B: 1 to 5) and Electrode (E: Fz, Cz, Pz) as within-subject factors and Group (G: HC, EM) as the between-subject factor. The degrees of freedom for this analysis were: B[4,160], BxG[4,160], E[2,80], ExG[2,80], BxE[8,320], BxExG[8,320], and G[1,40]. Bold values represent *p* < .05.

Spectral power of repetitive stimuli. The anticipated frequency bands of interest, theta (3-8 Hz), alpha (8-12 Hz), and beta-gamma (12-40 Hz), were identified in both groups. For a visual representation of the results and rmANOVA statistics, see Figure 53 and Table 23. First, a main effect of Electrode Location for all three frequencies indicated a central distribution. Next, a main effect of Block was detected in both theta and alpha, but not beta-gamma (see Table 23). These results would imply normal habituation across blocks for theta and alpha but not beta-gamma. The spectral power of theta, alpha and beta-gamma was comparable between EM and HC as confirmed by no main effect of Group or Group x Block interaction. No differences in habituation were detected between groups.
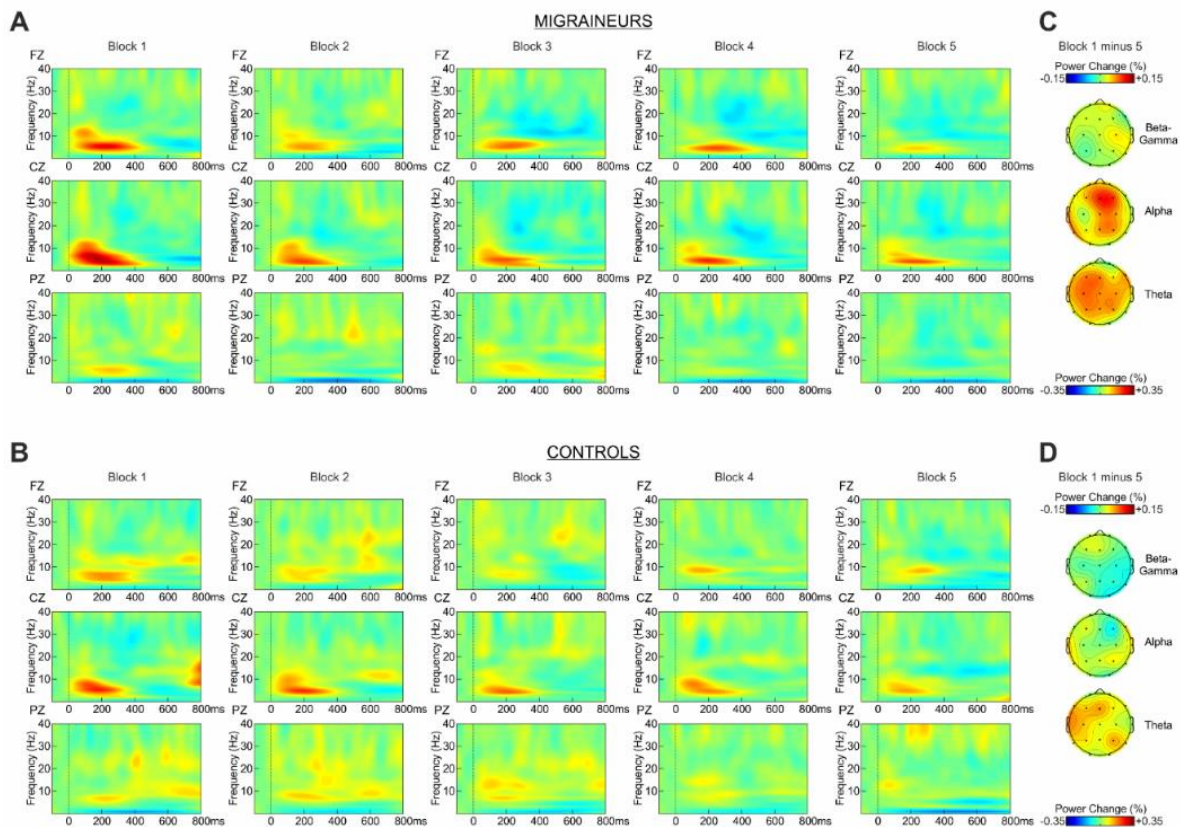
Figure 53. Grand mean event-related spectral perturbations (ERSPs) representing the change in power with respect to the baseline of standard trials, separated by blocks, at the midline electrodes (Fz, Cz, Pz) for both EM (A) and HC (B). Power is represented as a function of percentage change (-100 to +100%) over -100 ms to 800 ms. Topographical maps of the spectral power difference between the 1st and 5th block are depicted for each frequency of interest (theta: 3 – 8 Hz, 0-400 ms; alpha: 8 – 12 Hz, 0-200 ms; and beta-gamma: 12-40 Hz, 0-200 ms) and group.

Table 23. Results of the repeated measures analysis of variance on the ERP components related to standard trials.

TF	B F	B p	B x G F	B x G p	E F	E p	E x G F	E x G p	B x E F	B x E p	B x E x G F	B x E x G p	G F	G p
Theta	5.543	**.001**	.902	.452	41.601	**<.001**	2.293	.111	1.060	.386	.462	.824	2.373	.131
Alpha	2.276	**.034**	1.774	.141	10.388	**<.001**	1.226	.299	1.958	.070	.499	.814	.701	.407
Betag	.578	.660	.827	.499	5.390	**.007**	.467	.788	.788	.580	.354	.907	2.230	.143

Theta (3-8 Hz, 0-400 ms), alpha (8-12 Hz, 0-200ms), and beta-gamma (12-40 Hz, 0-200 ms) frequencies were assessed. The rmANOVA included Block (B: 1 to 5) and Electrode (E: Fz, Cz, Pz) as within-subject factors and Group (G: HC, EM) as the between-subject factor. The degrees of freedom for this analysis were: B(4,160), BxG(4,160), E(2,80), ExG(2x80), BxE(8,320), BxExG(8,320), and G(1,40). Bold values represent $p < .05$.

Time and phase-synchronization analyses of repetitive stimuli. For a visual representation of the results and statistics related to the rmANOVAs, see Table 24 and Figure 54. A visual inspection of Figure 54 would appear to indicate an increment of the phase-synchronization of theta, alpha, and beta-gamma on standard trials, with EM appearing to show increased phase at all three frequencies as compared to HC. Furthermore, the ITC would appear to habituate across blocks for all frequencies. The results of the ANOVA yielded a main effect of Electrode Location for all three frequencies, which would indicate increased ITC at central electrodes. Similarly, to the results of spectral power, a main effect of Block was found for both theta and alpha but not beta-gamma, which would support habituation of theta and alpha over blocks but not beta-gamma. Next, in terms of group comparisons, a main effect of Group for theta indicated that EM had increased phase synchronization as compared to HC. No significant differences were observed in the phase synchronization of alpha and beta-gamma between groups, as confirmed by a lack of main effect of Group and no Group interactions. Once again, no differences in the habituation of these frequencies were observed between groups.
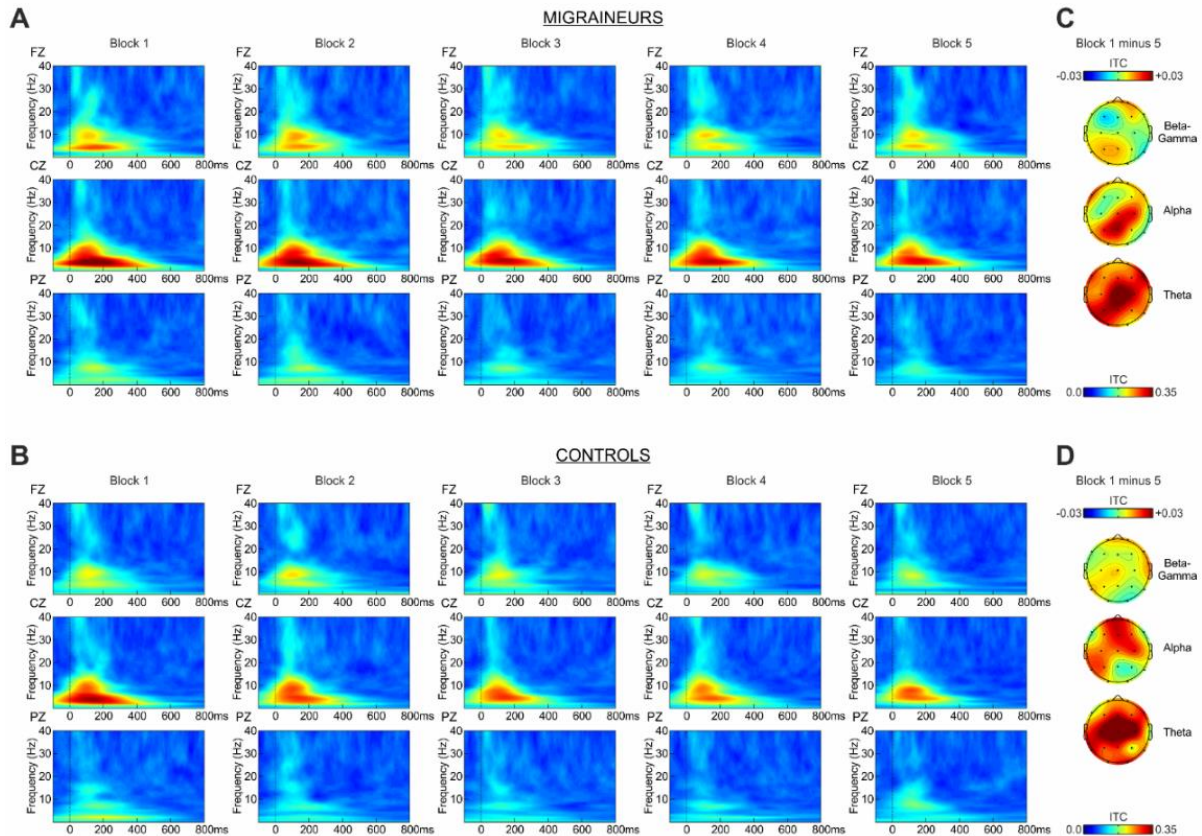
Figure 54. Grand mean of the inter-trial coherence (ITC, also known as phase synchronization) on standard trials, separated as a function of Block, at midline electrodes (Fz, Cz, Pz) and EM (A) and HC (B). The ITC was plotted over a scale from 0 to 0.35 and over the time window from -100 ms to 800 ms. Topographical maps of the ITC difference (-0.03 to +0.03) between the 1st and 5th block are shown in terms of the frequency of interest (theta: 3 – 8 Hz, 0-400 ms, alpha: 8 – 12 Hz, 0-200 ms, and beta-gamma: 12-40 Hz, 0-200 ms) and group.

Table 24. Results of the repeated measures analysis of variance on the event-related potential (ERP) components related to standard trials.

P-sync	B		B x G		E		E x G		B x E		B x E x G		G	
	F	p	F	p	F	p	F	p	F	p	F	p	F	p
Theta	14.599	**<.001**	.679	.577	43.583	**<.001**	1.577	.216	1.198	.308	.480	.825	5.986	**.019**
Alpha	3.659	**.009**	1.070	.370	39.114	**<.001**	.138	.853	.967	.447	1.608	.148	2.377	.131
Betag	1.203	.312	.134	.957	14.338	**<.001**	2.924	.062	1.386	.219	.650	.695	.339	.564

The following frequencies were analyzed: theta (3-8 Hz, 0-400 ms), alpha (8-12 Hz, 0-200 ms), and beta-gamma (12-40 Hz, 0-200 ms). A rmANOVA was carried out including Block (B: 1 to 5) and Electrode (E: Fz, Cz, Pz) as within-subject factors and Group (G: EM, HC) as the between-subject factor. The degrees of freedom for this analysis were as follows: B(4,160), BxG(4,160), E(2,80), ExG(2,80), BxE(8,320), BxExG(8,320), and G(1,40). Bold values represent $p < .05$.

Target/novel ERPs. The anticipated cascade of ERPs was observed in response to target stimuli in both EM and HC, including a frontocentral MMN, a centro-parietal P3b, and a frontocentral RON (see Figure 55). For a visual representation of the results and statistics related to the rmANOVAs, see Figure 55 and Table 25. The results of the rmANOVA on target stimuli yielded a significant main effect of Electrode for all three components with the anticipated topographic distributions. Furthermore, no significant main effect of Group was found at any of the components, indicating that EM and HC did not significantly differ with respect to either MMN, P3b, or RON to target stimuli. Finally, the Block x Group interaction was not significant for any of the components.

In terms of novel stimuli, once again the anticipated cascade of ERPs was observed and consisted of a frontocentral MMN, a central early P3a, a frontal and parietal late P3b, and a frontocentral RON (see Figure 55). The rmANOVA indicated a main effect of Electrode Location supporting the expected topographic distributions. In terms of group comparisons, although the main effect of Group was not significant for any component, a significant Electrode x Group interaction was found for the early P3a, late P3a, and RON. Upon decomposing this interaction using post-hoc *t*-tests, the amplitude of the early P3a was found to be significantly reduced at the Pz electrode ($t(40) = 3.747$, $p = .001$) with a trend at Cz ($t(40) = 1.967$, $p = .056$) in EM as compared to HC. The late P3a, on the other hand, was found to be significantly increased at frontal sites in EM, as confirmed by a significant effect at the Fz electrode ($t(40) = -2.087$, $p = .043$). RON was also found to be altered at frontal sites, with a reduced amplitude in EM at the Fz electrode ($t(40) = 2.801$, $p = .008$).

Table 25. Repeated measures ANOVA for the ERP difference waveforms related to target and novel stimuli.

Component	E		E x G		G	
	F	*p*	*F*	*p*	*F*	*p*
Target						
MMN	43.807	**<.001**	0.647	.488	0.061	.806
P3b	204.806	**<.001**	2.300	.125	0.068	.796
RON	119.858	**<.001**	3.260	.062	0.052	.820
Novel						
MMN	27.929	**<.001**	1.699	.196	0.382	.540
Early P3a	45.876	**<.001**	18.103	**<.001**	1.310	.259
Late P3a	223.141	**<.001**	5.025	**.015**	0.097	.757
RON	78.174	**<.001**	6.586	**.005**	0.002	.968

Components and time windows for target stimuli: mismatch negativity (MMN) (175-225 ms), P3b (450-550 ms), and re-orienting negativity (RON) (350-450 ms). For novel stimuli: MMN (175-225 ms), early P3a (225-275 ms), late P3a (275-325 ms), and RON (400-600 ms). The rmANOVA included Electrode (E: Fz, Cz, and Pz) as within-subject factor and Group (G: HC, EM) as between-subject factor. The degrees of freedom were as follows: E(2,80), E x G(2,80), and G(1,40). Bold values represent *p* < .05.
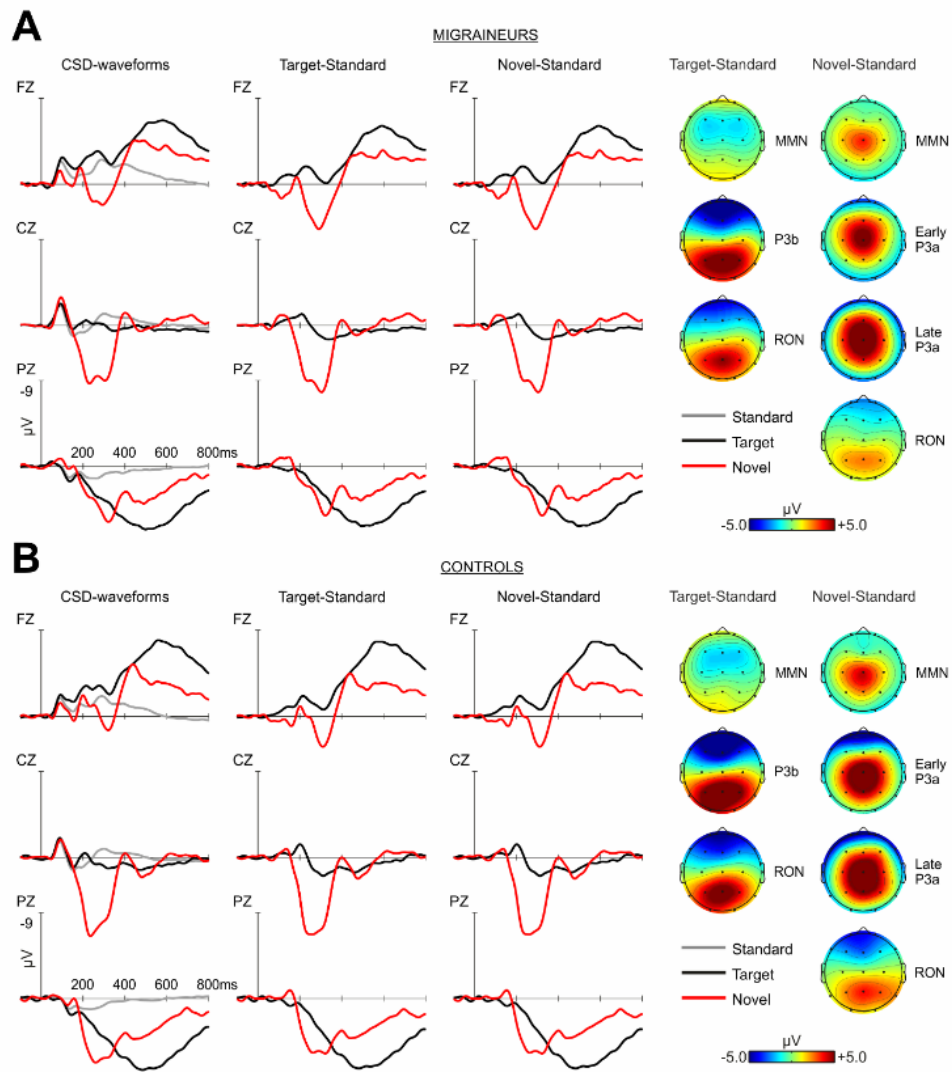
Figure 55. Grand mean event-related potential (ERP) waveforms for standard (grey line), target (black line), and novel (red line), at midline electrodes (Fz, Cz, Pz) over the time window of interest from -100 ms to 800 ms and between -9 and +9 µV for both EM (A) and HC (B). Difference waveforms associated to the target minus standard (black line) and novel minus standard (red line) are shown. Scalp distribution between -5 to + 5 µV for target minus standard trials involve the mismatch negativity (MMN), P3b, and RON. Scalp distribution between -5 to +5 µV for novel minus standard involve the MMN, early P3a, late P3a, and RON).

6. DISCUSSION

In this section, the results of the previously described research studies 1 through 4 will be described, in light of the main and secondary objectives of the present PhD thesis.

6.1. Developing a task to study the exogenous and endogenous mechanisms of sensory-attentional processing

The first SO of this PhD thesis was to design a task, that would enable us to study the exogenous and endogenous mechanisms of sensory-attentional processing. To accomplish this objective, in Research Study 1 we modified a pre-existing neural entrainment paradigm (484) and checked that the resulting signal met the requirements for neural entrainment in the narrow sense.(482,491) Past research would provide evidence against the conceptualization of neural entrainment as a succession of ERPs,(484,525,757) however it remains unclear whether the reported behavioral benefits of neural entrainment are a side-effect of expectancy-related ERPs elicited in response to task predictability.(758,759) In our modified version of the neural entrainment paradigm,(484) the following changes were made: [i] an entrainer stream of variable length (8-12 entrainers), [ii] a detection task with bilateral targets, and [iii] a greater proportion of target-absent trials to which participants were told to withhold their response. These modifications were made to reduce inherent task predictability, typical to most neural entrainment paradigms, while augmenting the number of target-absent trials used to assess endogenous neural activity. We also ran the analyses at both the Pz [based on past literature (484,514,740)] and Oz [based on the site of maximum signal in our research study] electrodes and found the same effects at both sites, indicating that Oz is also a valid choice for future studies. Our modified neural entrainment task effectively permitted us to study both exogenous (throughout the entrainment period) and endogenous mechanisms (in the absence of entrainers and targets) of sensory-attentional processing. The results of this research study would support the presence of a neural mechanism with the capacity to synchronize internal oscillatory activity to the temporal structure of external stimuli.(210,482). Specifically, we found:

[i] alignment of internal oscillatory activity to the periodic external stimuli,

[ii] persistence of this entrained signal (phase alignment) for a number of cycles post-entrainer offset,

[iii] no behavioral benefits for targets aligned (in-phase) to the entrainers.

179

Neural entrainment in the narrow sense

First, we observed an increase in the ITC at the entrained frequency during the entrainer period, alongside a significant peak in the cross-coherence between the internal and external signals. Specifically, following the phase reset in response to the first entrainer, the neural oscillatory activity remained aligned to the external rhythm (12 Hz) throughout the stream of entrainers. This is consistent with findings indicating that the brain has a natural tendency to synchronize its endogenous oscillatory activity to external rhythms.(189,486,514,760) However, the presence of significant cross-coherence is a requirement of neural entrainment in the narrow sense, but it is not sufficient to conclude that the alignment between the internal and external signals occurs due to neural entrainment. To investigate this further, phase alignment was inspected to see whether it persisted for at least two cycles, post-entrainer offset. The results of our research study showed that not only did phase alignment between the internal and external signals persist for a minimum of three cycles post-entrainer but there was also a phase separation of approximately 180° between in-phase and anti-phase temporal moments, even on target-absent trials. This is in line with previous literature indicating reverberation, or the persistence of the entrained signal for some time post-entrainer offset.(476,484,761) Additionally, the results of our study build on past literature by demonstrating that neural reverberation occurs despite reduced temporal predictability with regard to possible target onsets and a variable entrainer stream. Importantly, this was seen on all trials, including target-absent ones where activity was uncontaminated by the appearance of a target or response-related ERP activity. In fact, our experimental design, which included a greater number of absent-target trials, a variable length of entrainers, and four different target SOAs, not only removed the influence of motor response-related ERPs but also reduced the probability of the appearance of ERPs related with expectation, thus supporting the presence of neural entrainment.(210,494,495,758,759,762)

Neural entrainment and behavior

Despite previous research indicating behavioral benefits for targets in-phase with the entrainers,(484,514) the results of this research study did not yield the expected behavioral effects. To make sense of these findings, it is important to begin by reviewing the literature related to alpha phase concentration. Although some studies have shown a benefit of alpha phase concentration on detection or discrimination tasks,(189,237,484,493,740) others have not reported these benefits.(457,763–766) In fact, a review of the literature would suggest that reported phasic effects tend to be weak and highly related to experimental features [e.g.,(765)]. In terms of alpha entrainment, several studies have indicated a behavioral benefit in response to in-phase, with respect to the neural entrainers, as opposed to anti-phase targets, when phase was concentrated.(237,484,514) However,

in another study, despite an effect of alpha phase, the authors reported an unexpected opposite effect on behavior, with enhanced accuracy in response to anti-phase as compared to in-phase targets.(525)

The paradigm used in this research study, was methodologically similar to the one used by Kizuk & Mathewson (484) with the most relevant modification being a reduction in temporal predictability inherent to other neural entrainment paradigms, through the use of an entrainer stream of variable length (8-12 entrainers). We do not believe that the results of the current study directly contradict previous work, but rather appear to suggest that the net effect of rhythmic neural entrainment on behavioral measures, particularly when anticipation is reduced, may be weaker than previously stipulated. Therefore, we propose that performance benefits described in other research studies may be a mix of the effects of neural entrainment, as demonstrated here, and other processes, such as expectation,(761) or memory,(759) elicited as a result of task predictability.

6.2. Assessing the exogenous and endogenous mechanisms of sensory-attentional processing in interictal EM and HC, using a neural entrainment task

The second SO of this PhD thesis was to examine the exogenous and endogenous mechanisms of sensory-attentional processing in patients with EM during the interictal phase, using the previously validated neural entrainment task [Research Study 1], and time-frequency analyses. The neural oscillatory activity during the entrainer and target periods permitted us to assess exogenous mechanisms whereas target-absent trials allowed us to assess endogenous mechanisms without the contamination of evoked (exogenous) activity. The results of this research study yielded three main findings:

[i] no differences in behavioral performance between HC and EM,

[ii] the presence of neural entrainment in the narrow sense as confirmed by significant phase alignment between the internal and external signals and persistence of this neural entrainment post-entrainer offset in both HC and EM,

[iii] a similar index of lateralization in both HC and EM.

Behavioral performance

Regarding behavioral performance, no significant differences between groups in terms of hit rates and RTs were found, which was confirmed by a lack of a significant main effect or interaction/s with the between-subject factor, Group. These findings are in line with those of other studies, using the Posner cueing paradigm to study selective attention in patients with migraine compared to headache-free controls.(669–671,767) Furthermore, they are also consistent with the literature evaluating attentional mechanisms in patients with migraine using the Stroop task, where similar behavioural performance between patients and controls was also reported [(648,768,769) despite (659)]. Intriguingly, recent studies have suggested that alterations in attentional mechanisms may occur at the level of attentional executive function in patients with migraine in the interictal phase.(661,663,769,770) In fact, the executive component of attentional function is thought to underlie, among other things, the ability to navigate cognitively demanding tasks as well as suppress irrelevant information.(645) Nevertheless, although our research study made use of a neural entrainment task that may be considered more attentionally demanding than the classic Posner paradigm,(388) our task is more associated with selective attention than executive function, which could explain the lack of significant differences in behavior between patients and controls.

183

Importantly, the task was working correctly, as confirmed by a main effect of spatial validity, no main effect of relative phase, and a lack of interaction between spatial validity and relative phase. The main effect of spatial validity was anticipated given the vast literature on the topic of spatial cueing and its resulting impact on preferential processing and consequently behavioral benefits, including greater accuracy and/or faster RTs in response to attended as compared to unattended locations.(367,388,660,771,772). In contrast, we did not find a main effect of relative phase or an interaction between any of the variables (relative phase, spatial validity, participant group). This is consistent with the results of our previous study [Research Study 1] as well as several other studies, which also reported a lack of relative phase effects and/or interactions with other variables.(457,763–765) Nonetheless, some other studies did report a main effect of relative phase (189,740) and/or an interaction between relative phase and spatial validity.(237,484,773) What these findings would appear to show us is the importance of the effects of task predictability on the presence of relative phase effects,(739) also discussed in other studies.(759,761) In particular, decreasing task predictability seems to reduce the likelihood of certain behavioral benefits occurring, which might suggest that the impact of neural entrainment on behaviour may be more limited than previously stipulated.

IAF

Next, differences in IAF between the offset of the cue and the onset of the first entrainer were assessed to see if there were any differences in the frequency of the IAF. Differences in the IAF between groups are relevant because neural entrainment tends to occur more easily when the external rhythms are closer to the eigenfrequency of the internal oscillators.(482) Similar IAF between groups in our research study might explain the lack of significant behavioural differences.

Neural entrainment (exogenous and endogenous mechanisms)

After having assessed both the IAF and the resulting behavioral performance, neural entrainment was inspected as a function of both exogenous and endogenous mechanisms of sensory-attentional processing. However, prior to breaking down the results, it was important to confirm the presence of neural entrainment in the narrow sense, according to a series of requirements.(482,491) [i] First, endogenous neural oscillatory activity should occur without the necessity of exogenous stimuli and synchronize to external rhythmicities when present. In our research study, this was seen in both EM and HC, by an increase in the ITC alongside a significant peak in the cross-coherence and phase alignment between the internal oscillators and the external signal at the 12 Hz frequency. [ii] Endogenous neural oscillatory activity should also be resilient to perturbations and be able to adapt its eigenfrequency within certain bounds. Once again, this was confirmed in our research study by

the IAF, indicating that the internal oscillators did in fact adapt their natural frequencies within certain bounds to the external periodicity. [iii] Lastly, neural entrainment should persist for some time once the driving signal has disappeared, and the neural oscillators should not recover their eigenfrequencies right away. This was confirmed according to the persistence for at least three cycles post-entrainer offset, of the entrained signal as well as by analyses on the phase separation between anti-phase and in-phase moments, which was approximately 180° difference in both participant groups. Given that we successfully verified the requirements for neural entrainment in the narrow sense, results will now be discussed as a function of exogenous and endogenous mechanisms.

With regard to exogenous sensory-attentional processing, we examined the activity throughout the stream of entrainers. Both EM and HC yielded similar activity as could be seen by a lack of significant differences in the ITC. These results are consistent with past research on photic driving,(774) which may be considered a rudimentary form of neural entrainment,(506) although they may not meet all of the requirements for neural entrainment in the narrow sense. In EM interictally compared to HC, similar photic driving has been reported below 18 Hz,(687) and specifically at 12 Hz.(774) This would appear to suggest that exogenous mechanisms of neural entrainment, as measured by this task and over the alpha frequency band, may be preserved in low-frequency EM patients, interictally.

Next, endogenous activity was examined using target-absent trials, where the influence of motor response and/or expectation-related ERPs was largely reduced. Similar phase alignment on target-absent trials was observed in both participant groups over the target window, along with a 180° phase separation between anti-phase and in-phase temporal moments. No significant differences between groups in terms of the mean direction on target-absent trials, assessed using the Watson-Williams test, were observed. Concentration metrics such as kappa, mean vector length, and mean angular direction were also found to be similar between EM and HC. Target-present trials yielded the same pattern of results despite the contamination from the evoked responses. Nonetheless, the results from target-absent trials are of particular interest, because they would appear to suggest that the endogenous mechanisms of neural entrainment and their top-down regulatory control may be unaffected in low-frequency EM interictally, at least according to this task. These results are consistent with other studies that have divided top-down mechanisms into either facilitatory or inhibitory processes and concluded that patients with migraine and HC do not differ with respect to facilitatory processes (i.e., similar alpha power decrease).(671,683,775) This would appear to indicate that patients with EM do not struggle in processing relevant inputs, which is consistent with our results. Nevertheless, deficient inhibitory mechanisms, related to an impaired suppression of irrelevant sensory information have been reported.(671,683,775)

6.3. Studying the exogenous mechanisms of visual sensory processing in interictal EM and HC, using a pattern-reversal task

The third SO of this PhD thesis was to assess the exogenous mechanisms of visual processing in patients with EM during the interictal phase, using the PR task and evoked potentials (Research Study 3). Two separate experiments were carried out. The first was comprised of a sample of young adults from the general population diagnosed with EM and their HC, and the second consisted of middle-aged adults, recruited from an outpatient clinic, with EM and their HC. In both experiments, a perceptual measure of sensory sensitivity [the SPQ (252)] was provided to the participant groups. This was followed by an EEG recording to obtain PR-VEPs and by extension metrics related to cortical excitability and habituation. The results of this research study yielded three main findings in both experiments:

[i] significant differences in sensory sensitivity between EM and HC, with EM patients reporting significantly lower scores (or sensory hypersensitivity),

[ii] similar cortical excitability between EM and HC, as quantified using the N1-P1 first block peak-to-peak amplitude,

[iii] normal habituation, evidenced by an expected decrease in N1-P1 peak-to-peak amplitude across blocks in both EM and HC.

Visual sensitivity

Patients with migraine often report visual hypersensitivity, both ictally and interictally, as measured using self-report questionnaires and visual thresholds.(263,535,547) In this research study, the SPQ self-report questionnaire, a validated instrument, was used to obtain a perceptual measure of sensory sensitivity.(252) This questionnaire was selected due to its use in both neurological and pain research.(776,777) In both Experiments 1 and 2, EM had significantly lower values on the Vision scale of the SPQ, indicating enhanced sensory sensitivity to visual stimuli, as compared to HC. These results are consistent with patient complaints, in the clinical setting, of altered sensory processing, reported discomfort to certain patterns, colors, and contrasts, and interictal sensitivity to light.(571,778) Furthermore, the interictal visual hypersensitivity reported in this research study, would be in line with studies using self-report measures, which found that patients with migraine report more visual sensitivities in their environment as compared to headache-free controls (779) and greater sensitivity to light when exposed to the same stimulus at different intensities.(547) Lastly,

studies using psychophysical methods to determine sensory discomfort thresholds in patients with migraine and headache-free controls, have found decreased visual discomfort thresholds in patients, signaling visual hypersensitivity.(263,535) In sum, given that we found visual hypersensitivity in both experiments and also taking into account past literature,(263,535,547,571,779) it would appear that interictal visual hypersensitivity in patients with EM is quite robust.

Cortical excitability

The joint use of EEG and the PR task has been shown to provide a good measure of cortical properties, such as cortical excitability (first block N1-P1 peak-to-peak amplitude) and habituation (difference between first block and last block N1-P1 amplitude). In terms of cortical excitability in patients with EM, interictally, two different theories have been proposed to explain possible alterations. First, a theory of reduced cortical excitability (or hypoexcitability) has been suggested, related to decreased preactivation levels of the sensory cortices.(101,581) Specifically, these reduced preactivation levels, which may result in deficits of habituation or even response potentiation, have been thought to occur as a consequence of thalamocortical dysrhythmia in patients with migraine.(101) Second, a theory of increased cortical excitability (or hyperexcitability),(610,611) has also been proposed, stating the opposite. Accordingly, in patients with migraine, hyperexcitability has been suggested to occur due to either increased neuronal excitation (612) or decreased inhibition (581) [for a review, see (576)]. In fact, as a result of these discrepancies, the broader term of "cortical dysexcitability" has been proposed to better summarize the reported alterations in cortical excitability in patients with migraine.(615)

The results of both experiments in our research study yielded similar first block N1-P1 peak-to-peak amplitudes in both EM and HC, which would suggest that patients and controls do not differ with respect to cortical excitability. This is consistent with a growing body of evidence using PR tasks in patients with migraine having found no differences between patients and controls on measures of cortical excitability (341,607,609,616) [for a review see (615)]. Nonetheless, it remains difficult to provide a definitive picture as to the state of cortical excitability in patients with EM, interictally. One plausible explanation is that both theories coexist, hinting at the presence of different profiles of cortical excitability in patients with migraine, which may affect their electrophysiological responses. In fact, the presence and sum of both profiles might explain why some studies, including ours, found a lack of significant differences in cortical excitability when compared to healthy controls. To sum up, at the moment it is not possible to discard the hypothesis that patients with migraine might have normal cortical excitability, during the interictal period.

Habituation

Perhaps the most well-known apparent deficit in EM is a reported lack of habituation during the interictal phase, which some have proposed as a hallmark of migraine electrophysiology.(622,693) This alteration has been found in some studies (101,341,347,607,616,617) despite some controversy.(604,609,623–626) Nonetheless, in this research study and in both experiments, we did not find the expected deficit of habituation, quantified according to the N1-P1 peak-to-peak amplitude difference across blocks/trials. In fact, in both experiments patients showed normal habituation. Furthermore, in Experiment 2 middle-aged patients appeared to show steeper habituation slopes as compared to headache-free controls, which may suggest more pronounced habituation. This result is consistent with a growing body of literature, which has shown normal habituation in patients with migraine (604,609,623–626) and which has not been able to replicate the interictal habituation deficit in patients with migraine.(573,626–629) The negative results in our study and others, do not necessarily discard the existence of a habituation deficit in specific subsets of patients with migraine (601) and under certain conditions (747,780) but they do suggest that perhaps this alteration should not be considered a general and defining characteristic of patients with migraine, at least in the visual modality. An alternative explanation might be that the habituation deficit exists but that the stimulation being used, in this case the PR, is unable to adequately reproduce real-world conditions. The effect may also be there, but the study may not have a large enough sample size (statistical power) to detect finer differences.

Furthermore, in Experiment 1, we found a correlation between cortical excitability and habituation in EM, with a reduced first block amplitude being associated with less habituation (and perhaps even potentiation). This finding is consistent with several past studies, which also found a negative correlation between first block amplitude and habituation.(101,601,607,619,781) In fact, decreased cortical excitability, or lower preactivation levels, may be a consequence of the hypothesized thalamocortical dysrhythmia thought to occur in patients with migraine.(347) Furthermore, Knott and Irwin's ceiling theory,(782) as applied to migraine,(328) further states that diminished preactivation levels of the sensory cortices during the interictal phase might explain the reported deficit of habituation. However, this theoretical link remains speculative, seeing that in Experiment 2 of this research study, we did not find a correlation between cortical excitability and habituation in EM.

Age and migraine frequency

Next, keeping in mind the concepts discussed above, we wanted to explore whether hypersensitivity, cortical excitability, or habituation might be modulated by either age or migraine

frequency (EM only). Past studies would appear to indicate the presence of an inverse U-shaped relationship between age and migraine frequency. Specifically, migraine frequency has a tendency to peak around mid-life with a peak in prevalence between 30-39 years old,(783) and decline with older age, although this is not always the case. Furthermore, sensory sensitivity follows a similar profile of activity with patients reporting greater hypersensitivity with increasing age and migraine frequency with a peak between 46-60 years old, quantified according to the mean number of visual stressors,(779) and declining as of approximately 50 years old.(784) Other studies have also reported a positive correlation between photophobia and migraine frequency using self-perception reports [age range: 18-55 years old; (785)] and photophobia scores [age range: 20-79 years old;(786) despite (787)]. This would provide support for a link between visual sensitivity and disease severity, with increased migraine frequency being correlated with greater hypersensitivity.

In recent years, patients with high-frequency EM have been proposed to be more clinically similar to those with CM than those with low-frequency EM. This might suggest that beyond clinical measures, symptomatology such as visual sensitivity, might be more similar to patients with CM than low-frequency EM.(788) The results of both Experiments 1 and 2 in our research study indicated visual hypersensitivity in EM as compared to HC, despite a lack of correlations to either age or migraine frequency.

Finally, to the best of our knowledge, no previous studies have directly evaluated the relationship between cortical excitability and habituation to age and migraine frequency. In fact, a recent meta-analysis,(744) discussed the lack of information in a number of research studies that made it impossible to evaluate the relationship between migraine frequency and amplitude/habituation of VEPs. The same authors also discussed the difficulties in generalizing results due to the effects of age on VEP attenuation.(744) Nonetheless, given our lack of significant correlations between age, migraine frequency, cortical excitability, and habituation, as well as the negative results between EM and HC, the relationship between these variables remains unclear.

Methodological considerations

One of the major criticisms related to PR-VEP research in migraine, is the difficulty in generalizing and establishing conclusions, when each study uses vastly different methodologies, clinical samples, interictal criteria, statistical analyses, task instructions, and blinding procedures. It goes without saying, that the standardization of methodological techniques is extremely important in electrophysiology, particularly in light of a replicability crisis in the field of cognitive neuroscience.(789) This is why, in our study, we selected our stimulus parameters as a function of recommendations made by other authors in the field.(623–626,747,780) Furthermore, in terms of

statistical analyses, we implemented LMMs, which provide a methodologically superior approach as compared to previously used analyses (such as rmANOVAs). By implementing LMMs we hoped to increase the precision of our measures and improve our ability to uncover subtle group differences, while also running the typical rmANOVAs as control analyses. In fact, our research study is one of few (618,621) that implement LMMs in analyzing PR data in patients with migraine given that past research studies have primarily made use of linear regression slopes, least squares slopes, or rmANOVAs of amplitude, to study both cortical excitability and habituation.(601) LMMs, when compared to these methods, hold several advantages, particularly with regard to clinical studies. First, the use of LMMs allows the researcher to conserve all of the information and variability in the data, particularly with regard to individual and temporal factors.(790,791) In EEG research, this is particularly important, given that the EEG technique introduces a high degree of complexity to the data. Second, LMMs are better at handling missing data and are more robust to unbalanced data or a small number of observations.(790,791) When using EEG, there is usually high variability in the data due to the nature of electrophysiological artifacts and how they impact the number of trials included in the final analysis, therefore LMMs provide a statistically-sound method to deal with these differences.(792) Migraine patients can also be quite heterogeneous,(793) therefore LMMs can also reduce the impact of within-participant differences, which are often ignored when using classic analysis methods. Nonetheless, despite a more powerful statistical method, we did not find differences in either cortical excitability or habituation between groups, with the exception of Experiment 2, where we found increased cortical excitability in EM on the trial LMM.

Relationship between sensory sensitivity and the concepts of cortical excitability and habituation

Looking at the results of this research study, it is interesting to comment on what appears to be a dissociation between the three processes of sensory sensitivity, cortical excitability, and habituation. In particular, it would be interesting to assess whether an electrophysiological correlate of the reported hypersensitivity in patients with migraine exists at the neural level, in terms of brain responses. In other clinical disorders such as autism and obsessive-compulsive disorder, where patients also frequently complain of sensory sensitivities, some studies have suggested that a lack of habituation to environmental stimuli might reduce the ability to properly suppress stimuli, leading to the development of hypersensitivities.(794,795) However, a link between visual evoked potentials and sensory measures (e.g., visual discomfort thresholds) has not been found in patients with migraine.(609) In fact, direct links between behavior or perceptual measures and EEG metrics are frequently implied but seldom supported through statistics. Therefore, it remains essential to continue investigating the relationship between subjective, perceptual measures provided by patients with

migraine and objective neural metrics, given that these processes would appear to share a link. Despite this research study not finding a link between the three measures, which might suggest that they are independent processes, an alternative explanation might be that PR-VEPs do not provide the adequate tool to tap into these processes and their interactions effectively.

6.4. Investigating the exogenous and endogenous mechanisms of auditory sensitivity processing in interictal EM and HC, using an oddball task

The final SO of this PhD thesis was to assess the exogenous and endogenous mechanisms of sensory-attentional processing in the auditory modality and in patients with EM during the interictal phase, using an active oddball task and ERPs as well as time-frequency analyses (Research Study 4). The early, primarily stimulus-driven components including N1 and P2 were used to assess sensory processing whereas later components including the MMN, early and late P3a, P3b, and RON were used to assess sensory-attentional mechanisms. Furthermore, our research study added spectral power and phase synchronization metrics to expand on the information provided by classic ERP analyses. The results of this research study yielded three main findings:

[i] significant differences in the amplitude of the N1 component and theta-phase synchronization between EM and HC, with EM patients indicating increased responses to auditory stimuli,

[ii] normal habituation to repetitive auditory stimuli in both EM and HC, as a function of ERP amplitudes, spectral power, and phase-synchronization,

[iii] significantly reduced early P3a, incremented P3b, and reduced RON in EM, suggesting an impaired attentional response pattern to novel stimuli.

Early sensory-attentional processing

Past literature would appear to indicate a hypersensitivity to sound between attacks in patients with migraine.(561) The results of this research study would be consistent with these findings, suggesting altered exogenous mechanisms of auditory sensory-attentional processing in patients with EM interictally. In fact, the presence of an increased amplitude of N1 in patients with EM suggests that patients attribute increased saliency and subsequently destine more attentional resources to the processing of environmental sounds.(146,350) This may, in turn, have an impact on the neural representation of sound within the auditory cortex.(796) Furthermore, the amplitude of both P2 and N2 components were similar between groups in our research study, which would suggest that higher-order perceptual processes along with their top-down, endogenous modulation by attentional mechanisms are preserved in patients with migraine.(428)

Aside from the alterations in N1 amplitude, the main finding of this research study was the incremented theta phase-synchronization in response to repetitive stimuli in patients with EM. During

active auditory oddball tasks, the theta frequency range has been shown to underlie the neural response to standard stimuli.(379) Furthermore, metrics such as power and phase-synchronization of neural oscillatory activity have been linked to the generation and modulation of ERPs (797,798) a particular role for phase-synchronization in the maintenance (and progressive habituation) of ERP amplitudes over repetitive stimulation.(353) In fact, theta phase synchronization would appear to have a relevant and dynamic role in early sensory processing by providing an internal form of information coding in the sensory cortex,(799) through constant monitoring of external sensory stimuli.(800) Furthermore, this process would appear to be tightly related to the N1 component, at least in the auditory modality.(353) Consequently, in this research study, the reported increase in theta phase-synchronization in EM could lead to the incremented auditory processing, confirmed by an enhanced N1 amplitude. The results of our research study are also consistent with findings in the visual domain, indicating increased phase-synchronization in interictal patients with EM without aura, in alpha during repetitive visual stimulation (102,695,801) as well as altered connectivity between salience and auditory-related structures as measured using resting-state fMRI. Ultimately, these results would provide support to the hypothesized thalamocortical dysrhythmia,(101) thought to result in increased low-frequency oscillations in thalamic structures leading to a hyperresponsivity of sensory cortices.

Habituation

The habituation of ERPs, spectral power, and phase-synchronization measures across blocks was analyzed in both patients with EM and HC and yielded normal habituation in both groups. These findings are consistent with our results using visual stimuli (Research Study 1) and also previous studies, which did not find significant differences in N1 and P2 habituation to auditory stimuli between patients with EM and HC.(673,675,676,678,802) Importantly, the thalamocortical dysrhythmia hypothesis states that the reported hyperresponsivity in patients with migraine is due to a deficit of habituation in response to sensory stimuli,(102) however, an increased number of negative findings related to this proposed lack of habituation would open this up for debate.(673,675,676,678,802) In fact, it remains unclear whether this deficit of habitation, often found in patients with migraine interictally, is a hallmark of the disease itself or may be related to a specific subtype of migraine (i.e., episodic, chronic, with or without aura) or some other confounding factor such as treatment, psychiatric comorbidity, age, or methodological differences.(803) For a more in-depth discussion see Section 6.3.

Late sensory-attentional processing

Following the appearance of earlier ERP components, the subsequent ERP cascade can shed light on the response to novel and target stimuli, which would appear to be impaired in patients with

EM. In line with the results of some previous studies (678,679) and despite others,(675,676) we found similar MMN amplitude in response to novel stimuli between groups. This might suggest that processes related to the early sensory detection of unexpected change, or stimuli, are preserved in patients with EM, interictally. Next, we explored the P3a component. In relation to literature, some studies have found no difference (676,680) whereas others have reported increased P3a in EM as compared to HC.(675) Additionally, given that previous basic research studies have separated P3a into two peaks (early and late) associated to different brain generators, we decided to divide the P3a accordingly. The results of our research study yielded a reduced early P3a and increased late P3a in EM as compared to HC. This would suggest that, in response to novel stimuli, patients with EM showed a reduced post-sensory response (decreased early P3a), quickly compensated by an enhanced allocation of attentional resources (increased late P3a). In terms of P3b, EM and HC showed similar amplitudes of this component in response to auditory stimuli, which is consistent with some studies,(672,673,681) but in contrast to others.(674,679,804) Finally, results from this research study yielded a reduced RON in response to both target and novel stimuli in patients with EM. This would suggest that patients with migraine struggle to disengage from the presence of distracting, novel stimuli as well as re-orienting back to the task, which might indicate impaired cognitive flexibility.(170)

6.5. Research study limitations

Limitations of RS1

The current study primarily focused on the alpha frequency band via selective visual attention, therefore it remains to be determined whether these results can be generalized to other frequency bands, sensory modalities, and cognitive processes. Nonetheless, past studies investigating other frequencies and cognitive processes including target detection,(514) visual discrimination,(237) speech perception,(805) cross-modal illusory perception,(806) and source memory performance,(807) did not account for the effects of inherent task predictability. In our study, it appears rather clear that the putative effect of neural entrainment on behavioral performance, if any, must have been much smaller than the significant effect of spatial validity, replicating the findings of a number of past studies on discrimination accuracy,(367,808,809) and stimulus detection.(388,810,811) Additionally, the spatial attention effect occurred alongside lateralization of alpha activity at posterior sites,(186) which would provide support to the role of alpha in suppressing irrelevant information, in this case related to spatial location.(402,812–814) Also, despite our study reducing the effect of absolute expectation (one fixed timepoint) as a potential confounding factor, we did not modulate factors related to relative expectation (a varying possible timepoint, with fixed spacing). Future studies should attempt to dissociate these effects from neural entrainment by adding jitter to target onset times, similarly to Spaak et al.(525)

Limitations of RS2

One of the explanations for the lack of significant differences in this research study could be due to the characteristics of our patient sample which was comprised of young adults with EM in the interictal phase. Previously, one of the possible explanations for discrepancies in the research on migraine has been attributed to the type of patient being assessed,[(815) for a review see (816)] with a large proportion of studies finding negative results recruiting patients from the general population in contrast to those reporting significant differences where patients were frequently sampled from out-patient clinics. Importantly, the patients originating from out-patient clinics frequently report a higher headache frequency and headache-related disability, more psychiatric comorbidities such as anxiety and depression, as well as the effects of medication, all of which could impact the results.(815–817) Although, and importantly, this is not so clear; please keep in mind the results of RS3, where we also recruited a sample of patients from an out-patient clinic and did not find between group differences (with the exception of sensory sensitivity as measured by the SPQ). Therefore, it is possible that endogenous processing could be altered in patients with a more severe disease

pathophysiology. In fact, we are currently analyzing the results of a follow-up experiment, which applied the same cued visual detection task with bilateral entrainment to patients recruited from a specialized Headache Clinic with a higher headache frequency (the same sample of participants as those in Research Study 3, Experiment 2). Furthermore, the patients in this study did not report sensory hypersensitivity, according to the scores of the SPQ, which did not differ significantly from their HC. However, these patients were taken from the same pool of patients used for RS3 and RS4 and in the other studies we did find significant differences in sensory sensitivity between groups. Therefore, it may be the case that in reducing the sample size of this research study, due to a greater number of exclusions, we removed those patients with greater sensory sensitivity.

Limitations of RS3

First, in terms of limitations, sensory sensitivity in our study was assessed using a perceptual metric (SPQ) but we were unable to measure it directly using an objective measure, unlike the other experimental variables (cortical excitability and habituation). However, despite this limitation, PR tasks with simultaneous EEG recording provide a well-validated and frequently used tool to study visual processing as well as the ability to select stimulation parameters based on recommendations from other authors.(623–626,747,780) Migraine is also three times more frequent in women than in men (818) and this should be taken into account when considering the relationship of different experimental measures to gender. However, in this research study we were unable to examine the relationship of gender to other demographic and experimental variables. Specifically, in Experiment 1, the sample was comprised of all women, whereas in Experiment 2, we maintained a 3 to 1 ration of women to men, equivalent to the prevalence reported in the population (105) with our EM and HC samples being gender-matched in both studies to avoid potential distortion of our results. Nonetheless, in previous studies on these concepts, the effects of gender were also not considered, despite some evidence suggesting that there are structural and functional brain differences in men and women, related to migraine.(819) Also, in terms of correlations, it is possible that we did not find a significant correlation due to the small sample sizes and homogeneity of our participant groups. Finally, we did not evaluate MA and MwoA separately due to small sample sizes, despite having collected information relative to aura. However, past literature on cortical excitability and habituation in patients with MA also did not find abnormal cortical excitability or a lack of habituation.(609,625)

Limitations of RS4

The first limitation in this study, similarly to RS2 (although in this case we still found significant differences between groups) consisted of the features of our sample of patients with migraine, which were young women between the ages of 19-28 years old, diagnosed with low-

frequency EM. Given their age and disease severity, it is possible that the results of our research study are unable to unequivocally explain migraine symptomatology particularly in patients with higher frequency of attacks and greater comorbidities, such as those frequently treated in out-patient clinics. Furthermore, the age of migraine onset may have an effect on sensory-attentional auditory processes but in this research study we were unable to evaluate its impact given that patients were unaware or unsure of their diagnosis, having never been formally diagnosed, and were therefore unable to pinpoint an onset time. Furthermore, although this study assessed habituation it is important to note that the presentation of other stimuli (particularly strong or salient ones) may result in recovery or disruption of habituation to standard repetitive stimuli.(331) Given that the experimental design consisted of an active three-stimulus oddball task it is possible that the presentation of target and novel stimuli may have affected the chain of habituation and biased data. Therefore, habituation results should be interpreted with some degree of caution.

General limitations

Migraine research is in a constant state of evolution as researchers seek to understand this complex neurological disease and to improve its research designs, methods, and analyses. Given that past literature is somewhat conflicting, it is particularly important to reflect on the reasons as to why this may be the case and to make the necessary improvements for future studies. For starters, a number of general limitations can be discussed, both in light of the research carried out in this PhD thesis, but also with respect to the field of migraine research as a whole. These limitations and factors to consider include patient and attack heterogeneity, the concept of migraine phase and our methods to control for it, experimental design, method, and analysis discrepancies, and limitations inherent to our research techniques, among others.

It goes without saying that patients with migraine showcase significant intraindividual but also interindividual heterogeneity in terms of both attack and disease characteristics.(793) For example, in terms of attacks, some patients report aura while others do not alongside differences in duration, intensity, and accompanying symptoms.(793) Additionally, migraine as a disease is also highly variable, with different onset times, occurrences, comorbidities, and evolution, leading to a variety of different subtypes based on self-reported symptoms.(793,820) Despite constant improvements being made to the classification system used to group patients with migraine into different diagnostic categories (ICHD-3), migraine nosology remains somewhat imprecise, closely related to a lack of distinct disease biomarkers. Furthermore, migraine is a multifactorial disease most likely elicited by a number of different input combinations,(821–823) which makes it difficult to generalize findings. Migraine subtypes frequently refer to disease symptomatology (i.e., MA and

MwoA) but also attack frequency (i.e., EM and CM). However, it remains unclear whether MA and MwoA are truly separate entities, with some researchers arguing against their etiological distinction [for a review see (824)] and others for it.(825) According to Nyholt et al., MA and MwoA exist on the same spectrum,(824) as supported by evidence indicating that [i] patients diagnosed with MA frequently report attacks without aura (826) [ii] MwoA and MA appear to coexist within the same families,(827) as well as [iii] the development of MA in patients previously diagnosed with MwoA and vice versa.(828,829) Additionally, in a research study using latent class analysis on twin unselected community samples, MwoA and MA were found to co-occur on a spectrum but with MA being more related to increased disease severity. Furthermore, the differentiation between EM and CM is also somewhat arbitrary. The current distinction is based on the number of attacks, meaning that patients with 15 or more headache days a month for at least three months, of which 8 or more should present with migraine-like symptoms, are diagnosed with CM. However, in recent years some studies have indicated that patients with high-frequency EM (8-14 headache days/month) may actually be more clinically similar to those with CM than those with low-frequency EM.(788) This might suggest that aside from clinical symptoms, these patients resemble CM in terms of experimental measures as well. In sum, the current criteria used to classify patients into distinct subtypes remains somewhat imprecise therefore until the debate as to distinct or similar etiologies is clarified, researchers should proceed with caution when generalizing results to a specific migraine subtype. Furthermore, migraine is also frequently associated with a high level of psychiatric comorbidities, such as anxiety and depression.(110,111) In fact, as previously mentioned the type of patient assessed may have an important impact on the results. For example, in studies of visual processing, many studies sampling from the general population reported negative results, which was not the case for studies using patients recruited from out-patient clinics.(815) This may be related to the fact that patients in out-patient clinics tend to have greater headache frequency and headache-related disability, more severe comorbidities including anxiety and depression, as well as pharmaceutical treatments, which may have an impact on sensory-attentional, as well as cognitive function.(815–817) In this PhD thesis, we attempted to recruit for the most part, young adults from the general population with low-frequency EM and great care was taken regarding comorbidities and medication to ensure that our patient and control samples were as homogeneous as possible. Although this approach is important to minimize the third variable problem on our measures of interest and the internal validity of our experiments, it is true that it reduces our ability to study the whole spectrum of migraine and may remove important information related to disease heterogeneity. This is why, in Research Study 3 we also assessed a sample from an out-patient clinic, to see whether increased disease severity and age, might impact the results with similar findings being reported in both experiments. In sum, it is

important to carry out and replicate previous studies with different samples of well-matched migraine patients, to reduce the likelihood of previous findings being associated with something other than migraine itself.

Next, in terms of phase it is important to note that this variable is most often controlled using a daily headache calendar. This tool was first introduced by Russell et al. seeing as patients often had difficulty recalling headache presence and its characteristics, resulting in recall bias and a lack of descriptive accuracy.(830) Nonetheless, adherence continued to remain a problem, despite eDiaries improving this issue through ease of access, branching questions, and accessible patient reports. In fact, one of the criticisms when reviewing the literature on migraine has been attributed to the lack of consistency when defining different phases of the migraine cycle,(703) which makes it difficult to conduct literature reviews, particularly with regard to phase effects. Research studies on migraine should utilize baseline headache diaries (and throughout the experimental period as well as after the session) for both patients and controls as standard procedure. For both phase effects and patient heterogeneity, longitudinal studies may provide an excellent research tool.

Also, with regard to the experimental design themselves, a number of authors have emphasized the difficulty in generalizing findings and establishing clear conclusions when the majority of studies have used different methodological parameters, clinical samples and selection criteria, task instructions, and blinding (see 6.3. for more details). In our research studies, we were careful to select parameters based on the recommendations of previous authors. Sample size is also an issue in research on patients with migraine, particularly when using EEG due to the necessity for a certain number of artifact-free trials, which often excludes a number of participants from further analyses. Also, given that the majority of research studies focus on a specific migraine phase, patients are frequently excluded for being outside of this phase post-recording and revision of the eDiary results. As migraine frequency and disease severity increases, more patients are excluded, which may introduce bias into the remaining sample, seeing as the patients that are excluded (especially when the number is high) may be different from those that are left in the final analysis sample. Unfortunately, this is a big problem in migraine research and might be resolved by increasing the initial sample size to account for a large number of fall-out. Furthermore, increasing the sample size also has a positive effect on statistical power, which may permit us to uncover more subtle effects, particularly in patients with low-frequency and low burden of disease.

Finally, the EEG technique provides a number of advantages including high temporal resolution and the ability to evaluate the stages of sensory-attentional processing, however neither ERPs nor time-frequency analyses provide a direct relationship between these processes and specific brain areas or neurotransmitters. A number of previous studies have identified alterations in both

structure and function of certain brain areas [for a review see (97,831)], associated with sensory-attentional processing, including reduced grey matter in areas related to pain including the amygdala, operculum, anterior cingulate cortex, insula, and frontal, precentral, and temporal gyri,(832) increased activation of the visual cortex.(833,834) Nonetheless, given that ERPs are unable to directly assess these aspects, future studies should attempt to combine different techniques to better understand exogenous and endogenous sensory-attentional processing in patients with migraine.

6.6. Research study conclusions

The MO of this research thesis was to study sensory-attentional processing in patients with EM interictally. To accomplish this, four research studies were conducted investigating exogenous and endogenous mechanisms as well as a variety of processes, in the visual and auditory domains. The overarching results would appear to indicate certain sensory-attentional alterations, particularly with regard to sensory sensitivity, attentional re-orienting, and the allocation of attentional resources to novel or unexpected stimuli. On the other hand, other processes were found to be normal or preserved in patients with EM interictally, including cortical excitability, habituation, and neural synchronization. The implications of these results will be discussed upon continuation.

Conclusions of RS1

The results of this research study would provide additional evidence for neural entrainment, as defined by the synchronization of endogenous oscillatory activity to external, rhythmic stimuli, which persists beyond the presence of a driving signal. It would also provide support to the body of literature against the conceptualization of neural entrainment as a succession of ERPs. Furthermore, the effect of neural entrainment on behavioral performance may be more limited than previously suggested, although it remains to be seen how this internal predictive mechanism may modulate visual perception and affect behavior. Nonetheless, neural entrainment is maintained despite reduced temporal predictability. Importantly, this task permits the study of both exogenous and endogenous mechanisms as they relate to neural synchronization, which makes it a suitable candidate for use in clinical studies.

Conclusions of RS2

In this subset of patients with EM, assessed during the interictal phase, both the exogenous and endogenous mechanisms of neural entrainment were found to be preserved. This would suggest that in patients with a low burden of disease, neural synchronization processes as they relate to sensory-attentional processing are comparable to HC. However, future studies should attempt to broaden these findings further to see whether these results may differ in patients with a greater disease burden or in the auditory modality.

Conclusions of RS3

The results of both experiments in this research study yielded a significant hypersensitivity to visual stimuli in interictal EM but no differences in cortical excitability or habituation, as assessed

with PR-VEPs. This would suggest that in the visual domain, the exogenous mechanisms underlying sensory-attentional processing in response to PR stimulation may be relatively intact.

Conclusions of RS4

In this research study, the findings indicated a hypersensitivity to auditory stimuli in EM patients, interictally. Additionally, EM showed a reduced post-sensory response and a rapid compensatory mechanism of increased allocation of attentional resources in contrast to HC. Taken together, these results would suggest that patients attribute increased saliency and attentional resources to repetitive stimuli and their surrounding environment. Furthermore, in response to salient or biologically relevant stimuli (i.e., target and novel), patients struggled to re-orient back to the current task after being exposed to a distracting stimulus, indicating decreased cognitive flexibility in EM as compared to HC. Ultimately, EM patients would appear to exhibit hypersensitivity to auditory stimuli, impaired allocation of attentional resources, and trouble re-orienting, which might explain the reported auditory alterations in EM interictally.

7. GENERAL CONCLUSIONS

1. Cued visual detection tasks with bilateral entrainment can provide a good measure of both exogenous and endogenous mechanisms of sensory-attentional processing.

2. In patients with episodic migraine during the interictal phase, the brain's capacity to synchronize its neural oscillatory activity to rhythmic external stimuli, measured using a cued visual detection task with bilateral entrainment, is not significantly different from headache-free controls. This would suggest that the exogenous and endogenous mechanisms of sensory-attentional processing, related to neural entrainment, are preserved in this type of patient.

3. Patients with episodic migraine in the interictal phase report similar cortical excitability and normal habituation on a pattern-reversal task, as compared to headache-free controls. Additionally, patients exhibit visual hypersensitivity in contrast to controls, which would suggest some level of altered exogenous mechanisms related to visual processing.

4. Patients with interictal, episodic migraine compared to headache-free controls show normal habituation but heightened responses to auditory stimuli, in response to an oddball task, as well as an increased allocation of attentional resources to novel or unexpected stimuli and difficulty shifting attention back to the task. This would appear to indicate the presence of certain altered exogenous and endogenous mechanisms of auditory sensory-attentional processing.

In conclusion, patients with episodic migraine exhibit some level of sensory-attentional processing impairments, although the results, as compared to the past literature in migraine, appear to be more limited than previously thought.

8. FUTURE LINES OF RESEARCH

This research thesis has highlighted the importance of studying the exogenous and endogenous mechanisms of sensory-attentional processing in patients with migraine. In particular, the results from the case-control studies (Research Studies 2-4) would suggest some future lines of research, which will be detailed upon continuation.

First, with regard to Research Study 2, it would be interesting to extend these results to other modalities and frequencies, particularly taking into account the results from Research Study 4, which indicated a number of altered sensory-attentional processes in EM as compared to HC, among others increased theta phase-synchronization. Applying a theta frequency entrainment task in the auditory modality, would enable us to determine whether the alterations reported in this modality in Research Study 4, might be explained by differences in the ability to synchronize internal oscillatory activity to external periodicities [neural entrainment] in patients with migraine as compared to HC.

Next, in terms of Research Study 3, it would be of interest to continue exploring the interplay between sensory sensitivity, cortical excitability, and habituation using a paradigm that could permit us to directly measure all three processes objectively. This way we could attempt to more definitively delineate the relationship between these three variables and their interaction in patients with migraine.

In Research Study 4, the results would appear to indicate that novelty processing mechanisms might be impaired in patients with migraine, therefore future studies should consider using paradigms that tap into this cognitive process specifically. Furthermore, although we did not find a deficit of habituation on this task, the results should be interpreted with caution and instead it may be interesting to apply a 'purer' auditory habituation paradigm in patients with migraine interictally, to see whether there is the expected deficit of habituation as well.

Finally, as we have seen, migraine is a complex disorder comprised of different subtypes and symptomatology, therefore future studies should examine different types of patients, phases of the migraine cycle, disease evolution, and other aspects related to patient heterogeneity as well as sociodemographic characteristics such as gender.

9. BIBLIOGRAPHY

1.   Pearce JM. Historical aspects of migraine. J Neurol Neurosurg Psychiatry. 1986 Oct 1;49(10):1097–103.

2.   Magiorkinis E, Diamantis A, Mitsikostas DD, Androutsos G. Headaches in antiquity and during the early scientific era. J Neurol. 2009 Aug;256(8):1215–20.

3.   Friedman AP. The headache in history, literature, and legend. Bull N Y Acad Med. 1972 May;48(4):661–81.

4.   Jones JM. Great pains: Famous people with headaches. Cephalalgia Int J Headache. 1999 Sep;19(7):627–30.

5.   Safiri S, Pourfathi H, Eagan A, Mansournia MA, Khodayari MT, Sullman MJM, et al. Global, regional, and national burden of migraine in 204 countries and territories, 1990 to 2019. Pain. 2022 Feb 1;163(2):e293–309.

6.   Headache Classification Committee of the International Headache Society (IHS) The International Classification of Headache Disorders, 3rd edition. Cephalalgia. 2018;38(1):1–211.

7.   Rizzoli P, Mullally WJ. Headache. Am J Med. 2018 Jan 1;131(1):17–24.

8.   Lipton RB, Silberstein SD. Episodic and chronic migraine headache: Breaking down barriers to optimal treatment and prevention. Headache. 2015 Mar;55 Suppl 2:103–22; quiz 123–6.

9.   van de Graaf DL, Schoonman GG, Habibović M, Pauws SC. Towards eHealth to support the health journey of headache patients: A scoping review. J Neurol. 2021 Oct;268(10):3646–65.

10.   Wittrock DA, Ficek SK, Cook TM. Headache-free controls? Evidence of headaches in individuals who deny having headaches during diagnostic screening. Headache J Head Face Pain. 1996;36(7):416–8.

11.   Peng KP, May A. Redefining migraine phases – A suggestion based on clinical, physiological, and functional imaging evidence. Cephalalgia. 2020 Jul 1;40(8):866–70.

12.   Linde M, Mellberg A, Dahlöf C. The natural course of migraine attacks. A prospective analysis of untreated attacks compared with attacks treated with a triptan. Cephalalgia Int J Headache. 2006 Jun;26(6):712–21.

13.   Linde M. Migraine: A review and future directions for treatment. Acta Neurol Scand. 2006;114(2):71–83.

14.   Gil-Gouveia R, Martins IP. Clinical description of attack-related cognitive symptoms in migraine: A systematic review. Cephalalgia Int J Headache. 2018 Jun;38(7):1335–50.

15.   Blau JN. Migraine prodromes separated from the aura: Complete migraine. Br Med J. 1980 Sep 6;281(6241):658–60.

16.   Drummond P, Lance J. Neurovascular disturbances in headache patients. Clin Exp Neurol. 1984 Feb 1;20:93–9.

17.   Kelman L. The premonitory symptoms (prodrome): A tertiary care study of 893 migraineurs. Headache. 2004 Oct;44(9):865–72.

18.   Pop MG, Crivii C, Opincariu I, Pop MG, Crivii C, Opincariu I. Anatomy and function of the hypothalamus. IntechOpen; 2018.

19.   Maniyar FH, Sprenger T, Monteith T, Schankin C, Goadsby PJ. Brain activations in the premonitory phase of nitroglycerin-triggered migraine attacks. Brain J Neurol. 2014 Jan;137(Pt 1):232–41.

20.   Schulte LH, May A. The migraine generator revisited: Continuous scanning of the migraine cycle over 30 days and three spontaneous attacks. Brain. 2016 Jul 1;139(7):1987–93.

21.   Gollion C, De Icco R, Dodick DW, Ashina H. The premonitory phase of migraine is due to hypothalamic dysfunction: Revisiting the evidence. J Headache Pain. 2022 Dec 13;23(1):158.

22.   Stankewitz A, Aderjan D, Eippert F, May A. Trigeminal nociceptive transmission in migraineurs predicts migraine attacks. J Neurosci Off J Soc Neurosci. 2011 Feb 9;31(6):1937–43.

23.   Patel NM, Jozsa F, M Das J. Neuroanatomy, spinal trigeminal nucleus. In: StatPearls. Treasure Island (FL): StatPearls Publishing; 2022.

24.   Schulte LH, Peng KP. Current understanding of premonitory networks in migraine: A window to attack generation. Cephalalgia. 2019 Nov 1;39(13):1720–7.

25.   Noseda R, Burstein R. Migraine pathophysiology: Anatomy of the trigeminovascular pathway and associated neurological symptoms, cortical spreading depression, sensitization, and modulation of pain. PAIN®. 2013 Dec 1;154:S44–53.

26.   Jensen R, Stovner LJ. Epidemiology and comorbidity of headache. Lancet Neurol. 2008 Apr;7(4):354–61.

27.   Kunkel RS. Migraine aura without headache: Benign, but a diagnosis of exclusion. Cleve Clin J Med. 2005 Jun 1;72(6):529–34.

28.   Ziegler DK, Hassanein RS. Specific headache phenomena: Their frequency and coincidence. Headache. 1990 Feb;30(3):152–6.

29.   Russell MB, Olesen J. A nosographic analysis of the migraine aura in a general population. Brain J Neurol. 1996 Apr;119 (Pt 2):355–61.

30.   O'Connor PS, Tredici TJ. Acephalgic migraine. Fifteen years experience. Ophthalmology. 1981 Oct;88(10):999–1003.

31.   Fisher CM. Late-life migraine accompaniments as a cause of unexplained transient ischemic attacks. Can J Neurol Sci J Can Sci Neurol. 1980 Feb;7(1):9–17.

32.   Wijman CA, Wolf PA, Kase CS, Kelly-Hayes M, Beiser AS. Migrainous visual accompaniments are not rare in late life: The Framingham Study. Stroke. 1998 Aug;29(8):1539–43.

33.   Mattsson P, Lundberg PO. Characteristics and prevalence of transient visual disturbances indicative of migraine visual aura. Cephalalgia Int J Headache. 1999 Jun;19(5):479–84.

34.   Russell WR, Whitty CW. Studies in traumatic epilepsy. 3. Visual fits. J Neurol Neurosurg Psychiatry. 1955 May;18(2):79–96.

35.   Benke T, Hochleitner M, Bauer G. Aura phenomena during syncope. Eur Neurol. 1997;37(1):28–32.

36.   Medina JL, Diamond S. The clinical link between migraine and cluster headaches. Arch Neurol. 1977 Aug;34(8):470–2.

37.   Krymchantowski AV. Aura with non-migraine headache. Curr Pain Headache Rep. 2005 Aug;9(4):264–7.

38.   Silberstein SD, Niknam R, Rozen TD, Young WB. Cluster headache with aura. Neurology. 2000 Jan 11;54(1):219–219.

39.   Peres MFP, Siow HC, Rozen TD. Hemicrania continua with aura. Cephalalgia Int J Headache. 2002 Apr;22(3):246–8.

40.   Matharu MJ, Goadsby PJ. Post-traumatic chronic paroxysmal hemicrania (CPH) with aura. Neurology. 2001 Jan 23;56(2):273–5.

41.   Denuelle M, Fabre N. Functional neuroimaging of migraine. Rev Neurol (Paris). 2013 May 1;169(5):380–9.

42. Weiller C, May A, Limmroth V, Jüptner M, Kaube H, Schayck RV, et al. Brain stem activation in spontaneous human migraine attacks. Nat Med. 1995 Jul;1(7):658–60.

43. Afridi SK, Giffin NJ, Kaube H, Friston KJ, Ward NS, Frackowiak RSJ, et al. A positron emission tomographic study in spontaneous migraine. Arch Neurol. 2005 Aug;62(8):1270–5.

44. Afridi SK, Matharu MS, Lee L, Kaube H, Friston KJ, Frackowiak RSJ, et al. A PET study exploring the laterality of brainstem activation in migraine using glyceryl trinitrate. Brain J Neurol. 2005 Apr;128(Pt 4):932–9.

45. Denuelle M, Fabre N, Payoux P, Chollet F, Geraud G. Hypothalamic activation in spontaneous migraine attacks. Headache. 2007;47(10):1418–26.

46. Borsook D, Burstein R. The enigma of the dorsolateral pons as a migraine generator. Cephalalgia Int J Headache. 2012 Aug;32(11):803–12.

47. Casey KL, Minoshima S, Berger KL, Koeppe RA, Morrow TJ, Frey KA. Positron emission tomographic analysis of cerebral structures activated specifically by repetitive noxious heat stimuli. J Neurophysiol. 1994 Feb;71(2):802–7.

48. Rosen SD, Paulesu E, Frith CD, Frackowiak RS, Davies GJ, Jones T, et al. Central nervous pathways mediating angina pectoris. Lancet Lond Engl. 1994 Jul 16;344(8916):147–50.

49. Jones AK, Friston K, Frackowiak RS. Localization of responses to pain in human cerebral cortex. Science. 1992 Jan 10;255(5041):215–6.

50. Blau JN. Resolution of migraine attacks: Sleep and the recovery phase. J Neurol Neurosurg Psychiatry. 1982 Mar;45(3):223–6.

51. Kelman L. The postdrome of the acute migraine attack. Cephalalgia Int J Headache. 2006 Feb;26(2):214–20.

52. Quintela E, Castillo J, Muñoz P, Pascual J. Premonitory and resolution symptoms in migraine: A prospective study in 100 unselected patients. Cephalalgia Int J Headache. 2006 Sep;26(9):1051–60.

53. Giffin NJ, Lipton RB, Silberstein SD, Olesen J, Goadsby PJ. The migraine postdrome: An electronic diary study. Neurology. 2016 Jul 19;87(3):309–13.

54. Bose P, Goadsby PJ. The migraine postdrome. Curr Opin Neurol. 2016 Jun;29(3):299–301.

55. Main A, Dowson A, Gross M. Photophobia and phonophobia in migraineurs between attacks. Headache. 1997 Sep;37(8):492–5.

56. Ashkenazi A, Mushtaq A, Yang I, Oshinsky ML. Ictal and interictal phonophobia in migraine - A quantitative controlled study. Cephalalgia Int J Headache. 2009 Oct;29(10):1042–8.

57. Meylakh N, Henderson LA. Exploring alterations in sensory pathways in migraine. J Headache Pain. 2022 Jan 12;23(1):5.

58. Brandes JL. The migraine cycle: Patient burden of migraine during and between migraine attacks. Headache. 2008 Mar;48(3):430–41.

59. Asmundson GJ, Norton PJ, Veloso F. Anxiety sensitivity and fear of pain in patients with recurring headaches. Behav Res Ther. 1999 Aug;37(8):703–13.

60. Vincent M, Viktrup L, Nicholson RA, Ossipov MH, Vargas BB. The not so hidden impact of interictal burden in migraine: A narrative review. Front Neurol. 2022;13.

61. Latham PW. Clinical lecture on nervous or sick-headaches. Br Med J. 1872 Mar 30;1(587):336–7.

62. Latham PW. On nervous or sick-headache, its varieties and treatment, 2 lectures. 1873. 96 p.

63.   Graham JR, Wolff HG. Mechanism of migraine headache and action of ergotamine tartrate. Arch Neurol Psychiatry. 1938 Apr 1;39(4):737–63.

64.   Wolff HG. Headache and other head pain. Oxford University Press; 1963. 810 p.

65.   Charles A, Brennan KC. The neurobiology of migraine. Handb Clin Neurol. 2010;97:99–108.

66.   Mason BN, Russo AF. Vascular contributions to migraine: Time to revisit? Front Cell Neurosci. 2018 Aug 3;12:233.

67.   Thomsen LL, Kruuse C, Iversen HK, Olesen J. A nitric oxide donor (nitroglycerin) triggers genuine migraine attacks. Eur J Neurol. 1994 Sep;1(1):73–80.

68.   Tfelt-Hansen P, Saxena PR, Dahlöf C, Pascual J, Láinez M, Henry P, et al. Ergotamine in the acute treatment of migraine: A review and European consensus. Brain. 2000 Jan 1;123(1):9–18.

69.   Wang F, Wang J, Cao Y, Xu Z. Serotonin-norepinephrine reuptake inhibitors for the prevention of migraine and vestibular migraine: A systematic review and meta-analysis. Reg Anesth Pain Med. 2020 May;45(5):323–30.

70.   Rahmann A, Wienecke T, Hansen JM, Fahrenkrug J, Olesen J, Ashina M. Vasoactive intestinal peptide causes marked cephalic vasodilation, but does not induce migraine. Cephalalgia Int J Headache. 2008 Mar;28(3):226–36.

71.   Friberg L, Olesen J, Iversen HK, Sperling B. Migraine pain associated with middle cerebral artery dilatation: Reversal by sumatriptan. Lancet Lond Engl. 1991 Jul 6;338(8758):13–7.

72.   Caekebeke JF, Ferrari MD, Zwetsloot CP, Jansen J, Saxena PR. Antimigraine drug sumatriptan increases blood flow velocity in large cerebral arteries during migraine attacks. Neurology. 1992 Aug;42(8):1522–6.

73.   Olesen J, Larsen B, Lauritzen M. Focal hyperemia followed by spreading oligemia and impaired activation of rCBF in classic migraine. Ann Neurol. 1981 Apr;9(4):344–52.

74.   Kruuse C, Thomsen LL, Birk S, Olesen J. Migraine can be induced by sildenafil without changes in middle cerebral artery diameter. Brain J Neurol. 2003 Jan;126(Pt 1):241–7.

75.   Schoonman GG, van der Grond J, Kortmann C, van der Geest RJ, Terwindt GM, Ferrari MD. Migraine headache is not associated with cerebral or meningeal vasodilatation - A 3T magnetic resonance angiography study. Brain J Neurol. 2008 Aug;131(Pt 8):2192–200.

76.   Asghar MS, Hansen AE, Amin FM, van der Geest RJ, Koning P van der, Larsson HBW, et al. Evidence for a vascular factor in migraine. Ann Neurol. 2011 Apr;69(4):635–45.

77.   Liveing E. On megrim, sick-headache, and some allied disorders, a contribution to the pathology of nerve-storms. New Burlington Street: London, J. and A. Churchill; 1873.

78.   Lance JW, Lambert GA, Goadsby PJ, Duckworth JW. Brainstem influences on the cephalic circulation: Experimental data from cat and monkey of relevance to the mechanism of migraine. Headache. 1983 Nov;23(6):258–65.

79.   Cutrer FM. Pathophysiology of migraine. Semin Neurol. 2010 Apr;30(2):120–30.

80.   Cutrer FM, Charles A. The neurogenic basis of migraine. Headache J Head Face Pain. 2008;48(9):1411–4.

81.   Moskowitz MA. The neurobiology of vascular head pain. Ann Neurol. 1984 Aug;16(2):157–68.

82.   Moskowitz MA, Reinhard JF, Romero J, Melamed E, Pettibone DJ. Neurotransmitters and the fifth cranial nerve: Is there a relation to the headache phase of migraine? Lancet Lond Engl. 1979 Oct 27;2(8148):883–5.

83. Russell FA, King R, Smillie SJ, Kodji X, Brain SD. Calcitonin gene-related peptide: Physiology and pathophysiology. Physiol Rev. 2014 Oct;94(4):1099–142.

84. Humphrey PP, Goadsby PJ. The mode of action of sumatriptan is vascular? A debate. Cephalalgia Int J Headache. 1994 Dec;14(6):401–10; discussion 393.

85. Alpuente A, Gallardo VJ, Asskour L, Caronna E, Torres-Ferrus M, Pozo-Rosich P. Salivary CGRP can monitor the different migraine phases: CGRP (in)dependent attacks. Cephalalgia. 2022 Mar 1;42(3):186–96.

86. Peroutka SJ. Neurogenic inflammation and migraine: Implications for the therapeutics. Mol Interv. 2005 Oct;5(5):304–11.

87. Charles AC, Baca SM. Cortical spreading depression and migraine. Nat Rev Neurol. 2013 Nov;9(11):637–44.

88. Matsuura T, Bures J. The minimum volume of depolarized neural tissue required for triggering cortical spreading depression in rat. Exp Brain Res. 1971;12(3):238–49.

89. Tang YT, Mendez JM, Theriot JJ, Sawant PM, López-Valdés HE, Ju YS, et al. Minimum conditions for the induction of cortical spreading depression in brain slices. J Neurophysiol. 2014 Nov 15;112(10):2572–9.

90. Leão AAP, Morison RS. Propagation of spreading cortical depression. J Neurophysiol. 1945 Jan;8(1):33–45.

91. Arulmozhi DK, Veeranjaneyulu A, Bodhankar SL. Migraine: Current concepts and emerging therapies. Vascul Pharmacol. 2005 Sep;43(3):176–87.

92. Lauritzen M. Pathophysiology of the migraine aura. The spreading depression theory. Brain J Neurol. 1994 Feb;117 (Pt 1):199–210.

93. Ayata C. Cortical spreading depression triggers migraine attack: Pro. Headache. 2010 Apr;50(4):725–30.

94. Charles A. Does cortical spreading depression initiate a migraine attack? Maybe not. Headache. 2010 Apr;50(4):731–3.

95. Ferrari MD, Klever RR, Terwindt GM, Ayata C, van den Maagdenberg AMJM. Migraine pathophysiology: Lessons from mouse models and human genetics. Lancet Neurol. 2015 Jan;14(1):65–80.

96. Jacobs B, Dussor G. Neurovascular contributions to migraine: Moving beyond vasodilation. Neuroscience. 2016 Dec 3;338:130–44.

97. Goadsby PJ, Holland PR, Martins-Oliveira M, Hoffmann J, Schankin C, Akerman S. Pathophysiology of migraine: A disorder of sensory processing. Physiol Rev. 2017 Apr;97(2):553–622.

98. Hoffmann J, Baca SM, Akerman S. Neurovascular mechanisms of migraine and cluster headache. J Cereb Blood Flow Metab. 2019 Apr;39(4):573–94.

99. Akerman S, Holland PR, Goadsby PJ. Diencephalic and brainstem mechanisms in migraine. Nat Rev Neurosci. 2011 Sep 20;12(10):570–84.

100. Burstein R, Jakubowski M, Garcia-Nicas E, Kainz V, Bajwa Z, Hargreaves R, et al. Thalamic sensitization transforms localized pain into widespread allodynia. Ann Neurol. 2010 Jul;68(1):81–91.

101. Coppola G, Pierelli F, Schoenen J. Is the cerebral cortex hyperexcitable or hyperresponsive in migraine? Cephalalgia Int J Headache. 2007 Dec;27(12):1427–39.

102. de Tommaso M, Ambrosini A, Brighina F, Coppola G, Perrotta A, Pierelli F, et al. Altered processing of sensory stimuli in patients with migraine. Nat Rev Neurol. 2014 Mar;10(3):144–55.

103. Messlinger K, Fischer MJM, Lennerz JK. Neuropeptide effects in the trigeminal system: Pathophysiology and clinical relevance in migraine. Keio J Med. 2011;60(3):82–9.

104. GBD 2016 Neurology Collaborators. Global, regional, and national burden of neurological disorders, 1990-2016: a systematic analysis for the Global Burden of Disease Study 2016. Lancet Neurol. 2019 May;18(5):459–80.

105. Bigal ME, Lipton RB. The epidemiology, burden, and comorbidities of migraine. Neurol Clin. 2009 May;27(2):321–34.

106. Steiner TJ, Stovner LJ, Vos T, Jensen R, Katsarava Z. Migraine is first cause of disability in under 50s: Will health politicians now take notice? J Headache Pain. 2018 Feb 21;19(1):17.

107. Raggi A, Giovannetti AM, Quintas R, D'Amico D, Cieza A, Sabariego C, et al. A systematic review of the psychosocial difficulties relevant to patients with migraine. J Headache Pain. 2012 Nov 1;13(8):595–606.

108. Alonso J, Petukhova M, Vilagut G, Chatterji S, Heeringa S, Üstün TB, et al. Days out of role due to common physical and mental conditions: Results from the WHO World Mental Health surveys. Mol Psychiatry. 2011 Dec;16(12):1234–46.

109. Lampl C, Thomas H, Stovner LJ, Tassorelli C, Katsarava Z, Laínez JM, et al. Interictal burden attributable to episodic headache: Findings from the Eurolight project. J Headache Pain. 2016 Feb 16;17:9.

110. Buse DC, Reed ML, Fanning KM, Bostic R, Dodick DW, Schwedt TJ, et al. Comorbid and co-occurring conditions in migraine and associated risk of increasing headache pain intensity and headache frequency: Results of the migraine in America symptoms and treatment (MAST) study. J Headache Pain. 2020 Mar 2;21(1):23.

111. Irimia P, Garrido-Cumbrera M, Santos-Lasaosa S, Aguirre-Vazquez M, Correa-Fernández J, Colomina I, et al. Impact of monthly headache days on anxiety, depression and disability in migraine patients: Results from the Spanish Atlas. Sci Rep. 2021 Apr 15;11(1):8286.

112. D'Amico D, Sansone E, Grazzi L, Giovannetti AM, Leonardi M, Schiavolin S, et al. Multimorbidity in patients with chronic migraine and medication overuse headache. Acta Neurol Scand. 2018 Dec;138(6):515–22.

113. Lipton R, Bigal M. Migraine: Epidemiology, impact, and risk factors for progression. Headache. 2005 May 1;45 Suppl 1:S3–13.

114. Dickter C, Kieffaber P. EEG methods for the psychological sciences. Arts Sci Book Chapters. 2013 Dec 20;1–8.

115. Purves D, editor. Neuroscience. 3rd ed. Sunderland, Mass: Sinauer Associates, Publishers; 2004. 1 p.

116. Lodish H, Berk A, Matsudaira P, Kaiser CA, Krieger M, Scott MP, et al. Molecular cell biology. 5th ed. New York: W.H. Freeman and Co; 2005.

117. Niedermeyer E. Dipole theory and electroencephalography. Clin Electroencephalogr. 1996 Jul 1;27(3):121–31.

118. Buzsáki G, Anastassiou CA, Koch C. The origin of extracellular fields and currents - EEG, ECoG, LFP and spikes. Nat Rev Neurosci. 2012 May 18;13(6):407–20.

119. Bear MF, Connors BW, Paradiso MA. Neuroscience: Exploring the brain. Wolters Kluwer; 2016. 975 p.

120. Luck SJ. An introduction to the event-related potential technique. 2005.

121.   Blackwood DH, Muir WJ. Cognitive brain potentials and their application. Br J Psychiatry Suppl. 1990;(9):96–101.

122.   Posner MI. Chronometric explorations of mind. Oxford, England: Lawrence Erlbaum; 1978. xiii, 271 p. (Chronometric explorations of mind).

123.   Luck SJ, Woodman GF, Vogel EK. Event-related potential studies of attention. Trends Cogn Sci. 2000 Nov 1;4(11):432–40.

124.   Rinker T. Auditory processing in children with specific language impairment (SLI): An electrophysiological study. 2006 Jan 1;

125.   Regan D. Human brain electrophysiology: Evoked potentials and evoked magnetic fields in science and medicine. New York: Elsevier; 1989. 672 p.

126.   García-Larrea L, Lukaszewicz AC, Mauguière F. Somatosensory responses during selective spatial attention: The N120-to-N140 transition. Psychophysiology. 1995 Nov;32(6):526–37.

127.   Näätänen R, Picton T. The N1 wave of the human electric and magnetic response to sound: A review and an analysis of the component structure. Psychophysiology. 1987;24(4):375–425.

128.   Liang M, Mouraux A, Chan V, Blakemore C, Iannetti GD. Functional characterisation of sensory ERPs using probabilistic ICA: Effect of stimulus modality and stimulus location. Clin Neurophysiol Off J Int Fed Clin Neurophysiol. 2010 Apr;121(4):577–87.

129.   Kelly SP, Schroeder CE, Lalor EC. What does polarity inversion of extrastriate activity tell us about striate contributions to the early VEP? A comment on Ales et al. (2010). NeuroImage. 2013 Aug 1;76:442–5.

130.   Rauss K, Schwartz S, Pourtois G. Top-down effects on early visual processing in humans: A predictive coding framework. Neurosci Biobehav Rev. 2011 Apr;35(5):1237–53.

131.   Johannes S, Münte TF, Heinze HJ, Mangun GR. Luminance and spatial attention effects on early visual processing. Cogn Brain Res. 1995 Jul 1;2(3):189–205.

132.   Ellemberg D, Hammarrenger B, Lepore F, Roy MS, Guillemot JP. Contrast dependency of VEPs as a function of spatial frequency: The parvocellular and magnocellular contributions to human VEPs. Spat Vis. 2001 Jan 1;15(1):99–111.

133.   Hillyard SA, Vogel EK, Luck SJ. Sensory gain control (amplification) as a mechanism of selective attention: Electrophysiological and neuroimaging evidence. Philos Trans R Soc Lond B Biol Sci. 1998 Aug 29;353(1373):1257–70.

134.   Handy TC, Mangun GR. Attention and spatial selection: Electrophysiological evidence for modulation by perceptual load. Percept Psychophys. 2000 Jan 1;62(1):175–86.

135.   Handy TC, Soltani M, Mangun GR. Perceptual load and visuocortical processing: Event-related potentials reveal sensory-level selection. Psychol Sci. 2001 May 1;12(3):213–8.

136.   Olofsson JK, Nordin S, Sequeira H, Polich J. Affective picture processing: An integrative review of ERP findings. Biol Psychol. 2008 Mar 1;77(3):247–65.

137.   Mangun GR. Neural mechanisms of visual selective attention. Psychophysiology. 1995;32(1):4–18.

138.   Hopf JM, Vogel E, Woodman G, Heinze HJ, Luck SJ. Localizing visual discrimination processes in time and space. J Neurophysiol. 2002 Oct;88(4):2088–95.

139.   Vogel EK, Luck SJ. The visual N1 component as an index of a discrimination process. Psychophysiology. 2000 Mar;37(2):190–203.

140.   Eimer M. "Sensory gating" as a mechanism for visuospatial orienting: Electrophysiological evidence from trial-by-trial cuing experiments. Percept Psychophys. 1994 Nov 1;55(6):667–75.

141.   Luck SJ, Hillyard SA, Mouloua M, Woldorff MG, Clark VP, Hawkins HL. Effects of spatial cuing on luminance detectability: Psychophysical and electrophysiological evidence for early selection. J Exp Psychol Hum Percept Perform. 1994;20:887–904.

142.   Mangun GR, Hillyard SA. Modulations of sensory-evoked brain potentials indicate changes in perceptual processing during visual-spatial priming. J Exp Psychol Hum Percept Perform. 1991;17:1057–74.

143.   Bentin S, Allison T, Puce A, Perez E, McCarthy G. Electrophysiological studies of face perception in humans. J Cogn Neurosci. 1996 Nov;8(6):551–65.

144.   Rossion B, Campanella S, Gomez CM, Delinte A, Debatisse D, Liard L, et al. Task modulation of brain activity related to familiar and unfamiliar face processing: An ERP study. Clin Neurophysiol. 1999 Mar 1;110(3):449–62.

145.   Luck SJ, Hillyard SA. Electrophysiological correlates of feature analysis during visual search. Psychophysiology. 1994;31(3):291–308.

146.   Naatanen R, Näätänen R. Attention and brain function. Psychology Press; 1992. 518 p.

147.   Patel SH, Azzam PN. Characterization of N200 and P300: Selected studies of the event-related potential. Int J Med Sci. 2005 Oct 1;2(4):147–54.

148.   Walter WG, Cooper R, Aldridge VJ, Mccallum WC, Winter AL. Contingent negative variation: An electric sign of sensorimotor association and expectancy in the human brain. Nature. 1964 Jul 25;203:380–4.

149.   Young A, Cornejo J, Spinner A. Auditory brainstem response. In: StatPearls. Treasure Island (FL): StatPearls Publishing; 2022.

150.   Goldstein R, Rodman LB. Early components of averaged evoked responses to rapidly repeated auditory stimuli. J Speech Hear Res. 1967 Dec;10(4):697–705.

151.   Figueiredo Frizzo AC, Rodrigues Funayama CA, Isaac ML, Colafêmina JF. Auditory middle latency responses: A study of healthy children. Braz J Otorhinolaryngol. 2007;73(3):398–403.

152.   Neves IF, Gonçalves IC, Leite RA, Leite Magliaro FC, Matas CG. Middle latency response study of auditory evoked potentials' amplitudes and latencies audiologically normal individuals. Braz J Otorhinolaryngol. 2015 Oct 20;73(1):69–74.

153.   Picton TW, Hillyard SA, Krausz HI, Galambos R. Human auditory evoked potentials. I. Evaluation of components. Electroencephalogr Clin Neurophysiol. 1974 Feb;36(2):179–90.

154.   Adler G, Adler J. Influence of stimulus intensity on AEP components in the 80- to 200-millisecond latency range. Audiol Off Organ Int Soc Audiol. 1989;28(6):316–24.

155.   Herrmann CS, Knight RT. Mechanisms of human attention: Event-related potentials and oscillations. Neurosci Biobehav Rev. 2001 Aug 1;25(6):465–76.

156.   Key APF, Dove GO, Maguire MJ. Linking brainwaves to the brain: An ERP primer. Dev Neuropsychol. 2005;27(2):183–215.

157.   Jones SJ, Longe O, Vaz Pato M. Auditory evoked potentials to abrupt pitch and timbre change of complex tones: Electrophysiological evidence of "streaming"? Electroencephalogr Clin Neurophysiol Potentials Sect. 1998 Mar 1;108(2):131–42.

158.   Hink RF, Hillyard SA, Benson PJ. Event-related brain potentials and selective attention to acoustic and phonetic cues. Biol Psychol. 1978 Jan 1;6(1):1–16.

159.   Näätänen R, Gaillard AW, Mäntysalo S. Early selective-attention effect on evoked potential reinterpreted. Acta Psychol (Amst). 1978 Jul;42(4):313–29.

160.   Picton TW, Hillyard SA. Human auditory evoked potentials. II. Effects of attention. Electroencephalogr Clin Neurophysiol. 1974 Feb;36(2):191–9.

161.   Escera C, Corral MJ. Role of mismatch negativity and novelty-P3 in involuntary auditory attention. J Psychophysiol. 2007 Jan;21(3–4):251–64.

162.   Ritter W, Simson R, Vaughan HG, Friedman D. A brain event related to the making of a sensory discrimination. Science. 1979 Mar 30;203(4387):1358–61.

163.   Picton TW. Human auditory evoked potentials. Plural Publishing; 2010. 649 p.

164.   Scheer M, Bülthoff HH, Chuang LL. Steering demands diminish the early-P3, late-P3 and RON components of the event-related potential of task-irrelevant environmental sounds. Front Hum Neurosci. 2016;10.

165.   Polich J. Theoretical overview of P3a and P3b. In: Polich J, editor. Detection of change: Event-related potential and fMRI findings. Boston, MA: Springer US; 2003. p. 83–98.

166.   Picton T. The P300 wave of the human event-related potential. J Clin Neurophysiol Off Publ Am Electroencephalogr Soc. 1992 Nov 1;9:456–79.

167.   Polich J, Comerchero MD. P3a from visual stimuli: Typicality, task, and topography. Brain Topogr. 2003;15(3):141–52.

168.   Polich J. Updating P300: An integrative theory of P3a and P3b. Clin Neurophysiol. 2007 Oct 1;118(10):2128–48.

169.   Rugg MD, Coles MGH, editors. Electrophysiology of mind: Event-related brain potentials and cognition. Oxford University Press; 1995. 236 p.

170.   Schröger E, Wolff C. Attentional orienting and reorienting is indicated by human event-related brain potentials. Neuroreport. 1998 Oct 26;9(15):3355–8.

171.   Makeig S, Delorme A, Westerfield M, Jung TP, Townsend J, Courchesne E, et al. Electroencephalographic brain dynamics following manually responded visual targets. PLOS Biol. 2004 Jun 15;2(6):e176.

172.   Roach BJ, Mathalon DH. Event-related EEG time-frequency analysis: An overview of measures and an analysis of early gamma band phase locking in schizophrenia. Schizophr Bull. 2008 Sep 1;34(5):907–26.

173.   Başar E. EEG-brain dynamics: Relation between EEG and brain evoked potentials. Elsevier/North-Holland Biomedical Press; 1980. 444 p.

174.   Buzsáki G, Draguhn A. Neuronal oscillations in cortical networks. Science. 2004 Jun 25;304(5679):1926–9.

175.   Buzsaki G. Rhythms of the brain. Oxford University Press; 2006. 465 p.

176.   Knyazev GG. Motivation, emotion, and their inhibitory control mirrored in brain oscillations. Neurosci Biobehav Rev. 2007 Jan 1;31(3):377–95.

177.   Long S, Ding R, Wang J, Yu Y, Lu J, Yao D. Sleep quality and electroencephalogram delta power. Front Neurosci. 2021;15.

178.   Knyazev GG, Slobodskoj-Plusnin JY, Bocharov AV. Event-related delta and theta synchronization during explicit and implicit emotion processing. Neuroscience. 2009 Dec 29;164(4):1588–600.

179.   Putman P. Resting state EEG delta-beta coherence in relation to anxiety, behavioral inhibition, and selective attentional processing of threatening stimuli. Int J Psychophysiol Off J Int Organ Psychophysiol. 2011 Apr;80(1):63–8.

180.   Klimesch W. Memory processes, brain oscillations and EEG synchronization. Int J Psychophysiol. 1996 Nov 1;24(1):61–100.

181.   Herweg NA, Solomon EA, Kahana MJ. Theta oscillations in human memory. Trends Cogn Sci. 2020 Mar;24(3):208–27.

182.   Goyal A, Miller J, Qasim SE, Watrous AJ, Zhang H, Stein JM, et al. Functionally distinct high and low theta oscillations in the human hippocampus. Nat Commun. 2020 May 18;11(1):2469.

183.   Klimesch W, Sauseng P, Hanslmayr S. EEG alpha oscillations: The inhibition–timing hypothesis. Brain Res Rev. 2007 Jan 1;53(1):63–88.

184.   Ergenoglu T, Demiralp T, Bayraktaroglu Z, Ergen M, Beydagi H, Uresin Y. Alpha rhythm of the EEG modulates visual detection performance in humans. Brain Res Cogn Brain Res. 2004 Aug;20(3):376–83.

185.   Babiloni C, Brancucci A, Del Percio C, Capotosto P, Arendt-Nielsen L, Chen ACN, et al. Anticipatory electroencephalography alpha rhythm predicts subjective perception of pain intensity. J Pain. 2006 Oct;7(10):709–17.

186.   Thut G, Nietzel A, Brandt SA, Pascual-Leone A. Alpha-band electroencephalographic activity over occipital cortex indexes visuospatial attention bias and predicts visual target detection. J Neurosci Off J Soc Neurosci. 2006 Sep 13;26(37):9494–502.

187.   Hanslmayr S, Aslan A, Staudigl T, Klimesch W, Herrmann CS, Bäuml KH. Prestimulus oscillations predict visual perception performance between and within subjects. NeuroImage. 2007 Oct 1;37(4):1465–73.

188.   Romei V, Brodbeck V, Michel C, Amedi A, Pascual-Leone A, Thut G. Spontaneous fluctuations in posterior α-band EEG activity reflect variability in excitability of human visual areas. Cereb Cortex. 2008 Sep 1;18(9):2010–8.

189.   Busch NA, Dubois J, VanRullen R. The phase of ongoing EEG oscillations predicts visual perception. J Neurosci. 2009 Jun 17;29(24):7869–76.

190.   Bazanova OM, Kondratenko AV, Kuz'minova OI, Muravleva KB, Petrova SE. [EEG alpha indices in dependence on the menstrual cycle phase and salivary progesterone]. Fiziol Cheloveka. 2014;40(2):31–40.

191.   Ray WJ, Cole HW. EEG alpha activity reflects attentional demands, and beta activity reflects emotional and cognitive processes. Science. 1985 May 10;228(4700):750–2.

192.   Weiss S, Mueller HM. "Too many betas do not spoil the broth": The role of beta brain oscillations in language processing. Front Psychol. 2012 Jun 25;3:201.

193.   Neuper C, Scherer R, Wriessnegger S, Pfurtscheller G. Motor imagery and action observation: Modulation of sensorimotor brain rhythms during mental control of a brain–computer interface. Clin Neurophysiol. 2009 Feb 1;120(2):239–47.

194.   Gola M, Magnuski M, Szumska I, Wróbel A. EEG beta band activity is related to attention and attentional deficits in the visual performance of elderly subjects. Int J Psychophysiol. 2013 Sep 1;89(3):334–41.

195.   Tallon-Baudry C, Bertrand O. Oscillatory gamma activity in humans and its role in object representation. Trends Cogn Sci. 1999 Apr;3(4):151–62.

196.   Romei V, Gross J, Thut G. On the role of prestimulus alpha rhythms over occipito-parietal areas in visual input regulation: Correlation or causation? J Neurosci Off J Soc Neurosci. 2010 Jun 23;30(25):8692–7.

197.   Kent JL. Psychedelic information theory: Shamanism in the age of reason. Inf Theory.

198.   Pfurtscheller G, Lopes da Silva FH. Event-related EEG/MEG synchronization and desynchronization: Basic principles. Clin Neurophysiol. 1999 Nov 1;110(11):1842–57.

199.   Nunez PL, Srinivasan R. Electric fields of the brain: The neurophysics of EEG. Oxford University Press; 2006. 629 p.

200.   Cohen MX. Analyzing neural time series data: Theory and practice. MIT Press; 2014. 615 p.

201.   Varela F, Lachaux JP, Rodriguez E, Martinerie J. The brainweb: Phase synchronization and large-scale integration. Nat Rev Neurosci. 2001 Apr;2(4):229–39.

202.   Sur S, Sinha VK. Event-related potential: An overview. Ind Psychiatry J. 2009;18(1):70–3.

203.   Fabiani M, Gratton G, Coles MGH. Event-related brain potentials. In: Handbook of psychophysiology, 2nd ed. New York, NY, US: Cambridge University Press; 2000. p. 53–84.

204.   Picton TW, Bentin S, Berg P, Donchin E, Hillyard SA, Johnson R, et al. Guidelines for using human event-related potentials to study cognition: Recording standards and publication criteria. Psychophysiology. 2000 Mar;37(2):127–52.

205.   Coles MGH, Rugg MD. Event-related brain potentials: An introduction. In: Electrophysiology of mind: Event-related brain potentials and cognition. New York, NY, US: Oxford University Press; 1995. p. 1–26. (Oxford psychology series, No. 25).

206.   Luck SJ, Kappenman ES. ERP components and selective attention. In: The Oxford handbook of event-related potential components. New York, NY, US: Oxford University Press; 2012. p. 295–327. (Oxford library of psychology).

207.   Vialatte FB, Maurice M, Dauwels J, Cichocki A. Steady-state visually evoked potentials: Focus on essential paradigms and future perspectives. Prog Neurobiol. 2010 Apr;90(4):418–38.

208.   Picton TW, John MS, Dimitrijevic A, Purcell D. Human auditory steady-state responses: Respuestas auditivas de estado estable en humanos. Int J Audiol. 2003 Jan 1;42(4):177–219.

209.   Niedermeyer E, Silva FHL da. Electroencephalography: Basic principles, clinical applications, and related fields. Lippincott Williams & Wilkins; 2005. 1342 p.

210.   Zoefel B, ten Oever S, Sack AT. The involvement of endogenous neural oscillations in the processing of rhythmic input: More than a regular repetition of evoked neural responses. Front Neurosci. 2018;12.

211.   Dumper K, Jenkins W, Lacombe A, Lovett M, Perimutter M. Introductory psychology. Simple Book Publishing;

212.   Mather G. Foundations of sensation and perception. 3rd ed. Psychology Press; 2016.

213.   Albright TD. Perceiving. Daedalus. 2015;144(1):22–41.

214.   Gescheider GA. Psychophysics: The fundamentals. Psychology Press; 1997.

215.   Ikumi N, Cerda-Company X, Marti-Marca A, Vilà-Balló A, Caronna E, Gallardo VJ, et al. Avoidance behaviour modulates but does not condition phonophobia in migraine. Cephalalgia. 2022 Nov 1;42(13):1305–16.

216.   Goldstein B, Shulman A. Tinnitus - Hyperacusis and the loudness discomfort level test - A preliminary report. Int Tinnitus J. 1996 Jan 1;2:83–9.

217.   Pause BM, Miranda A, Göder R, Aldenhoff JB, Ferstl R. Reduced olfactory performance in patients with major depression. J Psychiatr Res. 2001;35(5):271–7.

218.   de Lange FP, Heilbron M, Kok P. How do expectations shape perception? Trends Cogn Sci. 2018 Sep;22(9):764–79.

219.   Maksimenko VA, Runnova AE, Zhuravlev MO, Makarov VV, Nedayvozov V, Grubov VV, et al. Visual perception affected by motivation and alertness controlled by a noninvasive brain-computer interface. PLOS ONE. 2017 dic;12(12):e0188700.

220.   Doly M. Transduction of the light message: From the photon to the optic nerve. Fundam Clin Pharmacol. 1994;8(2):147–54.

221.   Schultze M. Zur anatomie und physiologie der retina. Arch Für Mikrosk Anat. 1866 Dec 1;2(1):175–286.

222.   Ingram NT, Sampath AP, Fain GL. Why are rods more sensitive than cones? J Physiol. 2016 Oct 1;594(19):5415–26.

223.   Purves D, Augustine GJ, Fitzpatrick D, Katz LC, LaMantia AS, McNamara JO, et al. The retina. In: Neuroscience. 2nd ed. Sinauer Associates; 2001.

224.   Coombs JL, Van Der List D, Chalupa LM. Morphological properties of mouse retinal ganglion cells during postnatal development. J Comp Neurol. 2007 Aug 20;503(6):803–14.

225.   Schmidt TM, Do MTH, Dacey D, Lucas R, Hattar S, Matynia A. Melanopsin-positive intrinsically photosensitive retinal ganglion cells: From form to function. J Neurosci Off J Soc Neurosci. 2011 Nov 9;31(45):16094–101.

226.   Kim US, Mahroo OA, Mollon JD, Yu-Wai-Man P. Retinal ganglion cells - Diversity of cell types and clinical relevance. Front Neurol. 2021 May 21;12:661938.

227.   Erskine L, Herrera E. Connecting the retina to the brain. ASN Neuro. 2014;6(6):1759091414562107.

228.   Rakic P. Prenatal genesis of connections subserving ocular dominance in the rhesus monkey. Nature. 1976 Jun 10;261(5560):467–71.

229.   Godement P, Salaün J, Imbert M. Prenatal and postnatal development of retinogeniculate and retinocollicular projections in the mouse. J Comp Neurol. 1984 Dec 20;230(4):552–75.

230.   Chalupa LM, Snider CJ. Topographic specificity in the retinocollicular projection of the developing ferret: An anterograde tracing study. J Comp Neurol. 1998 Mar 2;392(1):35–47.

231.   Creel DJ. Visually evoked potentials. Handb Clin Neurol. 2019;160:501–22.

232.   Ahirwal P. Correlation of neurochemical profile to the retinal fundus imaging feature: Pilot experiment. 2020.

233.   Di Russo F, Martínez A, Sereno MI, Pitzalis S, Hillyard SA. Cortical sources of the early components of the visual evoked potential. Hum Brain Mapp. 2002 Feb;15(2):95–111.

234.   Foxe JJ, Simpson GV. Flow of activation from V1 to frontal cortex in humans. A framework for defining "early" visual processing. Exp Brain Res. 2002 Jan;142(1):139–50.

235.   Foxe JJ, Strugstad EC, Sehatpour P, Molholm S, Pasieka W, Schroeder CE, et al. Parvocellular and magnocellular contributions to the initial generators of the visual evoked potential: High-density electrical mapping of the "C1" component. Brain Topogr. 2008 Sep;21(1):11–21.

236.   Herrmann CS. Human EEG responses to 1–100 Hz flicker: Resonance phenomena in visual cortex and their potential correlation to cognitive phenomena. Exp Brain Res. 2001 Apr 1;137(3):346–53.

237.   de Graaf TA, Gross J, Paterson G, Rusch T, Sack AT, Thut G. Alpha-band rhythms in visual task performance: Phase-locking by rhythmic sensory stimulation. PloS One. 2013;8(3):e60035.

238.   Lopes da Silva F. Neural mechanisms underlying brain waves: From neural membranes to networks. Electroencephalogr Clin Neurophysiol. 1991 Aug 1;79(2):81–93.

239.   Sanchez G. Real-time electrophysiology in cognitive neuroscience: Towards adaptive paradigms to study perceptual learning and decision making in humans.

240.   Harris J. Sensation and perception. 1st ed. SAGE Publications Ltd; 2014.

241.   Appler JM, Goodrich LV. Connecting the ear to the brain: Molecular mechanisms of auditory circuit assembly. Prog Neurobiol. 2011 Apr;93(4):488–508.

242.   Møller AR. Auditory neurophysiology. J Clin Neurophysiol Off Publ Am Electroencephalogr Soc. 1994 May;11(3):284–308.

243.   Li S, Cheng C, Lu L, Ma X, Zhang X, Li A, et al. Hearing loss in neurological disorders. Front Cell Dev Biol. 2021 Aug 11;9:716300.

244.   Paulraj MP, Subramaniam K, Yaccob SB, Adom AHB, Hema CR. Auditory evoked potential response and hearing loss: A review. Open Biomed Eng J. 2015 Feb 27;9:17–24.

245.   Gorga MP, Kaminski JR, Beauchaine KL, Jesteadt W, Neely ST. Auditory brainstem responses from children three months to three years of age: Normal patterns of response. II. J Speech Hear Res. 1989 Jun;32(2):281–8.

246.   Thornton AR, Mendel MI, Anderson CV. Effects of stimulus frequency and intensity on the middle components of the averaged auditory electroencephalic response. J Speech Hear Res. 1977 Mar;20(1):81–94.

247.   Biau E, Wang D, Park H, Jensen O, Hanslmayr S. Auditory detection is modulated by theta phase of silent lip movements. Curr Res Neurobiol. 2021 Jan 1;2:100014.

248.   Tal I, Leszczynski M, Mesgarani N, Schroeder CE. Does the phase of ongoing EEG oscillations predict auditory perception? bioRxiv; 2020. p. 2020.07.17.209387.

249.   Butler BE, Lomber SG. Functional and structural changes throughout the auditory system following congenital and early-onset deafness: Implications for hearing restoration. Front Syst Neurosci. 2013 Nov 26;7:92.

250.   Khan I, Khan MA. Sensory and perceptual alterations. In: StatPearls. Treasure Island (FL): StatPearls Publishing; 2022.

251.   Schulz SE, Stevenson RA. Differentiating between sensory sensitivity and sensory reactivity in relation to restricted interests and repetitive behaviours. Autism Int J Res Pract. 2020 Jan;24(1):121–34.

252.   Tavassoli T, Hoekstra RA, Baron-Cohen S. The Sensory Perception Quotient (SPQ): Development and validation of a new sensory questionnaire for adults with and without autism. Mol Autism. 2014 Apr 24;5(1):29.

253.   Aron EN, Aron A, Jagiellowicz J. Sensory processing sensitivity: A review in the light of the evolution of biological responsivity. Personal Soc Psychol Rev Off J Soc Personal Soc Psychol Inc. 2012 Aug;16(3):262–82.

254.   Houghton DC, Stein DJ, Cortese BM. Review: Exteroceptive sensory abnormalities in childhood and adolescent anxiety and obsessive-compulsive disorder: A critical review. J Am Acad Child Adolesc Psychiatry. 2020 Jan;59(1):78–87.

255.   Greven CU, Lionetti F, Booth C, Aron EN, Fox E, Schendan HE, et al. Sensory Processing Sensitivity in the context of Environmental Sensitivity: A critical review and development of research agenda. Neurosci Biobehav Rev. 2019 Mar 1;98:287–305.

256.   Ghanizadeh A. Sensory processing problems in children with ADHD, a systematic review. Psychiatry Investig. 2011 Jun;8(2):89–94.

257.   Serafini G, Gonda X, Canepa G, Pompili M, Rihmer Z, Amore M, et al. Extreme sensory processing patterns show a complex association with depression, and impulsivity, alexithymia, and hopelessness. J Affect Disord. 2017 Mar 1;210:249–57.

258.   Ashwin E, Ashwin C, Rhydderch D, Howells J, Baron-Cohen S. Eagle-eyed visual acuity: An experimental investigation of enhanced perception in autism. Biol Psychiatry. 2009 Jan 1;65(1):17–21.

259.   Bonnel A, Mottron L, Peretz I, Trudel M, Gallun E, Bonnel AM. Enhanced pitch sensitivity in individuals with autism: A signal detection analysis. J Cogn Neurosci. 2003 Feb 15;15(2):226–35.

260.   Jones CRG, Happé F, Baird G, Simonoff E, Marsden AJS, Tregay J, et al. Auditory discrimination and auditory sensory behaviours in autism spectrum disorders. Neuropsychologia. 2009 Nov;47(13):2850–8.

261.   Khalfa S, Bruneau N, Rogé B, Georgieff N, Veuillet E, Adrien JL, et al. Increased perception of loudness in autism. Hear Res. 2004 Dec;198(1–2):87–92.

262.   Marco EJ, Hinkley LBN, Hill SS, Nagarajan SS. Sensory processing in autism: A review of neurophysiologic findings. Pediatr Res. 2011 May;69(5 Pt 2):48R-54R.

263.   Woodhouse A, Drummond PD. Mechanisms of increased sensitivity to noise and light in migraine headache. Cephalalgia Int J Headache. 1993 Dec;13(6):417–21.

264.   Gosling SD. From mice to men: What can we learn about personality from animal research? Psychol Bull. 2001;127:45–86.

265.   Wolf M, van Doorn GS, Weissing FJ. Evolutionary emergence of responsive and unresponsive personalities. Proc Natl Acad Sci U S A. 2008 Oct 14;105(41):15825–30.

266.   Wolf M, Van Doorn GS, Weissing FJ. On the coevolution of social responsiveness and behavioural consistency. Proc Biol Sci. 2011 Feb 7;278(1704):440–8.

267.   Berson DM, Dunn FA, Takao M. Phototransduction by retinal ganglion cells that set the circadian clock. Science. 2002 Feb 8;295(5557):1070–3.

268.   Hattar S, Liao HW, Takao M, Berson DM, Yau KW. Melanopsin-containing retinal ganglion cells: Architecture, projections, and intrinsic photosensitivity. Science. 2002 Feb 8;295(5557):1065–70.

269.   Duda M, Domaglik A, Orlowska-Freuer M, Krzysztynska-Kuleta O, Beldzik B, Smyk M, et al. Melanopsin: From a small molecule to brain functions. Neurosci Biobehav Rev. 2020 Jun;113.

270.   Gamlin PD, Zhang H, Clarke RJ. Luminance neurons in the pretectal olivary nucleus mediate the pupillary light reflex in the rhesus monkey. Exp Brain Res. 1995;106(1):169–76.

271.   McDougal DH, Gamlin PD. The influence of intrinsically-photosensitive retinal ganglion cells on the spectral sensitivity and response dynamics of the human pupillary light reflex. Vision Res. 2010 Jan;50(1):72–87.

272.   Young RSL, Kimura E. Pupillary correlates of light-evoked melanopsin activity in humans. Vision Res. 2008 Mar;48(7):862–71.

273.   Okamoto K, Thompson R, Tashiro A, Chang Z, Bereiter DA. Bright light produces Fos-positive neurons in caudal trigeminal brainstem. Neuroscience. 2009 Jun 2;160(4):858–64.

274.   Noseda R, Kainz V, Jakubowski M, Gooley JJ, Saper CB, Digre K, et al. A neural mechanism for exacerbation of headache by light. Nat Neurosci. 2010 Feb;13(2):239–45.

275.   Digre KB, Brennan KC. Shedding light on photophobia. J Neuro-Ophthalmol Off J North Am Neuro-Ophthalmol Soc. 2012 Mar;32(1):68–81.

276. Xue T, Do MTH, Riccio A, Jiang Z, Hsieh J, Wang HC, et al. Melanopsin signaling in mammalian iris and retina. Nature. 2011 Nov 2;479(7371):67–73.

277. Semo M, Gias C, Ahmado A, Vugler A. A role for the ciliary marginal zone in the melanopsin-dependent intrinsic pupillary light reflex. Exp Eye Res. 2014 Feb;119:8–18.

278. Matynia A, Nguyen E, Sun X, Blixt FW, Parikh S, Kessler J, et al. Peripheral sensory neurons expressing melanopsin respond to light. Front Neural Circuits. 2016 Aug 10;10:60.

279. Noseda R, Jakubowski M, Kainz V, Borsook D, Burstein R. Cortical projections of functionally identified thalamic trigeminovascular neurons: Implications for migraine headache and its associated symptoms. J Neurosci Off J Soc Neurosci. 2011 Oct 5;31(40):14204–17.

280. Dolgonos S, Ayyala H, Evinger C. Light-induced trigeminal sensitization without central visual pathways: Another mechanism for photophobia. Invest Ophthalmol Vis Sci. 2011 Oct 4;52(11):7852–8.

281. Noseda R, Constandil L, Bourgeais L, Chalus M, Villanueva L. Changes of meningeal excitability mediated by corticotrigeminal networks: A link for the endogenous modulation of migraine pain. J Neurosci Off J Soc Neurosci. 2010 Oct 27;30(43).

282. Hubel DH, Wiesel TN. Receptive fields, binocular interaction and functional architecture in the cat's visual cortex. J Physiol. 1962 Jan;160(1):106–54.

283. Ly JQM, Gaggioni G, Chellappa SL, Papachilleos S, Brzozowski A, Borsu C, et al. Circadian regulation of human cortical excitability. Nat Commun. 2016 Jun 24;7(1):11828.

284. Aron EN, Aron A. Sensory-processing sensitivity and its relation to introversion and emotionality. J Pers Soc Psychol. 1997 Aug;73(2):345–68.

285. Miceli S, Nadif Kasri N, Joosten J, Huang C, Kepser L, Proville R, et al. Reduced inhibition within layer IV of sert knockout rat barrel cortex is associated with faster sensory integration. Cereb Cortex. 2017 Feb 1;27(2):933–49.

286. Jones LA, Hills PJ, Dick KM, Jones SP, Bright P. Cognitive mechanisms associated with auditory sensory gating. Brain Cogn. 2016 Feb;102:33–45.

287. Lozano-Soto E, Soto-León V, Sabbarese S, Ruiz-Alvarez L, Sanchez-del-Rio M, Aguilar J, et al. Transcranial static magnetic field stimulation (tSMS) of the visual cortex decreases experimental photophobia. Cephalalgia. 2018 Jul 1;38(8):1493–7.

288. Coppola G, Schoenen J. Measures of cortical excitability. In: Borsook D, May A, Goadsby PJ, Hargreaves R, editors. The migraine brain: Imaging structure and function. Oxford University Press; 2012. p. 0.

289. van Vreeswijk C, Sompolinsky H. Chaos in neuronal networks with balanced excitatory and inhibitory activity. Science. 1996 Dec 6;274(5293):1724–6.

290. Zhou Y, Danbolt NC. Glutamate as a neurotransmitter in the healthy brain. J Neural Transm. 2014;121(8):799–817.

291. Barnard EA, Skolnick P, Olsen RW, Mohler H, Sieghart W, Biggio G, et al. International Union of Pharmacology. XV. Subtypes of gamma-aminobutyric acidA receptors: Classification on the basis of subunit structure and receptor function. Pharmacol Rev. 1998 Jun;50(2):291–313.

292. Bormann J. The "ABC" of GABA receptors. Trends Pharmacol Sci. 2000 Jan 1;21(1):16–9.

293. Bowery NG, Bettler B, Froestl W, Gallagher JP, Marshall F, Raiteri M, et al. International Union of Pharmacology. XXXIII. Mammalian gamma-aminobutyric acid(B) receptors: Structure and function. Pharmacol Rev. 2002 Jun;54(2):247–64.

294.   Buzsáki G. Feed-forward inhibition in the hippocampal formation. Prog Neurobiol. 1984;22(2):131–53.

295.   Nelson SB, Valakh V. Excitatory/inhibitory balance and circuit homeostasis in autism spectrum disorders. Neuron. 2015 Aug 19;87(4):684–98.

296.   Vogels TP, Sprekeler H, Zenke F, Clopath C, Gerstner W. Inhibitory plasticity balances excitation and inhibition in sensory pathways and memory networks. Science. 2011 Dec 16;334(6062):1569–73.

297.   Heiss JE, Katz Y, Ganmor E, Lampl I. Shift in the balance between excitation and inhibition during sensory adaptation of S1 neurons. J Neurosci Off J Soc Neurosci. 2008 Dec 3;28(49):13320–30.

298.   Shu Y, Hasenstaub A, Badoual M, Bal T, McCormick DA. Barrages of synaptic activity control the gain and sensitivity of cortical neurons. J Neurosci. 2003 Nov 12;23(32):10388–401.

299.   Davis GW. Homeostatic control of neural activity: From phenomenology to molecular design. Annu Rev Neurosci. 2006 Jul 21;29(1):307–23.

300.   Marder E, Goaillard JM. Variability, compensation and homeostasis in neuron and network function. Nat Rev Neurosci. 2006 Jul;7(7):563–74.

301.   Turrigiano GG, Nelson SB. Homeostatic plasticity in the developing nervous system. Nat Rev Neurosci. 2004 Feb;5(2):97–107.

302.   Turrigiano G. Homeostatic synaptic plasticity: Local and global mechanisms for stabilizing neuronal function. Cold Spring Harb Perspect Biol. 2012 Jan 1;4(1):a005736.

303.   Ferguson BR, Gao WJ. PV interneurons: Critical regulators of E/I balance for prefrontal cortex-dependent behavior and psychiatric disorders. Front Neural Circuits. 2018;12:37.

304.   Shen W, McKeown CR, Demas JA, Cline HT. Inhibition to excitation ratio regulates visual system responses and behavior in vivo. J Neurophysiol. 2011 Nov;106(5):2285–302.

305.   Yizhar O, Fenno LE, Prigge M, Schneider F, Davidson TJ, O'Shea DJ, et al. Neocortical excitation/inhibition balance in information processing and social dysfunction. Nature. 2011 Sep;477(7363):171–8.

306.   Ghatak S, Talantova M, McKercher SR, Lipton SA. Novel therapeutic approach for excitatory/inhibitory imbalance in neurodevelopmental and neurodegenerative diseases. Annu Rev Pharmacol Toxicol. 2021 Jan 6;61:701–21.

307.   Liu Y, Ouyang P, Zheng Y, Mi L, Zhao J, Ning Y, et al. A selective review of the excitatory-inhibitory imbalance in schizophrenia: Underlying biology, genetics, microcircuits, and symptoms. Front Cell Dev Biol. 2021 Oct 21;9:664535.

308.   Uzunova G, Pallanti S, Hollander E. Excitatory/inhibitory imbalance in autism spectrum disorders: Implications for interventions and therapeutics. World J Biol Psychiatry Off J World Fed Soc Biol Psychiatry. 2016 Apr;17(3):174–86.

309.   Nguyen BN, McKendrick AM, Vingrys AJ. Abnormal inhibition-excitation imbalance in migraine. Cephalalgia. 2016 Jan 1;36(1):5–14.

310.   Byrne J. Neuroscience online: An electronic textbook for the neurosciences. Department of Neurobiology and Anatomy: The University of Texas Medical School at Houston; 1997.

311.   Hebb DO. The organization of behavior. John Wiley & Sons, New York, USA; 1949.

312.   Fox K, Stryker M. Integrating Hebbian and homeostatic plasticity: Introduction. Philos Trans R Soc Lond B Biol Sci. 2017 Mar 5;372(1715):20160413.

313. Desai NS, Rutherford LC, Turrigiano GG. BDNF regulates the intrinsic excitability of cortical neurons. Learn Mem. 1999 Jan 5;6(3):284–91.

314. Turrigiano GG, Leslie KR, Desai NS, Rutherford LC, Nelson SB. Activity-dependent scaling of quantal amplitude in neocortical neurons. Nature. 1998 Feb;391(6670):892–6.

315. Mahon S, Charpier S. Bidirectional plasticity of intrinsic excitability controls sensory inputs efficiency in layer 5 barrel cortex neurons in vivo. J Neurosci Off J Soc Neurosci. 2012 Aug 15;32(33):11377–89.

316. Daoudal G, Debanne D. Long-term plasticity of intrinsic excitability: Learning rules and mechanisms. Learn Mem Cold Spring Harb N. 2003;10(6):456–65.

317. Folger HT. The effects of mechanical shock on locomotion in Amoeba proteus. J Morphol. 1926;42(2):359–70.

318. Grave C. The tentacle reflex in a holothurian, cucumaria pulcherrima. Science. 1905 May 12;

319. Prosser CL, Hunter WS. The extinction of startle responses and spinal reflexes in the white rat. Am J Physiol-Leg Content. 1936;

320. Humphrey G. The nature of learning in its relation to the living system. Oxford, England: Harcourt, Brace; 1933. 296 p.

321. Fantz RL. Visual experience in infants: Decreased attention to familiar patterns relative to novel ones. Science. 1964 Oct 30;146(3644):668–70.

322. Pinsker H, Kupfermann I, Castellucci V, Kandel E. Habituation and dishabituation of the gill-withdrawal reflex in aplysia. Science. 1970 Mar 27;167(3926):1740–2.

323. Harris JD. Habituatory response decrement in the intact organism. Psychol Bull. 1943;40:385–422.

324. Thorpe WH. Learning and instinct in animals. Cambridge, MA, US: Harvard University Press; 1956. viii, 493 p.

325. Glaser EM. The physiological basis of habituation. Lond Oxf Univ Press. 1966;

326. Sharpless S, Jasper H. Habituation of the arousal reaction. Brain. 1956 Dec 1;79(4):655–80.

327. Rankin CH, Abrams T, Barry RJ, Bhatnagar S, Clayton DF, Colombo J, et al. Habituation revisited: An updated and revised description of the behavioral characteristics of habituation. Neurobiol Learn Mem. 2009 Sep 1;92(2):135–8.

328. Schoenen J. Deficient habituation of evoked cortical potentials in migraine: A link between brain biology, behavior and trigeminovascular activation? Biomed Pharmacother Biomedecine Pharmacother. 1996;50(2):71–8.

329. Thompson RF, Spencer WA. Habituation: A model phenomenon for the study of neuronal substrates of behavior. Psychol Rev. 1966;73:16–43.

330. Groves PM, Thompson RF. Habituation: A dual-process theory. Psychol Rev. 1970;77:419–50.

331. Thompson RF. Habituation: A history. Neurobiol Learn Mem. 2009 Sep;92(2):127–34.

332. Groves PM, Lee D, Thompson RF. Effects of stimulus frequency and intensity on habituation and sensitization in acute spinal cat. Physiol Behav. 1969 May 1;4(3):383–8.

333. Solomon RL, Corbit JD. An opponent-process theory of motivation: I. Temporal dynamics of affect. Psychol Rev. 1974;81:119–45.

334. Solomon RL. The opponent-process theory of acquired motivation. 1980;

335. Starr MD. An opponent-process theory of motivation: VI. Time and intensity variables in the development of separation-induced distress calling in ducklings. J Exp Psychol Anim Behav Process. 1978;4:338–55.

336. Sokolov EN. Higher nervous functions; the orienting reflex. Annu Rev Physiol. 1963;25:545–80.

337. Konorski J. Integrative activity of the brain: An interdisciplinary approach. In: Learning, perception, and the brain. Chicago: University of Chicago Press; 1967.

338. Wagner A. Habituation and memory. In: Mechanisms of learning and motivation: A memorial volume for Jerry Konorski. Hillsdale, NJ: Lawrence Earlbaum Assoc.; 1979. p. 53–82.

339. Kirvelis D, Vanagas V. E. N. Sokolov's neural model of stimuli as neuro-cybernetic approach to anticipatory perception. 2014.

340. Barry RJ. Habituation of the orienting reflex and the development of Preliminary Process Theory. Neurobiol Learn Mem. 2009 Sep 1;92(2):235–42.

341. Schoenen J, Wang W, Albert A, Delwaide PJ. Potentiation instead of habituation characterizes visual evoked potentials in migraine patients between attacks. Eur J Neurol. 1995 Apr;2(2):115–22.

342. Odom JV, Bach M, Barber C, Brigell M, Marmor MF, Tormene AP, et al. Visual evoked potentials standard (2004). Doc Ophthalmol Adv Ophthalmol. 2004;108(2):115–23.

343. Asheri B, Haratian A, Mohamadi M, Asadi F, Yasini P, Zarepak N, et al. Enhancing detection of steady-state visual evoked potentials using frequency and harmonics of that frequency in OpenVibe. Biomed Eng Adv. 2021 Dec 1;2:100022.

344. Shibata K, Yamane K, Iwata M, Ohkawa S. Evaluating the effects of spatial frequency on migraines by using pattern-reversal visual evoked potentials. Clin Neurophysiol. 2005 Sep 1;116(9):2220–7.

345. Algin Dİ, Erdinç OO. Impaired visual habituation in idiopathic generalized epilepsy with photosensitivity patients. Arch Neuropsychiatry. 2018 Apr 20;57(2):108–12.

346. Brazzo D, Di Lorenzo G, Bill P, Fasce M, Papalia G, Veggiotti P, et al. Abnormal visual habituation in pediatric photosensitive epilepsy. Clin Neurophysiol Off J Int Fed Clin Neurophysiol. 2011 Jan;122(1):16–20.

347. Coppola G, Di Lorenzo C, Schoenen J, Pierelli F. Habituation and sensitization in primary headaches. J Headache Pain. 2013;14(1):65.

348. Sand T, Kvaløy MB, Wader T, Hovdal H. Evoked potential tests in clinical diagnosis. Tidsskr Den Nor Legeforening. 2013 May 7;

349. Lee SJ, Jeon J, Park Y, Lee JS. A comparative study of pattern visual evoked potentials between amblyopia, optic atrophy. Ann Optom Contact Lens. 2015 Jan 1;14(4):194–8.

350. Rinne T, Särkkä A, Degerman A, Schröger E, Alho K. Two separate mechanisms underlie auditory change detection and involuntary control of attention. Brain Res. 2006 Mar 10;1077(1):135–43.

351. Näätänen R, Alho K. Mismatch negativity – The measure for central sound representation accuracy. Audiol Neurotol. 1997;2(5):341–53.

352. Näätänen R. The mismatch negativity: A powerful tool for cognitive neuroscience. Ear Hear. 1995 Feb;16(1):6.

353.   Fuentemilla L, Marco-Pallarés J, Grau C. Modulation of spectral power and of phase resetting of EEG contributes differentially to the generation of auditory event-related potentials. NeuroImage. 2006 Apr 15;30(3):909–16.

354.   Styles EA. The psychology of attention. 2nd ed. Psychology Press; 2006.

355.   Shiffrin RM. Attention. In: Stevens' handbook of experimental psychology: Perception and motivation; Learning and cognition, Vols 1-2, 2nd ed. Oxford, England: John Wiley & Sons; 1988. p. 739–811.

356.   Johnson A, Proctor RW. Attention: Theory and practice. SAGE Publications, Inc.; 2004.

357.   Broadbent DE. Immediate memory and the shifting of attention. In: Perception and communication. Elmsford, NY, US: Pergamon Press; 1958. p. 210–43.

358.   Jackson D, Cottrell G. Attention and U-shaped learning in the acquisition of the past tense. 1999 Apr 17;

359.   Treisman AnneM. Selective attention in man. Br Med Bull. 1964 Jan;20(1):12–6.

360.   Cherry EC. Some experiments on the recognition of speech, with one and with two ears. J Acoust Soc Am. 1953 Sep;25(5):975–9.

361.   Moray N. Attention in dichotic listening: Affective cues and the influence of instructions. Q J Exp Psychol. 1959 Feb 1;11(1):56–60.

362.   Erlbeck H, Kübler A, Kotchoubey B, Veser S. Task instructions modulate the attentional mode affecting the auditory MMN and the semantic N400. Front Hum Neurosci. 2014;8.

363.   Chun MM. Contextual cueing of visual attention. Trends Cogn Sci. 2000 May;4(5):170–8.

364.   Chun MM, Jiang Y. Contextual cueing: Implicit learning and memory of visual context guides spatial attention. Cognit Psychol. 1998 Jun;36(1):28–71.

365.   Tris Atmaja B. The mechanism on how auditory system solves the cocktail party problem. 2019.

366.   Deutsch JA, Deutsch D. Attention: Some theoretical considerations. Psychol Rev. 1963;70:80–90.

367.   Carrasco M. Visual attention: The past 25 years. Vision Res. 2011 Jul 1;51(13):1484–525.

368.   Clarke DD, Sokoloff L. Circulation and energy metabolism of the brain. Basic Neurochem Mol Cell Med Asp 6th Ed. 1999;

369.   Attwell D, Laughlin SB. An energy budget for signaling in the grey matter of the brain. J Cereb Blood Flow Metab Off J Int Soc Cereb Blood Flow Metab. 2001 Oct;21(10):1133–45.

370.   Lee K, Choo H. A critical review of selective attention: An interdisciplinary perspective. Artif Intell Rev - AIR. 2011 Jun 1;40.

371.   Allport A. Visual attention. In: Foundations of cognitive science. Cambridge, MA, US: The MIT Press; 1989. p. 631–82.

372.   Pashler H, editor. Attention. Hove, England: Psychology Press/Erlbaum (UK) Taylor & Francis; 1998. viii, 407 p. (Attention).

373.   Lavie N. Perceptual load as a necessary condition for selective attention. J Exp Psychol Hum Percept Perform. 1995 Jun;21(3):451–68.

374.   Lavie N. Distracted and confused? Selective attention under load. Trends Cogn Sci. 2005 Feb 1;9(2):75–82.

375.   Friedman D, Cycowicz YM, Gaeta H. The novelty P3: An event-related brain potential (ERP) sign of the brain's evaluation of novelty. Neurosci Biobehav Rev. 2001 Jun;25(4):355–73.

376.   Bradley MM. Natural selective attention: Orienting and emotion. Psychophysiology. 2009 Jan;46(1):1–11.

377.   Schomaker J, Meeter M. Short- and long-lasting consequences of novelty, deviance and surprise on brain and cognition. Neurosci Biobehav Rev. 2015 Aug;55:268–79.

378.   Goschke T. Voluntary action and cognitive control from a cognitive neuroscience perspective. In: Voluntary action: Brains, minds, and sociality. New York, NY, US: Oxford University Press; 2003. p. 49–85.

379.   Marco-Pallarés J, Nager W, Krämer UM, Cunillera T, Càmara E, Cucurell D, et al. Neurophysiological markers of novelty processing are modulated by COMT and DRD4 genotypes. NeuroImage. 2010 Nov 15;53(3):962–9.

380.   Corbetta M, Patel G, Shulman GL. The reorienting system of the human brain: From environment to theory of mind. Neuron. 2008 May 8;58(3):306–24.

381.   Barcelo F, Escera C, Corral MJ, Periáñez JA. Task switching and novelty processing activate a common neural network for cognitive control. J Cogn Neurosci. 2006 Oct;18(10):1734–48.

382.   Barceló F, Periáñez JA, Knight RT. Think differently: A brain orienting response to task novelty. Neuroreport. 2002 Oct 28;13(15):1887–92.

383.   Yantis S, Jonides J. Abrupt visual onsets and selective attention: Evidence from visual search. J Exp Psychol Hum Percept Perform. 1984;10:601–21.

384.   Theeuwes J. Exogenous and endogenous control of attention: The effect of visual onsets and offsets. Percept Psychophys. 1991 Jan 1;49(1):83–90.

385.   Egeth H, Yantis S. Visual attention: Control, representation, and time course. Annu Rev Psychol. 1997 Feb 1;48:269–97.

386.   Wolfe JM, Horowitz TS. What attributes guide the deployment of visual attention and how do they do it? Nat Rev Neurosci. 2004 Jun;5(6):495–501.

387.   Chica AB, Bartolomeo P, Lupiáñez J. Two cognitive and neural systems for endogenous and exogenous spatial attention. Behav Brain Res. 2013 Jan 15;237:107–23.

388.   Posner MI. Orienting of attention. Q J Exp Psychol. 1980 Feb;32(1):3–25.

389.   Coull J, Nobre A. Dissociating explicit timing from temporal expectation with fMRI. Curr Opin Neurobiol. 2008 Apr 1;18(2):137–44.

390.   Doherty JR, Rao A, Mesulam MM, Nobre AC. Synergistic effect of combined temporal and spatial expectations on visual attention. J Neurosci. 2005 Sep 7;25(36):8259–66.

391.   O'Reilly JX, McCarthy KJ, Capizzi M, Nobre AC. Acquisition of the temporal and ordinal structure of movement sequences in incidental learning. J Neurophysiol. 2008 May;99(5):2731–5.

392.   Müller HJ, Rabbitt PM. Reflexive and voluntary orienting of visual attention: Time course of activation and resistance to interruption. J Exp Psychol Hum Percept Perform. 1989;15:315–30.

393.   Carrasco M. Spatial covert attention: Perceptual modulation. In: The Oxford handbook of attention. New York, NY, US: Oxford University Press; 2014. p. 183–230. (Oxford library of psychology).

394.   Carretié L. Exogenous (automatic) attention to emotional stimuli: A review. Cogn Affect Behav Neurosci. 2014 Dec;14(4):1228–58.

395.   Katsuki F, Constantinidis C. Bottom-up and top-down attention: Different processes and overlapping neural systems. The Neuroscientist. 2014 Oct 1;20(5):509–21.

396.   Rohenkohl G, Coull JT, Nobre AC. Behavioural dissociation between exogenous and endogenous temporal orienting of attention. PloS One. 2011 Jan 28;6(1):e14620.

397.   Kiehl KA, Laurens KR, Duty TL, Forster BB, Liddle PF. Neural sources involved in auditory target detection and novelty processing: An event-related fMRI study. Psychophysiology. 2001 Jan;38(1):133–42.

398.   Berger A, Henik A, Rafal R. Competition between endogenous and exogenous orienting of visual attention. J Exp Psychol Gen. 2005 May;134(2):207–21.

399.   Theeuwes J. Top-down search strategies cannot override attentional capture. Psychon Bull Rev. 2004 Feb 1;11(1):65–70.

400.   Theeuwes J. Perceptual selectivity for color and form. Percept Psychophys. 1992 Nov 1;51(6):599–606.

401.   Desimone R, Duncan J. Neural mechanisms of selective visual attention. Annu Rev Neurosci. 1995;18:193–222.

402.   Corbetta M, Shulman GL. Control of goal-directed and stimulus-driven attention in the brain. Nat Rev Neurosci. 2002 Mar;3(3):201–15.

403.   Corbetta M, Kincade JM, Ollinger JM, McAvoy MP, Shulman GL. Voluntary orienting is dissociated from target detection in human posterior parietal cortex. Nat Neurosci. 2000 Mar;3(3):292–7.

404.   Shulman GL, Astafiev SV, Franke D, Pope DLW, Snyder AZ, McAvoy MP, et al. Interaction of stimulus-driven reorienting and expectation in ventral and dorsal frontoparietal and basal ganglia-cortical networks. J Neurosci Off J Soc Neurosci. 2009 Apr 8;29(14):4392–407.

405.   Awh E, Belopolsky AV, Theeuwes J. Top-down versus bottom-up attentional control: A failed theoretical dichotomy. Trends Cogn Sci. 2012 Aug 1;16(8):437–43.

406.   Vuilleumier P. How brains beware: Neural mechanisms of emotional attention. Trends Cogn Sci. 2005 Dec 1;9(12):585–94.

407.   Anderson BA, Laurent PA, Yantis S. Learned value magnifies salience-based attentional capture. PloS One. 2011;6(11):e27926.

408.   Jigo M, Heeger DJ, Carrasco M. An image-computable model of how endogenous and exogenous attention differentially alter visual perception. Proc Natl Acad Sci U S A. 2021 Aug 17;118(33):e2106436118.

409.   Fernández A, Okun S, Carrasco M. Differential effects of endogenous and exogenous attention on sensory tuning. J Neurosci Off J Soc Neurosci. 2022 Feb 16;42(7):1316–27.

410.   Beck DM, Kastner S. Top-down and bottom-up mechanisms in biasing competition in the human brain. Vision Res. 2009 Jun;49(10):1154–65.

411.   McMains S, Kastner S. Interactions of top-down and bottom-up mechanisms in human visual cortex. J Neurosci. 2011 Jan 12;31(2):587–97.

412.   Folk CL, Remington RW, Johnston JC. Involuntary covert orienting is contingent on attentional control settings. J Exp Psychol Hum Percept Perform. 1992 Nov;18(4):1030–44.

413.   Ogawa T, Komatsu H. Neuronal dynamics of bottom-up and top-down processes in area V4 of macaque monkeys performing a visual search. Exp Brain Res. 2006 Aug;173(1):1–13.

414.   Frintrop S, Rome E, Christensen HI. Computational visual attention systems and their cognitive foundations: A survey. ACM Trans Appl Percept. 2010;7(1):1–46.

415.   Hoffman JE, Subramaniam B. The role of visual attention in saccadic eye movements. Percept Psychophys. 1995 Jan 1;57(6):787–95.

416.   Spong P, Haider M, Lindsley DB. Selective attentiveness and cortical evoked responses to visual and auditory stimuli. Science. 1965 Apr 16;148(3668):395–7.

417.   Eason RG, Harter MR, White CT. Effects of attention and arousal on visually evoked cortical potentials and reaction time in man. Physiol Behav. 1969 May 1;4(3):283–9.

418.   Van Voorhis S, Hillyard SA. Visual evoked potentials and selective attention to points in space. Percept Psychophys. 1977 Jan 1;22(1):54–62.

419.   Mangun GR, Hillyard SA, Luck SJ. Electrocortical substrates of visual selective attention. In: Attention and performance 14: Synergies in experimental psychology, artificial intelligence, and cognitive neuroscience. Cambridge, MA, US: The MIT Press; 1993. p. 219–43.

420.   Hillyard SA, Anllo-Vento L. Event-related brain potentials in the study of visual selective attention. Proc Natl Acad Sci. 1998 Feb 3;95(3):781–7.

421.   Martínez A, Anllo-Vento L, Sereno MI, Frank LR, Buxton RB, Dubowitz DJ, et al. Involvement of striate and extrastriate visual cortical areas in spatial attention. Nat Neurosci. 1999 Apr;2(4):364–9.

422.   Di Russo F, Martínez A, Hillyard SA. Source analysis of event-related cortical activity during visuo-spatial attention. Cereb Cortex. 2003 May 1;13(5):486–99.

423.   Baumgartner HM, Graulty CJ, Hillyard SA, Pitts MA. Does spatial attention modulate the C1 component? The jury continues to deliberate. Cogn Neurosci. 2018;9(1–2):34–7.

424.   Fu S, Fedota JR, Greenwood PM, Parasuraman R. Dissociation of visual C1 and P1 components as a function of attentional load: An event-related potential study. Biol Psychol. 2010 Sep 1;85(1):171–8.

425.   Kelly SP, Gomez-Ramirez M, Foxe JJ. Spatial attention modulates initial afferent activity in human primary visual cortex. Cereb Cortex N Y N 1991. 2008 Nov;18(11):2629–36.

426.   Rauss KS, Pourtois G, Vuilleumier P, Schwartz S. Attentional load modifies early activity in human primary visual cortex. Hum Brain Mapp. 2009;30(5):1723–33.

427.   Luck SJ, Heinze HJ, Mangun GR, Hillyard SA. Visual event-related potentials index focused attention within bilateral stimulus arrays. II. Functional dissociation of P1 and N1 components. Electroencephalogr Clin Neurophysiol. 1990 Jun 1;75(6):528–42.

428.   Luck SJ, Hillyard SA. Electrophysiological correlates of feature analysis during visual search. Psychophysiology. 1994 May;31(3):291–308.

429.   Picton TW, Stapells DR, Campbell KB. Auditory evoked potentials from the human cochlea and brainstem. J Otolaryngol Suppl. 1981 Aug 1;9:1–41.

430.   Hackley SA, Woldorff M, Hillyard SA. Cross-modal selective attention effects on retinal, myogenic, brainstem, and cerebral evoked potentials. Psychophysiology. 1990;27(2):195–208.

431.   Pratt H, Starr A, Michalewski HJ, Bleich N, Mittelman N. The auditory P50 component to onset and offset of sound. Clin Neurophysiol. 2008 Feb 1;119(2):376–87.

432.   Lukas JH. Human auditory attention: The olivocochlear bundle may function as a peripheral filter. Psychophysiology. 1980;17(5):444–52.

433.   Lehmann A, Schönwiesner M. Selective attention modulates human auditory brainstem responses: Relative contributions of frequency and spatial cues. PLOS ONE. 2014 ene;9(1):e85442.

434.   McCallum WC, Curry SH, Pocock PV, Papakostopoulos D. Brain event-related potentials as indicators of early selective processes in auditory target localization. Psychophysiology. 1983;20(1):1–17.

435.   Woldorff M, Hansen JC, Hillyard SA. Evidence for effects of selective attention in the mid-latency range of the human auditory event-related potential. Electroencephalogr Clin Neurophysiol Suppl. 1987;40:146–54.

436.   Hillyard SA, Hink RF, Schwent VL, Picton TW. Electrical signs of selective attention in the human brain. Science. 1973 Oct 12;182(4108):177–80.

437.   Näätänen R. Selective attention and evoked potentials inhumans - A critical review. Biol Psychol. 1975 May 1;2(4):237–307.

438.   Hansen JC, Hillyard SA. Endogeneous brain potentials associated with selective auditory attention. Electroencephalogr Clin Neurophysiol. 1980 Aug 1;49(3):277–90.

439.   Näätänen R, Gaillard AWK. The orienting reflex and the N2 deflection of the event-related potential (ERP). In: Gaillard AWK, Ritter W, editors. Advances in psychology. North-Holland; 1983. p. 119–41. (Tutorials in event related potential research: Endogenous components; vol. 10).

440.   Näätänen R. Processing negativity: An evoked-potential reflection. Psychol Bull. 1982;92:605–40.

441.   Isreal JB, Wickens CD, Chesney GL, Donchin E. The event-related brain potential as an index of display-monitoring workload. Hum Factors. 1980 Apr 1;22(2):211–24.

442.   Kramer AF, Wickens CD, Donchin E. An analysis of the processing requirements of a complex perceptual-motor task. Hum Factors. 1983 Dec;25(6):597–621.

443.   Knight RT, Scabini D, Woods DL, Clayworth CC. Contributions of temporal-parietal junction to the human auditory P3. Brain Res. 1989 Nov 13;502(1):109–16.

444.   Schröger E, Giard MH, Wolff C. Auditory distraction: Event-related potential and behavioral indices. Clin Neurophysiol Off J Int Fed Clin Neurophysiol. 2000 Aug;111(8):1450–60.

445.   Woldorff MG, Hillyard SA. Modulation of early auditory processing during selective listening to rapidly presented tones. Electroencephalogr Clin Neurophysiol. 1991 Sep;79(3):170–91.

446.   Köster M, Gruber T. Rhythms of human attention and memory: An embedded process perspective. Front Hum Neurosci. 2022;16 (2022).

447.   VanRullen R, Carlson T, Cavanagh P. The blinking spotlight of attention. Proc Natl Acad Sci U S A. 2007 Dec 4;104(49):19204–9.

448.   Armstrong KM, Chang MH, Moore T. Selection and maintenance of spatial information by frontal eye field neurons. J Neurosci. 2009 Dec 16;29(50):15621–9.

449.   Ibos G, Duhamel JR, Hamed SB. A functional hierarchy within the parietofrontal network in stimulus selection and attention control. J Neurosci. 2013 May 8;33(19):8359–69.

450.   Palva S, Palva JM. New vistas for α-frequency band oscillations. Trends Neurosci. 2007 Apr 1;30(4):150–8.

451.   Jensen O, Mazaheri A. Shaping functional architecture by oscillatory alpha activity: Gating by inhibition. Front Hum Neurosci. 2010;4.

452.   Lakatos P, Karmos G, Mehta AD, Ulbert I, Schroeder CE. Entrainment of neuronal oscillations as a mechanism of attentional selection. Science. 2008 Apr 4;320(5872):110–3.

453.   Friese U, Daume J, Göschl F, König P, Wang P, Engel AK. Oscillatory brain activity during multisensory attention reflects activation, disinhibition, and cognitive control. Sci Rep. 2016 Sep 8;6(1):32775.

454.   Banerjee S, Snyder AC, Molholm S, Foxe JJ. Oscillatory alpha-band mechanisms and the deployment of spatial attention to anticipated auditory and visual target locations: Supramodal or sensory-specific control mechanisms? J Neurosci. 2011 Jul 6;31(27):9923–32.

455.   Ahveninen J, Huang S, Belliveau JW, Chang WT, Hämäläinen M. Dynamic oscillatory processes governing cued orienting and allocation of auditory attention. J Cogn Neurosci. 2013 Nov;25(11):1926–43.

456. Sauseng P, Klimesch W, Gerloff C, Hummel FC. Spontaneous locally restricted EEG alpha activity determines cortical excitability in the motor cortex. Neuropsychologia. 2009 Jan 1;47(1):284–8.

457. Busch NA, VanRullen R. Spontaneous EEG oscillations reveal periodic sampling of visual attention. Proc Natl Acad Sci U S A. 2010 Sep 14;107(37):16048–53.

458. Händel BF, Haarmeier T, Jensen O. Alpha oscillations correlate with the successful inhibition of unattended stimuli. J Cogn Neurosci. 2011 Sep 1;23(9):2494–502.

459. Kelly SP, Lalor EC, Reilly RB, Foxe JJ. Increases in alpha oscillatory power reflect an active retinotopic mechanism for distractor suppression during sustained visuospatial attention. J Neurophysiol. 2006 Jun;95(6):3844–51.

460. Rihs TA, Michel CM, Thut G. Mechanisms of selective inhibition in visual spatial attention are indexed by α-band EEG synchronization. Eur J Neurosci. 2007;25(2):603–10.

461. Worden MS, Foxe JJ, Wang N, Simpson GV. Anticipatory biasing of visuospatial attention indexed by retinotopically specific alpha-band electroencephalography increases over occipital cortex. J Neurosci Off J Soc Neurosci. 2000 Mar 15;20(6):RC63.

462. Yamagishi N, Callan DE, Goda N, Anderson SJ, Yoshida Y, Kawato M. Attentional modulation of oscillatory activity in human visual cortex. NeuroImage. 2003 Sep 1;20(1):98–113.

463. Frey JN, Ruhnau P, Weisz N. Not so different after all: The same oscillatory processes support different types of attention. Brain Res. 2015 Nov 11;1626:183–97.

464. Peylo C, Hilla Y, Sauseng P. Cause or consequence? Alpha oscillations in visuospatial attention. Trends Neurosci. 2021 Sep 1;44(9):705–13.

465. van Diepen RM, Cohen MX, Denys D, Mazaheri A. Attention and temporal expectations modulate power, not phase, of ongoing alpha oscillations. J Cogn Neurosci. 2015 Mar 16;27(8):1573–86.

466. Hanslmayr S, Sauseng P, Doppelmayr M, Schabus M, Klimesch W. Increasing individual upper alpha power by neurofeedback improves cognitive performance in human subjects. Appl Psychophysiol Biofeedback. 2005 Mar 1;30(1):1–10.

467. Fontolan L, Morillon B, Liegeois-Chauvel C, Giraud AL. The contribution of frequency-specific activity to hierarchical information processing in the human auditory cortex. Nat Commun. 2014 Sep 2;5(1):4694.

468. Bastos AM, Litvak V, Moran R, Bosman CA, Fries P, Friston KJ. A DCM study of spectral asymmetries in feedforward and feedback connections between visual areas V1 and V4 in the monkey. NeuroImage. 2015 Mar 1;108:460–75.

469. Clayton MS, Yeung N, Cohen Kadosh R. The roles of cortical oscillations in sustained attention. Trends Cogn Sci. 2015 Apr 1;19(4):188–95.

470. Lisman J. Working memory: The importance of theta and gamma oscillations. Curr Biol. 2010 Jun 8;20(11):R490–2.

471. Fries P. Rhythms for cognition: Communication through coherence. Neuron. 2015 Oct 7;88(1):220–35.

472. VanRullen R. Perceptual cycles. Trends Cogn Sci. 2016 Oct 1;20(10):723–35.

473. Fiebelkorn IC, Kastner S. A rhythmic theory of attention. Trends Cogn Sci. 2019 Feb 1;23(2):87–101.

474.   Karakaş S, Başar E. Models and theories of brain function in cognition within a framework of behavioral cognitive psychology. Int J Psychophysiol Off J Int Organ Psychophysiol. 2006 May;60(2):186–93.

475.   Gaillard C, Ben Hadj Hassen S, Di Bello F, Bihan-Poudec Y, VanRullen R, Ben Hamed S. Prefrontal attentional saccades explore space rhythmically. Nat Commun. 2020 Feb 17;11(1):925.

476.   Helfrich RF, Breska A, Knight RT. Neural entrainment and network resonance in support of top-down guided attention. Curr Opin Psychol. 2019 Oct 1;29:82–9.

477.   Bauer EA, Wilson KA, MacNamara A. Cognitive and affective psychophysiology. In: Asmundson GJG, editor. Comprehensive clinical psychology. 2nd ed. Oxford: Elsevier; 2022. p. 49–61.

478.   Llinás RR. Intrinsic electrical properties of mammalian neurons and CNS function: A historical perspective. Front Cell Neurosci. 2014;8.

479.   Van Quyen ML, Botella-Soler V, Valderrama M. Neuronal oscillations scale up and scale down brain dynamics. In: Multiscale analysis and nonlinear dynamics. John Wiley & Sons, Ltd; 2013. p. 205–16.

480.   Hahn G, Ponce-Alvarez A, Deco G, Aertsen A, Kumar A. Portraits of communication in neuronal networks. Nat Rev Neurosci. 2019 Feb;20(2):117–27.

481.   Chapeton JI, Haque R, Wittig JH, Inati SK, Zaghloul KA. Large-scale communication in the human brain is rhythmically modulated through alpha coherence. Curr Biol. 2019 Sep 9;29(17):2801-2811.e5.

482.   Obleser J, Kayser C. Neural entrainment and attentional selection in the listening brain. Trends Cogn Sci. 2019 Nov 1;23(11):913–26.

483.   Lakatos P, Schroeder CE, Leitman DI, Javitt DC. Predictive suppression of cortical excitability and its deficit in schizophrenia. J Neurosci. 2013 Jul 10;33(28):11692–702.

484.   Kizuk SAD, Mathewson KE. Power and phase of alpha oscillations reveal an interaction between spatial and temporal visual attention. J Cogn Neurosci. 2017 Mar;29(3):480–94.

485.   Stefanics G, Hangya B, Hernádi I, Winkler I, Lakatos P, Ulbert I. Phase entrainment of human delta oscillations can mediate the effects of expectation on reaction speed. J Neurosci. 2010 Oct 13;30(41):13578–85.

486.   Schroeder CE, Lakatos P. Low-frequency neuronal oscillations as instruments of sensory selection. Trends Neurosci. 2009 Jan;32(1).

487.   Henry MJ, Obleser J. Frequency modulation entrains slow neural oscillations and optimizes human listening behavior. Proc Natl Acad Sci. 2012 Dec 4;109(49):20095–100.

488.   Mathewson KE, Fabiani M, Gratton G, Beck DM, Lleras A. Rescuing stimuli from invisibility: Inducing a momentary release from visual masking with pre-target entrainment. Cognition. 2010 Apr;115(1):186–91.

489.   Henry MJ, Herrmann B, Obleser J. Entrained neural oscillations in multiple frequency bands comodulate behavior. Proc Natl Acad Sci. 2014 Oct 14;111(41):14935–40.

490.   Lakatos P, O'Connell MN, Barczak A, Mills A, Javitt DC, Schroeder CE. The leading sense: Supramodal control of neurophysiological context by attention. Neuron. 2009 Nov 12;64(3):419–30.

491.   Thut G, Schyns P, Gross J. Entrainment of perceptually relevant brain oscillations by non-invasive rhythmic stimulation of the human brain. Front Psychol. 2011;2.

492.   Obleser J, Henry MJ, Lakatos P. What do we talk about when we talk about rhythm? PLOS Biol. 2017 Sep 19;15(9):e2002794.

493.   Lakatos P, Gross J, Thut G. A new unifying account of the roles of neuronal entrainment. Curr Biol. 2019 Sep 23;29(18):R890–905.

494.   Capilla A, Pazo-Alvarez P, Darriba A, Campo P, Gross J. Steady-state visual evoked potentials can be explained by temporal superposition of transient event-related responses. PLOS ONE. 2011 ene;6(1):e14543.

495.   Keitel C, Quigley C, Ruhnau P. Stimulus-driven brain oscillations in the alpha range: Entrainment of intrinsic rhythms or frequency-following response? J Neurosci. 2014 Jul 30;34(31):10137–40.

496.   Vetri L, Maniscalco L, Diana P, Guidotti M, Matranga D, Bonnet-Brilhault F, et al. A preliminary study on photic driving in the electroencephalogram of children with autism across a wide cognitive and behavioral range. J Clin Med. 2022 Jan;11(13):3568.

497.   von Gizycki H, Jean-Louis G, Snyder M, Zizi F, Green H, Giuliano V, et al. The effects of photic driving on mood states. J Psychosom Res. 1998 May;44(5):599–604.

498.   Coull BM, Pedley TA. Intermittent photic stimulation. Clinical usefulness of non-convulsive responses. Electroencephalogr Clin Neurophysiol. 1978 Mar;44(3):353–63.

499.   Politoff AL, Monson N, Hass P, Stadter R. Decreased alpha bandwidth responsiveness to photic driving in Alzheimer disease. Electroencephalogr Clin Neurophysiol. 1992 Jan;82(1):45–52.

500.   Erkinjuntti T, Larsen T, Sulkava R, Ketonen L, Laaksonen R, Palo J. EEG in the differential diagnosis between Alzheimer's disease and vascular dementia. Acta Neurol Scand. 1988 Jan;77(1):36–43.

501.   Simon RH, Zimmerman AW, Sanderson P, Tasman A. EEG markers of migraine in children and adults. Headache. 1983 Sep;23(5):201–5.

502.   Gronseth GS, Greenberg MK. The utility of the electroencephalogram in the evaluation of patients presenting with headache: A review of the literature. Neurology. 1995 Jul;45(7):1263–7.

503.   de Tommaso M, Sciruicchio V, Bellotti R, Guido M, Sasanelli G, Specchio LM, et al. Photic driving response in primary headache: Diagnostic value tested by discriminant analysis and artificial neural network classifiers. Ital J Neurol Sci. 1999 Feb;20(1):23–8.

504.   Calderone DJ, Lakatos P, Butler PD, Castellanos FX. Entrainment of neural oscillations as a modifiable substrate of attention. Trends Cogn Sci. 2014 Jun 1;18(6):300–9.

505.   Jin Y, Potkin SG, Rice D, Sramek J, Costa J, Isenhart R, et al. Abnormal EEG responses to photic stimulation in schizophrenic patients. Schizophr Bull. 1990;16(4):627–34.

506.   Fisher RS, Harding G, Erba G, Barkley GL, Wilkins A, Epilepsy Foundation of America Working Group. Photic- and pattern-induced seizures: A review for the Epilepsy Foundation of America Working Group. Epilepsia. 2005 Sep;46(9):1426–41.

507.   Lazarev VV, Simpson DM, Schubsky BM, Deazevedo LC. Photic driving in the electroencephalogram of children and adolescents: Harmonic structure and relation to the resting state. Braz J Med Biol Res Rev Bras Pesqui Medicas E Biol. 2001 Dec;34(12):1573–84.

508.   Walter VJ, Walter WG. The central effects of rhythmic sensory stimulation. Electroencephalogr Clin Neurophysiol. 1949 Jan 1;1(1):57–86.

509.   Morse DR. Brain wave synchronizers: A review of their stress reduction effects and clinical studies assessed by questionnaire, galvanic skin resistance, pulse rate, saliva, and electroencephalograph. Stress Med. 1993;9:111–26.

510.   Guo Y, Bufacchi RJ, Novembre G, Kilintari M, Moayedi M, Hu L, et al. Ultralow-frequency neural entrainment to pain. PLoS Biol. 2020 Apr;18(4):e3000491.

511.   Thaut MH, McIntosh GC, Hoemberg V. Neurobiological foundations of neurologic music therapy: Rhythmic entrainment and the motor system. Front Psychol. 2015;5.

512.   Fox PT, Raichle ME. Stimulus rate dependence of regional cerebral blood flow in human striate cortex, demonstrated by positron emission tomography. J Neurophysiol. 1984 May;51(5):1109–20.

513.   Takashima R, Tanaka H, Kimoto K, Watanabe Y, Hirata K. The photic driving response in electroencephalogram in migraine patients. In: 2012 ICME International Conference on Complex Medical Engineering (CME). 2012. p. 312–5.

514.   Mathewson KE, Prudhomme C, Fabiani M, Beck DM, Lleras A, Gratton G. Making waves in the stream of consciousness: Entraining oscillations in EEG alpha and fluctuations in visual awareness with rhythmic visual stimulation. J Cogn Neurosci. 2012 Dec;24(12):2321–33.

515.   Cravo AM, Rohenkohl G, Wyart V, Nobre AC. Temporal expectation enhances contrast sensitivity by phase entrainment of low-frequency oscillations in visual cortex. J Neurosci Off J Soc Neurosci. 2013 Feb 27;33(9):4002–10.

516.   Jaegle A, Ro T. Direct control of visual perception with phase-specific modulation of posterior parietal cortex. J Cogn Neurosci. 2014 Feb 1;26(2):422–32.

517.   Neuling T, Rach S, Wagner S, Wolters CH, Herrmann CS. Good vibrations: Oscillatory phase shapes perception. NeuroImage. 2012 Nov 1;63(2):771–8.

518.   Ng BSW, Schroeder T, Kayser C. A precluding but not ensuring role of entrained low-frequency oscillations for auditory perception. J Neurosci. 2012 Aug 29;32(35):12268–76.

519.   Kostka JK, Hanganu-Opatz IL. Olfactory-driven beta band entrainment of limbic circuitry during neonatal development. Neuroscience; 2021 Oct.

520.   Haegens S, Nácher V, Luna R, Romo R, Jensen O. α-Oscillations in the monkey sensorimotor network influence discrimination performance by rhythmical inhibition of neuronal spiking. Proc Natl Acad Sci U S A. 2011 Nov 29;108(48):19377–82.

521.   Wälti MJ, Bächinger M, Ruddy KL, Wenderoth N. Steady-state responses in the somatosensory system interact with endogenous beta activity. bioRxiv; 2019. p. 690495.

522.   Ross B, Dobri S, Jamali S, Bartel L. Entrainment of somatosensory beta and gamma oscillations accompany improvement in tactile acuity after periodic and aperiodic repetitive sensory stimulation. Int J Psychophysiol. 2022 Jul 1;177:11–26.

523.   Besle J, Schevon CA, Mehta AD, Lakatos P, Goodman RR, McKhann GM, et al. Tuning of the human neocortex to the temporal dynamics of attended events. J Neurosci. 2011 Mar 2;31(9):3176–85.

524.   Gomez-Ramirez M, Kelly SP, Molholm S, Sehatpour P, Schwartz TH, Foxe JJ. Oscillatory sensory selection mechanisms during intersensory attention to rhythmic auditory and visual inputs: A human electrocorticographic investigation. J Neurosci Off J Soc Neurosci. 2011 Dec 14;31(50):18556–67.

525.   Spaak E, de Lange FP, Jensen O. Local entrainment of α oscillations by visual stimuli causes cyclic modulation of perception. J Neurosci Off J Soc Neurosci. 2014 Mar 5;34(10):3536–44.

526.   Mo J, Schroeder CE, Ding M. Attentional modulation of alpha oscillations in macaque inferotemporal cortex. J Neurosci. 2011 Jan 19;31(3):878–82.

527.   Schroeder CE, Lakatos P, Kajikawa Y, Partan S, Puce A. Neuronal oscillations and visual amplification of speech. Trends Cogn Sci. 2008 Mar 1;12(3):106–13.

528.   Klimesch W. Alpha-band oscillations, attention, and controlled access to stored information. Trends Cogn Sci. 2012 Dec 1;16(12):606–17.

529.   Breska A, Deouell LY. Automatic bias of temporal expectations following temporally regular input independently of high-level temporal expectation. J Cogn Neurosci. 2014 Jul 1;26(7):1555–71.

530.   Large EW, Jones MR. The dynamics of attending: How people track time-varying events. Psychol Rev. 1999;106(1):119–59.

531.   Polich J, Corey-Bloom J. Alzheimer's disease and P300: Review and evaluation of task and modality. Curr Alzheimer Res. 2005 Dec;2(5):515–25.

532.   Broglio SP, Pontifex MB, O'Connor P, Hillman CH. The persistent effects of concussion on neuroelectric indices of attention. J Neurotrauma. 2009 Sep;26(9):1463–70.

533.   Javitt DC, Spencer KM, Thaker GK, Winterer G, Hajós M. Neurophysiological biomarkers for drug development in schizophrenia. Nat Rev Drug Discov. 2008 Jan;7(1):68–83.

534.   Vilà-Balló A, François C, Cucurell D, Miró J, Falip M, Juncadella M, et al. Auditory target and novelty processing in patients with unilateral hippocampal sclerosis: A current-source density study. Sci Rep. 2017 May 9;7(1):1612.

535.   Vanagaite J, Pareja JA, Støren O, White LR, Sand T, Stovner LJ. Light-induced discomfort and pain in migraine. Cephalalgia Int J Headache. 1997 Nov;17(7):733–41.

536.   Hay KM, Mortimer MJ, Barker DC, Debney LM, Good PA. 1044 women with migraine: The effect of environmental stimuli. Headache. 1994 Mar;34(3):166–8.

537.   Lévêque Y, Masson R, Fornoni L, Moulin A, Bidet-Caulet A, Caclin A, et al. Self-perceived attention difficulties are associated with sensory hypersensitivity in migraine. Rev Neurol (Paris). 2020 Dec;176(10):829–38.

538.   Friedman DI, De Ver Dye T. Migraine and the environment. Headache J Head Face Pain. 2009;49(6):941–52.

539.   Zanchin G, Dainese F, Trucco M, Mainardi F, Mampreso E, Maggioni F. Osmophobia in migraine and tension-type headache and its clinical features in patients with migraine. Cephalalgia. 2007 Sep 1;27(9):1061–8.

540.   Lipton RB, Bigal ME, Ashina S, Burstein R, Silberstein S, Reed ML, et al. Cutaneous allodynia in the migraine population. Ann Neurol. 2008 Feb;63(2):148–58.

541.   Bigal ME, Ashina S, Burstein R, Reed ML, Buse D, Serrano D, et al. Prevalence and characteristics of allodynia in headache sufferers: A population study. Neurology. 2008 Apr 22;70(17):1525–33.

542.   Kelman L. Osmophobia and taste abnormality in migraineurs: A tertiary care study. Headache J Head Face Pain. 2004;44(10):1019–23.

543.   Sjöstrand C, Savic I, Laudon-Meyer E, Hillert L, Lodin K, Waldenlind E. Migraine and olfactory stimuli. Curr Pain Headache Rep. 2010 Jun 1;14(3):244–51.

544.   Schwedt TJ. Multisensory integration in migraine. Curr Opin Neurol. 2013 Jun;26(3):248–53.

545.   Demarquay G, Mauguière F. Central nervous system underpinnings of sensory hypersensitivity in migraine: Insights from neuroimaging and electrophysiological studies. Headache. 2016 Oct;56(9):1418–38.

546.   Llop SM, Frandsen JE, Digre KB, Katz BJ, Crum AV, Zhang C, et al. Increased prevalence of depression and anxiety in patients with migraine and interictal photophobia. J Headache Pain. 2016 Apr 14;17(1):34.

547.	Drummond PD. A quantitative assessment of photophobia in migraine and tension headache. Headache. 1986 Oct;26(9):465–9.

548.	Harle DE, Shepherd AJ, Evans BJW. Visual stimuli are common triggers of migraine and are associated with pattern glare. Headache J Head Face Pain. 2006;46(9):1431–40.

549.	Marek V, Potey A, Réaux-Le-Goazigo A, Reboussin E, Charbonnier A, Villette T, et al. Blue light exposure in vitro causes toxicity to trigeminal neurons and glia through increased superoxide and hydrogen peroxide generation. Free Radic Biol Med. 2019 Feb 1;131:27–39.

550.	Noseda R, Bernstein CA, Nir RR, Lee AJ, Fulton AB, Bertisch SM, et al. Migraine photophobia originating in cone-driven retinal pathways. Brain. 2016 Jul 1;139(7):1971–86.

551.	Drummond PD. Photophobia and autonomic responses to facial pain in migraine. Brain. 1997 Oct 1;120(10):1857–64.

552.	Kowacs P, Piovesan E, Werneck L, Tatsui C, Lange M, Ribas L, et al. Influence of intense light stimulation on trigeminal and cervical pain perception thresholds. Cephalalgia. 2001 Apr 1;21(3):184–8.

553.	Drummond PD, Woodhouse A. Painful stimulation of the forehead increases photophobia in migraine sufferers. Cephalalgia. 1993;13(5):321–4.

554.	Fillmore EP, Seifert MF. Anatomy of the trigeminal nerve. In: Tubbs RS, Rizk E, Shoja MM, Loukas M, Barbaro N, Spinner RJ, editors. Nerves and nerve injuries. San Diego: Academic Press; 2015. p. 319–50.

555.	Antal A, Polania R, Saller K, Morawetz C, Schmidt-Samoa C, Baudewig J, et al. Differential activation of the middle-temporal complex to visual stimulation in migraineurs. Cephalalgia. 2011 Feb 1;31(3):338–45.

556.	Datta R, Aguirre GK, Hu S, Detre JA, Cucchiara B. Interictal cortical hyperresponsiveness in migraine is directly related to the presence of aura. Cephalalgia. 2013 Apr 1;33(6):365–74.

557.	Cucchiara B, Wolf RL, Nagae L, Zhang Q, Kasner S, Datta R, et al. Migraine with aura is associated with an incomplete circle of willis: Results of a prospective observational study. PloS One. 2013;8(7):e71007.

558.	Schwedt TJ, Chong CD. Functional imaging and migraine: New connections? Curr Opin Neurol. 2015 Jun;28(3):265.

559.	Schwedt TJ, Chiang CC, Chong CD, Dodick DW. Functional MRI of migraine. Lancet Neurol. 2015 Jan 1;14(1):81–91.

560.	Niemann H, Bonnefoy X, Braubach M, Hecht K, Maschke C, Rodrigues C, et al. Noise-induced annoyance and morbidity results from the pan-European LARES study. Noise Health. 2006 Jan 4;8(31):63.

561.	Vingen JV, Pareja JA, Støren O, White LR, Stovner LJ. Phonophobia in migraine. Cephalalgia Int J Headache. 1998 Jun;18(5):243–9.

562.	Williams ZJ, He JL, Cascio CJ, Woynaroski TG. A review of decreased sound tolerance in autism: Definitions, phenomenology, and potential mechanisms. Neurosci Biobehav Rev. 2021 Feb 1;121:1–17.

563.	Kingdom FAA, Prins N. Psychophysics. 2nd ed. Elsevier Academic Press; 2016.

564.	Kröner-Herwig B, Ruhmland M, Zintel W, Siniatchkin M. Are migraineurs hypersensitive? A test of the stimulus processing disorder hypothesis. Eur J Pain. 2005 Dec 1;9(6):661–71.

565.	Evans BJW, Stevenson SJ. The Pattern Glare Test: A review and determination of normative values. Ophthalmic Physiol Opt J Br Coll Ophthalmic Opt Optom. 2008 Jul;28(4):295–309.

566.   Khalil NM. Investigations of visual function in migraine by visual evoked potentials and visual psychophysical tests [Ph.D.]. Imperial College London (University of London); 1991.

567.   Brighina F, Cosentino G, Fierro B. Brain stimulation in migraine. In: Lozano AM, Hallett M, editors. Handbook of clinical neurology. Elsevier; 2013. p. 585–98. (Brain Stimulation; vol. 116).

568.   Leao AAP. Spreading depression of activity in the cerebral cortex. J Neurophysiol. 1944 Nov;7(6):359–90.

569.   Pietrobon D, Striessnig J. Neurobiology of migraine. Nat Rev Neurosci. 2003 May;4(5):386–98.

570.   Aurora S, Wilkinson F. The brain is hyperexcitable in migraine. Cephalalgia. 2007 Dec 1;27(12):1442–53.

571.   Marcus DA, Soso MJ. Migraine and stripe-induced visual discomfort. Arch Neurol. 1989 Oct;46(10):1129–32.

572.   Coleston DM, Kennard C. Visual changes in migraine: Indications of cortical dysfunction. Cephalalgia. 1993;13.

573.   Brighina F, Bolognini N, Cosentino G, Maccora S, Paladino P, Baschi R, et al. Visual cortex hyperexcitability in migraine in response to sound-induced flash illusions. Neurology. 2015 May 19;84(20):2057–61.

574.   Wilkins AJ. Visual Stress. OUP Oxford; 1995. 217 p.

575.   Fong CY, Law WHC, Braithwaite JJ, Mazaheri A. Differences in early and late pattern-onset visual-evoked potentials between self- reported migraineurs and controls. NeuroImage Clin. 2020 Jan 1;25:102122.

576.   Vecchia D, Pietrobon D. Migraine: A disorder of brain excitatory–inhibitory balance? Trends Neurosci. 2012 Aug 1;35(8):507–20.

577.   Ophoff RA, Terwindt GM, Vergouwe MN, van Eijk R, Oefner PJ, Hoffman SMG, et al. Familial hemiplegic migraine and episodic ataxia type-2 are caused by mutations in the Ca2+ channel gene CACNL1A4. Cell. 1996 Nov 1;87(3):543–52.

578.   Fusco MD, Marconi R, Silvestri L, Atorino L, Rampoldi L, Morgante L, et al. Haploinsufficiency of ATP1A2 encoding the Na+/K+ pump α2 subunit associated with familial hemiplegic migraine type 2. Nat Genet. 2003 Feb;33(2):192–6.

579.   Dichgans M, Freilinger T, Eckstein G, Babini E, Lorenz-Depiereux B, Biskup S, et al. Mutation in the neuronal voltage-gated sodium channel SCN1A in familial hemiplegic migraine. The Lancet. 2005 Jul 30;366(9483):371–7.

580.   Aurora Sk, Cao Y, Bowyer Sm, Welch K m. a. The occipital cortex is hyperexcitable in migraine: Experimental evidence. Headache J Head Face Pain. 1999;39(7):469–76.

581.   Mulleners WM, Chronicle EP, Palmer JE, Koehler PJ, Vredeveld JW. Suppression of perception in migraine: Evidence for reduced inhibition in the visual cortex. Neurology. 2001 Jan 23;56(2):178–83.

582.   Aurora S, Welch K, Al-Sayed F. The threshold for phosphenes is lower in migraine. Cephalalgia. 2003 May 1;23(4):258–63.

583.   Gerwig M, Niehaus L, Kastrup O, Stude P, Diener HC. Visual cortex excitability in migraine evaluated by single and paired magnetic stimuli. Headache J Head Face Pain. 2005;45(10):1394–9.

584.   Gunaydin S, Soysal A, Atay T, Arpaci B. Motor and occipital cortex excitability in migraine patients. Can J Neurol Sci. 2006 Feb;33(1):63–7.

585. Afra P, Jouny CC, Bergey GK. Duration of complex partial seizures: An intracranial EEG study. Epilepsia. 2008;49(4):677–84.

586. Bohotin V, Fumai A, Vandenheede M, Bohotin C, Schoenen J. Excitability of visual V1-V2 and motor cortices to single transcranial magnetic stimuli in migraine: A reappraisal using a figure-of-eight coil. Cephalalgia. 2003 May 1;23(4):264–70.

587. Brigo F, Storti M, Nardone R, Fiaschi A, Bongiovanni LG, Tezzon F, et al. Transcranial magnetic stimulation of visual cortex in migraine patients: A systematic review with meta-analysis. J Headache Pain. 2012 Apr 27;13(5):339–49.

588. Antal A, Nitsche MA, Paulus W. Transcranial direct current stimulation and the visual cortex. Brain Res Bull. 2006 Feb 15;68(6):459–63.

589. Boylu E, Domaç FM, Koçer A, Unal Z, Tanridağ T, Us O. Visual evoked potential abnormalities in migraine patients. Electromyogr Clin Neurophysiol. 2010 Sep 1;50(6):303–8.

590. Nguyen BN, McKendrick AM, Vingrys AJ. Simultaneous retinal and cortical visually evoked electrophysiological responses in between migraine attacks. Cephalalgia Int J Headache. 2012 Sep;32(12):896–907.

591. El-Shazly AAEF, Farweez YA, Hamdi MM, El-Sherbiny NE. Pattern visual evoked potential, pattern electroretinogram, and retinal nerve fiber layer thickness in patients with migraine during and after aura. Curr Eye Res. 2017 Sep;42(9):1327–32.

592. Kennard C, Gawel M, Rudolph N de M, Rose FC. Visual evoked potentials in migraine subjects. Headache Today - Update 21 Experts. 1978;6:73–80.

593. Diener HC, Scholz E, Dichgans J, Gerber WD, Jäck A, Bille A, et al. Central effects of drugs used in migraine prophylaxis evaluated by visual evoked potentials. Ann Neurol. 1989;25(2):125–30.

594. Khalil NM, Legg NJ, Anderson DJ. Long term decline of P100 amplitude in migraine with aura. J Neurol Neurosurg Psychiatry. 2000 Oct 1;69(4):507–11.

595. Susvirkar AA, Velusami D, Srinivasan N. Evaluation of habituation to visual evoked potentials using pattern reversal among migraine individuals – A cross-sectional study. J Basic Clin Physiol Pharmacol. 2020 Mar 1;31(2).

596. Benna P, Bianco C, Costa P, Piazza D, Bergamasco B. Visual evoked potentials and brainstem auditory evoked potentials in migraine and transient ischemic attacks. Cephalalgia. 1985 May 1;5(2_suppl):53–8.

597. Drake ME, Pakalnis A, Hietter SA, Padamadan H. Visual and auditory evoked potentials in migraine. Electromyogr Clin Neurophysiol. 1990;30(2):77–81.

598. De Marinis M, Rinalduzzi S, Accornero N. Impairment in color perception in migraine with and without aura. Headache. 2007 Jun;47(6):895–904.

599. Khalil NM, Nicotra A, Wilkins AJ. Asymmetry of visual function in migraine with aura: Correlation with lateralisation of headache and aura. Cephalalgia Int J Headache. 2011 Jan;31(2):213–21.

600. Kalita J, Uniyal R, Misra UK, Bhoi SK. Neuronal dysexcitability may be a biomarker of migraine: A visual evoked potential study. Clin EEG Neurosci. 2018 Sep 1;49(5):342–50.

601. Lisicki M, Ruiz-Romagnoli E, D'Ostilio K, Piedrabuena R, Giobellina R, Schoenen J, et al. Familial history of migraine influences habituation of visual evoked potentials. Cephalalgia. 2017 Oct 1;37(11):1082–7.

602. Shibata K, Osawa M, Iwata M. Simultaneous recording of pattern reversal electroretinograms and visual evoked potentials in migraine. Cephalalgia. 1997 Nov 1;17(7):742–7.

603. Shibata K, Osawa M, Iwata M. Pattern reversal visual evoked potentials in migraine with aura and migraine aura without headache. Cephalalgia Int J Headache. 1998;18(6):319–23.

604. Oelkers R, Grosser K, Lang E, Geisslinger G, Kobal G, Brune K, et al. Visual evoked potentials in migraine patients: Alterations depend on pattern spatial frequency. Brain. 1999 Jun 1;122(6):1147–55.

605. Coutin-Churchman P, de Freytez AP. Vector analysis of visual evoked potentials in migraineurs with visual aura. Clin Neurophysiol. 2003 Nov 1;114(11):2132–7.

606. Wang W, Wang GP, Ding XL, Wang YH. Personality and response to repeated visual stimulation in migraine and tension-type headaches. Cephalalgia. 1999;19(8):718–24.

607. Afra J, Proietti Cecchini A, Sándor PS, Schoenen J. Comparison of visual and auditory evoked cortical potentials in migraine patients between attacks. Clin Neurophysiol Off J Int Fed Clin Neurophysiol. 2000 Jun;111(6):1124–9.

608. Afra J, Ambrosini A, Genicot R, Albert A, Schoenen J. Influence of colors on habituation of visual evoked potentials in patients with migraine with aura and in healthy volunteers. Headache. 2000 Jan;40(1):36–40.

609. Sand T, Vingen JV. Visual, long-latency auditory and brainstem auditory evoked potentials in migraine: Relation to pattern size, stimulus intensity, sound and light discomfort thresholds and pre-attack state. Cephalalgia. 2000 Nov 1;20(9):804–20.

610. Aurora SK, Ahmad BK, Welch KM, Bhardhwaj P, Ramadan NM. Transcranial magnetic stimulation confirms hyperexcitability of occipital cortex in migraine. Neurology. 1998 Apr;50(4):1111–4.

611. Antal A, Temme J, Nitsche M, Varga E, Lang N, Paulus W. Altered motion perception in migraineurs: Evidence for interictal cortical hyperexcitability. Cephalalgia. 2005 Oct 1;25(10):788–94.

612. Wilkinson F, Karanovic O, Wilson HR. Binocular rivalry in migraine. Cephalalgia Int J Headache. 2008 Dec;28(12):1327–38.

613. Ambrosini A, Schoenen J. Electrophysiological response patterns of primary sensory cortices in migraine. J Headache Pain. 2006 Dec 1;7(6):377–88.

614. Stankewitz A, May A. Cortical excitability and migraine. Cephalalgia. 2007 Dec 1;27(12):1454–6.

615. Valeriani M, Le Pera D. Abnormal brain excitability in migraine: A debated subject. Migraine Disord Res Trends Nova Sci N Y. 2007;35–60.

616. Afra J, Cecchini AP, De Pasqua V, Albert A, Schoenen J. Visual evoked potentials during long periods of pattern-reversal stimulation in migraine. Brain. 1998 Feb 1;121(2):233–41.

617. Judit Á, Sándor P, Schoenen J. Habituation of visual and intensity dependence of auditory evoked cortical potentials tends to normalize just before and during the migraine attack. Cephalalgia. 2000 Oct 1;20(8):714–9.

618. Bohotin V, Fumal A, Vandenheede M, Gérard P, Bohotin C, Maertens de Noordhout A, et al. Effects of repetitive transcranial magnetic stimulation on visual evoked potentials in migraine. Brain. 2002 Apr 1;125(4):912–22.

619. Ozkul Y, Bozlar S. Effects of fluoxetine on habituation of pattern reversal visually evoked potentials in migraine prophylaxis. Headache J Head Face Pain. 2002;42(7):582–7.

620.   Di Clemente L, Coppola G, Magis D, Fumal A, De Pasqua V, Schoenen J. Nociceptive blink reflex and visual evoked potential habituations are correlated in migraine. Headache J Head Face Pain. 2005;45(10):1388–93.

621.   Fumal A, Coppola G, Bohotin V, Gérardy PY, Seidel L, Donneau AF, et al. Induction of long-lasting changes of visual cortex excitability by five daily sessions of repetitive transcranial magnetic stimulation (rTMS) in healthy volunteers and migraine patients. Cephalalgia. 2006 Feb 1;26(2):143–9.

622.   Coppola G, Pierelli F, Schoenen J. Habituation and migraine. Neurobiol Learn Mem. 2009 Sep;92(2):249–59.

623.   Sand T, Zhitniy N, White LR, Stovner LJ. Visual evoked potential latency, amplitude and habituation in migraine: A longitudinal study. Clin Neurophysiol Off J Int Fed Clin Neurophysiol. 2008 May;119(5):1020–7.

624.   Sand T, White LR, Hagen K, Stovner LJ. Visual evoked potential and spatial frequency in migraine: A longitudinal study. Acta Neurol Scand Suppl. 2009;(189):33–7.

625.   Omland PM, Nilsen KB, Uglem M, Gravdahl G, Linde M, Hagen K, et al. Visual evoked potentials in interictal migraine: No confirmation of abnormal habituation. Headache J Head Face Pain. 2013;53(7):1071–86.

626.   Omland PM, Uglem M, Hagen K, Linde M, Tronvik E, Sand T. Visual evoked potentials in migraine: Is the "neurophysiological hallmark" concept still valid? Clin Neurophysiol Off J Int Fed Clin Neurophysiol. 2016 Jan;127(1):810–6.

627.   Brighina F, Cosentino G, Fierro B. Habituation or lack of habituation: What is really lacking in migraine? Clin Neurophysiol Off J Int Fed Clin Neurophysiol. 2016 Jan;127(1):19–20.

628.   Magis D, Lisicki M, Coppola G. Highlights in migraine electrophysiology: Are controversies just reflecting disease heterogeneity? Curr Opin Neurol. 2016 Jun;29(3):320–30.

629.   Sand T. We were blind, so now we can see: The EP/ERP story in migraine. Clin Neurophysiol. 2014 Mar 1;125(3):433–4.

630.   Lisicki M, D'Ostilio K, Erpicum M, Schoenen J, Magis D. Sunlight irradiance and habituation of visual evoked potentials in migraine: The environment makes its mark. Cephalalgia Int J Headache. 2018 Jun;38(7):1351–60.

631.   Ambrosini A, Rossi P, De Pasqua V, Pierelli F, Schoenen J. Lack of habituation causes high intensity dependence of auditory evoked cortical potentials in migraine. Brain J Neurol. 2003 Sep;126(Pt 9):2009–15.

632.   Wang W, Timsit-Berthier M, Schoenen J. Intensity dependence of auditory evoked potentials is pronounced in migraine: An indication of cortical potentiation and low serotonergic neurotransmission? Neurology. 1996 May 1;46(5):1404–1404.

633.   Siniatchkin M, Kropp P, Gerber WD. What kind of habituation is impaired in migraine patients? Cephalalgia. 2003 Sep 1;23(7):511–8.

634.   Siniatchkin M, Kropp P, Neumann M, Gerber WD, Stephani U. Intensity dependence of auditory evoked cortical potentials in migraine families. Pain. 2000 Mar 1;85(1):247–54.

635.   Ambrosini A, de Noordhout AM, Sándor PS, Schoenen J. Electrophysiological studies in migraine: A comprehensive review of their interest and limitations. Cephalalgia Int J Headache. 2003;23 Suppl 1:13–31.

636.   de Araújo CM, Barbosa IG, Lemos SMA, Domingues RB, Teixeira AL. Cognitive impairment in migraine: A systematic review. Dement Neuropsychol. 2012;6(2):74–9.

637.   Armitage SG. An analysis of certain psychological tests used for the evaluation of brain injury. Psychol Monogr. 1946;60:i–48.

638.   Reitan RM. Trail making test. Manual for administration, scoring, and interpretation. Indianapolis, IN: Indiana University Press; 1956.

639.   Wechsler D. A standardized memory scale for clinical use. J Psychol. 1945 Jan 1;19(1):87–95.

640.   Wechsler D. The psychometric tradition: Developing the Wechsler Adult Intelligence Scale. Contemp Educ Psychol. 1981;6:82–5.

641.   Hindmarch I, Parrott AC, Lanza M. The effects of an ergot alkaloid derivative (Hydergine) on aspects of psychomotor performance, arousal, and cognitive processing ability. J Clin Pharmacol. 1979;19(11–12):726–32.

642.   Baker EL, Letz R, Fidler A. A computer-administered neurobehavioral evaluation system for occupational and environmental epidemiology: Rationale, methodology, and pilot study results. J Occup Med. 1985;27(3):206–12.

643.   Comalli PE, Wapner S, Werner H. Interference effects of Stroop color-word test in childhood, adulthood, and aging. J Genet Psychol. 1962 Mar 1;100(1):47–53.

644.   Lavie N, Hirst A, de Fockert JW, Viding E. Load theory of selective attention and cognitive control. J Exp Psychol Gen. 2004;133:339–54.

645.   Fan J, McCandliss BD, Sommer T, Raz A, Posner MI. Testing the efficiency and independence of attentional networks. J Cogn Neurosci. 2002 Apr 1;14(3):340–7.

646.   Larrabee GJ, Curtiss G. Construct validity of various verbal and visual memory tests. J Clin Exp Neuropsychol. 1995 Aug 1;17(4):536–47.

647.   Salthouse TA. What cognitive abilities are involved in trail-making performance? Intelligence. 2011 Jul 1;39(4):222–32.

648.   Zeitlin C, Oddy M. Cognitive impairment in patients with severe migraine. Br J Clin Psychol. 1984;23(1):27–35.

649.   Camarda C, Monastero R, Pipia C, Recca D, Camarda R. Interictal executive dysfunction in migraineurs without aura: Relationship with duration and intensity of attacks. Cephalalgia Int J Headache. 2007 Oct;27(10):1094–100.

650.   Calandre E, Bembibre J, Arnedo M, Becerra D. Cognitive disturbances and regional cerebral blood flow abnormalities in migraine patients: Their relationship with the clinical manifestations of the illness. Cephalalgia. 2002 May 1;22(4):291–302.

651.   Lo Buono V, Bonanno L, Corallo F, Pisani LR, Lo Presti R, Grugno R, et al. Functional connectivity and cognitive impairment in migraine with and without aura. J Headache Pain. 2017 Jul 20;18(1):72.

652.   Baschi R, Monastero R, Cosentino G, Costa V, Giglia G, Fierro B, et al. Visuospatial learning is fostered in migraine: Evidence by a neuropsychological study. Neurol Sci Off J Ital Neurol Soc Ital Soc Clin Neurophysiol. 2019 Nov;40(11):2343–8.

653.   Cullum CM. Neuropsychological assessment of adults. In: Bellack AS, Hersen M, editors. Comprehensive clinical psychology. Oxford: Pergamon; 1998. p. 303–47.

654.   Chen C, Dong X, Gu P, Chen K, Wan Q, Xie H, et al. Attention impairment during the interictal state in migraineurs without aura: A cross-sectional study. J Pain Res. 2021;14:3073–83.

655. Le Pira F, Zappalà G, Giuffrida S, Lo Bartolo M, Reggio E, Morana R, et al. Memory disturbances in migraine with and without aura: A strategy problem? Cephalalgia. 2000 Jun 1;20(5):475–8.

656. Mulder EJ, Linssen WH, Passchier J, Orlebeke JF, de Geus EJ. Interictal and postictal cognitive changes in migraine. Cephalalgia Int J Headache. 1999 Jul;19(6):557–65; discussion 541.

657. Stebbins GT. Neuropsychological testing. In: Goetz CG, editor. Textbook of clinical neurology. 3rd ed. Philadelphia: W.B. Saunders; 2007. p. 539–57.

658. Leijdekkers MLA, Passchier J, Goudswaard P, Menges LJ, Orlebeke JF. Migraine patients cognitively impaired? Headache J Head Face Pain. 1990;30(6):352–8.

659. Su M, Wang R, Dong Z, Zhao D, Yu S. Decline in attentional inhibition among migraine patients: An event-related potential study using the Stroop task. J Headache Pain. 2021 May 3;22(1):34.

660. Posner MI, Petersen SE. The attention system of the human brain. Annu Rev Neurosci. 1990;13:25–42.

661. Han M, Hou X, Xu S, Hong Y, Chen J, Ma Y, et al. Selective attention network impairment during the interictal period of migraine without aura. J Clin Neurosci Off J Neurosurg Soc Australas. 2019 Feb;60:73–8.

662. Vallesi A. On the utility of the trail making test in migraine with and without aura: A meta-analysis. J Headache Pain. 2020 Jun 3;21(1):63.

663. Braganza DL, Fitzpatrick LE, Nguyen ML, Crowe SF. Interictal cognitive deficits in migraine sufferers: A meta-analysis. Neuropsychol Rev. 2022 Dec 1;32(4):736–57.

664. Foti M, Lo Buono V, Corallo F, Palmeri R, Bramanti P, Marino S. Neuropsychological assessment in migraine patients: A descriptive review on cognitive implications. Neurol Sci. 2017 Apr 1;38(4):553–62.

665. Bilder RM, Reise SP. Neuropsychological tests of the future: How do we get there from here? Clin Neuropsychol. 2019 Feb 17;33(2):220–45.

666. Howieson D. Current limitations of neuropsychological tests and assessment procedures. Clin Neuropsychol. 2019 Feb 17;33(2):200–8.

667. Kessels RPC. Improving precision in neuropsychological assessment: Bridging the gap between classic paper-and-pencil tests and paradigms from cognitive neuroscience. Clin Neuropsychol. 2019 Feb 17;33(2):357–68.

668. Treviño M, Zhu X, Lu YY, Scheuer LS, Passell E, Huang GC, et al. How do we measure attention? Using factor analysis to establish construct validity of neuropsychological tests. Cogn Res Princ Implic. 2021 Jul 22;6(1):51.

669. Mazzucchi A, Sinforiani E, Zinelli P, Agostinis C, Granella F, Miari A, et al. Interhemispheric attentional functioning in classic migraine subjects during paroxysmal and interparoxysmal phases. Headache. 1988 Sep 1;28:488–93.

670. Mickleborough MJS, Ekstrand C, Gould L, Lorentz EJ, Ellchuk T, Babyn P, et al. Attentional network differences between migraineurs and non-migraine controls: fMRI evidence. Brain Topogr. 2016 May;29(3):419–28.

671. Mickleborough MJS, Truong G, Handy TC. Top–down control of visual cortex in migraine populations. Neuropsychologia. 2011 Apr 1;49(5):1006–15.

672. Wang W, Schoenen J. Interictal potentiation of passive "oddball" auditory event-related potentials in migraine. Cephalalgia Int J Headache. 1998 Jun;18(5):261–5; discussion 241.

673.   Chen W, Shen X, Liu X, Luo B, Liu Y, Yu R, et al. Passive paradigm single-tone elicited ERPs in tension-type headaches and migraine. Cephalalgia Int J Headache. 2007 Feb;27(2):139–44.

674.   Drake ME, Pakalnis A, Padamadan H. Long-latency auditory event related potentials in migraine. Headache. 1989 Apr;29(4):239–41.

675.   Demarquay G, Caclin A, Brudon F, Fischer C, Morlet D. Exacerbated attention orienting to auditory stimulation in migraine patients. Clin Neurophysiol. 2011 Sep 1;122(9):1755–63.

676.   Morlet D, Demarquay G, Brudon F, Fischer C, Caclin A. Attention orienting dysfunction with preserved automatic auditory change detection in migraine. Clin Neurophysiol Off J Int Fed Clin Neurophysiol. 2014 Mar;125(3):500–11.

677.   Sable JJ, Patrick TA, Woody PL, Baker KR, Allen-Winters S, Andrasik F. Auditory event-related potentials in the interictal phase of migraine indicate alterations in automatic attention. Appl Psychophysiol Biofeedback. 2017 Dec;42(4):323–33.

678.   de Tommaso M, Guido M, Libro G, Losito L, Difruscolo O, Sardaro M, et al. Interictal lack of habituation of mismatch negativity in migraine. Cephalalgia. 2004 Aug 1;24(8):663–8.

679.   Valeriani M, Galli F, Tarantino S, Graceffa D, Pignata E, Miliucci R, et al. Correlation between abnormal brain excitability and emotional symptomatology in paediatric migraine. Cephalalgia Int J Headache. 2009 Feb;29(2):204–13.

680.   Koo YS, Ko D, Lee GT, Oh K, Kim MS, Kim KH, et al. Reduced frontal P3a amplitude in migraine patients during the pain-free period. J Clin Neurol Seoul Korea. 2013 Jan;9(1):43–50.

681.   Titlic M, Mise NI, Pintaric I, Rogosic V, Vanjaka-Rogosic L, Mihalj M, et al. The event-related potential P300 in patients with migraine. Acta Inform Medica. 2015 Dec;23(6):339–42.

682.   Wang R, Dong Z, Chen X, Zhang M, Yang F, Zhang X, et al. Gender differences of cognitive function in migraine patients: Evidence from event-related potentials using the oddball paradigm. J Headache Pain. 2014 Jan 27;15(1):6.

683.   Masson R, Lévêque Y, Demarquay G, ElShafei H, Fornoni L, Lecaignard F, et al. Auditory attention alterations in migraine: A behavioral and MEG/EEG study. Clin Neurophysiol Off J Int Fed Clin Neurophysiol. 2020 Aug;131(8):1933–46.

684.   Wagner D, Manahilov V, Loffler G, Gordon GE, Dutton GN. Visual noise selectively degrades vision in migraine. Invest Ophthalmol Vis Sci. 2010 Apr;51(4):2294–9.

685.   Guo Y, Tian Q, Xu S, Han M, Sun Y, Hong Y, et al. The impact of attack frequency and duration on neurocognitive processing in migraine sufferers: Evidence from event-related potentials using a modified oddball paradigm. BMC Neurol. 2019 Apr 27;19(1):73.

686.   Golshan F, Moss D, Sun G, Krigolson O, Cruz MT, Loehr J, et al. ERP evidence of heightened attentional response to visual stimuli in migraine headache disorders. Exp Brain Res. 2022 Sep 1;240(9):2499–511.

687.   Golla FL, Winter AL. Analysis of cerebral responses to flicker in patients complaining of episodic headache. Electroencephalogr Clin Neurophysiol. 1959 Aug 1;11(3):539–49.

688.   Battelli L, Black KR, Wray SH. Transcranial magnetic stimulation of visual area V5 in migraine. Neurology. 2002 Apr 9;58(7):1066–9.

689.   Ditchfield JA, McKendrick AM, Badcock DR. Processing of global form and motion in migraineurs. Vision Res. 2006 Jan;46(1–2):141–8.

690.   Fierro B, Ricci R, Piazza A, Scalia S, Giglia G, Vitello G, et al. 1 Hz rTMS enhances extrastriate cortex activity in migraine: Evidence of a reduced inhibition? Neurology. 2003 Nov 25;61(10):1446–8.

691.   Heinze HJ, Mangun GR, Burchert W, Hinrichs H, Scholz M, Münte TF, et al. Combined spatial and temporal imaging of brain activity during visual selective attention in humans. Nature. 1994 Dec 8;372(6506):543–6.

692.   Woldorff M g., Fox P t., Matzke M, Lancaster J l., Veeraswamy S, Zamarripa F, et al. Retinotopic organization of early visual spatial attention effects as revealed by PET and ERPs. Hum Brain Mapp. 1997;5(4):280–6.

693.   Brighina F, Palermo A, Fierro B. Cortical inhibition and habituation to evoked potentials: Relevance for pathophysiology of migraine. J Headache Pain. 2009 Apr;10(2):77–84.

694.   Chronicle E, Pearson A, Mulleners W. Objective assessment of cortical excitability in migraine with and without aura. Cephalalgia. 2006 Jul 1;26(7):801–8.

695.   Angelini L, Tommaso MD, Guido M, Hu K, Ivanov PCh, Marinazzo D, et al. Steady-state visual evoked potentials and phase synchronization in migraine patients. Phys Rev Lett. 2004 Jul 15;93(3):038103.

696.   de Tommaso M, Marinazzo D, Guido M, Libro G, Stramaglia S, Nitti L, et al. Visually evoked phase synchronization changes of alpha rhythm in migraine: Correlations with clinical features. Int J Psychophysiol. 2005 Sep 1;57(3):203–10.

697.   Thut G, Northoff G, Ives JR, Kamitani Y, Pfennig A, Kampmann F, et al. Effects of single-pulse transcranial magnetic stimulation (TMS) on functional brain activity: A combined event-related TMS and evoked potential study. Clin Neurophysiol Off J Int Fed Clin Neurophysiol. 2003 Nov;114(11):2071–80.

698.   Yum MK, Moon JH, Kang JK, Kwon OY, Park KJ, Shon YM, et al. Timely event-related synchronization fading and phase de-locking and their defects in migraine. Clin Neurophysiol Off J Int Fed Clin Neurophysiol. 2014 Jul;125(7):1400–6.

699.   Simon RH, Zimmerman AW, Tasman A, Hale MS. Spectral analysis of photic stimulation in migraine. Electroencephalogr Clin Neurophysiol. 1982 Mar;53(3):270–6.

700.   Clemens B, Bánk J, Piros P, Bessenyei M, Veto S, Tóth M, et al. Three-dimensional localization of abnormal EEG activity in migraine: A low resolution electromagnetic tomography (LORETA) study of migraine patients in the pain-free interval. Brain Topogr. 2008 Sep;21(1):36–42.

701.   Fong CY, Law WHC, Fahrenfort JJ, Braithwaite JJ, Mazaheri A. Attenuated alpha oscillation and hyperresponsiveness reveals impaired perceptual learning in migraineurs. J Headache Pain. 2022 Apr 5;23(1):44.

702.   Samaha J, Bauer P, Cimaroli S, Postle BR. Top-down control of the phase of alpha-band oscillations as a mechanism for temporal prediction. Proc Natl Acad Sci U S A. 2015 Jul 7;112(27):8439–44.

703.   Peng KP, May A. Migraine understood as a sensory threshold disease. PAIN. 2019 Jul;160(7):1494.

704.   Wang W, Timsit-Berthier M, Schoenen J. Intensity dependence of auditory evoked potentials is pronounced in migraine: An indication of cortical potentiation and low serotonergic neurotransmission? Neurology. 1996 May 1;46(5):1404–1404.

705.   Hundert AS, Huguet A, McGrath PJ, Stinson JN, Wheaton M. Commercially available mobile phone headache diary apps: A systematic review. JMIR MHealth UHealth. 2014 Aug 19;2(3):e36.

706.   Kessler RC, Adler L, Ames M, Demler O, Faraone S, Hiripi E, et al. The World Health Organization adult ADHD self-report scale (ASRS): A short screening scale for use in the general population. Psychol Med. 2005 Feb;35(2):245–56.

707.   Beck A, Steer R, Brown G. Manual for the Beck Depression Inventory-II (BDI-II). San Antonio, TX: The Psychological Corporation; 1996.

708.   Brainard DH. The Psychophysics toolbox. Spat Vis. 1997;10(4):433–6.

709.   Kleiner M, Brainard D, Pelli D, Ingling A, Murray R, Broussard C. What's new in psychtoolbox-3. Perception. 2007;36(14):1–16.

710.   Kaernbach C. A single-interval adjustment-matrix (SIAM) procedure for unbiased adaptive testing. J Acoust Soc Am. 1990 Dec;88(6):2645–55.

711.   Pasquereau B, Turner RS. Dopamine neurons encode errors in predicting movement trigger occurrence. J Neurophysiol. 2015 Feb 15;113(4):1110–23.

712.   Jennings JR, Wood CC. Letter: The epsilon-adjustment procedure for repeated-measures analyses of variance. Psychophysiology. 1976 May;13(3):277–8.

713.   Cohen J. A power primer. Psychol Bull. 1992 Jul;112(1):155–9.

714.   Wagenmakers EJ, Marsman M, Jamil T, Ly A, Verhagen J, Love J, et al. Bayesian inference for psychology. Part I: Theoretical advantages and practical ramifications. Psychon Bull Rev. 2018 Feb;25(1):35–57.

715.   Wagenmakers EJ, Love J, Marsman M, Jamil T, Ly A, Verhagen J, et al. Bayesian inference for psychology. Part II: Example applications with JASP. Psychon Bull Rev. 2018 Feb;25(1):58–76.

716.   Morey RD, Rouder JN, Jamil T, Morey MRD. Package 'bayesfactor' [Internet]. The Comprehensive R Archive Network (CRAN); 2017. Available from: https://cran.r-project.org/web/packages/BayesFactor/BayesFa

717.   Azzopardi P, Cowey A. Blindsight and visual awareness. Conscious Cogn. 1998 Sep;7(3):292–311.

718.   Delorme A, Makeig S. EEGLAB: An open source toolbox for analysis of single-trial EEG dynamics including independent component analysis. J Neurosci Methods. 2004 Mar 15;134(1):9–21.

719.   Lopez-Calderon J, Luck SJ. ERPLAB: An open-source toolbox for the analysis of event-related potentials. Front Hum Neurosci. 2014;8:213.

720.   Oostenveld R, Fries P, Maris E, Schoffelen JM. FieldTrip: Open source software for advanced analysis of MEG, EEG, and invasive electrophysiological data. Comput Intell Neurosci. 2011;2011:156869.

721.   Aydore S, Pantazis D, Leahy RM. A note on the phase locking value and its properties. NeuroImage. 2013 Jul 1;74:231–44.

722.   Haegens S, Cousijn H, Wallis G, Harrison PJ, Nobre AC. Inter- and intra-individual variability in alpha peak frequency. NeuroImage. 2014 May 15;92(100):46–55.

723.   Torralba Cuello M, Drew A, Sabaté San José A, Morís Fernández L, Soto-Faraco S. Alpha fluctuations regulate the accrual of visual information to awareness. Cortex J Devoted Study Nerv Syst Behav. 2022 Feb;147:58–71.

724.   Cohen MX. Effects of time lag and frequency matching on phase-based connectivity. J Neurosci Methods. 2015 Jul 30;250:137–46.

725.   Lachaux JP, Rodriguez E, Martinerie J, Varela FJ. Measuring phase synchrony in brain signals. Hum Brain Mapp. 1999;8(4):194–208.

726. Maris E, Oostenveld R. Nonparametric statistical testing of EEG- and MEG-data. J Neurosci Methods. 2007 Aug 15;164(1):177–90.

727. Ernst MD. Permutation methods: A basis for exact inference. Stat Sci. 2004;19(4):676–85.

728. Benjamini Y, Drai D, Elmer G, Kafkafi N, Golani I. Controlling the false discovery rate in behavior genetics research. Behav Brain Res. 2001 Nov 1;125(1–2):279–84.

729. Keitel C, Thut G, Gross J. Visual cortex responses reflect temporal structure of continuous quasi-rhythmic sensory stimulation. NeuroImage. 2017 Feb 1;146:58–70.

730. Biltoft CA, Pardyjak ER. Spectral coherence and the statistical significance of turbulent flux computations. J Atmospheric Ocean Technol. 2009 Feb 1;26(2):403–9.

731. Durand D, Greenwood JA. Modifications of the Rayleigh test for uniformity in analysis of two-dimensional orientation data. J Geol. 1958 May 1;66(3):229–38.

732. Berens P. CircStat: A MATLAB toolbox for circular statistics. J Stat Softw. 2009 Sep 23;31:1–21.

733. Fisher RA. Statistical methods for research workers. Oliver and Boyd; 1925.

734. Spielberger C, Gorsuch R, Lushene R, Vagg P, Jacobs G. Manual for the State-Trait Anxiety Inventory (Form Y1 – Y2). Vol. IV. Palo Alto, CA: Consulting Psychologists Press; 1983.

735. Spielberger CD, Gorsuch RL, Lushene RE, Buela-Casal G, Guillén-Riquelme A, Seisdedos Cubero N. STAI: Cuestionario de ansiedad estado-rasgo: Manual. 8a. ed. rev. y amp., [nuevos baremos]. Madrid: TEA; 2011. 40 p. (Publicaciones de psicología aplicada. Serie menor).

736. Kosinski M, Bayliss MS, Bjorner JB, Ware JE, Garber WH, Batenhorst A, et al. A six-item short-form survey for measuring headache impact: The HIT-6^{TM}. Qual Life Res. 2003 Dec 1;12(8):963–74.

737. Stewart WF, Lipton RB, Kolodner KB, Sawyer J, Lee C, Liberman JN. Validity of the Migraine Disability Assessment (MIDAS) score in comparison to a diary-based measure in a population sample of migraine sufferers. Pain. 2000 Oct;88(1):41–52.

738. Jhingran P, Osterhaus JT, Miller DW, Lee JT, Kirchdoerfer L. Development and validation of the Migraine-Specific Quality of Life questionnaire. Headache. 1998 Apr;38(4):295–302.

739. Vilà-Balló A, Marti-Marca A, Torralba Cuello M, Soto-Faraco S, Pozo-Rosich P. The influence of temporal unpredictability on the electrophysiological mechanisms of neural entrainment. Psychophysiology. 2022;59(11):e14108.

740. Mathewson KE, Gratton G, Fabiani M, Beck DM, Ro T. To see or not to see: Prestimulus α phase predicts visual awareness. J Neurosci. 2009 Mar 4;29(9):2725–32.

741. Coppola G, Bracaglia M, Di Lenola D, Di Lorenzo C, Serrao M, Parisi V, et al. Visual evoked potentials in subgroups of migraine with aura patients. J Headache Pain. 2015;16:92.

742. MATLAB. MathWorks - Makers of MATLAB and Simulink [Internet]. Available from: https://www.mathworks.com/

743. Coppola G, Bracaglia M, Di Lenola D, Di Lorenzo C, Serrao M, Parisi V, et al. Visual evoked potentials in subgroups of migraine with aura patients. J Headache Pain. 2015 Nov 2;16(1):92.

744. Sezai T, Murphy MJ, Riddell N, Nguyen V, Crewther SG. Visual processing during the interictal period between migraines: A meta-analysis. Neuropsychol Rev. 2022 Sep 17;

745. Pinheiro J, Bates D, R Core Team. nlme: Linear and nonlinear mixed effects models [Internet]. 2022. Available from: https://svn.r-project.org/R-packages/trunk/nlme/

746.   Pinheiro JC, Bates DM, editors. Linear mixed-effects models: Basic concepts and examples. In: Mixed-effects models in S and S-PLUS. New York, NY: Springer; 2000. p. 3–56. (Statistics and Computing).

747.   Omland PM, Nilsen KB, Sand T. Habituation measured by pattern reversal visual evoked potentials depends more on check size than reversal rate. Clin Neurophysiol. 2011 Sep 1;122(9):1846–53.

748.   Derogatis LR. Brief Symptom Inventory. APA PsycTests; 1982.

749.   Stewart WF, Lipton RB, Dowson AJ, Sawyer J. Development and testing of the Migraine Disability Assessment (MIDAS) questionnaire to assess headache-related disability. Neurology. 2001;56(6 Suppl 1):S20-28.

750.   Gil-Gouveia R, Oliveira AG, Martins IP. A subjective cognitive impairment scale for migraine attacks. The MIG-SCOG: Development and validation. Cephalalgia Int J Headache. 2011 Jul;31(9):984–91.

751.   Johns MW. A new method for measuring daytime sleepiness: The Epworth sleepiness scale. Sleep. 1991 Dec;14(6):540–5.

752.   Craig CL, Marshall AL, Sjöström M, Bauman AE, Booth ML, Ainsworth BE, et al. International physical activity questionnaire: 12-country reliability and validity. Med Sci Sports Exerc. 2003 Aug;35(8):1381–95.

753.   Khalfa S, Dubal S, Veuillet E, Perez-Diaz F, Jouvent R, Collet L. Psychometric normalization of a hyperacusis questionnaire. ORL J Oto-Rhino-Laryngol Its Relat Spec. 2002;64(6):436–42.

754.   Light GA, Williams LE, Minow F, Sprock J, Rissling A, Sharp R, et al. Electroencephalography (EEG) and event-related potentials (ERPs) with human participants. Curr Protoc Neurosci. 2010;52(1):6.25.1-6.25.24.

755.   Marco-Pallares J, Cucurell D, Münte TF, Strien N, Rodriguez-Fornells A. On the number of trials needed for a stable feedback-related negativity. Psychophysiology. 2011 Jun;48(6):852–60.

756.   Vilà-Balló A, Marti-Marca A, Torres-Ferrús M, Alpuente A, Gallardo VJ, Pozo-Rosich P. Neurophysiological correlates of abnormal auditory processing in episodic migraine during the interictal period. Cephalalgia Int J Headache. 2021 Jan;41(1):45–57.

757.   Wiesman AI, Wilson TW. Alpha frequency entrainment reduces the effect of visual distractors. J Cogn Neurosci. 2019 Sep;31(9):1392–403.

758.   Breska A, Deouell LY. When synchronizing to rhythms is not a good thing: Modulations of preparatory and post-target neural activity when shifting attention away from on-beat times of a distracting rhythm. J Neurosci Off J Soc Neurosci. 2016 Jul 6;36(27):7154–66.

759.   Breska A, Deouell LY. Neural mechanisms of rhythm-based temporal prediction: Delta phase-locking reflects temporal predictability but not rhythmic entrainment. PLOS Biol. 2017 Feb 10;15(2):e2001665.

760.   Jones MR, Moynihan H, MacKenzie N, Puente J. Temporal aspects of stimulus-driven attending in dynamic arrays. Psychol Sci. 2002 Jul;13(4):313–9.

761.   Helfrich RF, Huang M, Wilson G, Knight RT. Prefrontal cortex modulates posterior alpha oscillations during top-down guided visual perception. Proc Natl Acad Sci. 2017 Aug 29;114(35):9457–62.

762.   Herrmann B, Johnsrude IS. Neural signatures of the processing of temporal patterns in sound. J Neurosci Off J Soc Neurosci. 2018 Jun 13;38(24):5466–77.

763.   Benwell CSY, Tagliabue CF, Veniero D, Cecere R, Savazzi S, Thut G. Prestimulus EEG power predicts conscious awareness but not objective visual performance. eNeuro. 2017;4(6):ENEURO.0182-17.2017.

764.   Bompas A, Sumner P, Muthumumaraswamy SD, Singh KD, Gilchrist ID. The contribution of pre-stimulus neural oscillatory activity to spontaneous response time variability. NeuroImage. 2015 Feb 15;107:34–45.

765.   Ruzzoli M, Torralba M, Morís Fernández L, Soto-Faraco S. The relevance of alpha phase in human perception. Cortex J Devoted Study Nerv Syst Behav. 2019 Nov;120:249–68.

766.   Vigué-Guix I, Morís Fernández L, Torralba Cuello M, Ruzzoli M, Soto-Faraco S. Can the occipital alpha-phase speed up visual detection through a real-time EEG-based brain-computer interface (BCI)? Eur J Neurosci. 2022 Jun;55(11–12):3224–40.

767.   Sinforiani E, Zinelli P, Faglia L, Granella F, Mauri M, Manzoni GC, et al. Lateralization of visual attention in patients with classic migraine and unilateral prodromes. Funct Neurol. 1989 Sep;4(3):247–52.

768.   Gil-Gouveia R, Oliveira AG, Martins IP. Cognitive dysfunction during migraine attacks: A study on migraine without aura. Cephalalgia. 2015 Jul 1;35(8):662–74.

769.   Chen SP, Chang YA, Chou CH, Juan CC, Lee HC, Chen LK, et al. Circulating microRNAs associated with reversible cerebral vasoconstriction syndrome. Ann Neurol. 2021;89(3):459–73.

770.   Kaiser Pinotti L, Castro A da S, de Oliveira Garcia GH, Alvim PHP, Roza TH, Andrade FA, et al. Executive functions in migraine patients: A systematic review with meta-analysis. Cognit Neuropsychiatry. 2022 Nov 24;0(0):1–15.

771.   Coull JT, Nobre AC. Where and when to pay attention: The neural systems for directing attention to spatial locations and to time intervals as revealed by both PET and fMRI. J Neurosci Off J Soc Neurosci. 1998 Sep 15;18(18):7426–35.

772.   Marti-Marca A, Nguyen T, Grahn JA. Keep calm and pump up the jams: How musical mood and arousal affect visual attention. Music Sci. 2020;3.

773.   Lakatos P, Gross J, Thut G. A new unifying account of the roles of neuronal entrainment. Curr Biol. 2019 Sep 23;29(18):R890–905.

774.   Bjørk M, Hagen K, Stovner L, Sand T. Photic EEG-driving responses related to ictal phases and trigger sensitivity in migraine: A longitudinal, controlled study. Cephalalgia Int J Headache. 2011 Mar;31(4):444–55.

775.   Masson R, ElShafei HA, Demarquay G, Fornoni L, Lévêque Y, Caclin A, et al. Top-down inhibition of irrelevant information indexed by alpha rhythms is disrupted in migraine. Neurology; 2021 May.

776.   Isaacs D, Key AP, Cascio CJ, Conley AC, Walker HC, Wallace MT, et al. Sensory hypersensitivity severity and association with obsessive-compulsive symptoms in adults with tic disorder. Neuropsychiatr Dis Treat. 2020;16:2591–601.

777.   Dorris ER, Maccarthy J, Simpson K, McCarthy GM. Sensory Perception Quotient reveals visual, scent and touch sensory hypersensitivity in people with fibromyalgia syndrome. Front Pain Res Lausanne Switz. 2022;3:926331.

778.   Shepherd AJ. Visual contrast processing in migraine. Cephalalgia Int J Headache. 2000 Dec;20(10):865–80.

779.   Hay KM, Mortimer MJ, Barker DC, Debney LM, Good PA. 1044 women with migraine: The effect of environmental stimuli. Headache J Head Face Pain. 1994;34(3):166–8.

780. Shibata K, Yamane K, Nishimura Y, Kondo H, Otuka K. Spatial frequency differentially affects habituation in migraineurs: A steady-state visual-evoked potential study. Doc Ophthalmol Adv Ophthalmol. 2011 Oct;123(2):65–73.

781. Magis D, Allena M, Coppola G, Di Clemente L, Gérard P, Schoenen J. Search for correlations between genotypes and electrophysiological patterns in migraine: The MTHFR C677T polymorphism and visual evoked potentials. Cephalalgia Int J Headache. 2007 Oct;27(10):1142–9.

782. Knott JR, Irwin DA. Anxiety, stress, and the contingent negative variation. Arch Gen Psychiatry. 1973 Oct;29(4):538–41.

783. Bigal ME, Liberman JN, Lipton RB. Age-dependent prevalence and clinical features of migraine. Neurology. 2006 Jul 25;67(2):246–51.

784. Kelman L. Migraine changes with age: IMPACT on migraine classification. Headache. 2006;46(7):1161–71.

785. Pinheiro CF, Moreira JR, Carvalho GF, Zorzin L, Dach F, Bevilaqua-Grossi D. Interictal photophobia and phonophobia are related to the presence of aura and high frequency of attacks in patients with migraine. Appl Sci. 2021 Jan;11(6):2474.

786. Pearl TA, Dumkrieger G, Chong CD, Dodick DW, Schwedt TJ. Sensory hypersensitivity symptoms in migraine with vs without aura: Results from the American registry for migraine research. Headache. 2020 Mar;60(3):506–14.

787. Chong CD, Starling AJ, Schwedt TJ. Interictal photosensitivity associates with altered brain structure in patients with episodic migraine. Cephalalgia Int J Headache. 2016 May;36(6):526–33.

788. Torres-Ferrús M, Quintana M, Fernandez-Morales J, Alvarez-Sabin J, Pozo-Rosich P. When does chronic migraine strike? A clinical comparison of migraine according to the headache days suffered per month. Cephalalgia Int J Headache. 2017 Feb;37(2):104–13.

789. Pavlov YG, Adamian N, Appelhoff S, Arvaneh M, Benwell CSY, Beste C, et al. #EEGManyLabs: Investigating the replicability of influential EEG experiments. Cortex. 2021 Nov 1;144:213–29.

790. Molenberghs G, Verbeke G. Linear mixed models for longitudinal data. New York, NY: Springer; 2000. (Springer Series in Statistics).

791. Janmaat CJ, van Diepen M, Tsonaka R, Jager KJ, Zoccali C, Dekker FW. Pitfalls of linear regression for estimating slopes over time and how to avoid them by using linear mixed-effects models. Nephrol Dial Transplant Off Publ Eur Dial Transpl Assoc - Eur Ren Assoc. 2019 Apr 1;34(4):561–6.

792. Tibon R, Levy DA. Striking a balance: Analyzing unbalanced event-related potential data. Front Psychol. 2015;6:555.

793. Nappi G, Costa A, Tassorelli C, Santorelli FM. Migraine as a complex disease: Heterogeneity, comorbidity and genotype-phenotype interactions. Funct Neurol. 2000;15(2):87–93.

794. Sinha P, Kjelgaard MM, Gandhi TK, Tsourides K, Cardinaux AL, Pantazis D, et al. Autism as a disorder of prediction. Proc Natl Acad Sci. 2014 Oct 21;111(42):15220–5.

795. Podoly TY, Ben-Sasson A. Sensory habituation as a shared mechanism for sensory over-responsivity and obsessive-compulsive symptoms. Front Integr Neurosci. 2020;14:17.

796. Woldorff MG, Gallen CC, Hampson SA, Hillyard SA, Pantev C, Sobel D, et al. Modulation of early sensory processing in human auditory cortex during auditory selective attention. Proc Natl Acad Sci U S A. 1993 Sep 15;90(18):8722–6.

797.   Yordanova J, Devrim M, Kolev V, Ademoglu A, Demiralp T. Multiple time-frequency components account for the complex functional reactivity of P300. Neuroreport. 2000 Apr 7;11(5):1097–103.

798.   Başar-Eroglu C, Demiralp T. Event-related theta oscillations: An integrative and comparative approach in the human and animal brain. Int J Psychophysiol Off J Int Organ Psychophysiol. 2001 Jan;39(2–3):167–95.

799.   Kayser C, Ince RAA, Panzeri S. Analysis of slow (theta) oscillations as a potential temporal reference frame for information coding in sensory cortices. PLoS Comput Biol. 2012;8(10):e1002717.

800.   Luo H, Liu Z, Poeppel D. Auditory cortex tracks both auditory and visual stimulus dynamics using low-frequency neuronal phase modulation. PLoS Biol. 2010 Aug 10;8(8):e1000445.

801.   de Tommaso M, Stramaglia S, Marinazzo D, Trotta G, Pellicoro M. Functional and effective connectivity in EEG alpha and beta bands during intermittent flash stimulation in migraine with and without aura. Cephalalgia Int J Headache. 2013 Aug;33(11):938–47.

802.   Wang W, Schoenen J. Interictal potentiation of passive "Oddball" auditory event-related potentials in migraine. Cephalalgia. 1998 Jun 1;18(5):261–5.

803.   Brighina F, Cosentino G, Fierro B. Is lack of habituation a biomarker of migraine? A critical perspective. J Headache Pain. 2015 Dec;16(Suppl 1):A13.

804.   Wang W, Schoenen J, Timsit-Berthier M. Cognitive functions in migraine without aura between attacks: A psychophysiological approach using the "oddball" paradigm. Neurophysiol Clin Clin Neurophysiol. 1995;25(1):3–11.

805.   Kösem A, Bosker HR, Takashima A, Meyer A, Jensen O, Hagoort P. Neural entrainment determines the words we hear. Curr Biol. 2018 Sep 24;28(18):2867-2875.e3.

806.   Cecere R, Rees G, Romei V. Individual differences in alpha frequency drive crossmodal illusory perception. Curr Biol. 2015 Jan 19;25(2):231–5.

807.   Roberts BM, Clarke A, Addante RJ, Ranganath C. Entrainment enhances theta oscillations and improves episodic memory. Cogn Neurosci. 2018;9(3–4):181–93.

808.   Carrasco M, Eckstein M, Verghese P, Boynton G, Treue S. Visual attention: Neurophysiology, psychophysics, and cognitive neuroscience. Vision Res. 2009 Jun;49(10):1033–6.

809.   van Ede F, de Lange FP, Maris E. Attentional cues affect accuracy and reaction time via different cognitive and neural processes. J Neurosci Off J Soc Neurosci. 2012 Jul 25;32(30):10408–12.

810.   Bergen JR, Julesz B. Parallel versus serial processing in rapid pattern discrimination. Nature. 1983 Jun 23;303(5919):696–8.

811.   Posner MI, Snyder CR, Davidson BJ. Attention and the detection of signals. J Exp Psychol. 1980 Jun;109(2):160–74.

812.   Hopfinger JB, Buonocore MH, Mangun GR. The neural mechanisms of top-down attentional control. Nat Neurosci. 2000 Mar;3(3):284–91.

813.   Kastner S, Pinsk MA, De Weerd P, Desimone R, Ungerleider LG. Increased activity in human visual cortex during directed attention in the absence of visual stimulation. Neuron. 1999 Apr;22(4):751–61.

814.   Kastner S, Ungerleider LG. Mechanisms of visual attention in the human cortex. Annu Rev Neurosci. 2000;23:315–41.

815.   O'Bryant SE, Marcus DA, Rains JC, Penzien DB. Neuropsychology of migraine: Present status and future directions. Expert Rev Neurother. 2005 May;5(3):363–70.

816.   Gil-Gouveia R, Martins IP. Cognition and cognitive impairment in migraine. Curr Pain Headache Rep. 2019 Sep 11;23(11):84.

817.   Lake AE, Rains JC, Penzien DB, Lipchik GL. Headache and psychiatric comorbidity: Historical context, clinical implications, and research relevance. Headache. 2005 May;45(5):493–506.

818.   Al-Hassany L, Haas J, Piccininni M, Kurth T, Maassen Van Den Brink A, Rohmann JL. Giving researchers a headache - Sex and gender differences in migraine. Front Neurol. 2020;11.

819.   Maleki N, Becerra L, Upadhyay J, Burstein R, Borsook D. Direct optic nerve pulvinar connections defined by diffusion MR tractography in humans: Implications for photophobia. Hum Brain Mapp. 2012;33(1):75–88.

820.   Lee W, Min IK, Yang KI, Kim D, Yun CH, Chu MK. Classifying migraine subtypes and their characteristics by latent class analysis using data of a nation-wide population-based study. Sci Rep. 2021 Nov 3;11(1):21595.

821.   Cicchetti D, Rogosch FA. Equifinality and multifinality in developmental psychopathology. Dev Psychopathol. 1996;8(4):597–600.

822.   May A. Understanding migraine as a cycling brain syndrome: Reviewing the evidence from functional imaging. Neurol Sci Off J Ital Neurol Soc Ital Soc Clin Neurophysiol. 2017 May;38(Suppl 1):125–30.

823.   Feczko E, Miranda-Dominguez O, Marr M, Graham AM, Nigg JT, Fair DA. The heterogeneity problem: Approaches to identify psychiatric subtypes. Trends Cogn Sci. 2019 Jul 1;23(7):584–601.

824.   Nyholt DR, Gillespie NG, Heath AC, Merikangas KR, Duffy DL, Martin NG. Latent class and genetic analysis does not support migraine with aura and migraine without aura as separate entities. Genet Epidemiol. 2004 Apr;26(3):231–44.

825.   Russell MB, Olesen J. Increased familial risk and evidence of genetic factor in migraine. BMJ. 1995 Aug 26;311(7004):541–4.

826.   Launer LJ, Terwindt GM, Ferrari MD. The prevalence and characteristics of migraine in a population-based cohort: The GEM study. Neurology. 1999 Aug 11;53(3):537–42.

827.   Mochi M, Sangiorgi S, Cortelli P, Carelli V, Scapoli C, Crisci M, et al. Testing models for genetic determination in migraine. Cephalalgia. 1993 Dec 1;13(6):389–94.

828.   Kallela M, Wessman M, Färkkilä M. Validation of a migraine-specific questionnaire for use in family studies. Eur J Neurol. 2001;8(1):61–6.

829.   Ophoff RA, van Eijk R, Sandkuijl LA, Terwindt GM, Grubben CPM, Haan J, et al. Genetic heterogeneity of familial hemiplegic migraine. Genomics. 1994 Jul 1;22(1):21–6.

830.   Russell MB, Rasmussen BK, Brennum J, Iversen HK, Jensen RA, Olesen J. Presentation of a new instrument: The diagnostic headache diary. Cephalalgia Int J Headache. 1992 Dec;12(6):369–74.

831.   Ashina S, Bentivegna E, Martelletti P, Eikermann-Haerter K. Structural and functional brain changes in migraine. Pain Ther. 2021 Jun;10(1):211–23.

832.   Valfrè W, Rainero I, Bergui M, Pinessi L. Voxel-based morphometry reveals gray matter abnormalities in migraine. Headache. 2008 Jan;48(1):109–17.

833.   Vincent M, Pedra E, Mourão-Miranda J, Bramati IE, Henrique AR, Moll J. Enhanced interictal responsiveness of the migraineous visual cortex to incongruent bar stimulation: A functional MRI visual activation study. Cephalalgia Int J Headache. 2003 Nov;23(9):860–8.

834.   Boulloche N, Denuelle M, Payoux P, Fabre N, Trotter Y, Géraud G. Photophobia in migraine: An interictal PET study of cortical hyperexcitability and its modulation by pain. J Neurol Neurosurg Psychiatry. 2010 Sep;81(9):978–84.

835.   Polich J, Ehlers CL, Dalessio DJ. Pattern-shift visual evoked responses and EEG in migraine. Headache J Head Face Pain. 1986;26(9):451–6.

836.   Mariani E, Moschini V, Pastorino G, Rizzi F, Severgnini A, Tiengo M. Pattern-reversal visual evoked potentials and EEG correlations in common migraine patients. Headache J Head Face Pain. 1988;28(4):269–71.

837.   Raudino F. Visual evoked potential in patients with migraine. Headache J Head Face Pain. 1988;28(8):531–3.

838.   Lai CW, Dean P, Ziegler DK, Hassanein RS. Clinical and electrophysiological responses to dietary challenge in migraineurs. Headache. 1989 Mar;29(3):180–6.

839.   Mariani E, Moschini V, Pastorino GC, Rizzi F, Severgnini A, Tiengo M. Pattern reversal visual evoked potentials (VEP-PR) in migraine subjects with visual aura. Headache. 1990 Jun;30(7):435–8.

840.   Tsounis S, Milonas J, Gilliam F. Hemi-field pattern reversal visual evoked potentials in migraine. Cephalalgia Int J Headache. 1993 Aug;13(4):267–71.

841.   Tagliati M, Sabbadini M, Bernardi G, Silvestrini M. Multichannel visual evoked potentials in migraine. Electroencephalogr Clin Neurophysiol. 1995 Jan;96(1):1–5.

842.   Shibata K, Osawa M, Iwata M. Pattern reversal visual evoked potentials in classic and common migraine. J Neurol Sci. 1997 Feb 12;145(2):177–81.

843.   Sener HO, Haktanir I, Demirci S. Pattern-reversal visual evoked potentials in migraineurs with or without visual aura. Headache. 1997;37(7):449–51.

844.   Yücesan C, Sener Ö, Mutluer N. Influence of disease duration on visual evoked potentials in migraineurs. Headache J Head Face Pain. 2000;40(5):384–8.

845.   Logi F, Bonfiglio L, Orlandi G, Bonanni E, Iudice A, Sartucci F. Asymmetric scalp distribution of pattern visual evoked potentials during interictal phases in migraine. Acta Neurol Scand. 2001 Nov;104(5):301–7.

846.   Yilmaz M, Bayazit YA, Erbagci I, Pençe S. Visual evoked potential changes in migraine. Influence of migraine attack and aura. J Neurol Sci. 2001 Mar 1;184(2):139–41.

847.   Kochar K, Srivastava T, Maurya RK, Jain R, Aggarwal P. Visual evoked potential and brainstem auditory evoked potentials in acute attack and after the attack of migraine. Electromyogr Clin Neurophysiol. 2002;42(3):175–9.

848.   Ashjazadeh N, Varavipour B. Abnormalitites of visual evoked potential in migraine patients. Iran J Med Sci. 2015 Oct 28;28(2):65–8.

849.   Spreafico C, Frigerio R, Santoro P, Ferrarese C, Agostoni E. Visual evoked potentials in migraine. Neurol Sci Off J Ital Neurol Soc Ital Soc Clin Neurophysiol. 2004 Oct;25 Suppl 3:S288-290.

850.   Coppola G, Ambrosini A, Di Clemente L, Magis D, Fumal A, Gérard P, et al. Interictal abnormalities of gamma band activity in visual evoked responses in migraine: An indication of thalamocortical dysrhythmia? Cephalalgia Int J Headache. 2007 Dec;27(12):1360–7.

851.   Shibata K, Yamane K, Otuka K, Iwata M. Abnormal visual processing in migraine with aura: A study of steady-state visual evoked potentials. J Neurol Sci. 2008 Aug 15;271(1–2):119–26.

852.   Di Lorenzo C, Coppola G, Bracaglia M, Di Lenola D, Evangelista M, Sirianni G, et al. Cortical functional correlates of responsiveness to short-lasting preventive intervention with ketogenic diet in migraine: A multimodal evoked potentials study. J Headache Pain. 2016;17:58.

853.   Viganò A, D'Elia TS, Sava SL, Auvé M, De Pasqua V, Colosimo A, et al. Transcranial Direct Current Stimulation (tDCS) of the visual cortex: A proof-of-concept study based on interictal electrophysiological abnormalities in migraine. J Headache Pain. 2013 Mar 11;14(1):23.

854.   Lisicki M, Ruiz-Romagnoli E, D'Ostilio K, Piedrabuena R, Giobellina R, Schoenen J, et al. Familial history of migraine influences habituation of visual evoked potentials. Cephalalgia Int J Headache. 2017 Oct;37(11):1082–7.

855.   Omland PM, Uglem M, Engstrøm M, Linde M, Hagen K, Sand T. Modulation of visual evoked potentials by high-frequency repetitive transcranial magnetic stimulation in migraineurs. Clin Neurophysiol Off J Int Fed Clin Neurophysiol. 2014 Oct;125(10):2090–9.

856.   Ambrosini A, Iezzi E, Perrotta A, Kisialiou A, Nardella A, Berardelli A, et al. Correlation between habituation of visual-evoked potentials and magnetophosphene thresholds in migraine: A case-control study. Cephalalgia. 2016 Mar;36(3):258–64.

857.   Rauschel V, Ruscheweyh R, Krafczyk S, Straube A. Test-retest reliability of visual-evoked potential habituation. Cephalalgia Int J Headache. 2016 Aug;36(9):831–9.

858.   Verroiopoulos GV, Nitoda E, Ladas ID, Brouzas D, Antonakaki D, Moschos MM. Ophthalmological assessment of OCT and electrophysiological changes in migraine patients. J Clin Neurophysiol Off Publ Am Electroencephalogr Soc. 2016 Oct;33(5):431–42.

859.   Coppola G, Di Lorenzo C, Di Lenola D, Serrao M, Pierelli F, Parisi V. Visual evoked potential responses after photostress in migraine patients and their correlations with clinical features. J Clin Med. 2021 Mar 2;10(5):982.

860.   Kalita J, Misra UK, Kumar M, Bansal R, Uniyal R. Is palinopsia in migraineurs a phenomenon of impaired habituation of visual cortical neurons? Clin EEG Neurosci. 2022 May;53(3):196–203.

861.   Sándor PS, Afra J, Proietti-Cecchini A, Albert A, Schoenen J. Familial influences on cortical evoked potentials in migraine. Neuroreport. 1999 Apr 26;10(6):1235–8.

862.   Coppola G, Currà A, Sava SL, Alibardi A, Parisi V, Pierelli F, et al. Changes in visual-evoked potential habituation induced by hyperventilation in migraine. J Headache Pain. 2010 Dec;11(6):497–503.

863.   Coppola G, Currà A, Serrao M, Di Lorenzo C, Gorini M, Porretta E, et al. Lack of cold pressor test-induced effect on visual-evoked potentials in migraine. J Headache Pain. 2010 Apr;11(2):115–21.

864.   Coppola G, Crémers J, Gérard P, Pierelli F, Schoenen J. Effects of light deprivation on visual evoked potentials in migraine without aura. BMC Neurol. 2011 Jul 27;11:91.

865.   Hansen JM, Bolla M, Magis D, de Pasqua V, Ashina M, Thomsen LL, et al. Habituation of evoked responses is greater in patients with familial hemiplegic migraine than in controls: A contrast with the common forms of migraine. Eur J Neurol. 2011 Mar;18(3):478–85.

866.   Bednář M, Kubová Z, Kremláček J. Lack of visual evoked potentials amplitude decrement during prolonged reversal and motion stimulation in migraineurs. Clin Neurophysiol. 2014 Jun 1;125(6):1223–30.

867.   Ambrosini A, Kisialiou A, Coppola G, Finos L, Magis D, Pierelli F, et al. Visual and auditory cortical evoked potentials in interictal episodic migraine: An audit on 624 patients from three centres. Cephalalgia Int J Headache. 2017 Oct;37(12):1126–34.

868.   Ince F, Erdogan-Bakar E, Unal-Cevik I. Preventive drugs restore visual evoked habituation and attention in migraineurs. Acta Neurol Belg. 2017 Jun;117(2):523–30.

869.   Lisicki M, Ruiz-Romagnoli E, Piedrabuena R, Giobellina R, Schoenen J, Magis D. Migraine triggers and habituation of visual evoked potentials. Cephalalgia. 2018 Apr 1;38(5):988–92.

10. APPENDICES

10.1 Appendix 1

Supplementary Table 1. A summary list of studies, in patients with migraine, related to cortical excitability and specifically event-related potential (ERP) component latencies, amplitudes, and peak-to-peak amplitude differences in response to Pattern-Reversal stimulation.

Ref.	No of subjects and diagnosis	Mean age±SD (range)	Timing of session	Spatial freq.	Temporal freq.	No of trials	ERPs	Principal findings
Kennard et al.(592)	28 MA 30 HC	39	NA	NA	2 Hz	256	N1, P1, N2	**Increased latency and amplitude of P1 in MA compared to HC**
Benna et al.(596)	10 MwoA 10 with TIA	36 (25-46) 48 (44-52)	At least 8 days after attack	NA	NA	NA	N80, P1	No significant differences in latencies or amplitudes between groups
Polich et al.(835)	20 MA 20 HC	33±7 (23-44)	Headache-free at test	16x16	3.9 Hz	200x2	N75, P1, N145 N75-P1	No significant differences in latencies or amplitudes between groups
Mariani et al.(836)	22 MwoA 20 HC	39±11 (17-60) 40±12 (21-60)	At least 48 hours after attack	38'	1 Hz	128x2	P1 N1-P1	No significant differences in latencies or amplitudes between groups
Raudino (837)	34 MwoA 6 MA 20 HC	Female M: 37 (17-78) Male M: 30 (14-43) Female HC: 38 (17-54) Male HC: 37 (19-55)	Headache-free at test	NA	1.5 Hz	NA	P1	No significant differences in latencies or amplitudes between groups
Diener et al.(593)	54 MwoA 4 MA 87 HC	42 35	NA	60'x60'	1.56 Hz 8.33 Hz	64	P1 and (N1-Pl) + (N2-P1)/2	**Increased latency of P1 and larger amplitude in M at baseline compared to HC**
Lai et al.(838)	25 MA 13 MwoA	29 [median age] (17-38)	Not specified	27.6'	NA	128	N1, P1 N1-P1	No significant differences in latencies or amplitudes between groups
Drake et al.(597)	50 MwoA 37 HC	? (16-67)	NA	56'	1.88 Hz	200x2	N1, P1, N2	No significant differences in latencies or amplitudes between groups
Mariani et al.(839)	20 MA 20 HC	34±12 (19-55) 37±10 (21-51)	At least 48 hours after attack	38'	1 Hz	128x2	P1 N75-P1	**Increased latencies of P1 in MA compared to HC**

Tsounis et al.(840)	22 MwoA 22 MA 37 HC	37 (15-56) 32 (18-58)	At least 2 weeks after attack	49'	1 Hz	128x2	P1	No significant differences in latencies or amplitudes between groups
Tagliati et al.(841)	7 MwoA 8 visual prodromes 15 HC	32±9 (17-56) ? (18-50)	At least 1 week after attack	NA	NA	240	N70, P1 N70-P1	No significant differences in latencies or amplitudes between groups
Schoenen et al.(341)	27 MwoA 9 MA 16 HC	32 33	At least 1 week after attack	8'	3.1 Hz	50x5	N1, P1, N2 N1-P1 P1-N2	No significant differences in latencies or amplitudes between groups
Shibata et al. (842)	14 MwoA 19 MA 43 HC	40 (20-62) 42 (20-70) 41 (18-71)	At least 2-20 days after attack	30'	1 Hz	100x2	N75, P1, N145 N75-P1 P1-N145	**Increased N75-P1 amplitudes in MA compared with HC**
Sener et al.(843)	23 MwoA 16 MA 17 HC	33±7 36±9	At least 1 week after attack	NA	2 Hz	200x2	P1 N70-P1	No significant differences in latencies or amplitudes between groups
Shibata et al. (602)	14 MwoA 15 MA 23 HC	40 (22-65) 46 (22-65) 43 (20-65)	At least 5 days after attack	30'	2 Hz	100x2	P1 N75-P1	**Increased N75-P1 amplitude in MA as compared to HC**
Afra et al.(616)	25 MwoA 15 MA 25 HC	36 30	At least 5 days after attack	8'	3.1 Hz	100x15	N1, P1, N2 N1-P1 P1-N2	No significant differences in latencies or first block amplitudes between groups
Shibata et al.(603)	20 MA 19 ME (aura, no headache) 34 HC	41 (22-68) 48 (22-70) 48 (20-72)	At least 1-30 days after attack	30'	2 Hz	100x2	P1 N75-P1	**Increased amplitudes in MA and ME as compared to HC**
Oelkers et al.(604)	13 MwoA 13 MA 28 HC	29±6 27±4	± 3 days before and after attack	0.5 c.p.d. 1 c.p.d. 2 c.p.d. 4 c.p.d.	1 Hz	50x5 per cond.	N1, P1, N2 N1-P1 P1-N2	**Prolonged N2 latencies to 2, 4 c.p.d. as well as higher P1-N2 amplitude in response to 0.5 c.p.d. in MwoA and MA but not HC**
Wang et al.(606)	22 MwoA 13 ETH 20 CTH 26 HC	35±10 27±11 28±8 32±12	At least 1 week after attack	8'	3 Hz	50x5	N1, P1, N2 N1-P1 P1-N2	No significant differences in latencies or first block amplitudes between groups
Afra et al.(608)	12 MA 10 HC	34±16 28±6	± 3 days before and after attack	68'	3.1 Hz	50x5	N1, P1 N1-P1	No significant differences in latencies and amplitudes between groups

Afra et al.(607)	37 MwoA 22 MA 23 HC	36±11 27±7	± 3 days before and after attack	68'	3.1 Hz	50x5	N1, P1 N1-P1	No significant differences in latencies and first block amplitudes between groups
Yücesan et al.(844)	49 MwoA 17 HC	29±8 (18-48) 37±7 (23-52) 36±9 (18-48)	At least 1 week after attack	NA	2 Hz	250x2	P1 N70-P1	No significant differences in latencies and amplitudes between groups
Judit et al.(617)	69 MwoA 4 MA 4MwoA+ MA, no HC	34 35	± 3 days before and after attack (37 MwoA) 1 day before (8 M) during (15 M) 1-2 days after (32 M)	68'	3.1 Hz	50x5	N1, P1 N1-P1	No significant differences in latencies and amplitudes between groups
Khalil et al.(594)	47 MA 37 MwoA 8 MwoA + MA 62 HC	40±13 (16-59) 37±13 (17-58)	Headache-free at test	37.8'	2 Hz	240	P1	**Longer latencies and increased amplitudes of P1 in M compared to HC**
Sand & Vingen (609)	6 MA 15 MwoA 22 HC	39±9 40±9	Preattack group: headache 24 hours after (8 M) Interictal: no headache after (13M)	8' 33'	2 Hz	100x2	N70, P1, N145 N70-P1 P1-N145	No significant differences in amplitudes between groups
Logi et al.(845)	40 MwoA 19 MA 30 HC	36±14 38±10	At least 10 days after attack	14.3'	1 Hz	100x2 or x3	N70, P1 P60-N70 N70-P1	No significant differences in latencies and amplitudes between groups
Yilmaz et al.(846)	16 MwoA 29 MA 22 HC	32 (11-64) 34 (15-60)	During (26 M) Between (19 M) attacks	NA	2 Hz	200	N1, P1, N2 N1-P1	**Significantly longer N2 latency in MA interictally compared to HC**
Kochar et al.(847)	25 M ? HC	NA	During and 7 days after attack	NA	NA	NA	P1	**Prolonged P1 latency during the migraine attack, normal between attacks**
Ozkul and Bozlar (619)	44 MwoA 35 MA 40 HC	36±10 34±9 33±8	± 3 days before and after attack	68'	3.1 Hz	50x5	N1, P1 N1-P1	No significant differences in latencies and first block amplitudes between groups at baseline
Coutin-Churchman & de Freytez (605)	24 MA 50 HC	? (18-53) ? (18-47)	Interictal (not specified)	30'	2 Hz	100x2	P1 N1-P1 P1-N2	**Higher amplitudes in MA as compared to HC, no differences between groups in latencies**

Study	Subjects	Age	Timing	Duration	Frequency	Stimuli	Components	Results
Ashjazadeh & Varavipour (848)	27 MA 26 MwoA 55 HC	15-57 15-48	At least 1 week after attack	NA	2 Hz	200x2	N75, P1, N145 P1-N145	**Increased latencies of P1 in MA as compared to HC**
Spreafico et al.(849)	19 MA 34 MwoA 20 HC	38 35	At least 5 days after the last attack	240.5'	3 Hz	100x15	P1	**Lower P1 latencies in M with no preventive therapy compared to HC**
Coppola et al.(743)	27 MA 20 MA+ 30 HC	32±9 33±10 33±13	± 3 days before and after attack	15'	1.55 Hz	100x6	N1, P1, N2 N1-P1 P1-N2	**No differences in latencies, significantly increased N1-P1 amplitude in last block in MA not HC**
Coppola et al.(850)	15 MwoA 15 MA 15 HC	31±10 30±10 28±8	± 3 days before and after attack	15'	3.1 Hz	100x6	N1, P1 N1-P1	No significant differences in latencies and amplitudes between groups
Di Clemente et al.(620)	15 MwoA 15 HC	28±11 24±3	± 2 days before and after attack	68'	3.1 Hz	100x6	N1, P1 N1-P1	No significant differences in latencies and first block amplitudes between groups
Shibata et al.(344)	14 MwoA 11 MA 25 HC	41±11 44±15 40±10	± 72 hours before and after attack	0.5 c.p.d. 1.0 c.p.d. 4.0 c.p.d.	1 Hz	100x2	N75, P1, N135 P50-N75 N75-P1 P1-N135	**Increased N135 latency in M compared to HC at 4.0 c.p.d. Increased amplitudes with high contrasts and high spatial frequency, P100-N135 significantly increased at all spatial frequencies; P50-N75 at 1.0 and 4.0 c.p.d. and P100-N135 at 4.0 c.p.d.**
Sand et al.(623)	33 MwoA 8 MA 31 HC	37±13 37±16 40±11	Preattack (13 M) Attack (13 M) Postattack (10 M) Interictal (± 72 hours before and after attack; all M)	31' 62'	0.95 Hz	50x4	N1-P1 P1-N2	**Increased P1-N2 amplitudes in pre-attack phase as compared to interictal phase, as well as compared to MwoA and HC Increased N1-P1 amplitudes in MA as compared to MwoA and HC**
Sand et al.(624)	33 MwoA 8 MA 31 HC	37±13 37±16 40±11	Preattack (13 M) Interictal (±72 hours before and after attack)	31' 62'	0.95 Hz	50x4	N1-P1 P1-N2	No significant differences in amplitudes between HC and M **Increased P1-N2 amplitudes for medium and large checks and higher N1P1 amplitude for large checks in MA as compared to MwoA**
Marinis et al.(598)	40 MA 40 MwoA 40 HC	32±8 32±9 32±8	At least 72 hours after the last attack	38'	1 Hz	100x2	P1	No significant differences in latencies between groups

Study	Subjects	Age	Timing	Spatial	Temporal	Averages	Components	Results
Shibata et al.(851)	10 MA 10 MwoA 20 HC	39 (20-57) 41 (20-58) 39 (20-60)	At least 72 hours after and 48 hours before an attack	0.5 c.p.d. 2.0 c.p.d.	5 Hz 10 Hz	6 to 15s each	Ampl. and phase of 2nd and 4th harmonic (2F and 4F)	**For 2F: At 0.5 c.p.d. increased amplitude in M compared to HC.** **4F: At 2.0 c.p.d. significantly increased amplitude in MA compared to MwoA and HC at 10 Hz, high contrast**
Boylu et al.(589)	41 M ? HC	NA	NA	NA	NA	NA	N75, P1, N145 N75-P1	**Longer N75 and P1 latencies and lower amplitudes in migraine; N145 longer in M with longer disease**
Khalil et al.(599)	47 MA 62 HC	16-59	At least 3 days after an attack	38'	2 Hz	240	P1	No significant differences in amplitudes between groups
Nguyen et al.(590)	26 MwoA 19 MA 30 HC	28±6 (20-41) 33±6 (19-43) 26±7 (19-46)	At least 7 days after an attack 4 M had headache 72 hours after	48' 15' 960'	1 Hz 8.3 Hz	200 (100x2)	N75, P1, N135	**Reduced P1 amplitude for MA (transient PR-VEP) as compared to MwoA and HC**
Shibata et al.(780)	12 MwoA 12 MA 12 HC	41 (20-59) 43 (20-60) 42 (20-60)	± 72 hours before and after attack	0.5 c.p.d. 1.0 c.p.d. 2.0 c.p.d. 4.0 c.p.d.	7.5 Hz	20x4	Steady-state VEPs	**Increased amplitudes in MA in response to 2.0 c.p.d. as compared to MwoA and HC**
Coppola et al.(347)	21 MwoA 22 MA 22 Mict 21 HC	27±7 31±10 34±12 28±8	Interictal: ± 3 days before and after attack Ictal: ± 12 hours around attack	15'	1.55 Hz	100x6	N1-P1	No significant differences in first block or last block amplitudes between groups
Omland et al.(625)	12 MA 15 MwoA 34 HC	28±8 31±10	± 48 hours before and after attack	8' 65'	1.5 Hz	100x6	N70, P1, N145 N70-P1 P1-N145	No significant differences in latencies or amplitudes between groups
Di Lorenzo et al.(852)	14 MwoA 4 MA 18 HC	39 (19-54) 39	± 3 days before and after attack	15'	1.55 Hz	100x6	N1, P1, N2 N1-P1 P1-N2	No significant differences in latencies or amplitudes between groups
Vigano et al.(853)	13 MwoA 11 HC	29±5 26±6	± 72 hours before and after attack	15 mm side	3.1 Hz	100x6	N1-P1 P1-N2	No significant differences in first block amplitudes between groups
Lisicki et al.(854)	30 M 30 HC (15 with a first-	27±7 28±9 25±3	± 72 hours before and after attack	14'	3.1 Hz	100x6	N1-P1	**Reduced first block amplitudes in M and HC with first-degree relatives with migraine,**

	degree relative with M, and 15 without)							**negative correlation with habituation slope**
Omland et al.(855)	25 Mint (14 MwoA 11MA) 7 Mpreict (3 MwoA, 4 MA) 32 HC	27±8 27±9 30±10	Pre-ictal: < 48h before attack Interictal: ±48 hours before and after attack	8' 65'	1.5 Hz	100x6	N70-P1 P1-N145	No significant differences in amplitudes between groups at baseline
Ambrosini et al.(856)	13 MwoA 15 HC	33±10 (18-55) 30±8 (21-44)	± 3 days before and after attack	68'	3.1 Hz	100x6	N1-P1	No significant differences in amplitudes between groups
Coppola et al.(741)	27 MA 20 MA+ 30 HC	32±9 33±10 33±13	± 3 days before and after attack	15'	1.55 Hz	100x6	N1, P1, N2 N1-P1 P1-N2	**Increased last block amplitudes in M compared to HC**
Rauschel et al.(857)	41 M 40 HC	30±10 28±8	± 48 hours before and after attack	51'	3 Hz	75x6	N75-P1	No significant differences in amplitudes between groups
Omland et al.(626)	24 MwoA 15 both MwoA and MA 2 MA 30 HC	39±10 (19-56) 38±11 (21-59)	± 2 days before and after attack	16'	1.50 Hz	100x6	N70, P1, N145 N70-P1 P1-N145	No significant differences in latencies or first block amplitudes between groups
Verroiopoulos et al.(858)	15 MA 23 MwoA 20 HC	39±9 48±12 47±11	± 24 hours before and after attack	58.8'	1 Hz	200	P1 N80-P1	No significant differences in latencies or amplitudes between groups
El-Shazly et al.(591)	60 MA 30 HC	31±3 31±4	± 3 days before and after attack or during aura	60' (48'-72') Small: 16' Large: 64'	1 Hz	100x2	N75, P1 N75-P1	**P1 latency significantly longer and lower P1 amplitude during aura as compared to interictal MA and HC**
Kalita et al.(600)	65 M 30 HC	34±12 31±8	Phase not controlled, presence of headache at session noted	12'x16'	3 Hz	100x5	N75, P1	No significant differences in first block amplitudes between groups
Susvirkar et al.(595)	40 M 40 HC	21±0.4 21±0.4	± 3 days before and after attack	NA	1 Hz	300x4	N75, P1, N145	**Slower N75 and N145 latencies and increased P1 amplitudes in M as compared to HC**
Coppola et al.(859)	19 MA 22 MwoA 14 HC	30±10 29±8 30±6	± 3 days before and after attack or during attack (10 M)	15'	1 Hz	40x10	P1 N75-P1	No significant differences in latencies or amplitudes between groups at baseline

Kalita et al.(860)	91 M 25 HC	32±11 33±11	NA	12'x16'	3 Hz	100x5	N75, P1	**Significantly increased P1 amplitude during the first block as compared to HC**

Units of measurement: visual angle in minutes of arc ('); cycles per degree (c.p.d.); hertz (Hz). Abbreviations: migraine without aura (MwoA), migraine with aura (MA), migraine (M), transient ischemic attack (TIA), episodic tension-type headache (ETH), chronic tension-type headache (CTH), total number of patients with migraine with aura (MAtot), complex neurological aura (MA+), headache-free control (HC). Bold writing represents a significant group effect.

10.2 Appendix 2

Supplementary Table 2. A summary list of studies, in patients with migraine, related to habituation and specifically event-related potential (ERP) component latencies, amplitudes, and peak-to-peak amplitude differences in response to Pattern-Reversal stimulation.

Ref.	No of subjects and diagnosis	Mean age±SD (range)	Timing of session	Spatial freq.	Temp. freq.	No of trials	ERPs	Principal findings
Schoenen et al.(341)	27 MwoA 9 MA 16 HC	32 33	At least 1 week after attack	8'	3.1 Hz	50x5	N1-P1 P1-N2	**Loss of amplitude habituation in M, normal habituation in HC Potentiation of N1-P1 and P1-N2 amplitudes in M compared to HC**
Afra et al.(616)	25 MwoA 15 MA 25 HC	36 30	At least 5 days after attack	8'	3.1 Hz	100x15	N1-P1 P1-N2	**Loss of amplitude habituation and potentiation in M, normal hab. in HC**
Wang et al.(606)	22 MwoA 13 ETH 20 CTH 26 HC	35±10 27±10 28±8 32±12	At least 1 week after attack	8'	3 Hz	50x5	N1-P1 P1-N2	**Loss of amplitude habituation and potentiation of N1-P1 and P1-N2 amplitudes in M as compared to ETH, CTH, and HC**
Oelkers et al.(604)	13 MwoA 13 MA 28 HC	29±6 27±4	± 3 days before and after attack	0.5 c.p.d. 1.0 c.p.d. 2.0 c.p.d. 4.0 c.p.d.	1 Hz	50x5	N1-P1 P1-N2	No significant differences in habituation between groups (normal habituation)
Sándor et al.(861)	40 MwoA (20 parents and their children)	44±8 17±6	± 3 days before and after attack	8'	3.1 Hz	50x5	N1, P1	**Similar lack of habituation patterns in related migrainous pairs**
Áfra et al.(608)	12 MA 10 HC	34±16 28±6	± 3 days before and after attack	68'	3.1 Hz	50x5	N1-P1	No significant differences in habituation between groups (normal habituation)
Áfra et al.(607)	37 MwoA 22 MA 23 HC	36±11 27±7	± 3 days before and after attack	68'	3.1 Hz	50x5	N1-P1	**Loss of amplitude habituation in M as compared to HC Negative correlation between 1st block amplitude and habituation**
Judit et al.(617)	69 MwoA 4 MA 4MwoA+ MA	34 35	± 3 days before and after attack (37 MwoA) 1 day before (8 M) during (15 M) 1-2 days after attack (32 M)	68'	3.1 Hz	50x5	N1-P1	**Loss of amplitude habituation in M interictally, normalization just before and during the attack**

Study	Subjects	Age	Timing	Duration	Frequency	Stimulus	Components	Findings
Sand & Vingen (609)	6 MA 15 MwoA 22 HC	39±9 40±9	Preattack group: headache 24 hours after session (8 M) Interictal: no headache after (13 M)	8' 33'	2 Hz	100x2	N70-P1 P1-N145	No significant differences in habituation between M and HC to either 8' or 33' checks Neither HC nor M habituate to 33' checks
Bohotin et al.(586)	20 MwoA 10 MA 24 HC	34±10 24±3	± 3 days before and after attack	8'	3.1 Hz	100x6	N1-P1 P1-N2	**Loss of amplitude habituation, potentiation in M as compared to HC before rTMS**
Ozkul & Bozlar (619)	44 MwoA 35 MA 40 HC	36±10 34±9 33±8	± 3 days before and after attack	68'	3.1 Hz	50x5	N1-P1	**Loss of amplitude habituation in M as compared to HC Habituation negatively correlated with first block amplitude in HC and MwoA**
Di Clemente et al.(620)	15 MwoA 15 HC	28±11 24±3	± 2 days before and after attack	68'	3.1 Hz	100x6	N1-P1	**Loss of amplitude habituation and potentiation in M as compared to HC**
Coppola et al. (844)	15 MwoA 15 MA 15 HC	31±10 30±10 28±8	± 3 days before and after attack	15'	3.1 Hz	100x6	N1-P1	**Loss of amplitude habituation and potentiation in M as compared to HC**
Fumal et al.(621)	6 MwoA 2 MA 8 HC	23±1 23±2	± 3 days before and after attack	8'	3.1 Hz	100x6	N1-P1	**Loss of amplitude habituation and potentiation at baseline in M compared to HC**
Magis et al.(781)	24 MwoA 28 MA	32±14	72 hours before and after attack)	51' 33"	3.1 Hz	100x6	N1-P1	**Habituation deficit in M is more marked in patients with no mutation of the MTHFR C677T polymorphism as compared to those that are homozygous Lower first block amplitude correlated to greater habituation deficit**
Sand et al.(623)	33 MwoA 8 MA 31 HC	37±13 37±16 40±11	Preattack (13 M) Attack (13 M) Postattack (10 M) Interictal (± 72 hours before and after attack; all M)	31' 62'	0.95 Hz	50x4	N1-P1 P1-N2	No significant differences in habituation between M and HC to large check sizes

Sand et al.(624)	33 MwoA 8 MA 31 HC	37±13 37±16 40±11	Preattack (13 M) Interictal (±72 hours before and after attack)	31' 62'	0.95 Hz	50x4	N1-P1 P1-N2	No differences in habituation between groups for large checks (no habituation in both M and HC)
Coppola et al.(862)	18 MwoA 18 HC	31 27	± 3 days before and after attack	15'	3.1 Hz	100x6	N1-P1 P1-N2	**Loss of amplitude habituation and potentiation in MwoA as compared to HC at baseline**
Coppola et al.(863)	12 MwoA 19 HC	28±6 26±4	± 3 days before and after attack	15'	3.1 Hz	100x6	N1-P1	**Loss of amplitude habituation and potentiation in MwoA as compared to HC at baseline**
Coppola et al.(864)	17 MwoA 17 HC	29±12 29±11	± 3 days before and after attack	15'	3.1 Hz	100x6	N1-P1	**Loss of amplitude habituation and potentiation in MwoA as compared to HC at baseline**
Hansen et al.(865)	9 FHM 7 HC	38 (20-63) 29 (28-31)	Headache-free at recording	68'	3.1 Hz	100x6	N1-P1	**FHM habituated more than HC (who did not significantly habituate)**
Shibata et al.(780)	12 MwoA 12 MA 12 HC	41 (20-59) 43 (20-60) 42 (20-60)	± 72 hours before and after attack	0.5 c.p.d. 1.0 c.p.d. 2.0 c.p.d. 4.0 c.p.d.	7.5 Hz	20x4	Steady-state VEPs	No habituation in HC or lack of habituation in M
Coppola et al.(347)	21 MwoA 22 MA 22 Mict 21 HC	27±7 31±10 34±12 28±8	Interictal: ± 3 days before and after attack / Ictal: ± 12 hours before or after	15'	1.55 Hz	100x6	N1-P1	**Loss of amplitude habituation in MwoA and MA interictally but normal habituation in HC and Mict**
Omland et al(625)	15 MwoA 12 MA 34 HC	27±8 31±10	± 48 hours before and after attack	8' 65'	1.5 Hz	100x6	N1-P1 P1-N2	No significant differences in habituation measures between HC and M (normal habituation)
Vigano et al.(853)	13 MwoA 11 HC	29±5 26±6	± 72 hours before and after attack	15 mm side	3.1 Hz	100x6	N1-P1 P1-N2	No difference in habituation of N1-P1 between MwoA and HC **Loss of amplitude habituation of P1-N2 in MwoA but not HC**
Bednar et al.(866)	39 M 36 HC	41±11 (18-62) 37±12 (18-62)	Interictal: ± 72 hours before and after attack (19 M) Ictal (10 M)	13'	2 Hz	60x5	N75-P1 P1-N145	**Loss of amplitude habituation in M both interictally, ictally, and during treatment as compared to HC; particularly to high contrast**

Omland et al.(855)	25 Mint (14 MwoA, 11MA) 7 Mpreict (3 MwoA, 4 MA) 32 HC	27±8 27±9 30±10	Pre-ictal: < 48h before attack Interictal: ±48 hours before and after attack	8' 65'	1.5 Hz	100x6	N70-P1 P1-N145	No difference in habituation between Mint and HC at baseline
Ambrosini et al.(856)	13 MwoA 15 HC	33±10 (18-55) 30±8 (21-44)	± 3 days before and after attack	68'	3.1 Hz	100x6	N1-P1	**Loss of amplitude habituation and potentiation at baseline in MwoA compared to HC**
Coppola et al.(741)	27 MA 20 MA+ 30 HC	32±9 33±10 33±13	± 3 days before and after attack	15'	1.55 Hz	100x6	N1-P1 P1-N2	**Loss of N1-P1 amplitude habituation in M as compared to HC**
Rauschel et al.(857)	41 M 40 HC	30±10 28±8	± 48 hours before and after attack	51'	3 Hz	75x6	N75-P1	**Loss of amplitude habituation and potentiation at baseline in M compared to HC**
Ambrosini et al.(867)	624 EM 439 MwoA 185 MA 360 HC	(25-37)	± 3 days before and after attack	68' 15'	3.1 Hz	50x5 100x6	N1-P1	**Loss of amplitude habituation in M interictally compared to HC**
Omland et al.(626)	24 MwoA 15 both MwoA and MA 2 MA 30 HC	39±10 (19-56) 38±11 (21-59)	± 2 days before and after attack	16'	1.50 Hz	100x6	N70-P1 P1-N145	No significant differences in habituation measures between HC and M (normal habituation)
Verroiopoulos et al.(858)	15 MA 23 MwoA 20 HC	39±8 48±12 47±11	± 24 hours before and after attack	58.8'	1 Hz	200	N80-P1	No significant differences in habituation measures between HC and M (normal habituation)
Di Lorenzo et al.(852)	14 MwoA 4 MA 18 HC	39 (19-54) 39	± 3 days before and after attack	15'	1.55 Hz	100x6	N1-P1 P1-N2	**Loss of amplitude habituation at baseline in M compared to HC**
Lisicki et al.(854)	30 M 30 HC (15 with a first-degree relative with M, and 15 without)	27±7 28±9 25±3	± 72 hours before and after attack	14'	3.1 Hz	100x6	N1-P1	**Loss of amplitude habituation in M and HC with relative with migraine compared to HC without first-degree relatives with migraine**
Ince et al.(868)	52 M 35 HC	36±9 34±10	± 3 days before and after attack	NA	3.1 Hz	100x10	N1-P1 P1-N2	**Loss of amplitude habituation at baseline in M compared to HC**
Kalita et al.(600)	65 M 30 HC	34±12 30.7±8	Phase not controlled, presence of headache noted	12x16'	3 Hz	100x5	N75, P1	**Impaired habituation of N75 in M compared to HC at baseline**

Lisicki et al.(869)	25 MwoA	26±6	± 72 hours before and after attack	14'	3.1 Hz	100x6	N1-P1	**Preserved habituation in patients that do not perceive stress as a trigger, loss of amplitude habituation in rest**
Susvirkar et al.(595)	40 M 40 HC	21±0.4 21±0.4	± 3 days before and after attack	NA	1 Hz	300x4	P1	**Loss of amplitude habituation and potentiation in M compared to HC**
Kalita et al.(860)	91 M 25 HC	32±11 33±11	NA	12'x16'	3 Hz	100x5	N75, P1	**Loss of amplitude habituation and potentiation in M compared to HC**

Units of measurement: visual angle in minutes of arc ('); angle in seconds of arc ("), cycles per degree (c.p.d.); hertz (Hz). Abbreviations: migraine without aura (MwoA), migraine with aura (MA), migraine (M), episodic migraine (EM), episodic migraine interictally (EMint), episodic migraine ictally (EMict), migraine during the ictal phase (Mict), migraine in the pre-ictal phase (Mpreict), chronic migraine (CM), episodic tension-type headache (ETH), chronic tension-type headache (CTH), total number of patients with migraine with aura (MAtot), complex neurological aura (MA+), headache-free control (HC). Bold writing represents a significant group effect.

10.3 Appendix 3

Marti-Marca, A., Vilà-Balló, A., Torralba Cuello, M., Soto-Faraco, S., & Pozo-Rosich, P. (2022). The influence of temporal unpredictability on the electrophysiological mechanisms of neural entrainment. Psychophysiology, 59(11), e14108. © 2022 The Authors. Psychophysiology published by Wiley Periodicals LLC on behalf of Society for Psychophysiological Research. https://doi.org/10.1111/psyp.14108
Impact factor of journal: 4.348 (2021)

ORIGINAL ARTICLE

The influence of temporal unpredictability on the electrophysiological mechanisms of neural entrainment

Adrià Vilà-Balló[1,2] | Angela Marti-Marca[1] | Mireia Torralba Cuello[3] | Salvador Soto-Faraco[3,4] | Patricia Pozo-Rosich[1,5]

[1]Headache and Neurological Pain Research Group, Vall d'Hebron Research Institute, Department of Medicine, Autonomous University of Barcelona, Barcelona, Spain

[2]Department of Psychology, Faculty of Education and Psychology, University of Girona, Girona, Spain

[3]Multisensory Research Group, Center for Brain and Cognition, Pompeu Fabra University, Barcelona, Spain

[4]Catalan Institution for Research and Advanced Studies (ICREA), Barcelona, Spain

[5]Headache Unit, Department of Neurology, Vall d'Hebron University Hospital, Barcelona, Spain

Correspondence
Adrià Vilà-Balló, Headache Unit, Hospital Universitari Vall d'Hebron, Passeig de la Vall d'Hebron, 119-129, Barcelona 08035, Spain.
Email: adriavilaballo@gmail.com

Funding information
"la Caixa" Foundation, Grant/Award Number: LCF/PR/PR16/51110005; Fundació Institut de Recerca Hospital Universitari Vall d'Hebron", Grant/Award Number: VHIR/BEQUESPREDOC/2020/MARTI; Operative Programme for Catalunya 2014-2020; Open Access funding provided thanks to the CRUE-CSIC agreement with Wiley

Abstract

Neural entrainment, or the synchronization of endogenous oscillations to exogenous rhythmic events, has been postulated as a powerful mechanism underlying stimulus prediction. Nevertheless, studies that have explored the benefits of neural entrainment on attention, perception, and other cognitive functions have received criticism, which could compromise their theoretical and clinical value. Therefore, the aim of the present study was [1] to confirm the presence of entrainment using a set of pre-established criteria and [2] to establish whether the reported behavioral benefits of entrainment remain when temporal predictability related to target appearance is reduced. To address these points, we adapted a previous neural entrainment paradigm to include: a variable entrainer length and increased target-absent trials, and instructing participants to respond only if they had detected a target, to avoid guessing. Thirty-six right-handed women took part in this study. Our results indicated a significant alignment of neural activity to the external periodicity as well as a persistence of phase alignment beyond the offset of the driving signal. This would appear to indicate that neural entrainment triggers preexisting endogenous oscillations, which cannot simply be explained as a succession of event-related potentials associated with the stimuli, expectation and/or motor response. However, we found no behavioral benefit for targets in-phase with entrainers, which would suggest that the effect of neural entrainment on overt behavior may be more limited than expected. These results help to clarify the mechanistic processes underlying neural entrainment and provide new insights on its applications.

KEYWORDS
alpha rhythm, EEG, entrainment, endogenous oscillations, phase synchronization, temporal unpredictability

1 | INTRODUCTION

The synchronization of internal oscillations to rhythmic external events, known as neural entrainment, is thought to help organisms anticipate the environment's temporal structure (Obleser & Kayser, 2019; Thut et al., 2011; Zoefel et al., 2018). In particular, the alignment of the high excitability phase of the neural oscillation with the onset of the periodic, sensory input, may explain this predictive benefit by amplifying the relevant information for preferential processing and suppressing the random, less meaningful inputs (Large & Jones, 1999; Schroeder & Lakatos, 2009; Haegens & Zion Golumbic, 2018; Zoefel et al., 2018; Lakatos et al., 2019, for review). Recently, neural entrainment has been postulated as a useful tool for diagnostic and therapeutic procedures (Guo et al., 2020; Lakatos et al., 2013, 2019; Thaut et al., 2015).

Notwithstanding, some criticisms to the proposal that neural entrainment constitutes an anticipatory mechanism could compromise its theoretical importance and clinical value. One criticism is that many experiments have not managed to successfully provide evidence that entrainment is produced by the synchronization of already existing endogenous oscillations to rhythmic external stimuli, rather than being the result of a succession of event-related potentials (ERPs) (Capilla et al., 2011; Keitel et al., 2014; for review Zoefel et al., 2018). A second, important criticism is that, in past experiments, the temporal structure of the entrainer events as well as the underlying structure of the task did not change across trials, and therefore target onsets were highly predictable not only based on the entrainer periodicity, but also due to the time of target appearance. Under these conditions, behavioral benefits would most likely be a consequence of expectative mechanisms or high-level attention orienting strategies, rather than neural entrainment (for review see Helfrich et al., 2019; Obleser & Kayser, 2019; Zoefel et al., 2018). Finally, it is crucial to note the proper use of terminology. Recently, several authors have stressed the importance of using the term neural entrainment only when certain predetermined criteria are met (Haegens & Zion Golumbic, 2018; Helfrich et al., 2019; Obleser & Kayser, 2019), and using a different term such as "entrainment in the broad sense", "neural tracking", or "rhythmic tracking" otherwise. This subtle but important distinction allows one to differentiate synchronization of an independent internal and external rhythm, from a more general rhythmic response that could be explained by a different mechanistic process, such as resonance (Helfrich et al., 2019). To counteract the criticisms and characterize the observed phenomena, the following requirements have been proposed to delineate neural entrainment in the narrow sense: [1] The endogenous neural oscillations,

also known as eigenfrequencies, should occur spontaneously, without a driving, exogenous rhythm and synchronize to the external rhythm when the entrainer is present (Obleser & Kayser, 2019; Thut et al., 2011). [2] The neural oscillator should be resilient to perturbation, adapting its frequency within certain bounds (Obleser & Kayser, 2019). [3] Neural oscillators should not recover their eigenfrequency right away, rather they should remain at the entrained rhythm for a number of cycles, post-entrainer offset (Obleser & Kayser, 2019; Thut et al., 2011).

Recent studies investigating neural entrainment-related behavioral benefits have yet to resolve the criticisms highlighted above (Kösem et al., 2018; ten Oever et al., 2014; Wiesman & Wilson, 2019). A study by Kizuk and Mathewson (2017) explored the impact of neural entrainment on visual attention while addressing the first criticism. In their EEG study, participants discriminated the location of lateralized targets following a spatially informative cue and a stream of rhythmic, bilateral entrainers. Kizuk and Mathewson (2017) found the expected spatial attention advantage, and a rhythmicity effect so that targets presented in-phase (in-time) in contrast to the ones presented anti-phase (out-of-time), with the entrainers were better detected, especially at unattended locations. Importantly, they observed that neural entrainment persisted for two cycles post-entrainer offset even on target-absent trials. These findings support the presence of neural entrainment. However, activity during target-absent trials could still be contaminated, for instance by motor responses, given that participants were instructed to always guess a response. Furthermore, potential anticipatory confounds could be more exacerbated because the fixed length of the entrainer stream made target appearance highly predictable. Thus, despite using in-phase and anti-phase, the task did not completely address the second criticism about the potentially confounding effect of anticipation.

The aim of the present study was to examine whether endogenous oscillations synchronize to an external rhythm and meet the necessary requirements for neural entrainment, and whether the characteristic effects of this endogenous alignment continue to be observed when temporal predictability is strongly reduced. We reproduced the conditions in Kizuk and Mathewson (2017), but with a variable number of entrainers, increased target-absent trials, and instructions for participants to avoid guessing and respond only if they detected a target. These changes increase temporal unpredictability, avoiding the contamination of target-absent trials from motor response. The primary hypotheses of the present study were that, if the conditions for neural entrainment are met, then entrained, endogenous oscillations should persist and their effects on behavior, despite reducing temporal predictability. To

test this, three hypothesis-driven predictions were evaluated: (i) significant cross-coherence between the external rhythm and the neural oscillatory activity, (ii) persistence of phase alignment after entrainer offset for at least two cycles, and (iii) behavioral benefits of entrainment as seen by higher hit rates and faster reaction-times to targets in-phase with the previous entrainers, as compared to anti-phase.

2 | METHOD

2.1 | Participants

Thirty-six right-handed women (21.69 ± 2.06 years, range: 18–28 years) with normal or corrected-to-normal vision and hearing, and no previously diagnosed physical, neurological, or mental health conditions were initially selected to take part in this research study. The use of pharmaceutical or non-pharmaceutical drugs was also considered as a criterion for exclusion. The present data were collected from the control group of a prospective, case–control study on migraine (manuscript in preparation). For this reason, after providing their informed consent and before the EEG recording, participants filled out the Adult ADHD Self-Report Scale (ASRS) (Kessler et al., 2005) and the Beck Depression Inventory-II (BDI-II) (Beck et al., 1996). The entire session lasted approximately 3 h. At the end of the session, participants provided their payment details and were debriefed.

Six participants were discarded for the following reasons: mean false alarm rate > chance level 30% ($N = 1$), mean hit rate >90% on invalidly cued trials ($N = 2$; see Individual Detection Threshold section), technical problems ($N = 2$), and less than 50 trials per condition (see EEG analysis section) post-EEG artifact rejection ($N = 1$). The final sample consisted of 30 individuals (21.70 ± 2.18 years, range: 18–28 years). Scores on the psychological measures related to attention deficit disorder (ASRS 1.73 ± 1.62) and depression (BDI-II 4.83 ± 4.57) remained within the normal range. All participants gave their informed consent prior to participation and were compensated with 25€. This research was approved by the research Ethics Board at the Vall d'Hebron Hospital (PR [AG] 376/2017).

2.2 | Procedure

The experimental sessions were performed in a chamber with acoustic and electromagnetic attenuation. The lights were dimmed, and participants sat at a distance of approximately 0.75 m from the screen throughout the entire procedure. A cued, visual detection paradigm, with bilateral entrainment (see Figure 1a), based on Kizuk and Mathewson (2017), was used to assess attention on target-present and target-absent trials. Stimuli were programmed and presented, using custom-made scripts, with MATLAB R2015a and Psychophysics Toolbox Version 3.0.13 (Brainard, 1997; Kleiner et al., 2007), running on Windows XP. All stimuli were presented on a Sony Multiscan G520 Trinitron Color Monitor (CRT screen, resolution: 1024×768, 120 Hz refresh rate, background luminance: 21 cd/m2).

A black, fixation cross (height, width: 0.5°) was present throughout the entire duration of the experiment. Participants were asked to fixate on the cross throughout the entire duration of the trial, hence orienting their attention covertly. Each trial started with a black, directional arrow cue (isosceles triangle, height: 1°, width: 0.5°), which appeared 5.26° above the fixation cross for a duration of 200 ms, followed by a fixation period of 675 ms. After the fixation period, a stream of entrainers, of variable length (8–12; balanced across conditions, equiprobable within each block) was presented bilaterally at a rate of 12 Hz. The entrainers consisted of annuli (luminance: 7.3 cd/m2, 30.47% gray, external annulus diameter of 2.25°, internal annulus diameter of 1.25°, presented 1.13° above, and 4.1° to the left or right of the fixation cross), which were flashed on the screen for 8.33 ms and interleaved by blank intervals of 75 ms (hence, 83.33 periods for a 12 Hz rhythm). Entrainers were synchronous and of equal duration on both sides of the display. We varied the number of entrainers in each stream between 8 and 12, on a trial-by-trial basis, to reduce inherent task predictability.

After the last entrainer, a target was presented on 70% of trials, which consisted of two bilateral annuli (equal to the entrainers), but with a Gabor patch (spatial frequency: 1.68 cycles/pixel, orientation 90°; sigma 2.98 pixels; phase 0 cycles) on one side (for each block: 28 per cued side and 14 per SOA), whose contrast was set individually according to a detection threshold (see below). On the remaining 30% of trials, the target was absent and neither the annuli nor the resulting Gabor patch were presented (for each block: 12 per cued side and 6 per SOA). Participants were asked to respond to the target location on target-present trials (left/right side, pressing the z and m keys with their left and right index finger, respectively), and withhold their response if they did not see a target (such as would be the case on target-absent trials). Participants had a response deadline of 800 ms and were told to be conservative (refrain from guessing) if unsure, to prevent a high false alarm rate. The inter-trial interval (ITI) was chosen randomly between 500 ms and 700 ms.

On target-present trials, the target could appear at the location indicated by the spatial cue (valid trials, ~71%) or at the opposite location (invalid trials, ~29%). In addition, the
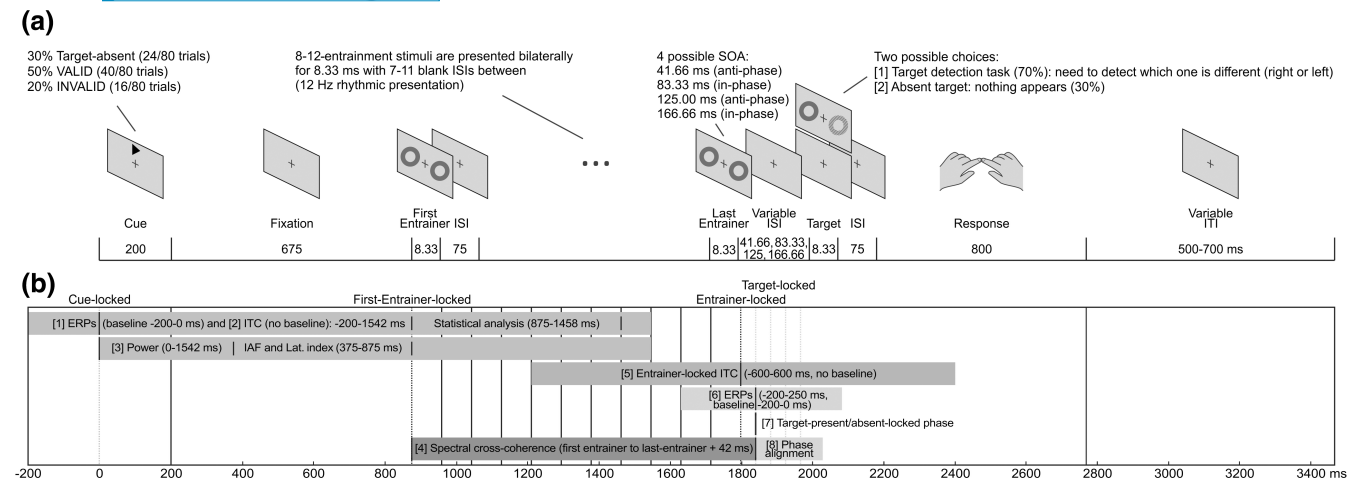
FIGURE 1 (a) Schematic illustration of a single trial of the cued, visual detection paradigm with bilateral entrainment. Participants were instructed to fixate on a central cross at all times. Each trial began with the appearance of a directional cue arrow pointing either to the right or to the left. After a fixed delay, a flashing sequence of synchronous bilateral annuli (entrainers) of variable length (8 to 12), with fixed inter-stimulus intervals, was presented around the target location. The inter-stimulus interval between the last entrainer and the target consisted of one of four possible options, with two target onsets occurring in-phase and two anti-phase with the rhythmic entrainers. On 70% of trials, otherwise referred to as target-present trials, a target could be presented at the spatially valid location (gray) or the spatially invalid one (black) and consisted of the same bilateral annuli but with one of the annuli containing a Gabor patch. Gabor patch contrast was set to a 60% detection threshold using a single-interval adjustment matrix prior to beginning the detection task. On the remaining 30% of trials, referred to as absent-target trials, the target was absent, and no annuli or Gabor patch were presented. Finally, participants were asked to indicate using the appropriate response keys the side on which the target had appeared, or to withhold their response if they did not see a target. The next trial began after a variable inter-trial interval. (b) Schematic illustration of the time windows used for each one of the analyses. For illustration purposes, entrainer stream length was fixed at 12 entrainers and target-locked analyses were fixed to the first anti-phase target onset. The first set of analyses were carried out using cue-locked data and were comprised of the following and their respective time windows. [1] ERP/SSVEP analyses, time window: 200 ms to 1542 ms (baseline: −200 ms to 0 ms). [2] ITC analysis, same analysis as [1] but without a baseline. The time window of interest to assess that data were significantly concentrated throughout the entire entrainer stream was from 875 ms to 1458 ms (from the 1st to the 8th entrainer). [3] Power analyses to explore IAF and lateralized alpha activity, time window: 0 ms to 1542 ms, once again no baseline was employed. The spectral power for the IAF and time-frequency for the lateralization index analysis were obtained from 375 ms to 875 ms. Additionally, [4] for the spectral cross coherence analysis, we selected from the onset of the first entrainer to the offset of the last entrainer plus one half-cycle (+42 ms), which corresponds to the first anti-phase target onset. The time window varied depending on the last entrainer (from 8 to 12). The next analysis was carried out using entrainer-locked data and is presented with its respective time window. Please note, that due to the variable length of the entrainer stream, the last entrainer could correspond to either one of the ordinal values between 8 and 12. [5] ITC analysis, time window: −600 ms to 600 ms, no baseline. The final set of analyses were carried out on target-locked (target-present/target-absent) data, along with their respective time windows. [6] ERP analyses, as a function of relative phase (anti-phase/in-phase) on target-present and target-absent trials, time window: −200 ms to 250 ms (baseline: −200 ms to 90 ms). [7] 12 Hz phase at target onset analysis. Here data were separately time-locked to target onset times (target-present trials) or to the moments in-time where targets were expected to occur (target-absent trials) and divided as a function of relative phase (anti-phase/in-phase). Finally, [8] to examine whether the phase continued aligned after the disappearance of the external rhythm, we restricted the analysis to target-absent correct trials. The time window was selected to contain 3 cycles of possible target onset times, where 1 cycle was equivalent to one anti-phase and consecutive in-phase presentation. The specific time window was 41.5 ms to 250 ms with respect to the last entrainer. (c) Schematic illustration of the time windows used for the control analyses which were performed using STFT instead of complex Morlet wavelets. For illustrative purposes, entrainer stream length was fixed at 12 entrainers and only one of the multiple contrasts was shown for each analysis. Please, note than the time-window and conditions employed for entrained-locked ITC [1] and for the [2] phase analyses at target-present/target-absent trials were the same as described above. [3] Circular correlations between the phase obtained at the offset of the last entrainer (10 ms post-onset) and the four target onsets (anti-phase 1, in-phase 1, anti-phase 2, and in-phase 2), on target-absent trials. [4] Circular correlation between the 12 Hz phase 166 ms pre-target onset and the reaction-times for target-present trials, separated as a function of the four possible target onset times (anti-phase 1, in-phase 1, anti-phase 2, and in-phase 2). [5] Phase (166 ms pre-target) opposition analysis between correct and incorrect trials. The four possible target onset times were collapsed into two groups (anti-phase and in-phase) to ensure we had a sufficient number of trials

rhythmic alignment of the targets was manipulated. The target could appear at four possible SOAs, two in anti-phase with the rhythmic entrainers (41.66 ms and 125.00 ms) and two in phase with the entrainers (83.33 ms and 166.66 ms). This resulted in four main conditions: spatially valid anti-phase, spatially valid in-phase, spatially invalid anti-phase, and spatially invalid in-phase. At the beginning of the experiment, participants received extensive instructions to respond as quickly as possible while maintaining accuracy.

The experimental session consisted of nine blocks of 80 trials and lasted approximately 40 minutes. Prior to the entrainment task, participants practiced using a training task with easily detectable targets, comprising 12 trials with the same trial structure as the main task (three trials of each main condition, random order). During training their performance was monitored and feedback provided. The individual detection threshold was calculated upon successful completion.

2.3 | Individual detection threshold

Stimulus contrast was adjusted to 60% of each participant's detection threshold using a single-interval adjustment matrix (SIAM) (Kaernbach, 1990). To calculate this threshold, a modified version of the entrainment task was used where the number of entrainers was fixed to 10 and only spatially valid, in-phase targets were presented. Participants were asked to indicate the side of target appearance as detailed above or withhold response in the perceived absence of a target. If the participant responded correctly (hit) the contrast was reduced according to the step size on the next trial. If they responded incorrectly (miss or false alarm) the contrast was increased by the step size on the next trial. An adjustment matrix was used to determine the step size of the resulting increment/decrement as a function of the number of reversals. Step size was set at 0.01 and was multiplied by four for the first and second reversal (step size: 0.04), by two for the third (step size: 0.02), and then maintained at 0.01 until all the reversals were complete. Once a total of 12 reversals were reached, the threshold procedure ended. The contrast values obtained during the last four reversals were averaged to calculate the final mean threshold. A separate threshold was obtained for both left and right sides. Participants with a mean hit rate higher than 90% were not considered for the study to guarantee that the spatial validity effect would be detectable and to avoid ceiling effects (Kizuk & Mathewson, 2017).

2.4 | EEG recording

Continuous EEGs (digitized, 500 Hz sampling rate, no online filters) were acquired using a BrainAmp Standard (001 10/2008) amplifier, connected to an actiCHamp Control Box (Brain Products). Data were recorded using 64 active electrodes (10–10 system). An online reference electrode was placed on the tip of the nose whereas a ground electrode was positioned at AFz in the cap. External electrodes included: left and right mastoids and vertical and horizontal electrooculograms. Impedances were kept below 10 kΩ.

2.5 | Analyses

This study followed a within-subjects design comprised of one session per participant and was not preregistered.

2.5.1 | Hazard rate

In order to obtain an objective index of task predictability and compare this index with that of Kizuk and Mathewson (2017), we decided to calculate the Hazard Rate (HR) for each target time of both tasks. We used the formula employed by Pasquereau and Turner (2015) to calculate the HR, which consisted of the probability that a target will occur at time t divided by the probability that it has not yet occurred:

$$h(t) = f(t) / [1 - F(t)]$$

where $f(t)$ referred to the probability distribution of target times and $F(t)$ is the cumulative distribution of probabilities. It is important to take into account, that our task was comprised of entrainer streams of varying lengths (five different time windows in total) and four different target appearance times post-last entrainer. Therefore, our design consisted of 12 temporal moments, from 625 ms to 1083 ms, between offset of the first entrainer and the appearance of a target.

2.5.2 | Behavioral analyses

We calculated hit rates, and RTs between spatially valid and invalid trials at each of the four SOAs (see Figure 2a–d). Trials with RTs < 100 ms or three standard deviations above the participant's mean RT on the condition (valid/invalid SOA pairings) were removed from further analyses (1.17 ± 1.00% of total trials on average, range: 0–3.04). The resulting data were analyzed to examine the effects of spatial validity and relative phase. The four SOAs were collapsed into in-phase and anti-phase conditions for the analysis. For hit rates and RTs, we ran two (spatial validity: valid/invalid) × 2 (relative phase: anti-phase/in-phase) repeated measures analyses of
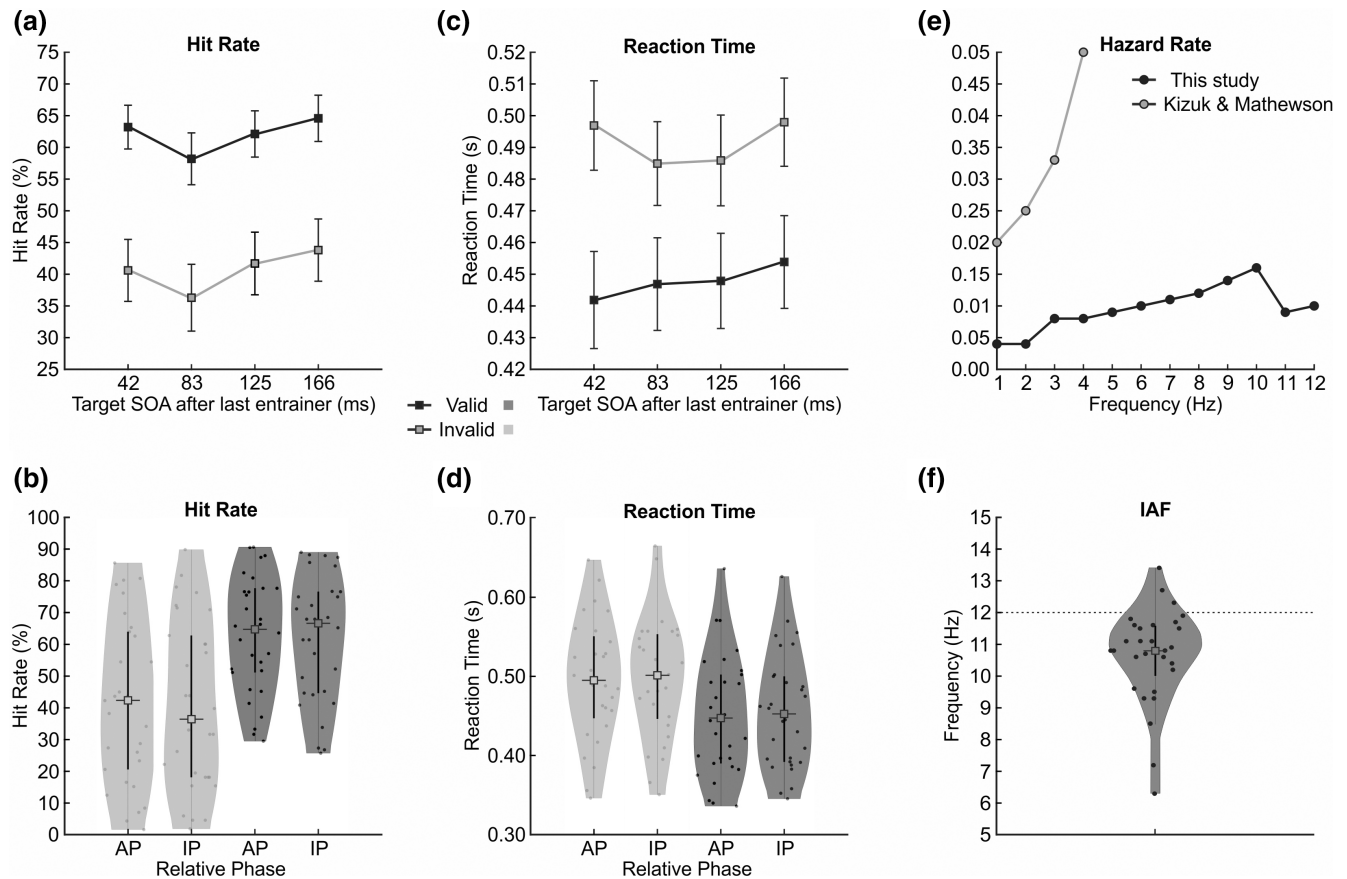
VILÀ-BALLÓ ET AL.

FIGURE 2 (a) Line graph of the mean hit rates and standard errors of the mean, as a function of relative phase (x axis) and spatial validity (separate lines). (b) Violin plots of the hit rates, separated as a function of spatial validity, while collapsing the four possible target onset times into two relative phases (anti-phase and in-phase). Dots represent individual data, the central squares the median, and vertical lines the interquartile range. (c) Line graph of the mean reaction-times and standard errors of the mean, as a function of relative phase (x axis) and spatial validity (separate lines). (d) Violin plots of the reaction-times, separated as a function of spatial validity, while collapsing the four possible target onset times into two relative phases (anti-phase and in-phase). Dots represent individual data, the central squares the median, and vertical lines the interquartile range. Line and bar colors indicate spatial validity (valid: dark gray, invalid: light gray). (e) Hazard Rate (HR) at each of the 12 times of our task and for the four times of Kizuk and Mathewson's (2017) task. (f) Violin plot of the IAF obtained between 5 and 15 Hz at the selected ROI. An alpha peak was detected in all participants with one exception

variance (rmANOVAs) where both factors were within-subjects. Post hoc t tests were carried out as needed. To correct potential violations of sphericity and estimate epsilon accordingly (Jennings & Wood, 1976), we used the Greenhouse–Geisser epsilon correction and the resulting, adjusted p values were reported. Cohen's d and f statistics were also calculated as measures of effect size for t tests and rmANOVAs, respectively (Cohen, 1992). We reported Bayes factors (BF10) for the rmANOVAs, which indicate whether the data provide evidence for the alternative model (H1) as compared to the null model (H0) (i.e., probability of the data given H1 relative to H0). This analysis was performed with JASP software, using the null model (Morey et al., 2017; Wagenmakers, Love, et al., 2018; Wagenmakers, Marsman, et al., 2018). For the model, we included spatial validity and relative phase as factors as well as their interaction.

We also added a metric to assess whether or not the participants in our study held a response bias, in either direction (more to less conservative). This measure is the response criterion, sometimes termed decision criterion, which is the mean of the z score of the hit rate and the z score of the false alarm rate (Azzopardi & Cowey, 1998).

2.5.3 | EEG preprocessing

EEG data analyses were performed using EEGLAB 13.5.4b (Delorme & Makeig, 2004), ERPLAB 7.0.0 (Lopez-Calderon & Luck, 2014), and FieldTrip version 20,161,103 (Oostenveld et al., 2011) toolboxes as well as MATLAB R2015a custom-made scripts. EEG activity was re-referenced offline to the mean activity of both mastoids. An offline 50 Hz notch filter (type

Parks-McClellan: padding factor: 2, smoothing factor: 50, sliding window length: 4, sliding window step: 1, order: 180) was applied to each recording. Phase analyses were performed without further preprocessing. For ERP analyses only, an offline Hamming windowed sinc finite impulse response (FIR) band-pass filter (zero-phase), from 0.1 to 40 Hz, was applied (high-pass: Frequency 0.1 Hz, order 16501, cutoff −6 dB; low-pass: frequency 40 Hz, order 167, cutoff −6 dB). It is important to note that no filters were used for inter-trial coherence (ITC), phase, and power analyses.

2.5.4 | EEG analyses

Please see Figure 1b for a detailed pipeline of EEG analyses and specific time windows. EEG activity was analyzed using five different time windows centered on different trial events. (1) Cue-locked analyses (from −200 ms to 1542 ms, with respect to the cue) included ERPs, power spectrum for the individual alpha frequency (IAF), time-resolved ITC, and power. (2) Cross-coherence analysis, from the onset of the first entrainer to the offset of the last entrainer plus one half-cycle (+42 ms). (3) Entrainer-locked analyses (from −600 ms to 600 ms, with respect to the last entrainer), which focused on ITC alone. (4) Target-locked analyses (−200 ms to 250 ms, with respect to the target onset), included ERPs and phase alignment at the entrainer frequency (12 Hz) at target onset times (for target-present) and times where targets should occur (for target-absent trials). (5) Phase alignment in the absence of external signal, which included three cycles of possible target onset times (a time window of interest from 41.5 ms to 250 ms, with respect to the last entrainer). These specific analyses are detailed below. In order to ensure that endogenous activity corresponded to trials where participants were attending to the task, only correct trials (i.e., hits and correct rejections) were included in the analyses. A minimum of 50 artifact-free trials for each condition was required, in order to have a non-biased estimation of the ITC (Aydore et al., 2013). For the ITC, phase alignment, and power analyses, data were reepoched with 2000 ms at both ends of the time window (or point) to avoid edge artifacts. Ocular (horizontal eye movements and blinks at points of interest) and muscular artifacts were removed through a process of visual inspection, using concatenated windows, which included cue-locked, entrainer-locked, and target-locked data. Once the artifact rejection was complete, all of the electrophysiological analyses, with the exception of the lateralized alpha activity analysis, were first carried out on the Pz electrode, to replicate (Kizuk & Mathewson, 2017). Results for the Oz electrode, where maximum ITC was observed, are also provided.

2.5.5 | IAF estimation

To estimate the IAF during the task, we selected the cue-locked epochs described above. Next, we calculated the power spectrum using a Short Time Fourier Transform (STFT, Hanning window, 4–30 Hz in 0.1 Hz steps, zero-padded to 10 s, time window: 375–875 ms post-cue). This time window was determined to avoid including ERP activity related to the cue and to ensure that we had enough cycles to estimate the frequencies of interest. The power spectrum was averaged across the electrodes of interest (PO3, POz, PO4, PO7, PO8, O1, Oz, and O2), and background noise was estimated by fitting a 1/fa curve to the power spectrum (Haegens et al., 2014; Torralba Cuello et al., 2022). A window between 5- and 15 Hz was used to calculate the individual alpha frequency peak.

2.5.6 | Event-related potentials

We extracted ERPs and Steady-State Visual Evoked Potentials (SSVEPs), for cue-locked analyses, from −200 ms to 1542 ms (baseline −200 ms to 0 ms), collapsing across target-present/target-absent trials given that this time window did not extend into the target period. For target-locked analyses, we calculated ERPs as a function of relative phase (anti-phase/in-phase) on target-present and target-absent trials from −200 ms to 250 ms (baseline −200 ms to 0 ms).

2.5.7 | Inter-trial coherence

We examined whether the effect of entrainment began with the first entrainers, continued throughout the entrainer period, and extended beyond the entrainers into the target-present/target-absent time windows. We obtained activity, locked to the onset of the cue (cue-locked) and to the onset of the last entrainer (entrainer-locked), respectively. Single-trial EEG epochs were convoluted via frequency-domain multiplication, in which the Fourier-derived spectrum was multiplied by the spectrum of a complex Morlet wavelet (variable number of cycles, 4–10 in logarithmic steps, wavelet time −2 to +2 s), and the inverse Fourier transform was taken. A separate time series of complex wavelet coefficients was obtained for each frequency, with a linear increase from 1 to 40 Hz, in 1 Hz steps. These complex coefficients, containing both real and imaginary components, were used to derive the ITC (Cohen, 2015), for each trial, time point, frequency, and participant. ITC is an index that measures phase consistency across trials, it can take values ranging from 0 (randomly distributed phases) to 1 (perfectly aligned phases).

For cue-locked epochs (from −2200 ms to 3542 ms, window of interest −200 ms to 1542 ms), ITC was calculated mixing epochs from both target-present and target-absent correct trials. For entrainer-locked epochs (from −2600 ms to 2600 ms, window of interest from −600 ms to 600 ms), ITC was separately obtained for target-present and target-absent correct trials, collapsing anti-phase and in-phase trials. No baseline was used.

To statistically assess that data were significantly concentrated throughout the entire entrainer stream, we used a Montecarlo permutation test (Maris & Oostenveld, 2007) on cue-locked data (from the 1st to the 8th entrainer, or a time window of interest from 875 ms to 1458 ms). Null ITC distributions were calculated for each participant and electrode of interest separately. Furthermore, for each trial, a phase from a random time inside the window of interest was selected. A surrogate ITC was calculated for the randomly selected phases (thus maintaining the number of trials). This procedure was repeated 10,000 times for each subject to obtain a distribution of surrogate ITCs. The surrogate ITC distributions were then averaged across subjects, and a p value (unbiased; Ernst, 2004) was obtained by computing the proportion of group-averaged surrogate ITCs that exceeded the measured ITC. Lastly, we ran a false discovery rate-based multiple comparison procedure (FDR) on the time series of p values to correct for multiple comparisons (Benjamini et al., 2001). Finally, corrected p values were inspected using an alpha of 0.05 as the cutoff for significance.

2.5.8 | Spectral cross-coherence

To provide additional evidence for entrainment, we performed a cross-coherence spectral analysis between the EEG activity and the entrainers (Keitel et al., 2017). Given that cross-coherence is a measure of the alignment between two signals (EEG activity and entrainers in our case), we expected a peak in the cross-coherence at 12 Hz. Epochs were classified based on the number of entrainers on each trial (8 to 12). For each type, we selected from the onset of the first entrainer to the offset of the last entrainer plus one half-cycle (+42 ms). Only correct trials were analyzed. Then, the next steps were separately performed for each epoch length: (i) For the purpose of this analysis, an artificial 12 Hz spiking signal was created. (ii) The entire spectrum was obtained using a STFT (2.048 s padding, Hanning window, frequency range 1 Hz to 40 Hz), for the empirical and the artificial signals, separately. (iii) Finally, the spectral cross-coherence value between the empirical and the artificial signal was obtained for each channel, frequency, and participant using the ft_connectivityanalysis function in the FieldTrip toolbox for EEG-MEG analysis.

Next, we calculated the weighted arithmetic mean of the cross-coherences across the five entrainer lengths (weighted by the number of trials per length), which resulted in a cross-coherence value for each frequency and participant. To assess the statistical significance of the peak at the entraining frequency (12 Hz), we used the procedure described by Biltoft and Pardyjak (2009). For the FFT estimation we employed 1024 samples, and we obtained an average number of trials of 351 ± 83 with a mean length of 418 points (335 for eight entrainers to 502 for 12 entrainers). At 500 Hz sampling rate, this results in degrees of freedom equal to 143. The cutoff for significance was established as a p value of <0.05, which implied a peak height of 0.0416 at 12 Hz.

2.5.9 | 12 Hz phase at target onset on target-present and target-absent trials

To assess phase opposition during the target period, EEG data from correct trials were time-locked to target onset or where target onset should occur, for target-present and target-absent trials respectively, as a function of in-phase and anti-phase temporal moments. The selection of target-absent trials was crucial to examine the effect of prior entrainment on the resulting phase without the contamination of ERP resulting from the presence of targets. For this analysis, epochs were selected from −2000 to 2000 ms, centered at the target onset (target-present trials) or where target onset should occur (target-absent trials). A minimum of 50 artifact-free trials per condition was required for each participant. Separately for each condition and participant, single-trial phases were obtained at 12 Hz. Next, a circular V-test (Durand & Greenwood, 1958), with phases pooled over all trials and participants, was performed to test whether there was a 180° separation between anti-phase and in-phase trials. In a complementary analysis used only for descriptive purposes, the mean angular difference between anti-phase versus in-phase trials was calculated for each participant, on target-present and target-absent trials. Circular statistics performed throughout the manuscript were obtained using the Circular Statistics Toolbox 1.21 (Berens, 2009).

2.5.10 | Phase alignment in the absence of external signal

To provide additional evidence for entrainment, we examined whether the phase alignment of the internal oscillators with the external signal was maintained even after the disappearance of the external rhythm. To evaluate this, we used a similar procedure to the one used for

cue-locked ITC data (see above). Here, we restricted the analysis to target-absent, correct trials. The time-window of interest was 41.5 ms to 250 ms after the last entrainer, which corresponds to three cycles of possible target onset times, where one cycle was equivalent to one anti-phase and consecutive in-phase presentation. Statistical significance was assessed using a Montecarlo procedure equivalent to the one described in the section titled *Inter-Trial Coherence (ITC)*.

2.5.11 | Control analyses

To avoid temporal smearing of evoked activity and to improve temporal resolution, we performed five control analyses, in which we estimated ITC and time-resolved phase at 12 Hz with a STFT of 166 ms length (two cycles of the frequency of interest), using a Hanning window to minimize spectral leakage (see Figure 1 for more detail about these analyses). Please, note that phases were free of contamination, apart from those at anti-phase 1.

For the first analysis, (i) we obtained ITC locked at the last entrainer during target-present and target-absent trials, using the same windows as the ones used with complex Morlet wavelets, which consisted of −2600 ms prior and 2600 ms after the first entrainer. We repeated the same phase concentration analysis as previously described for the complex Morlet wavelets.

Then, we carried out a series of analyses based on 12 Hz phase. For these analyses, we centered the activity at the temporal points mentioned below, and we added 2000 ms at each side. (ii) Phase opposition analyses between anti-phase and in-phase trials, at target onset (or where target onset should occur), were separately performed on target-present and target-absent conditions. Please, note that the statistical analyses were exactly the same as the ones performed with complex Morlex wavelets.

Next, to give additional support for the presence of entrainment, (iii) we carried out circular correlations between the phase obtained at the offset of the last entrainer (10 ms post-onset) and at the four temporal time points where targets should occur (anti-phase 1, in-phase 1, anti-phase 2, and in-phase 2), on target-absent trials. Data were calculated for each trial and participant. We combined the resulting *p* values across participants, using the Fisher method (Fisher, 1925), which provided us with a vector of *p* values as a function of time.

To explore the effect of 12 Hz phase on performance, we carried out two extra control analyses. In both cases, EEG data were time-locked to 166 ms pre-target and was divided both as a function of possible target onset time (anti-phase 1, in-phase 1, anti-phase 2, in-phase 2) and

response type (correct, incorrect). 12 Hz phase was calculated for each target onset, response type, trial, and participant. Furthermore, RTs for each trial were obtained. (iv) First, a circular correlation between 12 Hz phase and the RT was obtained for each participant and target onset time. *p* values were combined across participants, using the Fisher method (Fisher, 1925), to obtain a single *p* value for each target onset. (v) Finally, we carried out a phase opposition analysis between correct and incorrect trials. The four possible target onset times were collapsed into two groups (anti-phase and in-phase) to ensure we had a sufficient number of trials. For each participant, we computed the difference between the mean angle of correct and incorrect trials for each target onset and carried out a circular V-test (Durand & Greenwood, 1958) to test for 180° separation.

2.5.12 | Reality check: Lateralized alpha activity

To verify that subjects were indeed orienting attention, we analyzed the preparatory lateralization of the oscillatory alpha activity during the cue to target interval. We separately obtained epochs for cue-left/cue-right conditions (from −2200 ms to 3542 ms, window of interest from 0 ms to 1542 ms post-cue, no baseline was used) for valid, correct trials only, to ensure that participants were in fact orienting attention. For this analysis, the mean spectral power was calculated from the time window 375 ms to 875 ms after the cue onset, which corresponds to the 500 ms before the onset of the first entrainer. A FFT (zero padding to 1 s, Hanning window) was used to extract power in this time window of interest. Power was calculated for two ROIs of parieto-occipital electrodes (Thut et al., 2006; Worden et al., 2000). A left ROI (P3, PO3, PO7, P7, P5, P1, PO9, and O1) and a right ROI (P4, PO4, PO8, P8, P6, P2, PO10, and O2) were used. The average alpha power (7–14 Hz) for the electrodes ipsilateral and contralateral to the cue on both left and right cue (attended-left/attended-right) trials was computed. Next, an index of alpha lateralization was obtained by subtracting the previously obtained attended-left average alpha power (ipsi left-contra left) to the attended-right average alpha power (ipsi right-contra right) and dividing by the sum of the two (Thut et al., 2006). Finally, we ran a one-sided (right), paired *t* test against zero, to assess the statistical significance of the lateralization index. For illustrative purposes, the whole spectral power analysis was repeated (−2200 ms to 3542 ms time window) using a complex Morlet wavelet as described above for the ITC. The index of alpha lateralization was obtained for the entire window. Please notice that Morlet wavelets were not

used in the reality check to make sure that the latency of interest was not contaminated by post-entrainer activity.

3 | RESULTS

3.1 | Hazard rate

We obtained the HR to have an objective metric related to task predictability (see Figure 2e). We observed a low intercept and noted that the HR was quite similar between the first and last conditions. When this metric was calculated for the original paradigm (Kizuk & Mathewson, 2017) a higher intercept and higher overall values were recorded. Furthermore, there was a large difference between the HR of the first and later targets, a common bias in temporal attention paradigms. In comparison, our task clearly reduced this bias and increased unpredictability across target presentation times.

3.2 | Behavioral analyses

In order to explore spatial and temporal effects on performance, accuracy (hit rates) was separately obtained as a function of spatial validity (valid vs. invalid) and relative phase (anti-phase vs. in-phase) (see Figure 2a,b). An rmANOVA was conducted with spatial validity (valid/invalid) and relative phase (anti-phase/in-phase) as within-subject factors. Please note that the two anti-phase and in-phase SOAs were collapsed into two-levels: anti-phase and in-phase. The rmANOVA returned a significant main effect of spatial validity, $F(1,29) = 22.166$, $p = -5.7 \times 10^{-5}$, $f = .874$, $BF_{10} = 2.1 \times 10^{11}$, with higher hit rates on valid trials ($62.0 \pm 19.5\%$) as compared to invalid ones ($40.6 \pm 26.6\%$). On the other hand, there was no significant main effect of relative phase, $F(1,29) = 1.448$, $p = .239$, $f = .225$, $BF_{10} = .261$, indicating that there was no difference in hit rates between anti-phase ($M = 56.5 \pm 17.7\%$) and in-phase ($M = 55.3 \pm .19.8\%$) conditions. No significant interaction was detected between spatial validity and relative phase, $F(1,29) = .016$, $p = .901$, $f = .032$, $BF_{10} = .284$. Please note that Bayes Factors estimates indicated that there was strong evidence in favor of H1 for spatial validity and moderate evidence in favor of H0 for temporal validity and for the interaction between spatial validity and temporal validity.

The RTs on correct trials were analyzed using the same model, which included spatial validity (valid/invalid) and relative phase (anti-phase/in-phase) (see Figure 2c,d). Two of the participants' data were not accounted for in this analysis because they did not have any correct responses on invalid conditions, hence no RT average could be calculated (this was not a criterion for exclusion from remaining

analyses). The rmANOVA indicated a significant main effect of spatial validity, $F(1,27) = 43.432$, $p = 4.5 \times 10^{-7}$, $f = 1.269$, $BF_{10} = 1.3 \times 10^{9}$, with faster responses to validly-cued trials (454.5 ± 14.0 ms) as compared to invalid ones (493.1 ± 14.5 ms). Once again, the main effect of relative phase remained not significant, $F(1,27) = .968$, $p = .334$, $f = .190$, $BF_{10} = .217$, indicating that RTs were not modulated by anticipation based on preceding entrainers given that there was no significant difference between anti-phase (458.0 ± 14.3 ms) and in-phase (462.7 ± 13.7 ms) trials. The interaction between spatial and relative phase was also not significant, $F(1,27) = .257$, $p = .616$, $f = .095$, $BF_{10} = 0.287$. Similarly, to the results obtained for accuracy, for RT data, according to the resulting Bayes Factors estimates, there is strong evidence in favor of H1 for spatial validity and moderate evidence in favor of H0 for temporal validity and for the interaction between spatial validity and temporal validity.

In order to explore whether or not the participants in our experiment held a response bias, in either direction, the response criterion was calculated. The results indicated a lack of response bias as the response criterion was approximately equal to 0 ($c = -4.5103 \times 10^{-17}$).

3.3 | Individual alpha frequency

Next, we examined the IAF using a violin plot and corroborated that a large proportion of the data, as seen by the shaded area representing a kernel density estimation and the respective median and IQR values (Mdn: 10.80 Hz, IQR: 9.25–12.35 Hz) was concentrated around 11 Hz, very close to the entrained 12 Hz frequency (see Figure 2f).

3.4 | Cue-locked EEG data analyses

Given that it was not possible to depict an entire trial in one figure due to the variable number of entrainers and the four possible target onset times, we presented our data locked at different temporal points, throughout the manuscript. Here, to visualize the effects of entrainment on ERPs and ITC (see Figure 3), we time-locked EEG epochs from −200 ms to 1542 ms (baseline −200 ms to 0 ms), at Pz and Oz electrodes, during the presentation of the first eight entrainers (common to all trials). Valid and invalid target-present and target-absent trials were collapsed for this analysis. We observed an alignment of visual ERPs to entrainer onset times. Furthermore, and continuing with the visual inspection, we noticed an increase in ITC at the frequency of interest (12 Hz) and the persistence of this activity over the entire duration of the entrainer presentation period provided support for the presence of entrainment. Although the effect was visible at Pz electrode,
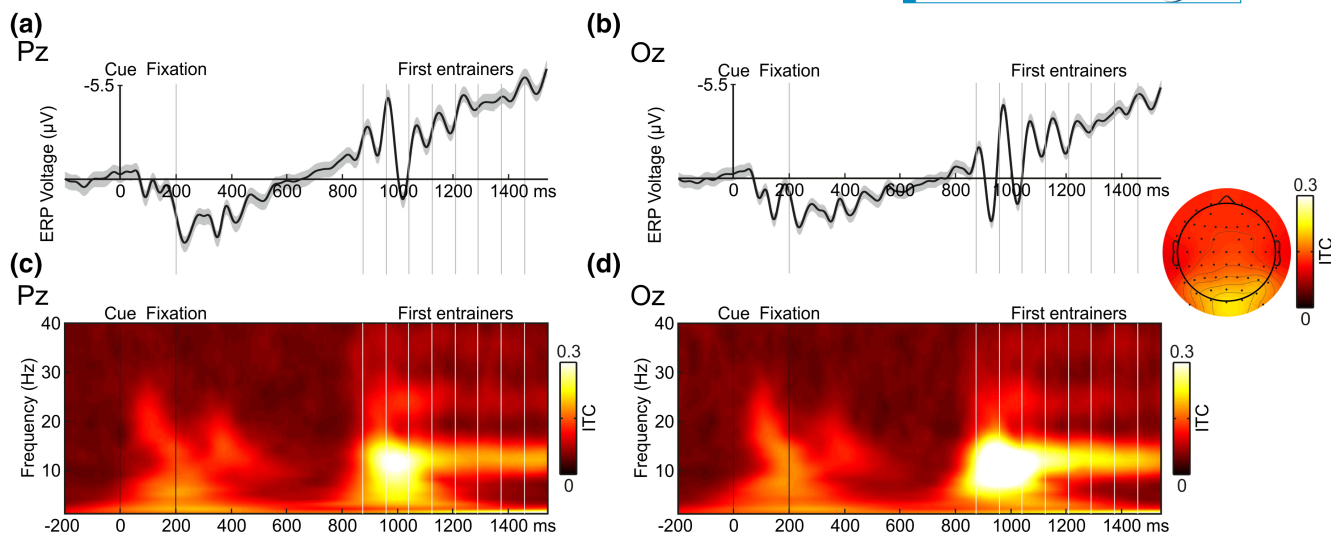
FIGURE 3 (a) Cue-locked grand average ERP with its SEM at Pz electrode. (b) Cue-locked grand average ERP with its SEM at Oz electrode. (c) Cue-locked ITC at Pz electrode. (d) Cue-locked ITC at Oz electrode. The time window selected for these graphs was −200 ms to 1542 ms (baseline from −200 ms to 0 ms). The cue, fixation cross, and first eight entrainers are depicted as vertical lines. Only correct trials were included, and epochs were collapsed across relative phase and spatial validity, as well as target-present and target-absent trials. An increase of ITC around 12 Hz was clearly observed throughout the entrainer period. A topographical map of the ITC at 10–14 Hz during the time-period comprising the first to the eighth entrainer is depicted

entrainment appeared to be even stronger, in terms of heightened ITC and increased alignment of SSVEPs with entrainer onset times, at the Oz electrode. See next paragraph for the statistical analysis on cue-locked data.

Post visual inspection, a statistical analysis was performed to evaluate the effects of entrainment. For this purpose, on cue-locked EEG data, and collapsing for valid and invalid, and for target-present and target-absent trials, a Montecarlo permutation test was performed to corroborate that the phase values were concentrated throughout the entrainment period (from the 1st to the 8th entrainer, or a time window of interest from 875 to 1458 ms). After correcting for multiple comparison, p values were statistically significant, according to the predefined alpha significance value of $p < .05$ at all examined time points at both Pz and Oz electrodes. The analysis thus provided evidence for phase alignment of the internal oscillatory activity with the external signal across the entrainment period.

3.5 | Cross-coherence between entrainers and EEG response

Continuing the statistical analysis of entrainment during entrainer presentation (see Figure 1), we used cross-coherence to determine whether the experimental paradigm successfully entrained neural oscillations to the external frequency. After having extracted the coherence for all frequencies and averaging across trials and participants, the output was examined for the presence of a

peak at 12 Hz. This resulted in an average peak height of 0.24 (Pz) and 0.28 (Oz) at 12 Hz, with a $p = 5 \times 10^{-9}$ and $p = 10^{-10}$, for Pz and Oz electrodes respectively, indicating the presence of a peak in coherence between the internal and external signal around the expected (12 Hz) frequency.

3.6 | Entrainer-locked analysis

To visualize whether entrainment continued beyond the last entrainer and into the target period, we time-locked the activity to the onset of the last entrainer (entrainer-locked). Then, we estimated the ITC by separating the trials as a function of correct target-present/target-absent trials, using complex Morlet wavelets (Figure 4). The analysis of both Pz and Oz electrodes allowed us to confirm the effect of the 12 Hz entrainment throughout the entire entrainer period. Furthermore, this activity persisted after the entrainers and throughout the potential target window, which contained no entrainers, on both target-present and, critically, on target-absent trials. Therefore, even though no target stimulus appeared, neural activity continued to oscillate following the entrainment rhythm.

3.7 | 12 Hz phase at target onset on target-present and target-absent trials

To statistically corroborate the 12 Hz phase alignment with the expected anti-phase and in-phase onsets, we locked
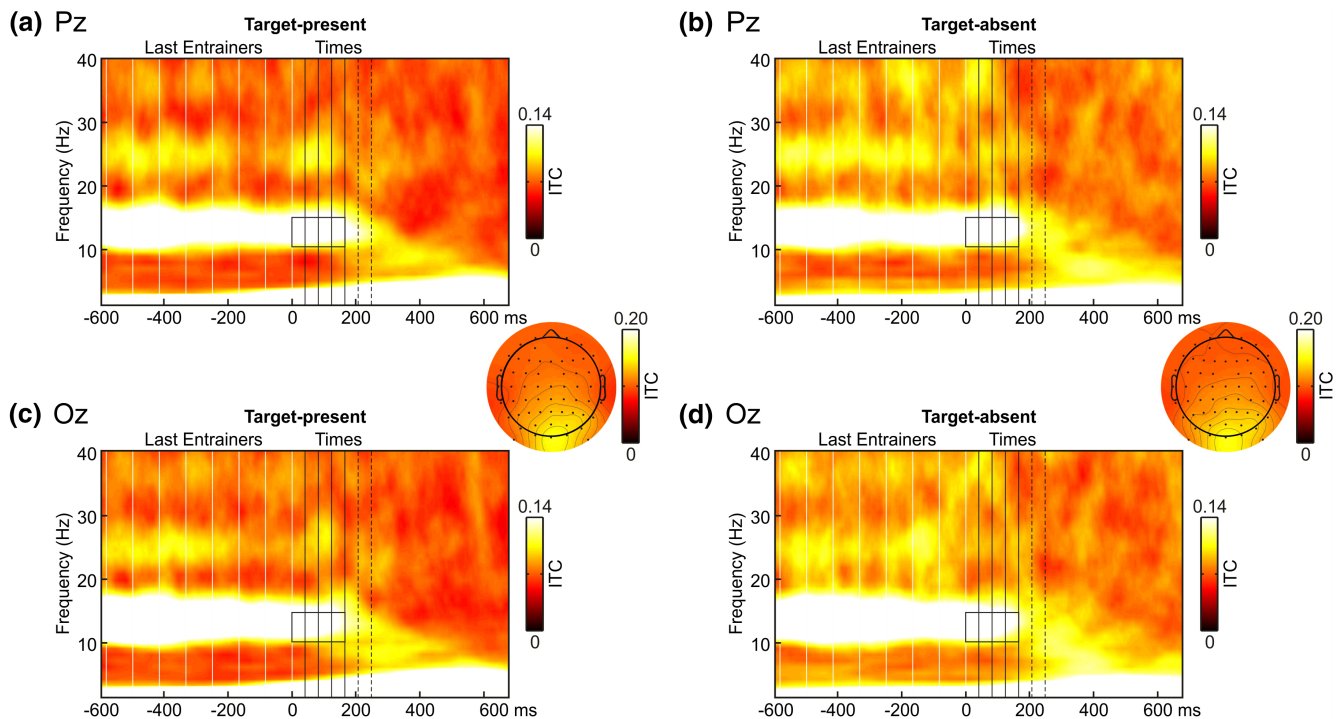
FIGURE 4 Entrainer-locked ITC graphs at 12 Hz obtained using complex Morlet wavelets. (a) Represents target-present trials at Pz electrode. (b) Represents target-absent trials at Pz electrode. (c) Represents target-present trials at Oz electrode. (d) Represents target-absent trials at Oz electrode. The time window for these graphs was −600 ms to 675 ms (no baseline). White, solid, vertical lines denote the last eight entrainers. Black, solid, vertical lines depict anti-phase and in-phase times (41.5, 83.3, 125, 166.6 ms after the last entrainer), whereas black, discontinuous, vertical lines represent one additional cycle of anti-phase and in-phase times (208.25 ms, 250 ms after the last entrainer) considered for the phase alignment analysis. Only correct trials were included and epochs were collapsed across relative phase and spatial validity. An increase of ITC around 12 Hz was clearly observed throughout the entrainer period and right through the target period. Separate topographical maps for target-present (left) and target-absent (right) trials of the ITC at 10–14 Hz are depicted. The time-period used for these maps consists of the time from the onset of the last entrainer to the last possible time point at which the target could appear

the EEG activity to the designated target-present/target-absent onset time for both Pz and Oz electrodes. As one of the primary objectives of this study was to focus on endogenous oscillations, above and beyond the target-related ERPs (Samaha et al., 2015; van Diepen et al., 2015), the mean phases at in- and anti-phase onsets were separately estimated for target-present and target-absent, correct trials, for all participants. Finally, the single-trial phase for each time and condition was separately obtained for each participant and the angular difference (anti-phase minus in-phase) was calculated. If entrainment had an effect that lasted beyond the entrainer presentation, then a 180° phase separation at 12 Hz was expected between moment's anti-phase and in-phase with the preceding entrainers. With this in mind, we performed further statistical analyses first on target-present trials, and next on target-absent trials, which allowed us to avoid the effects of target-related ERPs. We examined the phase difference between anti-phase and in-phase possible target moments on both target-present and target-absent trials (Figure 5), with the a-priori hypothesis of 180° separation between

the two. The results of the circular V-test were statistically significant for target-present and target-absent conditions, on both Pz (target-present: $p = 1.12 \times 10^{-5}$, target-absent: $p = 3.58 \times 10^{-4}$) and Oz (target-present: $p = 6.26 \times 10^{-6}$, target-absent: $p = 5.22 \times 10^{-5}$) electrodes. This indicated that the angular differences between the phases of the 12 Hz spontaneous oscillation at anti-phase versus in-phase moment were not uniformly distributed: what is more, the mean angular difference was 180°, as anticipated by our hypothesis (see Table 1 for descriptive data).

3.8 | Phase alignment in the absence of external signal

A complementary analysis to corroborate that the experimental paradigm resulted in true neural entrainment, was to examine whether the endogenous oscillations maintained the entrained rhythm after the external stimulation ended and before relaxing back to their original eigenfrequency. In order to evaluate phase concentration
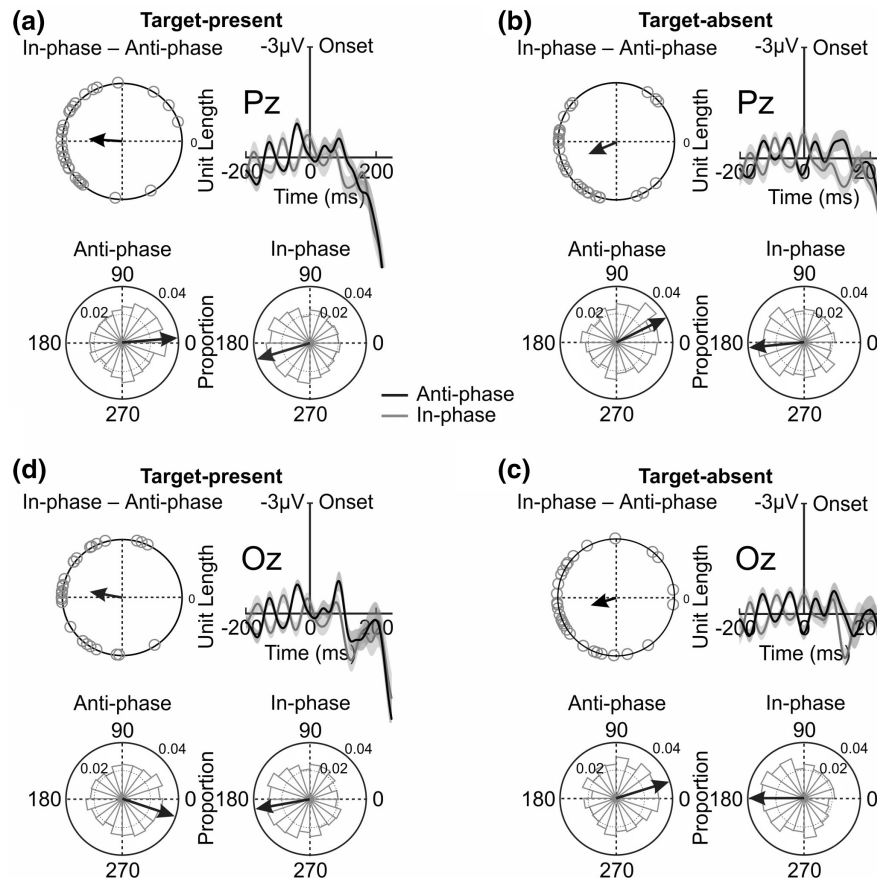
FIGURE 5 Schematic illustrations of the difference in activity on target-locked trials. Analyses were performed separately, using correct trials only, for target-present and target-absent data. Phases were obtained using complex Morlet wavelets. (a) Represents target-present trials at Pz electrode. (b) Represents target-absent trials at Pz electrode. (c) Represents target-present trials at Oz electrode. (d) Represents target-absent trials at Oz electrode. In each representation, four graphs are depicted. On the top right, the graphs represent the broadband ERPs with its SEMs, time-locked to target appearance (target-present trials) or expected target appearance (target-absent trials) (−200 ms to 250 ms, baseline: −200 ms to 0 ms). On the left, the circular graphs represent, for each participant (dots), the mean angular difference of the phase between in-phase and anti-phase trials. The length of the arrow is representative of the grand average of the mean differences. A clear 180° phase difference at 12 Hz between the phase of in-phase (red) and anti-phase (black) trials, with respect to the entrainers can be observed. Finally, the bottom rows show circular histograms where the bars represent the proportion of trials (pooled across all participants with no phase re-alignment for the 20 possible phase bins) for anti-phase (left) and in-phase (right). Upon closer examination, an opposite phase preference for in-phase and anti-phase can be observed on both target-present and target-absent trials

at 12 Hz, we performed a Montecarlo procedure equivalent to the one described in the cue-locked analysis, for the time-period comprising 41.5 ms to 250 ms after the last entrainer. This time window encompassed three anti-phase three in-phase moments (the equivalent of two additional cycles beyond the first expected target appearance, or 3 cycles after the last entrainer). After multiple comparison correction (FDR), all p values were statistically significant, according to the predefined alpha significance value of $p < 0.05$ for all of the examined time points at both Pz and Oz electrodes. This result thus provided evidence for phase alignment of the internal oscillators with the external signal even 3 cycles after the external signal had been removed, a result that is consistent with the ITC and 12 Hz phase results above.

3.9 | Control analyses

Several control analyses were performed using STFTs to replicate previous results but without the temporal smearing of evoked activity. (i) First, the analysis on last-entrainer-locked ITC data corroborated a significant phase concentration during the last eight entrainers ($p < 0.05$, FDR-corrected) on both Pz and Oz electrodes. (ii) Second, the phase opposition results continued to indicate that the phase was not uniformly distributed at anti-phase versus in-phase moments and that the separation between both phases was the anticipated 180° in support of our hypothesis, for both target-present (Pz: $p = 1.15 \times 10^{-3}$; Oz: $p = 2.99 \times 10^{-4}$) and target-absent trials (Pz: $p = 2.60 \times 10^{-4}$; Oz: $p = 3.65 \times 10^{-5}$) (see Table 2).

Electrode	Condition	Circular degrees (°)	Separation (in-phase – anti-phase)
Pz	Target-present anti-phase	4.69°	
	Target-present in-phase	163.1°	158.41°
	Target-absent anti-phase	26.5°	
	Target-absent in-phase	174.3°	147.8°
Oz	Target-present anti-phase	18.52°	
	Target-present in-phase	169.80°	151.28°
	Target-absent anti-phase	17.27°	
	Target-absent in-phase	179.40°	162.13°

TABLE 1 Analysis of the circular separation (in-phase – anti-phase) for target-present and target-absent trials extracted with complex Morlet wavelets

Electrode	Condition	Circular degrees (°)	Separation (in-phase – anti-phase)
Pz	Target-present anti-phase	18.34°	
	Target-present in-phase	160.00°	171.60°
	Target-absent anti-phase	21.91°	
	Target-absent in-phase	177.22°	163.93°
Oz	Target-present anti-phase	37.42°	
	Target-present in-phase	153.75°	165.52°
	Target-absent anti-phase	6.57°	
	Target-absent in-phase	169.02°	168.16°

TABLE 2 Analysis of the circular separation (in-phase – anti-phase) for target-present and target-absent trials extracted with short time Fourier transforms

	Last vs. Anti-phase 1	Last vs. In-phase 1	Last vs. Anti-phase 2	Last vs. In-phase 2
Pz	$p < 1.000 \times 10^{-100}$	$p = 7.545 \times 10^{-73}$	$p = 4.481 \times 10^{-26}$	$p = 6.470 \times 10^{-10}$
Oz	$p < 1.000 \times 10^{-100}$	$p = 6.727 \times 10^{-61}$	$p = 6.989 \times 10^{-14}$	$p = 2.816 \times 10^{-08}$

Note: p values for both Pz and Oz electrodes are reported.

TABLE 3 Circular correlations between the 12 Hz phase just after (10 ms) the offset of the last entrainer and on the temporal moment where targets should occur on target-absent trials, separated as a function of the four possible times

Besides the phase alignment analyses, (iii) we carried out correlations, on target-absent trials, between the 12 Hz phase just after the offset of the last entrainer (10 ms post-onset) and the 12 Hz phase at the four temporal time points where targets should occur (anti-phase 1, in-phase 1, anti-phase 2, in-phase 2). A significant correlation at all time points (see Table 3), at both Pz and Oz electrodes, was found which, provided additional evidence for the presence of entrainment.

To assess the influence of 12 Hz phase on performance, (iv) we performed a circular correlation between the resulting phases (166 ms pre-target onset, to avoid contamination from the target presentation) and RTs (for all four possible target onset times: anti-phase 1, in-phase 1, anti-phase 2, and in-phase 2), and a (v) phase opposition analysis as a function of response type (correct, incorrect) and type of target onset time (grouping the four onset times into two: anti-phase, in-phase). Interestingly, a significant correlation between 12 Hz phase and RTs was observed at

in-phase 1, at both Pz and Oz electrodes, but not at the other target onsets (see Table 4). Phase opposition analyses, however, were not significant between correct and incorrect trials (see Table 5).

3.10 | EEG alpha power lateralization

To ensure that the presence of the cue resulted in the expected inter-hemispheric imbalance of alpha power typical of spatial attention orienting, we examined the lateralization of alpha oscillatory activity on correct trials (7–14 Hz) following the cue. For this analysis, power was obtained from cue-locked data (0 ms to 1542 ms). The index of alpha power lateralization was assessed using the previously established time window (375 ms to 875 ms) and left ROI (P3, PO3, PO7, P7, P5, P1, PO9, and O1). A statistical analysis was performed comparing the inter-subject average lateralization index (ipsi–contra), using

TABLE 4 Circular correlation between the 12 Hz phase, at 166 ms pre-target onset and the reaction-times for target-present trials, separated as a function of the four possible target onset times

	Anti-phase 1	In-phase 1	Anti-phase 2	In-phase 2
Pz	$p = .595$	$p = .049$	$p = .656$	$p = .608$
Oz	$p = .948$	$p = .008$	$p = .855$	$p = .699$

Note: p values for both Pz and Oz electrodes are reported.

TABLE 5 Phase (166 ms pre-target) opposition between correct and incorrect trials, post-last entrainer offset, collapsed as a function of type of target onset time

	Anti-phase	In-phase
Pz	$p = .979$	$p = .976$
Oz	$p = .955$	$p = .999$

Note: p values for both Pz and Oz electrodes are reported.

a right-tailed paired *t* test (see violin plot in Figure 6 for individual distribution). As expected, a significant alpha lateralization index was obtained, $t(29) = 1.882$, $p = .035$, $d = .344$, suggesting that participants were, in fact, effectively orienting spatial attention as a function of cue direction throughout the task (see Figure 6).

4 | DISCUSSION

The present study addressed neural entrainment using a set of predetermined requisites to establish its presence and tested whether it could occur under conditions of temporal task unpredictability. The answer to these issues could help to interpret previous entrainment results, understand the processes underlying entrainment, and provide insights on application in clinical contexts and other fields. Previous results, by Kizuk and Mathewson (2017) among others (Spaak et al., 2014; Wiesman & Wilson, 2019), provided evidence against the interpretation of entrainment as the mere succession of ERPs. However, additional proof is required to discard the alternative explanation that entrainment and its ensuing behavioral benefits are a side-effect of ERPs related to expectancy and due to the inherent stimulus predictability built into the protocol (Breska & Deouell, 2016, 2017). Here, we introduced some modifications to the entrainment paradigm (Kizuk & Mathewson, 2017): [1] a stream of entrainers of variable, unpredictable length; [2] a detection task with bilateral targets; [3] an increased proportion of target-absent trials, to which participants were instructed not to respond. These modifications reduced the predictability inherent to most entrainment paradigms and ensured a larger number of target-absent trials
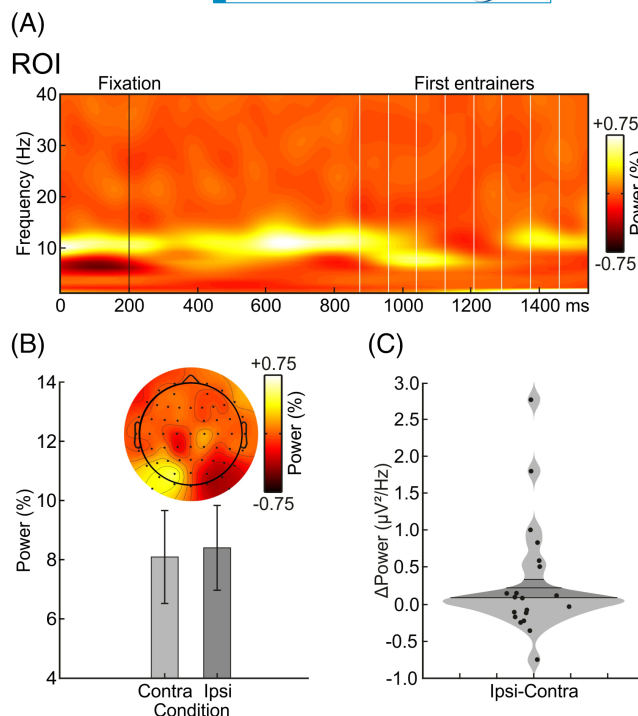

FIGURE 6 (a) Representation of alpha (7–14 Hz) power lateralization from 0 ms to 1542 ms post-cue (no baseline was used). Only correct trials were included in this analysis. The lateralization index was obtained by subtracting the previously obtained attended-left average alpha power (ipsi left-contra left) from the attended-right average alpha power (ipsi right-contra right) and dividing by the sum of the two. For the topographic plots, the average alpha power (7–14 Hz) for each electrode ipsilateral and contralateral to the cue on both left and right cue (attended-left/attended-right) trials was computed, at the time window 375 ms to 875 ms relative to cue onset (500 ms before the onset of the first entrainer). Please, note that we used the real activity for the left electrodes and the simulated activity for the right electrodes. Similarly, for the left cue, we used the real activity for the right electrodes, and the simulated for the left electrodes. (b) The bar graph represents the average power at 7–14 Hz, at the time window 375 ms to 875 ms relative to cue onset, for the electrodes contralateral (red) and ipsilateral (blue) to the cue on both left and right cue sides (attended-left/attended-right). (c) Finally, the lateralization index (explained above) for each participant was represented using a violin plot

to estimate interference-free, post-entrainer EEG activity. The main findings of this research study provide support for an adaptive mechanism based on endogenous oscillations capable of anticipating the temporal structure of external stimuli (Obleser & Kayser, 2019; Zoefel et al., 2018). More specifically, we found: [1] alignment of ongoing neural activity to the external rhythm and [2] persistence of phase alignment beyond the offset of the driving signal. However, [3] we found no behavioral benefits for targets aligned (in-phase) with the entrainer rhythm. We discuss the implications of these findings, below.

First, we confirmed our initial prediction: an increase in the ITC at the entrained frequency was observed during the presentation of the external rhythm, together with a significant cross-coherence between the neural activity and the entrainer. Specifically, after the phase reset produced by the first entrainer, the oscillatory activity remained aligned to the entrained frequency (12 Hz) throughout the entrainer stream. This is compatible with the hypothesis that the brain has a tendency to synchronize its endogenous oscillations to an external rhythm, in line with a number of other studies (Busch et al., 2009; Jones et al., 2002; Mathewson et al., 2010, 2012; Schroeder & Lakatos, 2009). Nevertheless, significant cross-coherence is necessary but not sufficient to conclude that the alignment between the internal and external signals is a result of neural entrainment. To address this, we examined whether phase alignment persisted for a minimum of 2 cycles, post-entrainer stream offset, which was our second prediction. We found that the alignment persisted for at least 3 cycles post-entrainer and observed a clear-cut 180° phase separation between out- and in-phase moments, even for uncontaminated target-absent trials. These results match those obtained by Kizuk and Mathewson (2017) and others, indicating the presence of oscillatory reverberation post-entrainer offset (Helfrich et al., 2017, 2019). However, our study adds to these past findings by showing that this neural reverberation occurs despite the temporally unpredictable nature of the target appearance and the variable entrainer length. Again, this was witnessed on all trials, included the subset of trials uncontaminated by stimulus or response-related activity within the post-entrainer period. Furthermore, target-absent trials as well as increased temporal unpredictability due to a variable number of entrainers and four different SOAs, allow us to remove the contamination of motor response-related ERPs while also reducing the likelihood of the appearance of ERPs associated with expectation, which strengthens our support for the presence of neural entrainment (Breska & Deouell, 2016, 2017; Capilla et al., 2011; Herrmann & Johnsrude, 2018; Keitel et al., 2014; Zoefel et al., 2018).

These findings support the hypothesis that neural entrainment constitutes an anticipatory adaptive mechanism that may help sensory parsing via predictive processes (Helfrich et al., 2019; Henry et al., 2014). Furthermore, validating the requirements for neural entrainment has a relevant impact because of its potential for clinical use (Lakatos et al., 2019; Thaut et al., 2015). Neural entrainment may be used as a diagnostic tool, for example in psychiatric (e.g., schizophrenia; Lakatos et al., 2013) or pain disorders (Guo et al., 2020). It may also be useful as a therapeutic procedure, to improve coordination and oral-motor synchronization in autism spectrum disorder (Bharathi et al., 2019) or stroke rehabilitation (Thaut & McIntosh, 2014). Further still, neural entrainment has been proposed to attenuate cognitive decline in Alzheimer's disease (Adaikkan & Tsai, 2020; Ferreira & Castellano, 2019; Iaccarino et al., 2016).

However, the results of this study failed to confirm our third prediction. We expected to obtain behavioral benefits for targets in-phase with the driving frequency, based on results from the EEG and previous studies, such as Mathewson et al. (2012) and Kizuk and Mathewson (2017). To explain this null finding, we can start by focusing beyond the specific concept of entrainment on the literature related to alpha phase concentration. Despite some studies indicating a benefit of this phase concentration on detection or discrimination tasks (Busch et al., 2009; de Graaf et al., 2013; Kizuk & Mathewson, 2017; Lakatos et al., 2019; Mathewson et al., 2009), other studies did not confirm this benefit (Benwell et al., 2017; Bompas et al., 2015; Busch & VanRullen, 2010; Ruzzoli et al., 2019; Vigué-Guix et al., 2020). Indeed, the accumulation of evidence seems to indicate that such phasic effects tend to be weak and highly dependent on experimental features, which remain to be clearly determined (e.g., Ruzzoli et al., 2019). With regard to neural entrainment of alpha phase, most studies showed benefits when targets were presented in-phase compared to anti-phase with the rhythmic entrainers and when phase was concentrated (de Graaf et al., 2013; Kizuk & Mathewson, 2017; Mathewson et al., 2012). On the other hand, in another neural entrainment study, despite observing an effect of alpha phase, the authors found an unexpected opposite effect on performance, with improved accuracy in anti-phase (Spaak et al., 2014) as compared to in-phase targets.

Furthermore, our study was methodologically quite similar to the Kizuk and Mathewson (2017) study, with the most notable difference being that our protocol reduced temporal predictability innate to previous entrainment paradigms by using a variable length of entrainers (8–12 entrainers). We do not believe that our results are in direct contradiction with previous studies, but we suggest that the net effect of rhythmic entrainment on behavior, particularly when other sources of anticipation are removed, may be weaker than previously thought. Therefore, the most plausible explanation so far is that, performance benefits observed in past studies may be a combination of neural entrainment, as demonstrated here, and other processes triggered by task predictability such as expectation (Helfrich et al., 2017) or memory-based mechanisms (Breska & Deouell, 2017).

Future studies should extend the present results beyond the parameters used in both our study and the one by Kizuk and Mathewson (2017). Since the task focuses

solely on one frequency and one cognitive function (visual attention), generalization to other stimulation frequencies, modalities, and cognitive processes should be investigated. But, other studies showing behavioral effects of entrainment at different oscillatory frequencies or cognitive processes such as visual discrimination (de Graaf et al., 2013), target detection (Mathewson et al., 2012), crossmodal illusory perception (Cecere et al., 2015), speech perception (Kösem et al., 2018), and source memory performance (Roberts et al., 2018), did not control for inherent task predictability. In our study, at the very least, we can claim that the putative effect of entrainment on performance, if any, must have been much smaller than the significant spatial attention effect, replicating the results of a myriad of past studies on discrimination accuracy (Carrasco, 2011; Carrasco et al., 2009; van Ede et al., 2012) and stimulus detection (Bergen & Julesz, 1983; Posner, 1980; Posner et al., 1980). Please note that this spatial attention effect was observed jointly with lateralization of alpha activity at posterior sites (Thut et al., 2006), supporting the hypothesis that alpha downregulates irrelevant information, in this case based on spatial location (Corbetta & Shulman, 2002; Hopfinger et al., 2000; Kastner et al., 1999; Kastner & Ungerleider, 2000). Finally, another aspect to take into account, is that we addressed the possible confound related to absolute expectation (one fixed timepoint) but did not modify the confounding factors related to "relative" expectation (a varying possible timepoint, with fixed spacing). We recommend that future studies examine the possible influence of relative expectation on entrainment, by adding jitter to the temporal timepoints at which targets can appear, as was done in Spaak et al. (2014).

Additionally, our analyses were initially focused on Pz electrode, similarly to past literature (e.g., Kizuk & Mathewson, 2017; Mathewson et al., 2009, 2012). However, after observing higher signal at the Oz electrode compared to Pz, we decided to run a series of exploratory analyses. We observed the same pattern of results in both electrodes, but with a greater effect in Oz. This result is in line with previous studies on visual stimulation and alpha oscillatory activity, which observed the peak of power activity (Alamia & VanRullen, 2019; Otero et al., 2020) and its highest signal to noise ratio at occipital sites (Ding et al., 2006; Srinivasan et al., 2006).

In conclusion, the results from the present study provide evidence for the neural entrainment hypothesis. Endogenous oscillations synchronize to external rhythms, and persist beyond these driving signals, forming a mechanistic basis for anticipatory parsing of the environment. Our study supported the hypothesis that neural entrainment most likely cannot be explained as a succession of ERPs. In addition, we have suggested that the net effect of this neural entrainment on overt behavior may be more limited than previously thought. It therefore remains to be tested whether and how this predictive mechanism modulates visual perception through the internal representation of the temporal properties of stimuli in a behaviorally relevant fashion. These results are important because they could clarify the processes underlying neural entrainment, which help interpret previous results, and provide insights on the application of these processes in clinical contexts and other fields.

AUTHOR CONTRIBUTIONS

Adrià Vilà-Balló: Conceptualization; data curation; formal analysis; investigation; methodology; project administration; software; visualization; writing – original draft; writing – review and editing. **Angela Marti-Marca:** Conceptualization; data curation; formal analysis; investigation; methodology; software; visualization; writing – original draft; writing – review and editing. **Mireia Torralba Cuello:** Conceptualization; data curation; formal analysis; methodology; software; writing – review and editing. **Salvador Soto-Faraco:** Conceptualization; methodology; resources; supervision; writing – review and editing. **Patricia Pozo-Rosich:** Conceptualization; funding acquisition; methodology; supervision; writing – review and editing.

ACKNOWLEDGMENTS

CONFLICT OF INTEREST

ORCID

Adrià Vilà-Balló https://orcid.org/0000-0001-7593-6012
Angela Marti-Marca https://orcid.org/0000-0002-9041-2943
Mireia Torralba Cuello https://orcid.org/0000-0003-3035-3918
Salvador Soto-Faraco https://orcid.org/0000-0002-4799-3762
Patricia Pozo-Rosich https://orcid.org/0000-0003-0796-4702

REFERENCES

Adaikkan, C., & Tsai, L.-H. (2020). Gamma entrainment: Impact on neurocircuits, glia, and therapeutic opportunities. *Trends in Neurosciences*, *43*(1), 24–41. https://doi.org/10.1016/j.tins.2019.11.001

Alamia, A., & VanRullen, R. (2019). Alpha oscillations and traveling waves: Signatures of predictive coding? *PLoS Biology*, *17*(10), e3000487. https://doi.org/10.1371/journal.pbio.3000487

Aydore, S., Pantazis, D., & Leahy, R. M. (2013). A note on the phase locking value and its properties. *NeuroImage*, *74*, 231–244. https://doi.org/10.1016/j.neuroimage.2013.02.008

Azzopardi, P., & Cowey, A. (1998). Blindsight and visual awareness. *Consciousness and Cognition*, *7*, 292–311. https://doi.org/10.1006/ccog.1998.0358

Beck, A., Steer, R., & Brown, G. (Eds.). (1996). *Manual for the Beck Depression Inventory-II*. Psychological Corporation.

Benjamini, Y., Drai, D., Elmer, G., Kafkafi, N., & Golani, I. (2001). Controlling the false discovery rate in behavior genetics research. *Behavioural Brain Research*, *125*(1–2), 279–284. https://doi.org/10.1016/s0166-4328(01)00297-2

Benwell, C. S. Y., Tagliabue, C. F., Veniero, D., Cecere, R., Savazzi, S., & Thut, G. (2017). Prestimulus EEG power predicts conscious awareness but not objective visual performance. *ENeuro*, *4*(6), ENEURO.0182–ENEU17.2017. https://doi.org/10.1523/ENEURO.0182-17.2017

Berens, P. (2009). CircStat: A MATLAB toolbox for circular statistics. *Journal of Statistical Software*, *31*(1), 1–21. https://doi.org/10.18637/jss.v031.i10

Bergen, J. R., & Julesz, B. (1983). Parallel versus serial processing in rapid pattern discrimination. *Nature*, *303*(5919), 696–698. https://doi.org/10.1038/303696a0

Bharathi, G., Jayaramayya, K., Balasubramanian, V., & Vellingiri, B. (2019). The potential role of rhythmic entrainment and music therapy intervention for individuals with autism spectrum disorders. *Journal of Exercise Rehabilitation*, *15*(2), 180–186. https://doi.org/10.12965/jer.1836578.289

Biltoft, C. A., & Pardyjak, E. R. (2009). Spectral coherence and the statistical significance of turbulent flux computations. *Journal of Atmospheric and Oceanic Technology*, *26*(2), 403–409. https://doi.org/10.1175/2008JTECHA1141.1

Bompas, A., Sumner, P., Muthumumaraswamy, S. D., Singh, K. D., & Gilchrist, I. D. (2015). The contribution of pre-stimulus neural oscillatory activity to spontaneous response time variability. *NeuroImage*, *107*, 34–45. https://doi.org/10.1016/j.neuroimage.2014.11.057

Brainard, D. H. (1997). The psychophysics toolbox. *Spatial Vision*, *10*(4), 433–436. https://doi.org/10.1163/156856897X00357

Breska, A., & Deouell, L. Y. (2016). When synchronizing to rhythms is not a good thing: Modulations of preparatory and post-target neural activity when shifting attention away from on-beat times of a distracting rhythm. *The Journal of Neuroscience: The Official Journal of the Society for Neuroscience*, *36*(27), 7154–7166. https://doi.org/10.1523/JNEUROSCI.4619-15.2016

Breska, A., & Deouell, L. Y. (2017). Neural mechanisms of rhythm-based temporal prediction: Delta phase-locking reflects temporal predictability but not rhythmic entrainment. *PLoS Biology*, *15*(2), e2001665. https://doi.org/10.1371/journal.pbio.2001665

Busch, N. A., Dubois, J., & VanRullen, R. (2009). The phase of ongoing EEG oscillations predicts visual perception. *Journal of Neuroscience*, *29*(24), 7869–7876. https://doi.org/10.1523/JNEUROSCI.0113-09.2009

Busch, N. A., & VanRullen, R. (2010). Spontaneous EEG oscillations reveal periodic sampling of visual attention. *Proceedings of the National Academy of Sciences of the United States of America*, *107*(37), 16048–16053. https://doi.org/10.1073/pnas.1004801107

Capilla, A., Pazo-Alvarez, P., Darriba, A., Campo, P., & Gross, J. (2011). Steady-state visual evoked potentials can be explained by temporal superposition of transient event-related responses. *PLoS One*, *6*(1), e14543. https://doi.org/10.1371/journal.pone.0014543

Carrasco, M. (2011). Visual attention: The past 25 years. *Vision Research*, *51*(13), 1484–1525. https://doi.org/10.1016/j.visres.2011.04.012

Carrasco, M., Eckstein, M., Verghese, P., Boynton, G., & Treue, S. (2009). Visual attention: Neurophysiology, psychophysics and cognitive neuroscience. *Vision Research*, *49*(10), 1033–1036. https://doi.org/10.1016/j.visres.2009.04.022

Cecere, R., Rees, G., & Romei, V. (2015). Individual differences in alpha frequency drive crossmodal illusory perception.

Current Biology: CB, *25*(2), 231–235. https://doi.org/10.1016/j.cub.2014.11.034

Cohen, J. (1992). A power primer. *Psychological Bulletin*, *112*(1), 155–159. https://doi.org/10.1037/0033-2909.112.1.155

Cohen, M. X. (2015). Effects of time lag and frequency matching on phase-based connectivity. *Journal of Neuroscience Methods*, *250*, 137–146. https://doi.org/10.1016/j.jneumeth.2014.09.005

Corbetta, M., & Shulman, G. L. (2002). Control of goal-directed and stimulus-driven attention in the brain. *Nature Reviews. Neuroscience*, *3*(3), 201–215. https://doi.org/10.1038/nrn755

de Graaf, T. A., Gross, J., Paterson, G., Rusch, T., Sack, A. T., & Thut, G. (2013). Alpha-band rhythms in visual task performance: Phase-locking by rhythmic sensory stimulation. *PLoS One*, *8*(3), e60035. https://doi.org/10.1371/journal.pone.0060035

Delorme, A., & Makeig, S. (2004). EEGLAB: An open source toolbox for analysis of single-trial EEG dynamics including independent component analysis. *Journal of Neuroscience Methods*, *134*(1), 9–21. https://doi.org/10.1016/j.jneumeth.2003.10.009

Ding, J., Sperling, G., & Srinivasan, R. (2006). Attentional modulation of SSVEP power depends on the network tagged by the flicker frequency. *Cerebral Cortex*, *16*(7), 1016–1029. https://doi.org/10.1093/cercor/bhj044

Durand, D., & Greenwood, J. A. (1958). Modifications of the rayleigh test for uniformity in analysis of two-dimensional orientation data. *The Journal of Geology*, *66*(3), 229–238. https://doi.org/10.1086/626501

Ernst, M. (2004). Permutation methods: A basis for exact inference. *Statistical Science*, *19*, 676–685. https://doi.org/10.1214/088342304000000396

Ferreira, A. C., & Castellano, J. M. (2019). Leaving the lights on using gamma entrainment to protect against neurodegeneration. *Neuron*, *102*(5), 901–902. https://doi.org/10.1016/j.neuron.2019.05.020

Fisher, R. A. (1925). *Statistical Methods for Research Workers*. Oliver and Boyd.

Guo, Y., Bufacchi, R. J., Novembre, G., Kilintari, M., Moayedi, M., Hu, L., & Iannetti, G. D. (2020). Ultralow-frequency neural entrainment to pain. *PLoS Biology*, *18*(4), e3000491. https://doi.org/10.1371/journal.pbio.3000491

Haegens, S., Cousijn, H., Wallis, G., Harrison, P. J., & Nobre, A. C. (2014). Inter- and intra-individual variability in alpha peak frequency. *NeuroImage*, *92*(100), 46–55. https://doi.org/10.1016/j.neuroimage.2014.01.049

Haegens, S., & Zion Golumbic, E. (2018). Rhythmic facilitation of sensory processing: A critical review. *Neuroscience and Biobehavioral Reviews*, *86*, 150–165. https://doi.org/10.1016/j.neubiorev.2017.12.002

Helfrich, R. F., Breska, A., & Knight, R. T. (2019). Neural entrainment and network resonance in support of top-down guided attention. *Current Opinion in Psychology*, *29*, 82–89. https://doi.org/10.1016/j.copsyc.2018.12.016

Helfrich, R. F., Huang, M., Wilson, G., & Knight, R. T. (2017). Prefrontal cortex modulates posterior alpha oscillations during top-down guided visual perception. *Proceedings of the National Academy of Sciences of the United States of America*, *114*(35), 9457–9462. https://doi.org/10.1073/pnas.1705965114

Henry, M. J., Herrmann, B., & Obleser, J. (2014). Entrained neural oscillations in multiple frequency bands comodulate behavior. *Proceedings of the National Academy of Sciences of the United States of America*, *111*(41), 14935–14940. https://doi.org/10.1073/pnas.1408741111

Herrmann, B., & Johnsrude, I. S. (2018). Neural signatures of the processing of temporal patterns in sound. *The Journal of Neuroscience: The Official Journal of the Society for Neuroscience*, *38*(24), 5466–5477. https://doi.org/10.1523/JNEUROSCI.0346-18.2018

Hopfinger, J. B., Buonocore, M. H., & Mangun, G. R. (2000). The neural mechanisms of top-down attentional control. *Nature Neuroscience*, *3*(3), 284–291. https://doi.org/10.1038/72999

Iaccarino, H. F., Singer, A. C., Martorell, A. J., Rudenko, A., Gao, F., Gillingham, T. Z., Mathys, H., Seo, J., Kritskiy, O., Abdurrob, F., Adaikkan, C., Canter, R. G., Rueda, R., Brown, E. N., Boyden, E. S., & Tsai, L.-H. (2016). Gamma frequency entrainment attenuates amyloid load and modifies microglia. *Nature*, *540*(7632), 230–235. https://doi.org/10.1038/nature20587

Jennings, J. R., & Wood, C. C. (1976). Letter: The epsilon-adjustment procedure for repeated-measures analyses of variance. *Psychophysiology*, *13*(3), 277–278. https://doi.org/10.1111/j.1469-8986.1976.tb00116.x

Jones, M. R., Moynihan, H., MacKenzie, N., & Puente, J. (2002). Temporal aspects of stimulus-driven attending in dynamic arrays. *Psychological Science*, *13*(4), 313–319. https://doi.org/10.1111/1467-9280.00458

Kaernbach, C. (1990). A single-interval adjustment-matrix (SIAM) procedure for unbiased adaptive testing. *The Journal of the Acoustical Society of America*, *88*(6), 2645–2655. https://doi.org/10.1121/1.399985

Kastner, S., Pinsk, M. A., De Weerd, P., Desimone, R., & Ungerleider, L. G. (1999). Increased activity in human visual cortex during directed attention in the absence of visual stimulation. *Neuron*, *22*(4), 751–761. https://doi.org/10.1016/s0896-6273(00)80734-5

Kastner, S., & Ungerleider, L. G. (2000). Mechanisms of visual attention in the human cortex. *Annual Review of Neuroscience*, *23*, 315–341. https://doi.org/10.1146/annurev.neuro.23.1.315

Keitel, C., Quigley, C., & Ruhnau, P. (2014). Stimulus-driven brain oscillations in the alpha range: Entrainment of intrinsic rhythms or frequency-following response? *The Journal of Neuroscience*, *34*(31), 10137–10140. https://doi.org/10.1523/JNEUROSCI.1904-14.2014

Keitel, C., Thut, G., & Gross, J. (2017). Visual cortex responses reflect temporal structure of continuous quasi-rhythmic sensory stimulation. *NeuroImage*, *146*, 58–70. https://doi.org/10.1016/j.neuroimage.2016.11.043

Kessler, R. C., Adler, L., Ames, M., Demler, O., Faraone, S., Hiripi, E., Howes, M. J., Jin, R., Secnik, K., Spencer, T., Ustun, T. B., & Walters, E. E. (2005). The World Health Organization Adult ADHD Self-Report Scale (ASRS): A short screening scale for use in the general population. *Psychological Medicine*, *35*(2), 245–256. https://doi.org/10.1017/s0033291704002892

Kizuk, S. A. D., & Mathewson, K. E. (2017). Power and phase of alpha oscillations reveal an interaction between spatial and temporal visual attention. *Journal of Cognitive Neuroscience*, *29*(3), 480–494. https://doi.org/10.1162/jocn_a_01058

Kleiner, M., Brainard, D. H., Pelli, D., Ingling, A., Murray, R., & Broussard, C. (2007). What's new in psychtoolbox-3. *Perception*, *36*, 1–16. https://doi.org/10.1068/v070821

Kösem, A., Bosker, H. R., Takashima, A., Meyer, A., Jensen, O., & Hagoort, P. (2018). Neural entrainment determines the words

we hear. *Current Biology: CB*, *28*(18), 2867–2875.e3. https://doi.org/10.1016/j.cub.2018.07.023

Lakatos, P., Gross, J., & Thut, G. (2019). A new unifying account of the roles of neuronal entrainment. *Current Biology: CB*, *29*(18), R890–R905. https://doi.org/10.1016/j.cub.2019.07.075

Lakatos, P., Schroeder, C. E., Leitman, D. I., & Javitt, D. C. (2013). Predictive suppression of cortical excitability and its deficit in schizophrenia. *The Journal of Neuroscience*, *33*(28), 11692–11702. https://doi.org/10.1523/JNEUROSCI.0010-13.2013

Large, E. W., & Jones, M. R. (1999). The dynamics of attending: How people track time-varying events. *Psychological Review*, *106*(1), 119–159. https://doi.org/10.1037/0033-295X.106.1.119

Lopez-Calderon, J., & Luck, S. J. (2014). ERPLAB: An open-source toolbox for the analysis of event-related potentials. *Frontiers in Human Neuroscience*, *8*, 213. https://doi.org/10.3389/fnhum.2014.00213

Maris, E., & Oostenveld, R. (2007). Nonparametric statistical testing of EEG- and MEG-data. *Journal of Neuroscience Methods*, *164*(1), 177–190. https://doi.org/10.1016/j.jneumeth.2007.03.024

Mathewson, K. E., Fabiani, M., Gratton, G., Beck, D. M., & Lleras, A. (2010). Rescuing stimuli from invisibility: Inducing a momentary release from visual masking with pre-target entrainment. *Cognition*, *115*(1), 186–191. https://doi.org/10.1016/j.cognition.2009.11.010

Mathewson, K. E., Gratton, G., Fabiani, M., Beck, D. M., & Ro, T. (2009). To see or not to see: Prestimulus alpha phase predicts visual awareness. *The Journal of Neuroscience: The Official Journal of the Society for Neuroscience*, *29*(9), 2725–2732. https://doi.org/10.1523/JNEUROSCI.3963-08.2009

Mathewson, K. E., Prudhomme, C., Fabiani, M., Beck, D. M., Lleras, A., & Gratton, G. (2012). Making waves in the stream of consciousness: Entraining oscillations in EEG alpha and fluctuations in visual awareness with rhythmic visual stimulation. *Journal of Cognitive Neuroscience*, *24*(12), 2321–2333. https://doi.org/10.1162/jocn_a_00288

Morey, R. D., Rouder, J. N., Jamil, T., & Morey, M. R. D. (2017, December 13). *Package 'bayesfactor'*. The Comprehensive R Archive Network (CRAN). https://cran.r-project.org/web/packages/BayesFactor/BayesFactor.pdf

Obleser, J., & Kayser, C. (2019). Neural entrainment and attentional selection in the listening brain. *Trends in Cognitive Sciences*, *23*(11), 913–926. https://doi.org/10.1016/j.tics.2019.08.004

Oostenveld, R., Fries, P., Maris, E., & Schoffelen, J. M. (2011). FieldTrip: Open source software for advanced analysis of MEG, EEG, and invasive electrophysiological data. *Computational Intelligence and Neuroscience*, *2011*, 156869. https://doi.org/10.1155/2011/156869

Otero, M., Prado-Gutiérrez, P., Weinstein, A., Escobar, M.-J., & El-Deredy, W. (2020). Persistence of EEG alpha entrainment depends on stimulus phase at offset. *Frontiers in Human Neuroscience*, *14*, 139. https://doi.org/10.3389/fnhum.2020.00139

Pasquereau, B., & Turner, R. S. (2015). Dopamine neurons encode errors in predicting movement trigger occurrence. *Journal of Neurophysiology*, *113*(4), 1110–1123. https://doi.org/10.1152/jn.00401.2014

Posner, M. I. (1980). Orienting of attention. *The Quarterly Journal of Experimental Psychology*, *32*(1), 3–25. https://doi.org/10.1080/00335558008248231

Posner, M. I., Snyder, C. R., & Davidson, B. J. (1980). Attention and the detection of signals. *Journal of Experimental Psychology*, *109*(2), 160–174. https://doi.org/10.1037/0096-3445.109.2.160

Roberts, B. M., Clarke, A., Addante, R. J., & Ranganath, C. (2018). Entrainment enhances theta oscillations and improves episodic memory. *Cognitive Neuroscience*, *9*(3–4), 181–193. https://doi.org/10.1080/17588928.2018.1521386

Ruzzoli, M., Torralba, M., Morís Fernández, L., & Soto-Faraco, S. (2019). The relevance of alpha phase in human perception. *Cortex; a Journal Devoted to the Study of the Nervous System and Behavior*, *120*, 249–268. https://doi.org/10.1016/j.cortex.2019.05.012

Samaha, J., Bauer, P., Cimaroli, S., & Postle, B. R. (2015). Top-down control of the phase of alpha-band oscillations as a mechanism for temporal prediction. *Proceedings of the National Academy of Sciences of the United States of America*, *112*(27), 8439–8444. https://doi.org/10.1073/pnas.1503686112

Schroeder, C. E., & Lakatos, P. (2009). Low-frequency neuronal oscillations as instruments of sensory selection. *Trends in Neurosciences*, *32*(1), 9–18. https://doi.org/10.1016/j.tins.2008.09.012

Spaak, E., de Lange, F. P., & Jensen, O. (2014). Local entrainment of α oscillations by visual stimuli causes cyclic modulation of perception. *The Journal of Neuroscience: The Official Journal of the Society for Neuroscience*, *34*(10), 3536–3544. https://doi.org/10.1523/JNEUROSCI.4385-13.2014

Srinivasan, R., Bibi, F. A., & Nunez, P. L. (2006). Steady-state visual evoked potentials: Distributed local sources and wave-like dynamics are sensitive to flicker frequency. *Brain Topography*, *18*(3), 167–187. https://doi.org/10.1007/s10548-006-0267-4

ten Oever, S., Schroeder, C. E., Poeppel, D., van Atteveldt, N., & Zion-Golumbic, E. (2014). Rhythmicity and cross-modal temporal cues facilitate detection. *Neuropsychologia*, *63*, 43–50. https://doi.org/10.1016/j.neuropsychologia.2014.08.008

Thaut, M. H., & McIntosh, G. C. (2014). Neurologic music therapy in stroke rehabilitation. *Current Physical Medicine and Rehabilitation Reports*, *2*(2), 106–113. https://doi.org/10.1007/s40141-014-0049-y

Thaut, M. H., McIntosh, G. C., & Hoemberg, V. (2015). Neurobiological foundations of neurologic music therapy: Rhythmic entrainment and the motor system. *Frontiers in Psychology*, *5*, 1185. https://doi.org/10.3389/fpsyg.2014.01185

Thut, G., Nietzel, A., Brandt, S. A., & Pascual-Leone, A. (2006). Alpha-band electroencephalographic activity over occipital cortex indexes visuospatial attention bias and predicts visual target detection. *The Journal of Neuroscience: The Official Journal of the Society for Neuroscience*, *26*(37), 9494–9502. https://doi.org/10.1523/JNEUROSCI.0875-06.2006

Thut, G., Schyns, P. G., & Gross, J. (2011). Entrainment of perceptually relevant brain oscillations by non-invasive rhythmic stimulation of the human brain. *Frontiers in Psychology*, *2*, 170. https://doi.org/10.3389/fpsyg.2011.00170

Torralba Cuello, M., Drew, A., Sabaté San José, A., Morís Fernández, L., & Soto-Faraco, S. (2022). Alpha fluctuations regulate the accrual of visual information to awareness. *Cortex; a Journal Devoted to the Study of the Nervous System and Behavior*, *147*, 58–71. https://doi.org/10.1016/j.cortex.2021.11.017

van Diepen, R. M., Cohen, M. X., Denys, D., & Mazaheri, A. (2015). Attention and temporal expectations modulate power, not phase, of ongoing alpha oscillations. *Journal of Cognitive*

Neuroscience, *27*(8), 1573–1586. https://doi.org/10.1162/jocn_a_00803

van Ede, F., de Lange, F. P., & Maris, E. (2012). Attentional cues affect accuracy and reaction time via different cognitive and neural processes. *Journal of Neuroscience*, *32*(30), 10408–10412. https://doi.org/10.1523/JNEUROSCI.1337-12.2012

Vigué-Guix, I., Morís Fernández, L., Torralba Cuello, M., Ruzzoli, M., & Soto-Faraco, S. (2020). Can the occipital alpha-phase speed up visual detection through a real-time EEG-based brain-computer interface (BCI)? *The European Journal of Neuroscience.* https://doi.org/10.1111/ejn.14931

Wagenmakers, E.-J., Love, J., Marsman, M., Jamil, T., Ly, A., Verhagen, J., Selker, R., Gronau, Q. F., Dropmann, D., Boutin, B., Meerhoff, F., Knight, P., Raj, A., van Kesteren, E.-J., van Doorn, J., Šmíra, M., Epskamp, S., Etz, A., Matzke, D., ... Morey, R. D. (2018). Bayesian inference for psychology. Part II: Example applications with JASP. *Psychonomic Bulletin & Review*, *25*(1), 58–76. https://doi.org/10.3758/s13423-017-1323-7

Wagenmakers, E.-J., Marsman, M., Jamil, T., Ly, A., Verhagen, J., Love, J., Selker, R., Gronau, Q. F., Šmíra, M., Epskamp, S., Matzke, D., Rouder, J. N., & Morey, R. D. (2018). Bayesian inference for psychology. Part I: Theoretical advantages and practical ramifications. *Psychonomic Bulletin & Review*, *25*(1), 35–57. https://doi.org/10.3758/s13423-017-1343-3

Wiesman, A. I., & Wilson, T. W. (2019). Alpha frequency entrainment reduces the effect of visual distractors. *Journal of Cognitive Neuroscience*, *31*(9), 1392–1403. https://doi.org/10.1162/jocn_a_01422

Worden, M. S., Foxe, J. J., Wang, N., & Simpson, G. V. (2000). Anticipatory biasing of visuospatial attention indexed by retinotopically specific alpha-band electroencephalography increases over occipital cortex. *The Journal of Neuroscience: The Official Journal of the Society for Neuroscience*, *20*(6), RC63. https://doi.org/10.1523/jneurosci.20-06-j0002.2000

Zoefel, B., Ten Oever, S., & Sack, A. T. (2018). The involvement of endogenous neural oscillations in the processing of rhythmic input: More than a regular repetition of evoked neural responses. *Frontiers in Neuroscience*, *12*, 95. https://doi.org/10.3389/fnins.2018.00095

10.4 Appendix 4

Vilà-Balló A, Marti-Marca A, Torres-Ferrús M, Alpuente A, Gallardo VJ, Pozo-Rosich P. Neurophysiological correlates of abnormal auditory processing in episodic migraine during the interictal period. Cephalalgia. 2021;41(1):45-57. Copyright © 2021 (Sage Publications). doi:10.1177/0333102420951509

Impact factor of journal: 4.70

Neurophysiological correlates of abnormal auditory processing in episodic migraine during the interictal period

Adrià Vilà-Balló[1] 🔳, Angela Marti-Marca[1] 🔳,
Marta Torres-Ferrús[1,2], Alicia Alpuente[1,2] 🔳,
Victor José Gallardo[1] and Patricia Pozo-Rosich[1,2]

Abstract

Background: The characteristics of the hypersensitivity to auditory stimuli during the interictal period in episodic migraine are discussed. The combined use of event-related potentials, time-frequency power and phase-synchronization can provide relevant information about the time-course of sensory-attentional processing in migraine and its underlying mechanisms.

Objective: The aim of this nested case-control study was to examine these processes in young, female, episodic migraine patients interictally and compare them to controls using an active auditory oddball task.

Method: We recorded, using 20 channels, the electrophysiological brain activity of 21 women with episodic migraine without aura and 21 healthy matched controls without family history of migraine, during a novelty oddball paradigm. We collected sociodemographic and clinical data as well as scores related to disability, quality of life, anxiety and depression. We calculated behavioural measures including reaction times, hit rates and false alarms. Spectral power and phase-synchronization of oscillatory activity as well as event-related potentials were obtained for standard stimuli. For target and novel stimuli, event-related potentials were acquired.

Results: There were no significant differences at the behavioural level. In migraine patients, we found an increased phase-synchronization at the theta frequency range and a higher N1 response to standard trials. No differences were observed in spectral power. No evidence for a lack of habituation in any of the measures was seen between migraine patients and controls. The Reorienting Negativity was reduced in migraine patients as compared to controls on novel but not on target trials.

Conclusion: Our findings suggest that migraine patients process stimuli as more salient, seem to allocate more of their attentional resources to their surrounding environment, and have less available resources to reorient attention back to the main task.

Introduction

Migraine is a neurosensory brain disorder involving altered sensory processing, which has been associated with thalamocortical dysrhythmia (1). Previous studies have reported abnormal neurophysiological responses in migraine, which can be summarized as enhanced sensory processing and a lack of habituation (1) during the interictal period. Nonetheless, while these

[1]Headache and Neurological Pain Research Group, Vall d'Hebron Research Institute, Department of Medicine, Universitat Autònoma de Barcelona, Barcelona, Spain
[2]Headache Unit, Department of Neurology, Hospital Universitari Vall d'Hebron, Barcelona, Spain

Corresponding author:
Adrià Vilà-Balló, Headache Unit, Department of Neurology, Hospital Universitari Vall d'Hebron, Passeig de la Vall d'Hebron, 119-129, 08035 Barcelona, Spain.
Email: adria.vila@vhir.org

abnormalities have been exhaustively analyzed in the visual modality, results obtained in audition remain inconsistent (2).

Auditory oddball tasks combined with electrophysiology (EEG) are one way of better understanding auditory processing, also allowing the study of attention and behavioural readjustments to environmental demands (3). In its active form, repetitive sounds, standard stimuli, and two types of less frequent, differential sounds, target and novel stimuli are presented to the participant, who is instructed to respond to targets only (4,5).

N1 and P2 Event-Related Potentials (ERPs) have been linked to early allocation of attention and to evaluative processing of repetitive standard stimuli. N1 is a negative electrophysiological component (peak 75–150 ms post-stimulus), which is affected by stimulus salience and the degree of attention (6,7). P2 (150–250 ms), a positive component, has been related to higher order perceptual processing (8,9), early allocation of attention and initial awareness (6). Most previous studies reported no group differences in either the N1 or P2 amplitude or habituation in migraine patients as compared to controls (3,10–13). However, other studies did observe an increased N1-P2 amplitude in migraine (14,15).

Target and novel sounds during active oddball tasks allow us to evaluate aspects of sensory-perceptual and attentional processing, which are essential to better comprehend the relationship between the evaluation of incoming information, the management of attentional resources, and the behavioural response to external stimuli (see Table 1 for a detailed description of the specific cascade of sensory and attentional processes, from the MMN to the RON, involved in the processing of novel and target stimuli) (4,16–19). Novel stimuli generate a cascade of electrophysiological components including the mismatch negativity (MMN), early P3a, late P3a and reorienting negativity (RON), which are related to detection and processing of unexpected events as well as subsequent attentional reorientation. Similarly, processing of target stimuli involves the MMN, P3b and RON, which are linked to contextual memory comparisons necessary for the behavioral response and the reorientation of attention back to the main task. Within the migraine literature, some studies have reported equal MMN amplitude (10,19) and similar P3a amplitude in patients as compared to controls (3,13,20). Furthermore, some studies have reported a reduced P3b amplitude in response to deviant or target stimuli (3,11,21,22), whereas others did not encounter group differences (19,23,24).

While ERPs can provide us with relevant information about the time-course of sensory-attentional processing, the transformation of data into time-frequency

Table 1. Cascade of effects of novel and target stimuli on the sensory-attentional system.

Type of stimuli	Component	Polarity	Peak (ms)	Site	Cognitive related processes
Novel	MMN	−	175–225	Fronto-central	Early sensory detection of unexpected changes. Automatic mechanisms of attentional capture
	Early P3a	+	225–275	Central	Post-sensory detection of unexpected events
	Late P3a	+	275–325	Frontal & parietal	Attentional processing of the unexpected event
	RON	−	350–450	Fronto-central	Attentional disengagement from the distractor stimuli and reorientation of attention back to the main task. Related to attentional resources, processing ease, and/or efficiency
Target	MMN	−	175–225	Fronto-central	Early sensory detection of unexpected changes. Automatic mechanisms of attentional capture
	P3b	+	300–600	Centro-parietal	Contextual memory comparisons, necessary to the behavioral response
	RON	−	400–600	Fronto-central	Attentional disengagement from the target stimuli and reorientation of attention back to the main task. Related to attentional resources, processing ease, and/or efficiency

Note: Novel stimuli lead to a cascade of event-related potentials, which include, in order of appearance, the Mismatch Negativity (MMN), the early and late P3a, and finally the Reorienting Negativity (RON) (4,17,18). ERPs associated with target stimuli include the MMN, the P3b and the RON (4,16–19).

(TF) measures of power and phase-synchronization (or inter-trial phase coherence) can give information about more general underlying processes. Power is related to the amount of simultaneously active neurons measured at any given point in time, whereas phase-synchronization gives an index of phase consistency across trials. For example, after the presentation of standard, target or novel stimuli, there is a rise in theta activity, which coincides with the period in which the N1 and P3a components have their maximum amplitude. Similarly, an increase in low-beta activity has been observed after the presentation of novel stimuli (5,25). Phase-synchronization, together with measures of power, could partially contribute to ERP activity (26), especially during the presentation of repetitive stimuli. However, despite these measures offering a more direct link to thalamocortical activity when compared to ERPs, to the best of our knowledge, neither power nor phase-synchronization have been studied in auditory processing, in migraine patients interictally.

Given the discrepancies seen within the auditory evoked potential literature in migraine and the lack of literature related to time-frequency measures in response to auditory stimuli, the objective of this study was to examine whether or not there were significant group differences in ERPs, power or phase-synchronization on an active auditory oddball task between young episodic migraineurs during the interictal period and controls.

Method

This is a double-blind study, using an observational, nested case-control study design.

Participants

We decided to focus on young patients with low-frequency episodic migraine (EM) interictally as compared to healthy controls. From a sample of 45 participants that underwent the EEG recording, 42 participants remained in the study after the EEG artifact rejection (see EEG recordings section and Supplemental material for more details). The final sample consisted of 21 right-handed females with EM without aura (age: 22.99 ± 1.99, attack frequency: 4.38 ± 2.91 days/month), according to the International Classification of Headache Disorders 3rd edition, beta version (ICHD-3 beta) (27), and 21 age- and gender-matched healthy controls (HC) (age: 21.95 ± 2.20, age: $t(40) = -1.598$, $p = 0.118$). The inclusion criteria for all participants was to be between 18–30 years old, right-handed, and with normal or corrected-to-normal vision and hearing. Specifically,

migraine patients chosen to take part in this study were all low-frequency, episodic migraineurs. There was a clear objective of having a very homogeneous and clinically-similar sample of participants to effectively compare brain responses and activity as well as to reduce possible biases. All participants were individuals who were unsure or unaware of their diagnosis. The exclusion criteria included the presence of other headache, neurological or psychiatric disorders as well as the use of specific medications/recreational drugs. Controls could not match the criteria for any headache (according to ICHD-3 beta), and they could not have any first-degree relatives with migraine (see Supplemental material for details about the recruitment process and exclusion criteria). The neurologist did not inform the participants of their diagnosis until the end of the EEG session to ensure that both the researcher and the participant remained double-blind.

Ethics approval: All participants gave their informed consent prior to participation and received 15 euros compensation at the end of the experimental session. This research study was approved by the Ethics Committee at the Vall d'Hebron Hospital (PR(AG) 376/2017).

Procedure

A neurologist confirmed the diagnosis of EM and the absence of migraine (or other headache) and familial antecedents of migraine in HCs. Participants that were designated as fit to continue completed a digital migraine diary during 30 days prior to the experimental session. All participants, including controls, completed the daily calendar to reduce possible biases such as the selection of controls who were not truly headache-free. The diary specifically collected headache presence, duration, intensity and the use of acute treatment, menses and the participant's sleep-wake cycle. Participants continued to fill in the diary 72 hours after the experiment. The experiment was done on a headache-free day preceded by a 72-hour headache-free window. During the session, participants completed patient-reported outcome (PRO) surveys (see Supplemental material) and underwent an EEG recording while performing an auditory oddball task. The entire session was 2.5 h long.

EEG recordings

We acquired continuous EEGs (digitized, sampling rate 500 Hz, no online filters, Neuroelectrics Enobio, Barcelona). Data was recorded using a 20-electrode EEG cap located over the scalp at standard positions (Fp1/Fp2, F3/F4, F7/F8, Fz, Cz, Pz, C3/C4, T7/T8, P3/P4, P7/P8, O1/O2), together with a common mode

sense (CMS), and a driven right leg electrode (DRL) placed on the right mastoid. Electrode impedances were kept below $15\,k\Omega$. EEG activity was re-referenced offline to the mean activity of all electrodes. Participants were instructed to keep their eyes open throughout the entire EEG session. Eye movements were monitored by an electrode placed at the infraorbital ridge of the right eye. From a sample of 45 participants, two EMs and one HC were not included in the final analyses based on EEG muscular and movement-related artifacts.

Auditory oddball paradigm

A variant of the active auditory oddball paradigm (5,25), in which an infrequent target tone (1620 Hz, 60 ms duration, 5 ms rise/fall times, probability of $p = 0.2$) occurred within a stream of standard tones (1500 Hz, 60 ms duration, 5 ms rise/fall times, probability of $p = 0.6$), was used. In addition to the standard and infrequent target tones, novel sounds (short excerpts of environmental sounds, such as the barking of a dog or the honking of a car) were also presented (average duration: 60.95 ± 7.61 ms, probability of $p = 0.2$). The stimuli were presented binaurally with the Presentation Software 18.1 (NeuroBehavioral Systems, San Francisco, CA, USA), through Sony MDR-ZX310APB headphones at 75 dB sound pressure level (SPL) in pseudo-random order with a stimulus onset asynchrony set to 1200 ms ($\pm$100 ms). A total of 500 trials (five blocks of 100 trials, 60/100 standard stimuli) were presented (duration $\cong$ 25 min). A central black fixation cross (height, width: 13 pixels) was presented on a black background throughout the entire duration of the experiment. Participants were instructed to keep their eyes open, avoid blinking, and remain fixated on the central cross, at all times, throughout the experiment. They were also instructed to respond as quickly and accurately as possible to the target tones while ignoring the standard and novel tones.

Behavioral analyses

Reaction times (RTs) for target stimuli were obtained. For each participant, RTs that were ± 3 standard deviations from their mean were excluded. The percentage of no-response ('miss') trials was also obtained by dividing the number of misses by the number of hits. Finally, the percentage of false alarms on standard and novel trials was calculated by dividing the number of standard/novel trials with a recorded response by the total number of standard/novel trials. Two-sample t-tests were used to compare these measures between groups. In addition, for standard stimuli, separate values were obtained for each block and submitted to repeated-measures analyses of variance (ANOVAs) with Time (Blocks 1–5) as a within-subject factor and Group (EM/HC) as a between-subject factor.

EEG pre-processing

First, the EEG was offline-filtered with a 50 Hz notch filter (type Parks-McClellan, order 180). Then, EEG data from ERP and TF analyses was pre-processed differently from ITC EEG data to avoid nonlinear phase distortions in ITC data (28). For ERP and TF, a Butterworth infinite impulse response (IIR) band-pass filter from 0.1 to 100 Hz was applied (high-pass: Frequency 0.1 Hz, order 2, cutoff -6 dB; low-pass: frequency 100 Hz, order 4, cutoff -6 dB). For ITC analyses, a Hamming windowed sinc finite impulse response (FIR) band-pass filter (zero-phase), from 0.1 to 100 Hz, was applied (high-pass: Frequency 0.1 Hz, order 16500, cutoff -6 dB; low-pass: frequency 100 Hz, order 66, cutoff -6 dB). Finally, epochs were separately obtained for standard, target and novel tones (ERPs: 100–1000 ms; power/phase-synchronization: -2000–2000 ms post-stimulus onset) and were baseline-corrected from -100 ms until 0 ms post-stimulus onset, as done in previous studies (5,25). Only correct trials were used to obtain the epochs. Correct trials were considered to be: Correct detections in response to target stimuli and no response to standard and novel tones. No participant had to be excluded due to an insufficient number of correct trials. Epochs exceeding ± 100 µV in the electro-oculogram (EOG) or EEG were automatically detected and removed from further analysis, then a visual inspection of the data was performed to confirm that artifacts were correctly detected.

Single trial convolution was performed via frequency-domain multiplication, in which the Fourier-derived spectrum of the ERP data was multiplied by the spectrum of the wavelet, and the inverse Fourier transform was taken. A six-cycle complex Morlet was used. A separate time series of complex wavelet coefficients was obtained for each frequency from 1 Hz to 40 Hz (linear increase). These complex coefficients, containing both real and imaginary components, were used to derive the power and phase-synchronization (i.e. inter-trial coherence). Power was computed with respect to baseline. Both measures were obtained for each trial and averaged for each participant before performing the grand-average.

Electrophysiological analyses

The EEG analyses were divided as a function of standard trials and target/novel trials. For standard trials, the individual amplitude was separately obtained for each component and for each of the five blocks.

The ERP mean amplitudes were set-centered on the peak activity of each component (N1: 75–125 ms; P2: 175–225 ms; N2: 250–350 ms). For spectral power and phase-synchronization, theta (3–8 Hz, 0–400 ms), alpha (8–12 Hz, 0–200 ms), and beta-gamma (12–40 Hz, 0–200 ms) frequency ranges were defined based on maximum activity and previous literature (5,25).

In the case of novel and target trials, the difference waveform ERPs were obtained between novel/target and standard trials. The following components were obtained, for novel: MMN (175–225 ms), Early P3a (225–275 ms), Late P3a (275–325 ms), and RON (350–450 ms); and for target stimuli: MMN (175–225 ms), P3b (450–550 ms), and RON (400–600 ms). For all ERP components, the mean amplitudes were set-centered on the peak activity. See Supplemental material for spectral power of target and novel trials.

Sample size was determined based on previous literature, which corroborated that 10–25 participants, with at least 20 artifact-free trials per condition, are enough for this kind of nested case-control EEG study (29,30). Consequently, participants with <20 correct responses or artifact-free trials of any condition were excluded from the analyses (30).

Standard trials were submitted to repeated-measures ANOVAs with Electrode location (Fz, Cz, Pz) and Block (1–5) as within-subject factors and Group (EM/HC) as a between-subject factor. A similar procedure was used for novel and target trials; however, the repeated-measures ANOVAs only had one within-subject factor: Electrode location (Fz, Cz, Pz) and one between-subject factor: Group (EM/HC). In addition, we used post-hoc t-tests comparisons when necessary.

For all analyses, p-values were corrected using the Greenhouse-Geisser correction for nonsphericity when appropriate.

Results

Behavioral results

In regards to behavioral measures, no significant differences between HC and EM were found on measures of RTs (HC: 512.53 ±73.29 ms, EM: 486.13 ±41.19 ms; $t(40) = 1.602$, $p = 0.117$), percentage of misses (HC 4.86 ±3.79%, EM 5.61 ±5.63%; $t(40) = -0.506$, $p = 0.616$), and false alarm rates on novel trials (HC 3.29 ±1.65%, EM:3.91 ±2.24%; $t(40) = -1.023$, $p = 0.312$). On standard trials, no modulation of the false alarm rate was observed across blocks (main effect of Block: $F(4,160) = 2.466$, $p = 0.106$), or as a function of group (main effect of Group: $F(1,40) = 0.001$, $p = 0.978$; Block × Group interaction: $F(4,160) = 0.102$, $p = 0.854$).

Electrophysiological results

Repetitive stimuli ERPs. See Figure 1 and Table 2 for repeated-measures ANOVAs. Typical N1, P2 and N2 ERP components were observed across blocks. A significant main effect of Electrode indicated the presence of a central distribution for N1 and P2, and a fronto-central distribution for N2. The lack of a significant main effect of Block together with the absence of a significant interaction of Block × Electrode for the N1 and N2 components, indicated that the amplitude of these components did not habituate across blocks. On the other hand, the amplitude of the P2 component was significantly reduced in the last block as compared to the first one, as seen by the significant main effect of Block and a significant Block × Electrode interaction.

In terms of group comparisons, a trend for increased N1 amplitude in the migraine group as compared to the control group was observed (see Table 2, N1, Group analyses, G). No differences were reported for P2 and N2 components between groups as reflected by a lack of a main effect of group and significant interactions. The lack of significant Block × Group interactions and Block × Electrode × Group interactions suggested that both groups presented a similar pattern of habituation (habituation of P2 and no habituation of N1 and N2).

Spectral power of repetitive stimuli. See Figure 2 and Table 3 for repeated-measures ANOVAs. As can be observed in Figure 2 and corroborated by statistical analyses, typical theta, alpha and beta-gamma activities were elicited in both groups, with certain habituation across blocks. The significant main effect of Electrode indicated the presence of a central distribution for all three frequencies. Habituation across blocks was confirmed for theta and alpha, but not for beta-gamma (see significant and non-significant main effects of Block in Table 3). No significant main effect of Group was obtained in theta, alpha, and beta-gamma power. Furthermore, a lack of significant Group × Block interactions implied that there were no differences between HC and EM in respect to the three frequencies. There were no significant group differences in habituation either.

Time and phase-synchronization analyses of repetitive stimuli. See Figure 3 and Table 4 for repeated-measures ANOVAs. In Figure 3, both groups had increased phase-synchronization of theta, alpha and beta-gamma on standard trials, with a clear habituation across blocks. Upon visual inspection, the phase-synchronization appeared higher in EM compared to HC. A central topographical distribution was supported by a significant main effect of electrode. Habituation
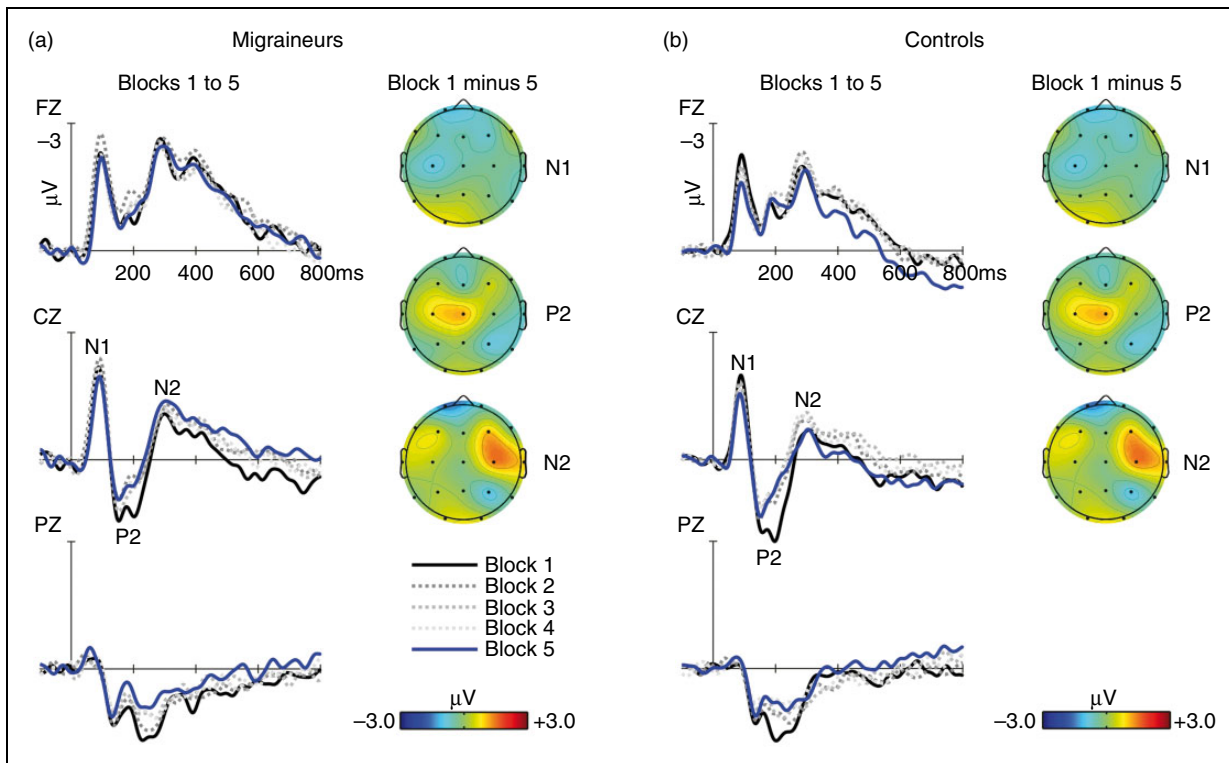
Figure 1. Grand mean ERP waveforms for standard trials, including the 1st (solid black line), 2nd (pointed dark grey line), 3rd (pointed medium grey line), 4th (pointed light grey line), 5th (solid blue line), at midline electrodes (Fz, Cz, and Pz), from −100 to 800 ms, −3/+3 μV, for both the EM (a) and HC (b) groups. Scalp distribution (−3/+3 μV) for 1st minus 5th block of standard trials involves the N1, P2 and N2.

Table 2. Repeated-measures ANOVA on the ERP components related to standard trials.

ERP	B F	B p	B × G F	B × G p	E F	E p	E × G F	E × G p	B × E F	B × E p	B × E × G F	B × E × G p	G F	G p
N1	0.830	0.498	1.412	0.237	34.504	**<0.001**	1.582	0.214	1.652	0.130	0.691	0.664	3.772	0.059
P2	3.968	**0.006**	0.919	0.447	68.364	**<0.001**	.303	0.713	2.562	**0.022**	0.554	0.757	0.019	0.891
N2	0.534	0.676	1.656	0.175	35.351	**<0.001**	1.933	0.153	0.957	0.447	1.114	0.354	2.582	0.116

Note: The following components and time-windows were studied: N1 (175–225 ms), P2 (350–450 ms), and N2 (250–350 ms). The repeated measures ANOVA included B: Block (1st, 2nd, 3rd, 4th, 5th) and E: Electrode location (Fz, Cz, Pz) as within-subject factors and G: Group (Control, Migraine) as the between-subject factor. The degrees of freedom were as follow: B (4,160), B × G (4,160), E (2,80), E × G (2,80), B × E (8,320), B × E × G (8,320), and G (1,40).
Bold values represent *P* < 0.05.

across blocks was also corroborated for theta and alpha but not for beta-gamma. Importantly, the significant main effect of Group confirmed the higher phase-synchronization in theta for the migraine group as compared to the control group (see Table 4, Theta, Group, G). No significant group differences were observed for the other frequencies (neither main effect of group, nor Group interactions). Similarly, no significant group differences were observed regarding the habituation of phase-synchronization of any of the three frequencies (see Table 4).

Target/Novel ERPs. See Figure 4 and Table 5 for repeated-measures ANOVAs. A cascade of ERP events was observed in response to target stimuli in both groups (see Figure 4) beginning with the appearance of a frontocentral MMN, a centro-parietal P3b, and a frontocentral RON. Topographical distributions were corroborated by the significant main effects of electrode. No significant group differences were observed (see Table 5).

Similarly, the time-course for responses to novel stimuli included the frontocentral MMN, a central
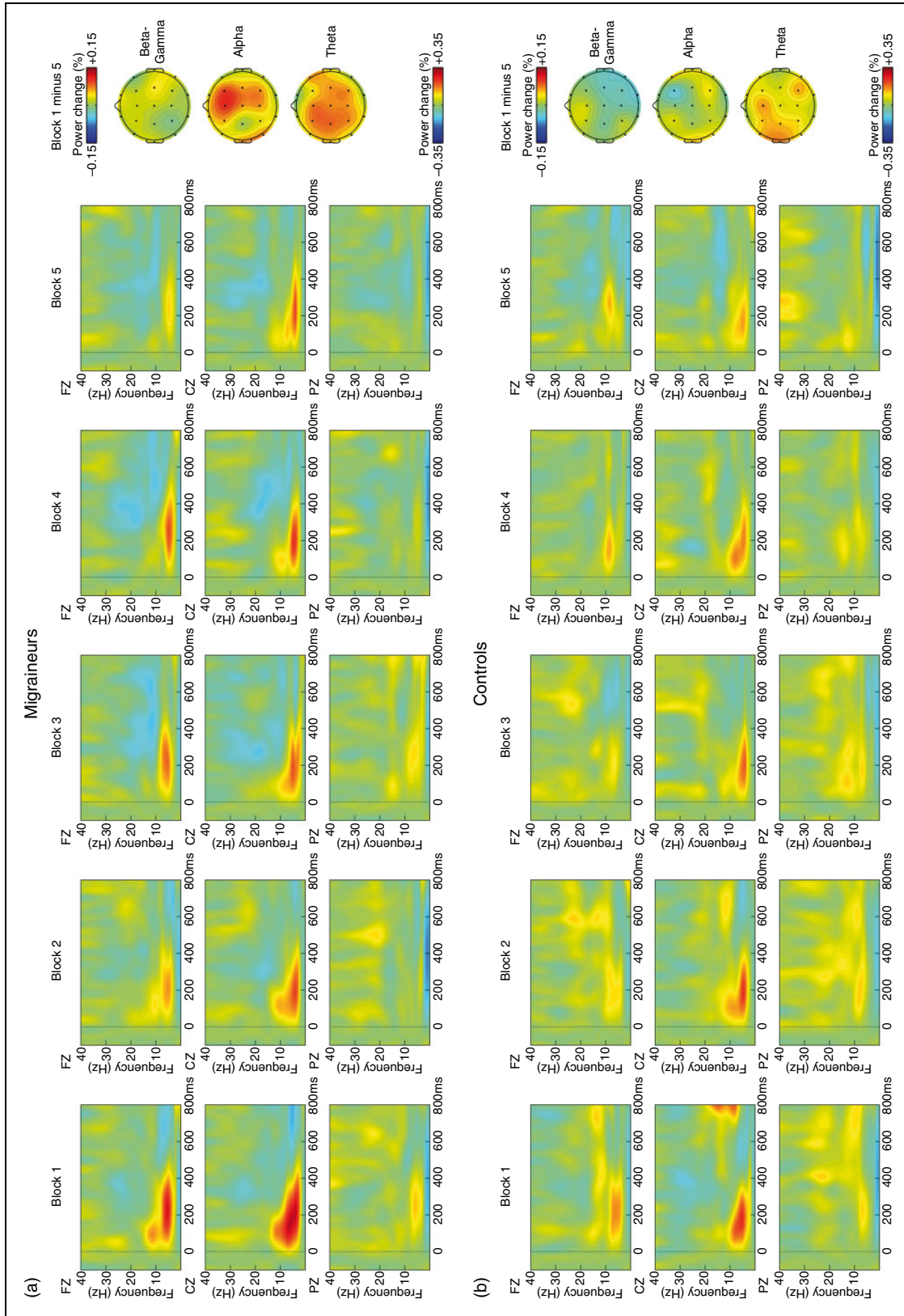
Figure 2. Grand mean event-related spectral perturbation representing changes in power with respect to baseline of standard trials, separated by blocks, at midline electrodes (Fz, Cz, Pz), for the migraine (a) and the control group (b). The increase/decrease of power is represented in percentage of change (−100/+100%), from −100 to 800 ms. Topographical maps of the spectral power difference between the 1st block and the 5th block, are depicted for each frequency of interest (theta: 3–8 Hz, 0–400 ms; alpha: 8–12 Hz, 0–200 ms; and Beta-Gamma: 12–40 Hz, 0–200 ms) and group.

Table 3. Repeated-measures ANOVA on the time-frequency spectral power of standard trials.

	B		B × G		E		E × G		B × E		B × E × G		G	
TF	F	p	F	p	F	p	F	p	F	p	F	p	F	p
Theta	5.543	**0.001**	0.902	0.452	41.601	**<0.001**	2.293	0.111	1.060	0.386	0.462	0.824	2.373	0.131
Alpha	2.726	**0.034**	1.774	0.141	10.388	**<0.001**	1.226	0.299	1.958	0.070	0.499	0.814	0.701	0.407
Beta-G	0.578	0.660	0.827	0.499	5.390	**0.007**	0.467	0.624	0.788	0.580	0.354	0.907	2.230	0.143

Note: The following frequency ranges and time-windows were studied: theta (3–8 Hz, 0–400 ms), alpha (8–12 Hz, 0–200 ms), and beta-gamma (12–40 Hz, 0–200 ms). The repeated measures ANOVA included B: Block (1st, 2nd, 3rd, 4th, 5th) and E: Electrode location (Fz, Cz, Pz) as within-subject factors and G: Group (Control, Migraine) as the between-subject factor. The degrees of freedom were: B (4,160), B × G (4,160), E (2,80), E × G (2,80), B × E (8,320), B × E × G (8,320), and G (1,40).
Bold value represent $P<0.05$.

early P3a, a frontal and parietal late P3b, and a frontocentral RON (see Figure 4). Topographical distributions were upheld by significant main effects of electrode. Despite a lack of main effects between groups, a significant Electrode × Group interaction was observed for the early P3a, late P3a, and RON. The post-hoc t-test analyses revealed that the early P3a trends to be reduced in EM as compared to HC at Cz ($t(40) = 1.967$, $p = 0.056$) and attains significance at Pz ($t(40) = 3.747$, $p = 0.001$). On the other hand, an increased late P3a was observed at frontal sites in EM as compared to HC (Fz: $t(40) = -2.087$, $p = 0.043$). A post-hoc analysis of the RON also indicated an amplitude reduction in EM at Fz ($t(40) = -2.801$, $p = 0.008$). For time-frequency see Supplemental results.

Discussion

The aim of this study was to investigate auditory sensory processing during an active oddball task in a group of young, female, low-frequency EM patients in the interictal phase as compared to healthy controls. Our research study proposed a novel approach by pairing classic ERP analyses with spectral power and phase-synchronization, which offer a more holistic approach to understanding the sensory alterations reported in EM. Patients presented: i) an increased response to auditory stimuli, as indicated by increased N1 amplitude and theta phase-synchronization, and ii) an abnormal response pattern to novel stimuli characterized by a reduced early P3a, an increased late P3a, and reduced RON.

Our results suggest that auditory sensory processing is increased in EM patients interictally, which supports previous findings indicating increased sensitivity to sound in patients between attacks (31). An increased N1 suggests that EM individuals process environmental sounds as more salient, and consequently allocate more attentional resources to their processing (6,7), affecting the representation of sound at the neural level, within the sensory auditory cortex (32). A lack of group differences in P2 and N2 components would suggest that higher order perceptual processes and their modulation by attentional top-down mechanisms remain preserved (8). Although some studies have failed to report differences in N1 or P2 amplitude (3,10–13,33), these results are compatible with data from other studies (14,15), which encountered higher N1-P2 amplitudes in families with migraine.

The main finding of the present study was the increased theta phase-synchronization in response to repetitive stimuli in EM. The theta wave is the main contributor to the brain's response to standard stimuli during active auditory oddball tasks (5). Notably, both power and phase-synchronization may be instrumental in generating and modulating ERPs. However, phase-synchronization may be also involved in maintenance (with progressive habituation) of ERP amplitudes across repetitions (26). Phase-synchronization of theta activity plays a relevant and active role in early sensory processing. It has been suggested to be an internal form of information coding in the sensory cortex (34), which acts by continuously tracking information related to external sensory stimuli (35). In the auditory modality, this process is closely linked to the N1 component (26). Therefore, an increase in phase-synchronization, as seen in our data, could underlie the increased sensory auditory processing seen in EM, confirmed by an increased amplitude of the N1 component. Our results are compatible with studies on visual processing, which also show increased phase-synchronization in EM without aura in particular within the alpha-band during visual stimulation (1,36,37) and with resting-state functional magnetic resonance imaging (rfMRI) studies indicating alterations in connectivity in salience- and auditory-related structures (38). Finally, our results are also congruent with the thalamocortical dysrhythmia hypothesis, suggesting the presence of increased low frequency oscillations in migraine in thalamic structures, which may lead to a hyperresponsiveness of the sensory cortices.
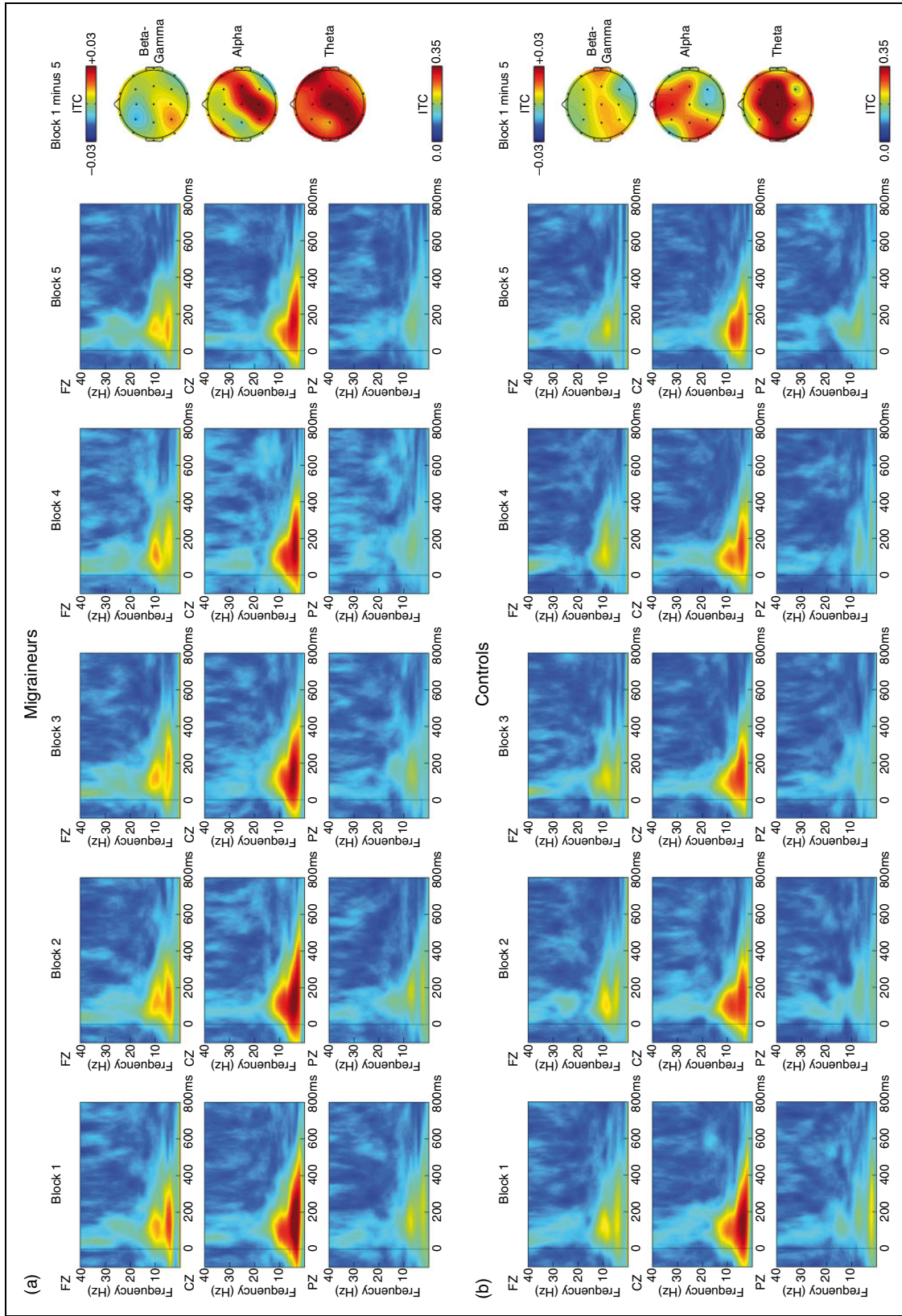
Figure 3. Grand mean inter-trial coherence (ITC, phase-synchronization) standard trials, separated by blocks, at midline electrodes (Fz, Cz, Pz), for the migraine (a) and the control group (b). The ITC (0/0.35) is depicted from −100 to 800 ms. Topographical maps of the ITC difference (−0.03/0.03) between the 1st block and the 5th block, are depicted for each frequency of interest (theta: 3–8 Hz, 0–400 ms; alpha: 8–12 Hz, 0–200 ms; and Beta-Gamma: 12–40 Hz, 0–200 ms) and group.

Table 4. Repeated-measures ANOVA on the phase-synchronization of standard trials.

P-Sync	B F	B p	B × G F	B × G p	E F	E p	E × G F	E × G p	B × E F	B × E p	B × E × G F	B × E × G p	G F	G p
Theta	14.599	**<0.001**	0.679	0.577	43.583	**<0.001**	1.577	0.216	1.198	0.308	0.480	0.825	5.986	**0.019**
Alpha	3.659	**0.009**	1.070	0.370	39.114	**<0.001**	0.138	0.853	0.967	0.447	1.608	0.148	2.377	0.131
Beta-G	1.203	0.312	0.134	0.957	14.338	**<0.001**	2.924	0.062	1.386	0.219	0.650	0.695	0.339	0.564

Note: The following frequency ranges and time-windows were studied: theta (3–8 Hz, 0–400 ms), alpha (8–12 Hz, 0–200 ms), and beta-gamma (12–40 Hz, 0–200 ms). The repeated measures ANOVA included B: Block (1st, 2nd, 3rd, 4th, 5th) and E: Electrode location (Fz, Cz, Pz) as within-subject factors and G: Group (Control, Migraine) as the between-subject factor. The degrees of freedom were: B (4,160), B × G (4,160), E (2,80), E × G (2,80), B × E (8,320), B × E × G (8,320), and G (1,40).
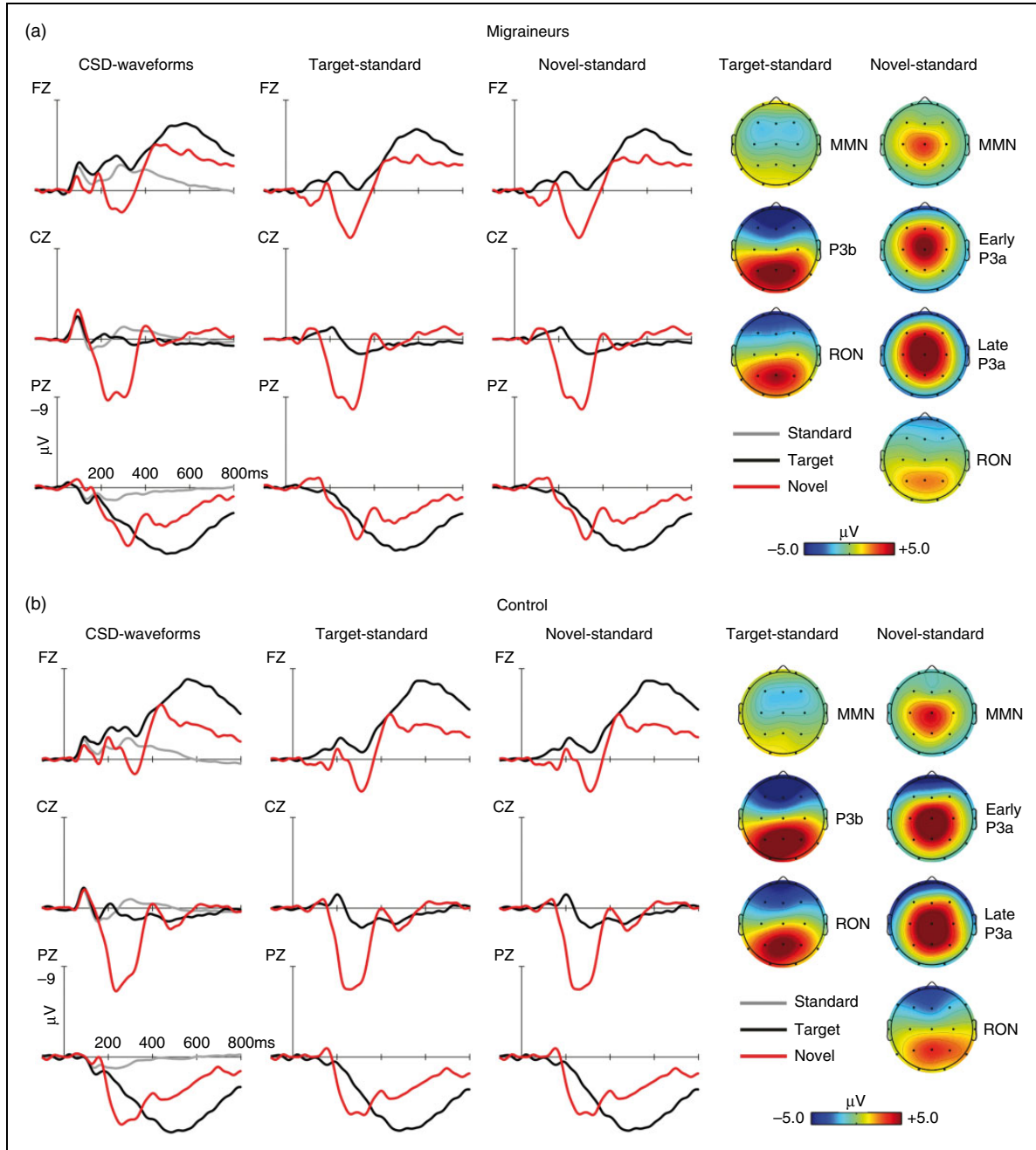Bold values represent $P<0.05$.

Figure 4. Grand mean ERP waveforms for standard (grey line), target (black line) and novel (red line), at midline electrodes (Fz, Cz, and Pz), from −100 to 800 ms, −9/+9 μV, for both the EM (a) and HC (b) groups. Difference waveforms associated to the target minus standard (black line) and novel minus standard (red line) are showed. Scalp distribution (−5/+5 μV) for target minus standard trials involve the MMN, P3b and RON. Scalp distribution (−5/+5 μV) for novel minus standard involve the MMN, early P3a, late P3a, and RON.

Table 5. Repeated-measures ANOVA for the ERP difference waveforms related to target and novel stimuli.

Component	E		E × G		G	
	F	p	F	p	F	p
Target						
MMN	43.807	**<0.001**	0.647	0.488	0.061	0.806
P3b	204.806	**<0.001**	2.300	0.125	0.068	0.796
RON	119.858	**<0.001**	3.260	0.062	0.052	0.820
Novel						
MMN	27.929	**<0.001**	1.699	0.196	0.382	0.540
Early P3a	45.876	**<0.001**	18.103	**<0.001**	1.310	0.259
Late P3a	23.141	**<0.001**	5.025	**0.015**	0.097	0.757
RON	78.174	**<0.001**	6.586	**0.005**	0.002	0.968

Note: The following components and time-windows were included for target stimuli: MMN (175–225 ms), P3b (450–550 ms), and RON (350–450 ms); and for novel stimuli: MMN (175–225 ms), early P3a (225–275 ms), late P3a (275–325 ms), and RON (400–600 ms). The repeated measures ANOVA included E: Electrode location (Fz, Cz, Pz) as the within-subject factor and G: Group (Control, Migraine) as the between-subject factor. The degrees of freedom were as follow: E (2,80), E × G (2,80), and G (1,40).
Bold values represent $P<0.05$.

In the current study, we observed habituation of ERPs, spectral power, and phase-synchronization processes in both EM and control groups across blocks. These results support previous studies, which did not find any differences in the habituation of N1 and P2 ERP components to auditory stimuli between migraine patients and healthy controls (3,10–13). Although the thalamocortical dysrhythmia hypothesis suggests that migraine hyperresponsiveness is due to a lack of habituation to sensory stimuli (1), current research findings have opened this up for debate. It remains unclear whether the deficit of habituation, frequently reported in migraine studies, is related to disease itself, or if it could be related with the subtype of migraine (such as episodic or chronic, with or without aura), or to a confounding variable (such as treatment, psychiatric comorbidity, age or methodological differences) (39).

In regards to the cascade of ERPs related to novel and target stimuli, we observed abnormalities in EM. Similarly to previous studies (10,19), but in contrast to others (12,13), no group differences were observed in MMN in response to novel stimuli, which may reflect that early sensory detection of unexpected change or stimuli, is preserved in migraine. Regarding P3a, previous studies reported no differences (13,20), while other studies showed an increased P3a in migraine compared to controls (12). Based on previous basic research studies indicating the presence of two P3a peaks (early and late) with different brain generators, we decided to divide the P3a in two. We observed an abnormal pattern of reduced early P3a and increased late P3a in patients as compared to controls. These results suggested that in EM there was a reduced post-sensory response to novel stimuli (reduced early P3a), which was quickly compensated by the

heightened allocation of attentional resources (increased late P3a). A reduced RON in both novel and target stimuli would indicate that patients had difficulty disengaging from distracting novel stimuli and reorienting attention back to the task, which could indicate decreased cognitive flexibility (16). Finally, consistent with one line of evidence, no group differences were observed between migraine patients and healthy controls with respect to the MMN (10,19) and P3b (3,11,22), despite findings from other studies (19,23,24).

Limitations: Our study has some limitations in relation to the features of our sample, which consisted of young adult women (19–28 years) with low-frequency EM without aura. It is possible that our sample can only partially explain migraine symptomology and might not be generalized to the usual population of migraine patients seen in clinical practice, which report higher frequency of attacks and more associated symptomology. Another factor that might have an impact on the results is the age of migraine onset, but unfortunately this variable was not collected in this research study, given that many of the participants that received a migraine diagnosis were unaware or unsure of whether or not they had migraine. Therefore, it was difficult to pinpoint a specific onset time. Future studies might evaluate how disease evolution and associated symptomatology may impact auditory sensory processing and consequently ERPs, spectral power, and phase-synchronization. There is also an important methodological aspect to consider, which is a basic principle of habituation: The presentation of other (usually strong or salient) stimuli results in a recovery or in a disruption of habituation to a standard repetitive stimulus (40). In this experiment,

habituation was examined using an active Oddball task, comprised of standard, novel and target stimuli. Thus, the results regarding habituation should be interpreted with caution, as the presence of target and novel stimuli could break the habituation chain and bias data.

Conclusions

In conclusion, the presence of an increased theta phase-synchronization and a larger N1 in EM could indicate the presence of a hypersensitivity to auditory stimuli in low-frequency EM patients between attacks. Patients appear to process repetitive stimuli as though they were more salient and seem to allocate more of their attentional resources to their surrounding environment. Finally, in the presence of particularly salient stimuli (such as novel and target), which could be considered biologically relevant, patients show a reduced RON, or a difficulty in reorienting their attention from the distracting stimulus back to the task at hand. This would suggest decreased cognitive flexibility in patients with EM as compared to controls. Ultimately, patients show a hypersensitivity to auditory stimuli and maladaptive allocation of attentional resources, which could explain the auditory alterations reported interictally in EM.

Article highlights

1. The perceived salience of auditory stimulus is increased in episodic migraine as seen in greater theta phase-synchronization and higher N1 amplitude.
2. The reduced amplitude of the reorienting negativity suggested that episodic migraine patients have less available resources to reorient attention back to the main task.

Declaration of conflicting interests

The authors declared the following potential conflicts of interest with respect to the research, authorship, and/or publication of this article: AVB, AMM, VJG report no conflicts of interest. AVB has received a postdoctoral contract courtesy of "La Caixa" Foundation, and was supported by the Spanish MICINN Juan de la Cierva postdoctoral grant (FJC2018-036804-I). AA has received honoraria as speaker for Allergan. MTF has received honoraria as a speaker for Allergan, Chiesi, Eli Lilly and Novartis. PPR has received honoraria as a consultant and speaker for Allergan, Almirall, Biohaven, Chiesi, Eli Lilly, Medscape, Neurodiem, Novartis and Teva. Her research group has received research grants from Allergan, AGAUR, la Caixa foundation, Migraine Research Foundation, Instituto Investigación Carlos III, MICINN, PERIS; and has received funding for clinical trials from Alder, Electrocore, Eli Lilly, Novartis and Teva. She is a trustee member of the board of the International Headache Society and a member of the Council of the European Headache Federation. She is on the editorial board of *Revista de Neurologia*. She is an editor for *Frontiers of Neurology* and the *Journal of Headache and Pain*. She is a member of the Clinical Trials Guidelines Committee of the International Headache Society. She has edited the Guidelines for the Diagnosis and Treatment of Headache of the Spanish Neurological Society. She is the founder of www.midolordecabeza.org. PPR does not own stocks from any pharmaceutical company. The authors report no disclosures relevant to the manuscript.

ORCID iDs

Adrià Vilà-Balló ![ORCID] https://orcid.org/0000-0001-7593-6012
Angela Marti-Marca ![ORCID] https://orcid.org/0000-0002-9041-2943
Alicia Alpuente ![ORCID] https://orcid.org/0000-0001-5296-9401

References

1. de Tommaso M, Ambrosini A, Brighina F, et al. Altered processing of sensory stimuli in patients with migraine. *Nat Rev Neurol* 2014; 10: 144–155.
2. Ambrosini A. Controversies about the role of the deficit of habituation of evoked potentials in migraine: A disease biomarker? PROS. *J Headache Pain* 2015; 16: A14.
3. Wang W and Schoenen J. Interictal potentiation of passive 'oddball' auditory event-related potentials in migraine. *Cephalalgia* 1998; 18: 261–265; discussion, 241.
4. Escera C and Corral MJ. Role of mismatch negativity and novelty-P3 in involuntary auditory attention. *J Psychophysiol* 2007; 21: 251–264.

5. Marco-Pallarés J, Nager W, Krämer UM, et al. Neurophysiological markers of novelty processing are modulated by COMT and DRD4 genotypes. *Neuroimage* 2010; 53: 962–969.

6. Näätänen R. *Attention and brain function.* Hillsdale, NJ: Lawrence Erlbaum Associates, 1992.

7. Rinne T, Särkkä A, Degerman A, et al. Two separate mechanisms underlie auditory change detection and involuntary control of attention. *Brain Res* 2006; 1077: 135–143.

8. Luck SJ and Hillyard SA. Electrophysiological correlates of feature analysis during visual search. *Psychophysiology* 1994; 31: 291–308.

9. Evans KM and Federmeier KD. The memory that's right and the memory that's left: Event-related potentials reveal hemispheric asymmetries in the encoding and retention of verbal information. *Neuropsychologia* 2007; 45: 1777–1790.

10. de Tommaso M, Guido M, Libro G, et al. Interictal lack of habituation of mismatch negativity in migraine. *Cephalalgia* 2004; 24: 663–668.

11. Chen W, Shen X, Liu X, et al. Passive paradigm single-tone elicited ERPs in tension-type headaches and migraine. *Cephalalgia* 2007; 27: 139–144.

12. Demarquay G, Caclin A, Brudon F, et al. Exacerbated attention orienting to auditory stimulation in migraine patients. *Clin Neurophysiol* 2011; 122: 1755–1763.

13. Morlet D, Demarquay G, Brudon F, et al. Attention orienting dysfunction with preserved automatic auditory change detection in migraine. *Clin Neurophysiol* 2014; 125: 500–511.

14. Wang W, Timsit-Berthier M, et al. Intensity dependence of auditory evoked potentials is pronounced in migraine: An indication of cortical potentiation and low serotonergic neurotransmission? *Neurology* 1996; 46: 1404–1409.

15. Siniatchkin M, Kropp P, Neumann M, et al. Intensity dependence of auditory evoked cortical potentials in migraine families. *Pain* 2000; 85: 247–254.

16. Schröger E and Wolff C. Attentional orienting and reorienting is indicated by human event-related brain potentials. *Neuroreport* 1998; 9: 3355–3358.

17. Polich J. Overview of P3a and P3b. In: Polich J (ed) *Detection of change: Event-related potential and fMRI findings.* Norwell, MA: Kluwer Academic Press, 2003, pp.83–98.

18. Scheer M, Bülthoff HH and Chuang LL. Steering demands diminish the early-P3, late-P3 and RON components of the event-related potential of task-irrelevant environmental sounds. *Front Hum Neurosci* 2016; 10: 73.

19. Valeriani M, Galli F, Tarantino S, et al. Correlation between abnormal brain excitability and emotional symptomatology in paediatric migraine. *Cephalalgia* 2009; 29: 204–213.

20. Koo YS, Ko D, Lee G-T, et al. Reduced frontal P3a amplitude in migraine patients during the pain-free period. *J Clin Neurol* 2013; 9: 43–50.

21. Wang R, Dong Z, Chen X, et al. Gender differences of cognitive function in migraine patients: evidence from event-related potentials using the oddball paradigm. *J Headache Pain* 2014; 15: 6.

22. Titlic M, Mise NI, Pintaric I, et al. The event-related potential P300 in patients with migraine. *Acta Inform Med* 2015; 23: 339–342.

23. Drake ME, Pakalnis A and Padamadan H. Long-latency auditory event related potentials in migraine. *Headache* 1989; 29: 239–241.

24. Wang W, Schoenen J and Timsit-Berthier M. Cognitive functions in migraine without aura between attacks: A psychophysiological approach using the 'oddball' paradigm. *Neurophysiol Clin* 1995; 25: 3–11.

25. Vilà-Balló A, François C, Cucurell D, et al. Auditory target and novelty processing in patients with unilateral hippocampal sclerosis: A current-source density study. *Sci Rep* 2017; 7: 1612.

26. Fuentemilla Ll, Marco-Pallarés J and Grau C. Modulation of spectral power and of phase resetting of EEG contributes differentially to the generation of auditory event-related potentials. *NeuroImage* 2006; 30: 909–916.

27. Olesen J, Bes A, Kunkel R, et al. The International Classification of Headache Disorders, 3rd edition (beta version). *Cephalalgia* 2013; 33: 629–808.

28. Cohen MX. *Analyzing neural time series data: Theory and practice.* Cambridge: MIT Press, 2014.

29. Light GA, Williams LE, Minow F, et al. Electroencephalography (EEG) and event-related potentials (ERPs) with human participants. *Curr Protoc Neurosci* 2010; 52: 6–25.

30. Marco-Pallares J, Cucurell D, Münte TF, et al. On the number of trials needed for a stable feedback-related negativity. *Psychophysiology* 2011; 48: 852–860.

31. Vingen JV, Pareja JA, Støren O, et al. Phonophobia in migraine. *Cephalalgia* 1998; 18: 243–249.

32. Woldorff MG, Gallen CC, Hampson SA, et al. Modulation of early sensory processing in human auditory cortex during auditory selective attention. Proc Natl Acad Sci USA 1993; 90: 8722–8726.

33. Ambrosini A, Rossi P, De Pasqua V, et al. Lack of habituation causes high intensity dependence of auditory evoked cortical potentials in migraine. *Brain* 2003; 126: 2009–2015.

34. Kayser C, Ince RAA and Panzeri S. Analysis of slow (theta) oscillations as a potential temporal reference frame for information coding in sensory cortices. *PLoS Comput Biol* 2012; 8: e1002717.

35. Luo H, Liu Z and Poeppel D. Auditory cortex tracks both auditory and visual stimulus dynamics using low-frequency neuronal phase modulation. *PLoS Biol* 2010; 8: e1000445.

36. Angelini L, de Tommaso M, Guido M, et al. Steady-state visual evoked potentials and phase synchronization in migraine patients. *Phys Rev Lett* 2004; 93: e038103.

37. de Tommaso M, Stramaglia S, Marinazzo D, et al. Functional and effective connectivity in EEG alpha and beta bands during intermittent flash stimulation in migraine with and without aura. *Cephalalgia* 2013; 33: 938–947.

38. Yang F-C, Chou K-H, Hsu A-L, et al. Altered brain functional connectome in migraine with and without restless legs syndrome: A resting-state functional MRI study. *Front Neurol* 2018; 9: e25.

39. Brighina F, Cosentino G and Fierro B. Is lack of habituation a biomarker of migraine? A critical perspective. *J Headache Pain* 2015;16: A13.

40. Thompson RF. Habituation: A history. *Neurobiol Learn Mem* 2009; 92: 127–134.